UQAC
Université du Québec
à Chicoutimi

PARAMÈTRES CONTRÔLANT LES PROPRIÉTÉS DE TRACTION À LA TEMPÉRATURE AMBIANTE ET ÉLEVÉE DES ALLIAGES Al-Cu ET Al-Si

PAR

ABRAM GIRGIS

MÉMOIRE PRÉSENTÉ À L'UNIVERSITÉ DU QUÉBEC À CHICOUTIMI
EN VUE DE L'OBTENTION DU GRADE DE MAÎTRE ÈS SCIENCES
APPLIQUÉES DU PROGRAMME DE MAÎTRISE EN INGÉNIERIE

QUÉBEC , CANADA

UQAC
Université du Québec
à Chicoutimi

PARAMETERS CONTROLLING THE AMBIENT AND ELEVATED TEMPERATURE TENSILE PROPERTIES OF AL-CU AND AL- SI CAST ALLOYS

BY

ABRAM GIRGIS

THESIS PRESENTED TO UNIVERSITY OF QUEBEC AT CHICOUTIMI
IN PARTIAL FULFILLMENT OF THE REQUIREMENT FOR THE
DEGREE OF MASTER OF SCIENCE IN ENGINEERING

QUÉBEC, CANADA

Dedicated to my late father Eng. Samir Girgis,
my mother, my sister and my brother

RÉSUMÉ

Au fil des années, de nombreux alliages ont été développés pour répondre aux exigences des différentes applications. Dans l'industrie automobile, les alliages légers destinés à la fonderie d'aluminium, notamment ceux à base d'Al-Si et d'Al-Cu, remplacent les matériaux à base ferreuse dans les culasses et les blocs moteurs. En consequence, de nouveaux alliages et traitements thermiques continuent à être développés au fur et à mesure que de nouveaux besoins et défis se présentent pour répondre aux demandes de réduction de la consommation de carburant et de performances à haute température des composants de moteur modernes.

La présente étude visait à étudier les propriétés mécaniques d'un nouvel alliage à base d'aluminium Al-6,5% Cu, portant le code HT200, et à déterminer comment ces propriétés pourraient être améliorées à l'aide du raffinage du grain et du traitement thermique. Les effets de différents traitements thermiques et additions d'alliages sur les propriétés de traction aux températures ambiante et à haute température ont été examinés. Trois alliages ont été utilisés: l'alliage de base HT200 (codé A) et deux autres, contenant 0,15% de Ti + 0,15% de Zr et 0,15% de Ti + 0,15% de Zr + 0,5% d'Ag (codés respectivement B et C). Les propriétés des trois alliages HT200 ont été comparées à celles des alliages 319 (codé D) et 356 (codé E), soumis aux mêmes conditions de traitement thermique. Sur la base de leur utilisation intensive dans l'industrie automobile, les alliages 319 et 356 ont été pris comme alliages de référence pour comparer les performances du nouvel alliage par rapport à ces deux alliages, afin de déterminer sa pertinence en tant que remplacement adéquat pour les applications automobiles.

Les alliages HT200, 319 et 356 ont été fondus en suivant les procédures habituelles de fusion, de coulée et les additions d'alliage spécifiées ont été effectuées. Des expériences d'analyse thermique ont été réalisées pour déterminer le comportement de solidification. La susceptibilité à la déchirure à chaud des alliages HT200 a également été examinée. Les barres d'essai de traction ont été préparées en utilisant un moule permanent ASTM B-108. Les barres telles que coulées ont été traitées thermiquement en utilisant douze conditions de traitement thermique différentes, en utilisant des temps de traitement en solution de 4 h et 8 h pour les alliages HT200, et six traitements thermiques en utilisant un temps de mise en solution de 8 h pour les alliages 319 et 356. Des essais de traction ont été effectués à température ambiante (25 °C) et à température élevée (250 °C), en utilisant une vitesse de déformation de 4 x 10-4 s-1, en utilisant une machine d'essais mécanique servohydraulique MTS pour les essais de température ambiante et un essai Instron Universal machine pour les tests de température élevée. Les microstructures ont été examinées par microscopie optique et électronique à balayage pour déterminer les phases et les intermétalliques présents dans la structure et les précipités formés. Les propriétés de traction (UTS, YS et% El) obtenues ont été analysées à l'aide d'une analyse statistique et de diagrammes de qualité utilisant le concept d'indice de qualité afin de déterminer la condition optimale de traitement de la composition de l'alliage-traitement thermique pour obtenir les meilleures propriétés de traction.

Les résultats ont montré que la surchauffe de l'alliage HT200 A pendant la fusion (température de coulée de 750 °C à 830 °C) diminuait la sensibilité de l'alliage au craquage

à chaud. L'ajout d'affineurs de grains comme dans les alliages B et C et le contrôle de la température du moule ont permis d'améliorer efficacement la résistance de l'alliage à la déchirure à chaud, ce qui a permis d'obtenir une pièce sans fissures. À la vitesse de refroidissement élevée de 8 °C / s obtenue avec les échantillons de barreaux d'essai de traction, la taille moyenne des grains dans l'alliage A était d'environ 85 µm, contre 350 µm pour les échantillons solidifiés à 0,8 °C / s analyses thermiques). Un taux de solidification élevé combiné à un affinage approprié des grains, à donné une taille de grain d'environ 50 µm dans l'alliage B.

À l'état brute de coulé, les alliages HT200, 319 et 356 présentaient des valeurs UTS, YS et% El de 283,45 MPa, 227,3 MPa et 2,2% (alliage A), 308,2 MPa, 213,5 MPa et 2,6% (alliage D) et 214,6 MPa, 140 MPa et 2,85% (alliage E). La résistance des alliages HT200 s'est améliorée de manière significative avec le traitement thermique. Les propriétés optimales de traction à la température ambiante (UTS, YS,% El) et les valeurs Q pour les cinq alliages et les conditions de traitement thermique T6 correspondantes donnant ces propriétés sont: 372,76 MPa, 297,3 MPa, 1,24%, 387,0 MPa (alliage A-S4WA1) 388,6 MPa, 292,24 MPa, 3,1%, 463,2 MPa (alliage B-S8WA2); 352 MPa, 274,86 MPa, 2,9%, 420,86 MPa (alliage C-S8WA1); 354,8 MPa, 324,36 MPa, 1,2%, 366,54 MPa (alliage D-S8WA2); 346,5 MPa, 298,5 MPa, 1,0%, 349,6 MPa (alliage E-S8WA2). Parmi les alliages HT200, l'alliage B dans la condition de traitement thermique S8WA2 (T6) a fourni la condition optimale de traitement thermique de la composition. L'amélioration des propriétés est due à la précipitation de particules ultrafines de la phase θ-Al2Cu, ainsi qu'à l'affinage du grain.

Pour les données de traction obtenues à 250 °C, l'alliage HT200 présentait des propriétés inférieures à celles des alliages 319 et 356 dans les conditions brutes de coulée et de traitement en solution. Les résistances plus élevées observées dans ces derniers alliages sont attribuées aux effets de renforcement résultant de leur teneur plus élevée en Si. En ce qui concerne l'alliage C, bien que l'ajout d'Ag n'ait entraîné aucune amélioration des propriétés de résistance de l'alliage HT200 à la température ambiante, lors des essais à haute température, la limite d'élasticité s'est améliorée d'environ 17%.

Les propriétés optimales de résistance à la traction à haute température et les valeurs Q pour les cinq alliages étudiés et les conditions de traitement thermique correspondantes fournissant ces propriétés sont: 281,2 MPa, 280,2 MPa, 1,97%, 325,3 MPa (alliage A-S8WA2); 307,9 MPa, 303,9 MPa, 2,3%, 361 MPa (alliage B-S8WA2); 276 MPa, 274,9 MPa, 3,2%, 351,9 MPa (alliage C-S8WA2); 309,1 MPa, 304,9 MPa, 2,8%, 375,6 MPa (alliage D-S8WA1); 282,6 MPa, 281,5 MPa, 2,4%, 338,7 MPa (alliage E-S8WA1). L'alliage B dans l'état traité thermiquement S8WA2 (T6) est considéré comme l'état optimal de composition d'alliage / traitement thermique.

Étant donné que l'alliage B offre les meilleures performances globales dans la gamme de traitements thermiques utilisés pour les alliages HT200, à la fois aux températures ambiantes et élevées, avec des propriétés comparables à celles des alliages 319 et 356, il peut être considéré comme une solution de remplacement très appropriée dans les applications automobiles.

ABSTRACT

Many alloys have been developed over the years to meet the requirements of different applications. In the automotive industry, lightweight aluminum casting alloys, among them Al-Si and Al-Cu based alloys, are replacing ferrous-based materials in cylinder heads and engine blocks. Accordingly, new alloys and heat treatments continue to be developed as new needs and challenges arise to meet the demands for reduced fuel consumption and high temperature performance of modern engine components.

The present study was undertaken to investigate the mechanical properties of a newly developed aluminum Al-6.5%Cu based alloy, coded HT200, and to determine how these properties could be further improved using grain refinement and heat treatment. The effects of different heat treatments and alloying additions on the ambient and high temperature tensile properties were examined. Three alloys were used: the base HT200 alloy (coded A), and two others, containing 0.15% Ti + 0.15%Zr, and 0.15% Ti + 0.15%Zr + 0.5%Ag additions (coded B and C, respectively). The properties of the three HT200 alloys were compared with those of 319 (coded D) and 356 (coded E) alloys, subjected to the same heat treatment conditions. Based on their extensive use in the automotive industry, the 319 and 356 alloys were taken as reference alloys, for comparing the performance of the new alloy with respect to these two alloys, to determine its suitability as a good alternative alloy for automotive applications.

Melts of the HT200, 319 and 356 alloys were prepared, following the usual melting and casting procedures, and the specified alloying additions made. Thermal analysis experiments were carried out to determine the solidification behavior. The hot tearing susceptibility of the HT200 alloys was also examined. Tensile test bars were prepared using an ASTM B-108 permanent mold. The as-cast bars were heat treated using twelve different heat treatment conditions, employing solution treatment times of 4 h and 8 h for the HT200 alloys, and six heat treatments using 8 h solution time for the 319 and 356 alloys. Tensile tests were carried out at ambient (25 ^{o}C) and elevated temperature (250 ^{o}C), using a strain rate of 4 x 10^{-4} s^{-1}, employing an MTS Servohydraulic mechanical testing machine for the room temperature testing and an Instron Universal testing machine for the elevated temperature tests. Microstructures were examined using optical and scanning electron microscopy to determine the phases and intermetallics present in the structure and the precipitates formed. The tensile properties (UTS, YS and %El) obtained were analyzed using statistical analysis and quality charts using the quality index concept to determine the optimum alloy composition-heat treatment condition for best tensile properties.

The results showed that while melt superheating of the HT200 alloy A (from 750 C to 830 C pouring temperature) decreased the alloy sensitivity to hot cracking. Addition of grain refiners as in alloys B and C and controlling the mold temperature were effective in improving the alloy resistance to hot tearing, resulting in a crack-free casting. At the high cooling rate of 8°C/s obtained with the tensile test bar castings, the average grain size in alloy A was found to be about 85 μm, compared to 350 μm reported for samples solidified at

0.8°C/s (from thermal analysis castings). A combined high solidification rate with proper grain refining resulted in a grain size of approximately 50 μm in alloy B.

In the as-cast condition, the HT200, 319 and 356 alloys exhibited UTS, YS and %El values of 283.45 MPa, 227.3 MPa and 2.2% (alloy A), 308.2 MPa, 213.5 MPa and 2.6% (alloy D) and 214.6 MPa, 140 MPa and 2.85% (alloy E). The strength of the HT200 alloys improved significantly with heat treatment. Optimum room temperature tensile properties (UTS, YS, %El) and Q-values for the five alloys and the corresponding T6 heat treatment conditions which provided these properties are: 372.76 MPa, 297.3 MPa, 1.24%, 387.0 MPa (alloy A-S4WA1); 388.6 MPa, 292.24 MPa, 3.1%, 463.2 MPa (alloy B-S8WA2); 352 MPa, 274.86 MPa, 2.9%, 420.86 MPa (alloy C-S8WA1); 354.8 MPa, 324.36 MPa, 1.2%, 366.54 MPa (alloy D-S8WA2); 346.5 MPa, 298.5 MPa, 1.0%, 349.6 MPa (alloy E-S8WA2). Among the HT200 alloys, alloy B in the S8WA2 (T6) heat-treated condition provided the optimum composition-heat treatment condition. The enhancement in properties is due to precipitation of ultra-fine particles of the θ-Al2Cu phase, as well as the grain refining.

For the tensile data obtained at 250 C, the HT200 alloy showed lower properties than the 319 and 356 alloys in the as-cast and solution treated conditions. The higher strengths observed in the latter alloys is attributed to the strengthening effects resulting from their higher Si content. With regard to alloy C, while the addition of Ag did not produce any improvement in strength properties of the HT200 alloy at room temperature, in the high temperature tests, the yield strength improved by about 17%.

Optimum high temperature tensile properties and Q-values for the five alloys investigated and the corresponding heat treatment conditions which provided these properties are: 281.2 MPa, 280.2 MPa, 1.97%, 325.3 MPa (alloy A-S8WA2); 307.9 MPa, 303.9 MPa, 2.3%, 361 MPa (alloy B-S8WA2); 276 MPa, 274.9 MPa, 3.2%, 351.9 MPa (alloy C-S8WA2); 309.1 MPa, 304.9 MPa, 2.8%, 375.6 MPa (alloy D-S8WA1); 282.6 MPa, 281.5 MPa, 2.4%, 338.7 MPa (alloy E-S8WA1). Alloy B in the S8WA2 (T6) heat-treated condition is considered the optimum alloy composition/heat treatment condition.

As alloy B gives the best overall performance across the range of heat treatments employed with respect to the HT200 alloys at both room and elevated temperatures, with properties comparable to those of 319 and 356 alloys, it may be considered as a very suitable alternate for use in automotive applications.

ACKNOWLEDGEMENTS

By the grace of Almighty God, I have been endowed the enthusiasm and strength to complete this work.

I would like to thank with feelings of gratitude my advisor Prof. Fawzy Hosny Samuel for his guidance, support, providing me with every opportunity, and believing in me in all aspects of my study from the very beginning to the final stages. His advice and guidance throughout this work have been of immeasurable help.

I must express my very profound gratitude and appreciation to Prof. Agnes-Marie Samuel, research professor at Université du Québec à Chicoutimi (Canada), for her continuous guidance, valuable assistance, and mentoring with kindness during the entire duration of the study, in addition to editing the thesis. Thank you for your care and gentleness.

I would also like to thank Dr. Salvador Valtierra of Nemak and Dr. Herbert Doty of General Motors for their encouragement and helpful comments during the course of my research.

My appreciation is extended to Dr. Mohamed Ibrahim for his technical assistance during the course of the study. Thanks are also due to Mr. Samuel Dessureault, technician at UQAC, for his help with preparation of castings and samples for metallography.

Financial support received from Natural Sciences and Engineering Research Council of Canada (NSERC), General Motors Powertrain Group (USA), and Corporativo Nemak (Mexico) is gratefully acknowledged.

Lastly but most importantly, I would like to express my heartfelt and deep gratitude to my mother Elham Morks-Girgis, my sister Youstina and my brother Arsany for their continuous encouragement, unfailing support, understanding and infinite love. I could never pay them back all their efforts, love, and all what they have done for me. This accomplishment would not have been possible without their love. Thank you all!

Abram Girgis

Table of Contents

List of Tables

Chapter 1

Chapter 2

Chapter 3

Chapter 4

Chapter 5

Chapter 6

List of Figures

Chapter 2

Chapter 3

Chapter 4

Chapter 5

Chapter 6

CHAPTER 1

DEFINING THE PROBLEM

CHAPTER 1

1 DEFINING THE PROBLEM

1.1 INTRODUCTION

By the second half of the 19th century, Aluminum became an economic competitor in engineering applications. It is the most abundant metal and the third most plentiful metallic element on earth [1] [2]. Aluminum and aluminum alloys are versatile and have many outstanding attributes that allow them to be used in a wide range of applications. These attributes include good corrosion and oxidation resistance, high thermal and electrical conductivities, high reflectivity, low density, high ductility and reasonably high strength, and relatively low cost [3].

The density of aluminum is 2.7 g/cm^3 (0.1 lb/in^3) which makes it a lightweight material. Aluminum and its alloys have the face-centered cubic (FCC) structure; that is, it is stable up to its melting point at 657 °C (1215 °F). This crystalline structure contributes in great part to the excellent formability of aluminum alloys because it contains multiple slip planes. Aluminum alloys are among the easiest of all metals to machine and form. They display a good combination of strength and ductility. They are considered among the easiest to recycle of any of the structural materials, also they are nontoxic [3]. Hence, aluminium and aluminum alloys are used in many industries and applications such as aerospace, automotive and marine. They are used in railway rolling stock, pipelines and pressure vessels,

buildings, civil and military bridging, in the packaging industry and in many other applications.

As pure aluminum is relatively ductile and weak, it is rarely used on its own, particularly in constructional applications. To increase its mechanical strength, pure aluminium can be alloyed with other elements. Included among them are silicon (Si), which increases strength and fluidity [4]; copper (Cu), which can give very high strength; manganese (Mn), which gives both strength and ductility improvements; magnesium (Mg) which enhances both strength and corrosion resistance; and zinc (Zn) which, in combination with Mg and/or Cu, improves the strength and helps in regaining some of the strength lost during welding. In addition, heat treatment is used to enhance the mechanical properties, as yield strength, toughness, hardness, of those alloys as well [5] [6].

Aluminium–copper (Al-Cu) alloy was one of the first alloys to be produced. It was around 1910 that the phenomenon of age hardening or precipitation hardening was discovered, in this family of alloys. Since then, a large range of alloys has been developed with strengths which can match that of good quality carbon steel but at a third of the weight [7]. Aluminum-copper alloys have been used extensively in wrought and cast form where strength and toughness are required [8]. These alloys are composed of a solid solution of copper in aluminum, which gives an increase in strength. However, the major part of the strength increase is caused by the formation of the copper aluminide or $CuAl_2$ precipitate. It should be present as a finely and evenly distributed submicroscopic precipitate within the grains, to gain the full benefits of this precipitate. This is achieved by solution treatment followed by a carefully controlled ageing heat treatment [9] [10]. This was the procedure adopted in the present study.

The early Al-Cu alloys contained around 2–4% of copper. This composition resulted in the alloys being so sensitive to hot shortness that for many years the 2XXX alloys were thought to be unweldable. However, increasing the amount of Cu to more than 4%, i.e., around 6% or more, markedly enhanced and improved weldability owing to the large amounts of eutectic available to back-fill hot cracks as they formed. The limit of solid solubility of Cu in Al is 5.8% at 548 °C. At ambient temperature, this copper is present as a saturated solid solution with particles of the hardening $CuAl_2$ phase as a fine or coarse precipitate within the grains or at the grain boundaries [7].

At ambient and elevated temperatures, these alloys exhibit high strength and hardness. Many alloys containing 2 to 8 wt% Cu have been developed. By using grain refining and heat treatment, and controlling the impurities, excellent strength and ductility are achieved. This combination of tensile properties and ductility provides exceptional toughness. This type of alloys is susceptible to solidification cracking and to interdendritic shrinkage. Examples of foundry techniques used to avoid these conditions are controlling the mold temperature and using grain refiners. This part is covered in the scope of this study under the section Hot Tearing. One of the drawbacks of Al-Cu alloys is that they are less resistant to corrosion [8] [11] [12].

Aluminum-copper alloys are used widely in aerospace applications, structural items, highly stressed parts, heavy goods vehicle wheels, duty forgings, cylinder heads and pistons. This study focuses on Al-Cu alloys, specifically a new alloy called HT200 that contains ~ 6.5wt% Cu. A detailed account of the problem investigated in this study, and the objectives formulated to address it are presented in the following sections.

1.2 DEFINITION OF THE PROBLEM

Over the years, a large number of alloys have been developed to meet the requirements of different application areas. Accordingly, new alloys and heat treatments continue to be developed as new needs arise. For example, in the automotive industry, lightweight aluminum casting alloys are replacing ferrous-based materials for engine heads and blocks. Not all producers use the same specific alloys, and alloys vary from producer to producer, but in general, heads are made from AA319 alloy and its variants, and blocks are being made from AA380 and its close variants [13].

Aluminum-copper alloys are the main alloys investigated in this study. As mentioned previously, adding Cu to Al alloys enhances the mechanical properties, but at some cost to ductility and corrosion resistance. With heat treatment, very good mechanical properties can be obtained. Adding grain refiners also increases the strength and decreases the hot tearing susceptibility [14].

In this study, a new aluminum Al-Cu based alloy, coded HT200, developed by Nemak, was investigated. This alloy has a relatively high Cu content of 6.5%. The mechanical properties of the proposed HT200 alloy were studied. The results were compared with those of 319 and 356 alloys, two aluminum alloys well known for their mechanical properties and widely used in the automotive industry. The two alloys were grain refined with 0.1-0.15%Ti and modified with 200ppm Sr before being used.

Alloy HT200 is the base alloy under investigation. From this base alloy, two other alloys were prepared, by adding certain alloying elements in each case, namely, HT200 with 0.15%Ti and 0.15%Zr additions, and HT200 with 0.15%Ti, 0.15%Zr and 0.5%Ag additions.

Titanium and zirconium were added as grain refiners. Silver was added as it accelerates the aging response and reduces the risk of stress corrosion [8].

Thus, five alloys were investigated in this study. For simplicity, they were coded as A, B, C, D, and E. The alloys together with their codes are listed in Table 1-1.

Table 1-1: Alloys used in this study.

Alloy Code	Alloy and Additions
Alloy **A**	HT200 (Al-6.5%Cu based alloy)
Alloy **B**	HT200 +0.15% Ti + 0.15%Zr
Alloy **C**	HT200 +0.15% Ti + 0.15%Zr + 0.5%Ag
Alloy **D**	319 +0.1-0.15%Ti + 200ppm Sr (0.02%)
Alloy **E**	356 + 0.1-0.15%Ti + 200ppm Sr (0.02%)
Ti: added as Al-5%Ti-1%B master alloy Zr: added as Al-15%Zr master alloy Ag: added in the form of pure metal Sr: added as Al-10%Sr master alloy	

The study focused on (i) determining the mechanical properties of the HT200 base alloy (Alloy A), and then (ii) investigating different techniques to further improve the mechanical properties of the alloy. Grain refinement and heat treatment were selected for this purpose. Grain refinement was done using Ti and Zr additions, while heat treatment conditions were varied using T6 and T7 tempers.

1.3 OBJECTIVES

The present study was undertaken to investigate the mechanical properties of the HT200 alloy (Alloy A) and to determine how these properties could be further improved

using grain refinement and heat treatment. The principal aim was to optimize the alloy composition and heat treatment conditions to provide optimum properties, and to compare them with the widely used 319 and 356 alloys to determine its suitability as a good alternative.

The main objectives of the study therefore were as follows:

- Carrying out thermal analysis of the alloys and obtaining the solidification curves to study the solidification behavior.

- Examining the microstructural features of the alloys to acquire a better understanding of the phases and intermetallics present in the structure, and the precipitates formed and their identifying characteristics and evolution during controlled exposure at different temperatures and times.

- Investigating the hot tearing susceptibility of the proposed base alloy A and its other versions, alloys B and C, and comparing the results with those of the reference alloys D and E.

- Heat treating the as-cast alloys using 12 different heat treatment conditions for alloys A, B and C, and 6 conditions for alloys D and E (these conditions being known to give better results for these two alloys). The aim is to obtain the optimum heat treatment conditions that give the best mechanical properties for alloys A, B and C.

- Running tensile tests on the as-cast and heat-treated alloys A, B, C, D and E at ambient temperature (25°C), to obtain their tensile properties (UTS, YS, El %) for each heat treatment condition.

- Running tensile tests on the as-cast and heat-treated alloys A, B, C, D and E at elevated temperature (250°C), to obtain their tensile properties (UTS, YS, El %) for each heat treatment condition.

- Compare the mechanical properties of alloys A, B, C, D, and E, for the different conditions, with those of the base alloy A in the as-cast condition, in order to (i) investigate the influence of the additives on the mechanical properties of the base alloy, and (ii) compare the mechanical properties of alloys A, B, and C with the reference alloys D and E. Comparisons are to be made using both ambient temperature (25°C) and elevated temperature (250°C) results.

- Analyze alloy quality using quality index Q values calculated from the tensile test data obtained for the five alloys at the two testing temperatures, in order to recommend the optimum alloy composition/heat treatment condition for HT200 alloy, and compare the Q values with those of the reference alloys D and E.

- Determine suitability of the HT200 alloy as a good alternative to 319 and 356 alloys.

1.4 STRUCTURE OF THE THESIS

This thesis is presented in seven chapters.

– Chapter 1 presents an introduction to the study undertaken in this research, a definition of the problem addressed, and the objectives to be achieved.

– Chapter 2 presents the literature review of the topic of this thesis.

- Chapter 3 describes the experimental procedures and testing methods that were employed in this research.

- Chapter 4 discusses the microstructural characterization of the alloys under study as well as their susceptibility to hot tearing.

- Chapter 5 presents the room temperature mechanical properties of the alloys.

- Chapter 6 presents the elevated temperature mechanical properties of the alloys.

- Chapter 7 presents conclusions, and recommendations for future work.

A list of references is provided at the end of the thesis.

CHAPTER 2

SURVEY OF THE LITERATURE

CHAPTER 2

2 SURVEY OF THE LITERATURE

2.1 INTRODUCTION

The mechanical properties of cast aluminum alloys can be enhanced by means of heat treatment and alloying elements. This chapter will present and discuss previous studies on solidification and heat treatment of aluminum-copper alloys, the alloys used in the present research study, and their effects on mechanical properties. As the alloy is primarily identified by its chemistry, the direct effect of alloying elements on the mechanical properties will be discussed in particular. Studies on the hot tearing susceptibility of Al-Cu alloys will also be presented. Finally the estimation of the quality of a casting alloy by quality index charts is presented.

2.2 ALUMINUM ALLOYS DESIGNATION SYSTEM

Aluminium alloys may be divided into two broad classes, cast aluminum alloys and wrought aluminum alloys, depending on their method of fabrication. These two classes can be further subdivided into families of alloys based on chemical composition and also on temper designation. Temper designations are used to identify the heat treatment condition of the alloy or the amount of cold work the alloy has undergone. [7]. Wrought alloys are those mechanically formed by rolling, forging, and extrusion into useful products. Cast alloys are those cast directly to the near final finished shape. The wrought alloys designation system

has four digits. This study is dealing with casting alloys whose designation system has four digits as well but it differs from the wrought alloys system in that a decimal point is used between the third and fourth digits to make clear that these are designations to identify alloys in the form of castings or foundry ingot [2].

In the casting alloy designation system, the various digits convey information about the alloy:

- The first digit indicates the alloy group or series the alloy belongs to. The alloy group is determined by the alloying element present in the greatest mean percentage, as seen in 2xx.x through 8xx.x alloys, as shown in Table 2-1.

- The second and third digits identify the specific aluminum alloy in the series or in the case of the 1xx.x series, they indicate the minimum percentage of aluminum [15] [16].

- The fourth digit, or the digit to the right of the decimal point, indicates the product form: 0 indicates casting piece is the final product and 1 or 2 when it is an ingot [15] [16].

- A modification of the original alloy or an impurity limit is indicated by a capital letter before the numerical designation (e.g., 356 and A356, or 319 and B319) [2] [17].

Table 2-1: Cast Alloy Designation System [2].

Alloy	Main Alloying Element
1xx.x	Pure aluminum, 99.00% maximum
2xx.x	Copper
3xx.x	Silicon, with added copper and/or magnesium
4xx.x	Silicon
5xx.x	Magnesium
7xx.x	Zinc
8xx.x	Tin
9xx.x	Other elements
6xx.x	Unused series

2.3 MICROSTRUCTURE

The chemical composition and the cooling rate control the microstructure of Al-Cu alloys. According to Bäckerud *et al.* [18], solidification of Al-Cu alloys starts by the development of a dendritic network then a eutectic reaction follows in the interdendritic regions thereby the eutectic Al_2Cu is formed in combination with the remaining aluminum. Thus, the microstructure of Al-Cu alloys consists mainly of α-A1 and the primary Al_2Cu phase. Some alloying elements may be added to Al-Cu alloys to improve their mechanical properties, such as Mg, Si, Mn, and Fe. Due to the addition of these elements, much more complex intermetallic compounds form. Some of these complex intermetallic compounds are insoluble, such as the β (Al_5Fe_2Si), π ($Al_8Mg_3FeSi_6$), and α-iron ($Al_{15}(Mn,Fe)_3Si_2$) phases,

which are introduced by iron addition. Iron intermetallics are harmful to mechanical properties as they are very brittle. Molinar and Cisneros [19] [20] found that by applying plastic deformation, stresses are imposed by the matrix on such intermetallic particles as α, β-iron and Al_2Cu. When these stresses reach the critical level of particle strength, the particles experience cracking, as an intraparticle micro-crack or void is formed and continues to grow, as illustrated in Figure 2-1. The presence of Fe-intermetallic compounds such as β-iron (Al_5FeSi) results in the formation of porosity, as they prevent the liquid metal feeding by blocking the interdendritic liquid-metal channels [21] [22] [23].

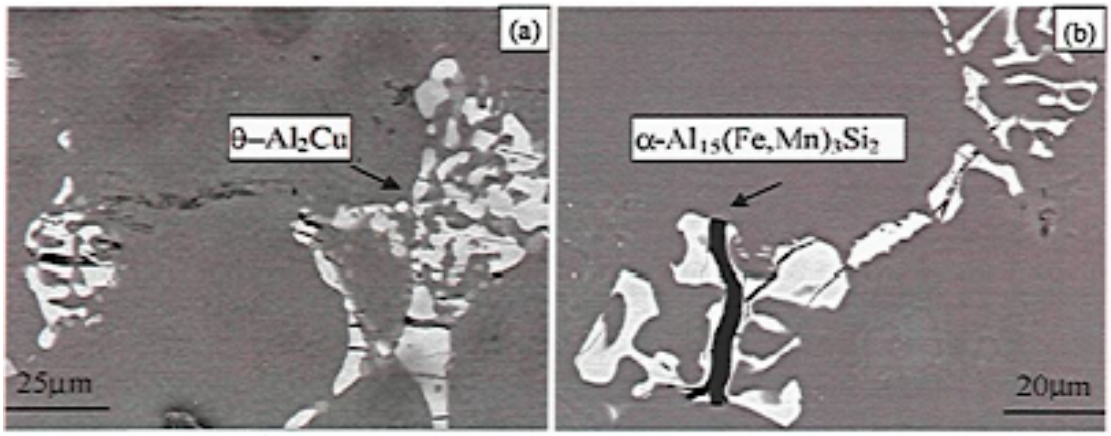

Figure 2-1: SEM micrographs of a region adjacent to the fracture surface of tensile specimens showing cracking of (a) θ-Al_2Cu intermetallics and (b) α-($Al_{15}(Mn,Fe)_3Si_2$) intermetallics. (A319 alloy) [20].

Porosity provides stress concentration sites as well as it facilitates crack propagation. Consequently, a high density of porosity causes a deterioration in the mechanical properties of the alloys. The effect of Mn addition on Al-Si-Cu casting alloys has been studied by Hwang *et al* [24]. They reported that the Mn is added mainly to improve the mechanical properties by transforming the elongated β-iron into the more compacted α-iron, which is less harmful. As for the Mg addition, if it occurs in a proportion greater than 0.2%, then,

together with Si, it forms Mg_2Si and the quaternary Q-phase, $Al_5Mg_8Cu_2Si_6$, which is formed in the last stages of solidification in combination with the Al_2Cu phase, as can be seen in Figure 2-2. If the level of silicon addition exceeds its solubility, eutectic silicon particles will be formed, as can be seen in Figure 2-3. Hwang *et al*. reported that under load application, primary silicon particles act as crack initiators, and hence have a harmful effect on the mechanical properties.

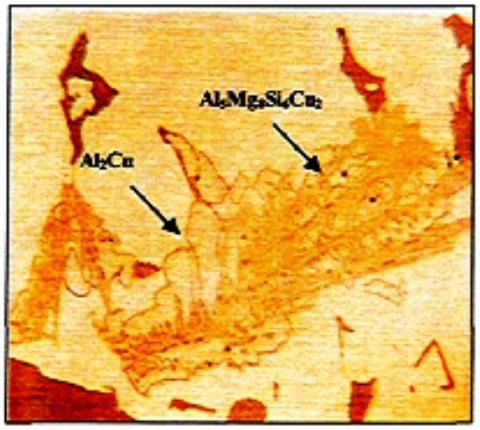

Figure 2-2: Microstructure of B319.1 alloy at cooling rate of 0.3°C/s, showing the $Al_5Mg_8Si_6Cu_2$ phase grown out from Al_2Cu particles [18].

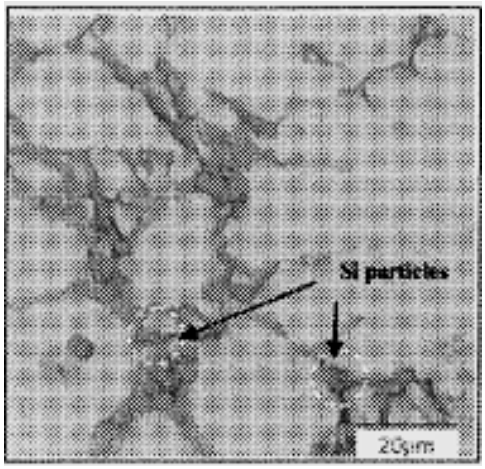

Figure 2-3: Microstructure of as-cast Al-4,5wt%Cu-2wt%Si alloy [25].

As mentioned previously, the microstructure of Al-Cu alloys is affected by the cooling rate. The dendrite arm spacing, size and distribution of the intermetallics, porosity, grain size, and morphology are the main microstructural features that are affected by the cooling rate. It has been reported by several researchers that the dendrite arm spacing (DAS) decreases as the cooling rate increases, [26] [27] [28], as illustrated in Figure 2-4. The equation $DAS = AV_c^{-n}$, is used in industry to determine the effect of cooling rate on DAS, where A is an alloy-dependent parameter, n is a parameter equal to 0.33 for aluminum alloys, and V_c is the cooling rate. Reducing the DAS leads to grain size refining, as well as homogeneous distribution of the intermetallic compounds; the refining and the homogeneous distribution reduces diffusion distances. This leads to an easier dissolution of the intermetallic compounds during solution heat treatment, reducing composition gradients, hence producing a higher degree of supersaturated solid solution. Consequently, a greater age-hardening response can be obtained [24] [29].

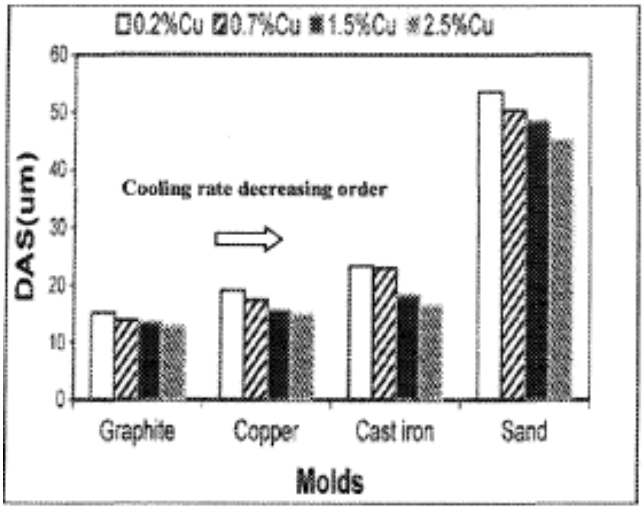

Figure 2-4: Variation of DAS of 319 alloys containing different levels of Cu and poured in different [27].

Argo and Gruzleski [30] and Emadi and Gruzleski [31], reported that as the DAS gets smaller, the shrinkage porosity is reduced since interdendritic feeding distances become shorter, whereby this type of porosity becomes less. Accordingly, with smaller dendrite arm spacings, improved mechanical properties of the alloy can be obtained.

2.4 HEAT TREATMENT PROCESS

There are several techniques to improve and enhance the mechanical properties of aluminum alloys. Strain hardening (or cold working) and heat treatment are two examples of these strengthening mechanisms. It should be noted that there are heat-treatable alloys, for which heat treatment is used to increase strength, and non-heat-treatable alloys, which depend primarily on cold work to increase strength. This section focuses on heat treatment of aluminum alloys, which generally refers to any of the heating and cooling operations that are performed for the purpose of increasing strength and hardness of precipitation-hardenable or age-hardenable aluminum alloys. [32]. Improving the mechanical properties is achieved by modifying the microstructure of the heat treatable alloy by optimizing certain parameters used in the heat treatment process which include temperature, time, heating and cooling rates [17].

The strengthening mechanism for heat-treatable aluminum alloys is termed precipitation hardening or age hardening. This mechanism is mainly based on the concept of the level of solid solubility of an alloying element (solute) in the matrix (solvent) depending on the temperature. This means that the solid solubility increases at a high temperature and vice versa. The strengthening is achieved by heating the alloy to a temperature that is slightly below the eutectic temperature or to a single-phase region for a sufficient period of time such that the solute atoms dissolve completely in the matrix. This step is commonly known as solution heat treatment or solutionizing. Following this step, the alloy is rapidly cooled or quenched to room temperature using a proper cooling medium in order to form a supersaturated solid solution at ambient temperature. The final step in this process is aging, during which fine precipitates begin to form, and age hardening occurs. While precipitation

of solute atoms may occur at room temperature (termed natural aging), aging is commonly carried out by heating to elevated temperatures in order to accelerate the formation of the precipitates (termed artificial aging). The response of the alloy mechanical properties to age-hardening is primarily dependent on the fraction, size, distribution, and coherency of the precipitates formed within the matrix [33] [34]. The three steps of the heat treatment process for aluminum alloys are illustrated in Figure 2-5.

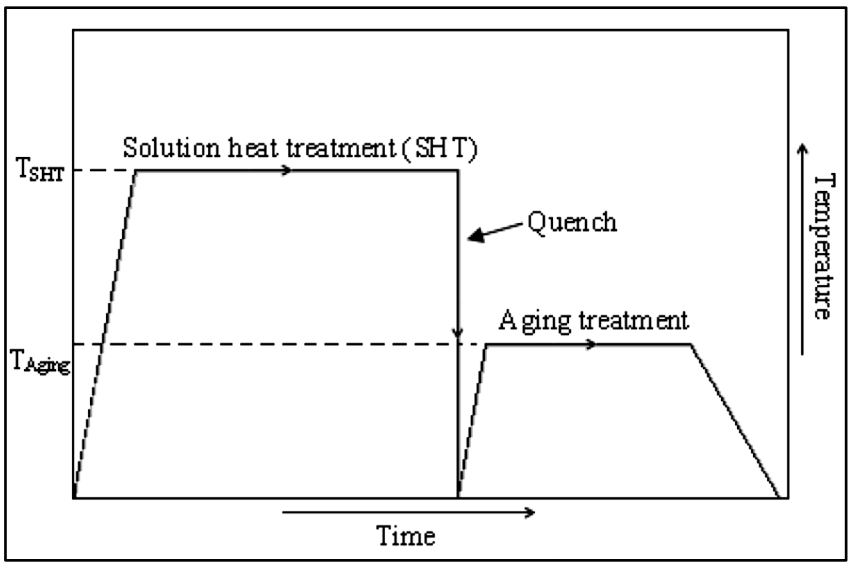

Figure 2-5: The three steps of the heat treatment process [35].

The amounts of soluble alloying elements contained in heat-treatable alloys exceed the equilibrium solid solubility limit at room and moderately higher temperatures. At the eutectic temperature, the amount of soluble alloying elements present may be less or more than the maximum that is soluble. These two cases and the fundamental solution-precipitation relationships involved are depicted in Figure 2-6, which shows a portion of the Al-Cu equilibrium diagram, with two selected alloys, Al-4.5% Cu, and Al-6.3% Cu, represented by the vertical dashed lines (a) and (b), respectively. These two compositions are

close to the commercial alloys 2025 and 2219, but generally the principles also apply to other heat treatable alloys. [36]

For the Al-4.5% Cu alloy, it can be seen from Figure 2-6 that, regardless of the initial structure, when solution heat treating is done by holding the alloy at 515 to 550 °C until equilibrium is reached, it causes the copper to go completely into solid solution. At temperatures below 515 °C, the solid solution becomes supersaturated, and the excess solute over the amount actually soluble at the lower temperature precipitates. With decreasing temperature, the degree of supersaturation increases and, consequently, the driving force for precipitation increases. The precipitation rate also depends on atom mobility, which is reduced as the temperature decreases. Precipitation enhances the mechanical properties, which depend not only on whether the solute is in or out of solution but also on specific atomic arrangements, as well as on size and dispersion of any precipitated phases.

Regarding the Al-6.3% copper alloy, which exceeds the maximum content soluble at the eutectic temperature, it can be seen in Figure 2-6 again, that when heated to a temperature slightly below the eutectic temperature, it consists of a solid solution plus additional undissolved $CuAl_2$. In this case, the solid solution has a higher copper concentration than that of the Al-4.5%Cu alloy, if the temperature exceeds 515 °C. This, in turn, provides greater driving force for precipitation at lower temperatures and increases the magnitude of property changes that may occur. Due to the $CuAl_2$ that is not dissolved at the high temperature, while remaining essentially unaltered through heating and cooling, the overall strength level rises noticeably.

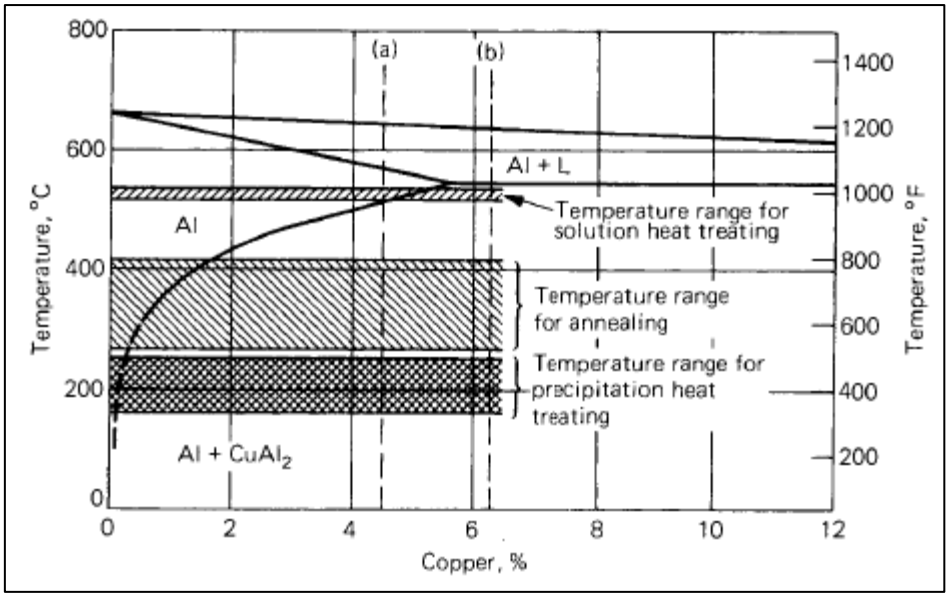

Figure 2-6: Portion of Al-Cu binary phase diagram. Temperature ranges for solution heat treating, annealing and precipitation heat treating are indicated. The range for solution treating is below the eutectic melting point of 548°C at 5.65 wt% Cu [32] [37].

To minimize having precipitation of the solute atoms as coarse and incoherent particles, the solid solution formed at a high temperature can be kept in a supersaturated state by quenching or cooling with sufficient rapidity. Controlled precipitation of fine particles at room or elevated temperatures after the quenching operation is used to enhance the mechanical properties of the heat-treated alloys. After quenching, mechanical properties of most alloys change at room temperature and it may start immediately or after a period of time; this is called “natural aging”. Whereas by heating above room temperature, precipitation can be accelerated in these alloys, and consequently their strengths increase; this operation is called “artificial aging” or “precipitation heat treating”.

A list of the common standardized heat treatments used for aluminum alloys is shown in Table 2-2 [8].

Table 2-2: Designations and practices of common heat treatments used for aluminum alloys [35]

Treatment	Solutionizing	Quenching	Aging
T4	Yes	Yes	Room Temperature only
T5	No	No	Elevated Temperature
T6	Yes	Yes	Elevated Temperature (Increased strength)
T7	Yes	Yes	Elevated Temperature (Dimensional stability)

Heat treatment starts with solution heat treatment that is achieved by heating cast or wrought products to a suitable temperature, holding at that temperature long enough to allow constituents to enter into solid solution, followed by quenching or cooling rapidly enough to hold the constituents in solution; the final step is aging, in which precipitation of solute atoms occurs, either at room temperature (natural aging) or at elevated temperature (artificial aging). The T6 and T7 heat treatments are commonly used for Al-Si and Al-Cu alloys in industry. They comprise solution heat treatment at a high temperature followed by rapid quenching to ambient temperature, and finally either natural aging at room temperature or artificial aging at higher temperatures [36].

As an example, Figure 2-7 and Figure 2-8 present schematically the precipitation hardening process, and the steps followed in carrying out the T6 heat treatment.

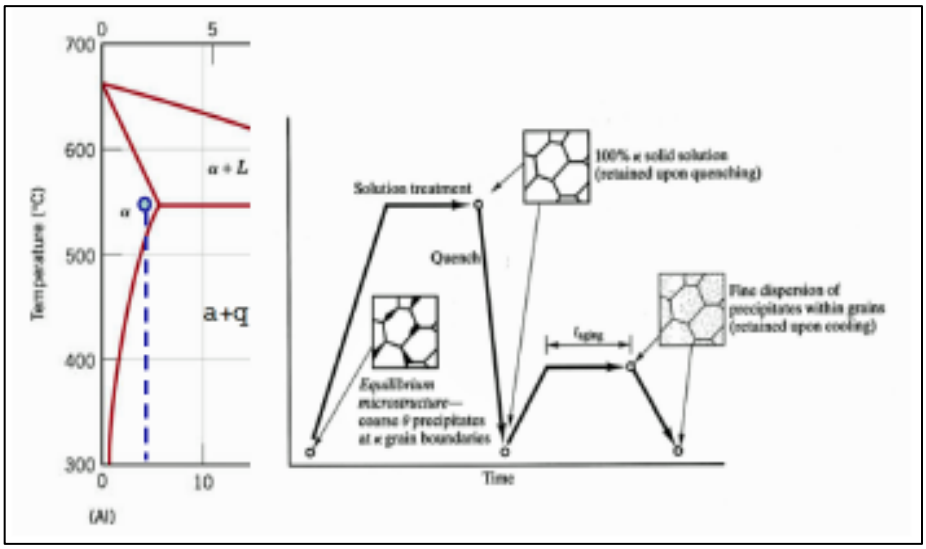

Figure 2-7: Illustration of precipitation hardening treatment [38].

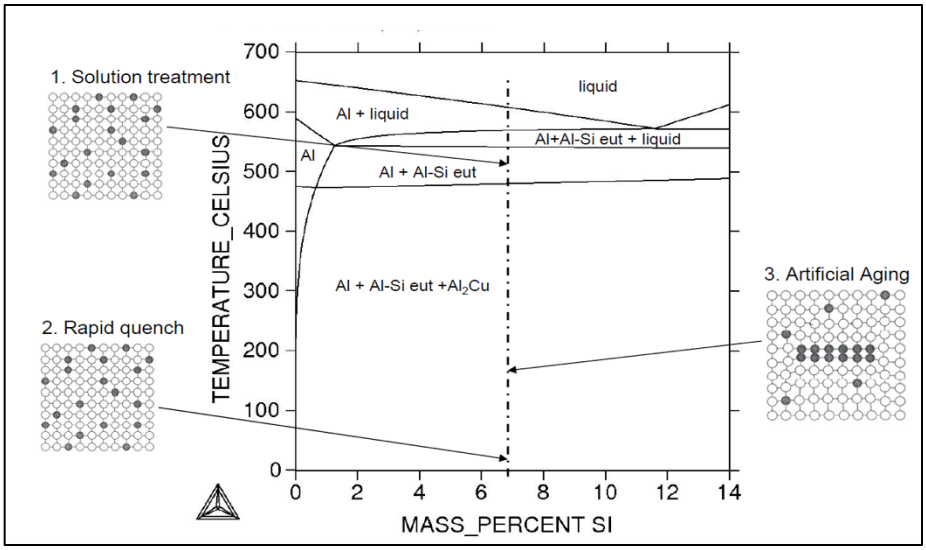

Figure 2-8: T6 heat treatment process [39].

The presence of Cu and Mg are known to improve the age-hardening tendency of aluminum alloys. Cáceres *et al.* [40] studied the effects of Si, Cu, Mg, Mn, and Fe, in addition to that of solidification rate on the mechanical properties of Al-Si-Cu-Mg alloys. They found that the increase in strength and decrease in ductility observed was related to the increase in the Cu and Mg content; whereas a detrimental effect on both strength and ductility was

observed by increasing the Fe content. They also reported that the content of Cu and Mg defines the alloy response to age-hardening, which depends on the volume fraction of the Cu-rich and Mg-rich intermetallic phases obtained [40].

The three steps for achieving precipitation strengthening in aluminum alloys through heat treatment for are reviewed in the subsections that follow.

2.4.1 SOLUTION HEAT TREATMENT

The objective of solution heat treatment is to achieve the maximum amount of hardening solutes such as Cu, Si, Mg or Zn in solid solution in the aluminum matrix. That is, to obtain a homogeneous supersaturated solid solution at elevated temperatures, by dissolving the existing phases in the as-cast structure into the solid solution; such phases are θ-Al_2Cu, β-Mg_2Si, Q-$Al_5Cu_2Mg_8Si_6$, π-$Al_9FeMg_3Si_5$ and β-Al_5FeSi. This makes the supersaturated solid solution like a reservoir of the strengthening precipitates. When the optimum solutionizing temperature and time are used, θ-Al_2Cu and β-Mg_2Si phases can be easily dissolved, whereas other phases, if present, are harder to dissolve; for example, the π-$Al_9FeMg_3Si_5$ phase is harder to dissolve due to the limited diffusivity of Fe in Al [34] [41] [42].

The solution treatment is controlled by the solution treating temperature and time. The temperature required for solution heat treatment is determined according to the alloy composition and solid solubility limit. However, it must be kept lower than the melting point of the existing phases in the as-cast structure to avoid incipient melting of these phases. For

some alloys, the eutectic temperature is the limit at which the maximum amount is soluble. Consequently, the solution treatment temperature for such alloys should be limited to a safe level, slightly below the eutectic temperature to avoid overheating and incipient or partial melting. Regarding the time required for solution heat treatment, it depends on the chemical composition of the alloy, the solution temperature, structural coarsening and casting procedure. It must be sufficient to ensure a uniformly homogeneous structure. A compromise between the mechanical properties required, alloy quality and economic efficiency should be made in deciding the solution treatment time [43] [44].

As for alloys with high Cu content, the solutionizing time must be carefully selected to allow maximum dissolution of the θ-Al_2Cu phase, as it is hard to achieve complete dissolution of this phase. Two points should be kept in mind while deciding the solution treatment time: the economic costs of long solution treatments, as well as the mechanical properties, which may deteriorate due to the formation of secondary porosity and coarsening of the microstructural constituents. [41] [45].

Some researchers have reported controversial conclusions regarding the solution treatment temperatures of Al-Cu alloys. Solution treatment at a temperature of 495°C or lower is preferred to avoid incipient melting of the Cu-rich phase, which can lead to overall deterioration in the mechanical properties. However, this range of temperatures is not sufficient either to maximize the dissolution of the Cu-rich phase or to modify the eutectic silicon morphology [46] [45]. Selecting the conservative temperature of 495°C for solution treating Al-Si-Cu-Mg alloys is still preferable, in order to avoid incipient melting as far as possible [47] [48].

2.4.2 QUENCHING

The next step in the heat treatment process is quenching. The cooling rate must be fast enough that the second phase does not have time to precipitate. If the second phase or the solute atoms precipitate in this step on grain boundaries or dispersoids and decrease vacancies, they will not be able to contribute to further strengthening in the subsequent age hardening treatment. [36]. The objective of quenching is therefore to preserve the supersaturated solid solution formed by rapidly cooling to some lower temperature, usually near the room temperature. This retains the solute atoms in solution and blocks them in the positions where they got to at the high temperature during solution treatment, and also maintains as many vacancies as possible within the lattice structure. These vacancies act as potential sites for the precipitates that will form in the subsequent step during aging treatment [44], and assist in promoting the low temperature diffusion required for zone formation.

If the cooling rate is too slow, retaining the precipitates in solution will fail. They will form on the grain boundaries as coarse particles that will have a very limited effect on mechanical properties, as they will not contribute to the subsequent strengthening. Consequently, the mechanical properties will remain close to those of an annealed metal or product. [7].

Generally, rapid quenching rates provide high strength and toughness and they improve resistance to corrosion and stress-corrosion cracking. However, the degree of distortion that occurs during quenching and the magnitude of residual stresses that develop in the products may increase with the rate of cooling. Therefore, an optimum quenching rate should be selected [36].

Quenching rate depends on the initial temperature of the solution-treated alloy/product, the final required microstructure and mechanical properties, and the alloy chemical composition. If the quenching rate is sufficiently fast to avoid the formation of precipitates during cooling, a final structure of finely distributed solute atoms within the matrix will be obtained [8].

In aluminum alloys, the cooling rate should be sufficiently high in the temperature range of 450°C to 200°C (critical temperature range), as within this range the precipitates may form rapidly due to the high level of supersaturation and the high diffusion rate within this range. At temperatures higher than this range, lower levels of supersaturation are obtained. At temperatures lower than this range, the diffusion rate is very low [49].

Quenching media in aluminum alloys include water, polymer solution, and brine solution. Despite the fact that water is frequently used as the quenching medium for aluminum alloys, Mohamed and Samuel [35] reported that water quenching can lead to distortion, residual stresses, and cracking. Therefore, temperatures between 60 and 70°C are recommended for water quenching to decrease the negative effects on the properties of cast aluminum alloys.

2.4.3 AGE HARDENING

Age hardening is the final stage in the heat treatment of aluminum alloys, after solution treatment and quenching. Looking at microstructures which have two or more phases present, there are a number of ways in which the phases can form. This depends on the relative amounts, size and shape of the phases, and whether the minor phase is dispersed within the grains or is present on the grain boundaries. The process by which the phases form is called *precipitation*, which is both temperature and time controlled [7].

Precipitation hardening or age hardening involves the development of coherent strengthening precipitates within the matrix. Generally, aging improves the tensile strength, reduces residual stresses, and results in stabilization of the microstructure. The time and temperature in an aging treatment play a major role in determining the mechanical properties obtained. Temperatures used to accelerate the precipitation process for Al alloys are generally within the range of 90-260°C [35].

The microstructure of a precipitation-hardenable alloy can be precisely controlled to give the desired mechanical properties. A complex sequence of time-dependent and temperature-dependent changes is involved in the age hardening of an alloy. First of all the metal is heated to a high temperature that is sufficient for the second phase to go into solution. Then the metal is quenched or rapidly cooled. The cooling rate must be fast enough that the second phase does not have time to precipitate. The second phase is retained in solution at room temperature as a *supersaturated* solid solution which is *metastable*. Then by *aging*, heating the alloy to a low temperature, the second phase precipitates. This allows atoms to diffuse and very fine precipitates begin to form. These precipitates are *coherent*, the lattice

is still continuous but distorted and this grants the alloy very high tensile strength, but accompanied by a drop in ductility. If the aging takes place at too high temperature or heating is held for longer time the alloy begins to *overage*, and the precipitate coarsens. Accordingly, the tensile strength drops whereas ductility increases. Allowing the over ageing process to continue results in getting the mechanical properties of the alloy to match those of the annealed structure. The heat treatment cycle and its effects on structure are displayed in Figure 2-9.

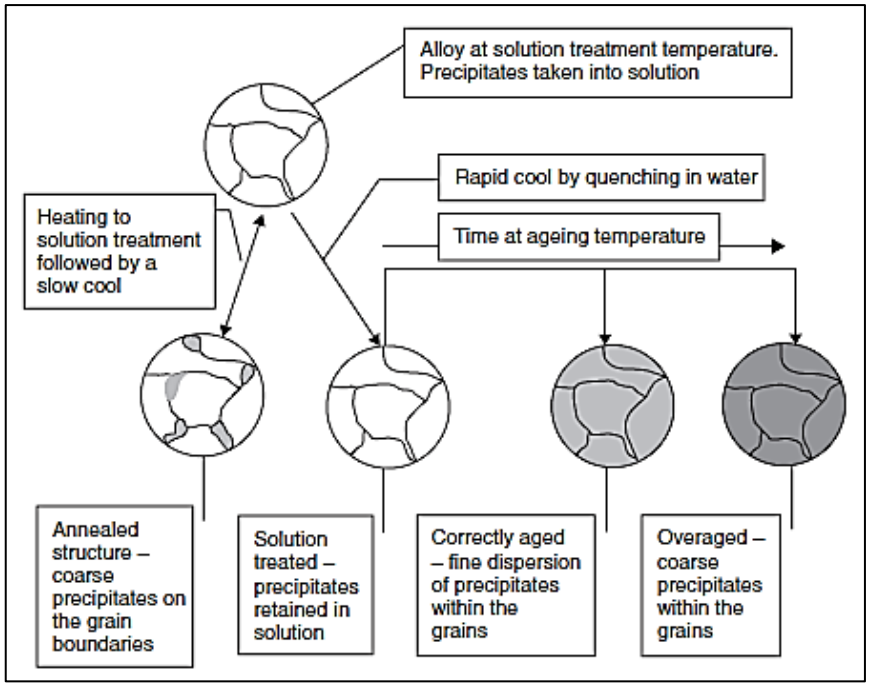

Figure 2-9: The solution treatment and age-(precipitation) hardening heat treatment cycle [7].

Generally, in aluminum alloys, the equilibrium precipitates are not formed at the beginning of the aging treatment, rather they are formed through a sequence of different forms of precipitates which occur successively during the treatment [50]. After solution treatment and quenching, the solute atoms, which exist in the supersaturated solid solution, SSSS, start to form clusters of atoms known as Guinier-Preston or GP zones. The solute

atoms in these GP zones consist of ordered groups, and they are coherent with the lattice structure and dispersed within the matrix. Usually these atoms have different sizes than those of the lattice structure of the aluminum matrix; therefore distortion occurs in the lattice structure, producing coherency-strain fields, which leads to a significant improvement in strength. These GP zones are metastable and they dissolve later in the presence of a more stable phase. As the aging treatment progresses, the GP zones dissolve, and metastable coherent or semi-coherent precipitates start forming. These precipitates continue to grow by diffusion of atoms from the SSSS, which results in achieving maximum or peak strength. As aging continues further, the metastable coherent precipitates later become totally incoherent. In this condition, the opposition of the precipitates to dislocation movement is reduced, which in turn leads to a consequent reduction in strength [50] [34]. The time needed for this sequence to complete depends on the chemical composition of the alloy, its thermal history, and the artificial aging temperature employed.

The main strengthening precipitates in Al-Si-Cu alloys are those of the θ-Al_2Cu phase [34] [51]. The sequence of forming these precipitates is as follows:

$$\alpha\text{sssss} \rightarrow \text{GP zones} \rightarrow \theta'' \rightarrow \theta' \rightarrow \theta\ (Al_2Cu)$$

It starts by clustering of Cu atoms which are formed from decomposition of the supersaturated solid solution. At room temperature, these clusters appear homogeneously, forming GP zones that are considerably enriched in solute. These GP zones exist as thin disks with a diameter of approximately 3-5 nm. As the time goes further, the GP zones increase in number, however, the size remains almost constant. By raising the aging temperature to above 100°C, the GP zones start to dissolve and form particles of θ'' precipitates. The θ''

fine particles nucleate uniformly and coherently with the matrix lattice structure. Extensive coherency-strain fields are developed due to the high degree of coherency, which leads to a significant increase in the peak strength of the alloy. The formation of θ'' precipitates lead to distortion in the lattice structure in, and around, their vicinity. These distortions impede the dislocation movements during plastic deformation, leading to high strength and hardness [17] [33] [51]. As aging continues, θ'' precipitates dissolve, later forming θ' phase which is plate-like in shape. As the precipitates of θ' grow, they lose coherency with the matrix, leading to reduction in the lattice distortion and consequently a decrease in strength. Further aging causes the formation of equilibrium θ-Al_2Cu particles. These equilibrium precipitates are totally incoherent with the matrix, relatively large in size, and have a coarse distribution in the matrix. These characteristics lead to further reduction in the strength. A schematic diagram of the strength or hardness as a function of the logarithm of the aging time is shown in Figure 2-10.

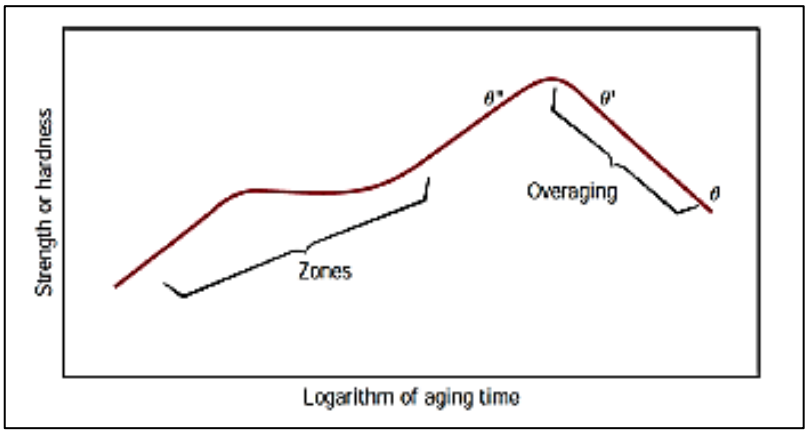

Figure 2-10: Schematic diagram showing strength and hardness as a function of the logarithm of aging time at constant temperature during aging treatment [38].

2.5 EFFECT OF ALLOYING ELEMENTS

Properties of aluminum casting alloys can be improved through the appropriate control of the different metallurgical parameters involved in the production of these castings. The addition of suitable alloying elements is one such parameter. Some alloying elements are used as grain refiners which improve the mechanical properties, reduce ingot cracking and gives better mechanical deformation characteristics. A very successful method to control the grain size is to introduce into the melt particles that nucleate new crystals during solidification. These nucleants are most commonly added in the form of aluminum master alloys [52]. It is a technique used in combination with heat treatment to further improve the mechanical properties of aluminum alloys [53]. Alloying elements affect the properties of aluminum alloys in different ways. If hard, non-ductile particles of a second phase are formed, strong barriers are produced. Edge dislocations are repelled by such particles and screw dislocations have difficulty in bypassing them [15]. The characteristics of the alloying elements that were used in this research study, and their effects on aluminum alloys are presented and discussed below.

Copper (Cu) when added to aluminum enhances and improves the mechanical properties. It increases the alloy strength and hardness in the as-cast and heat-treated conditions, at both ambient and elevated temperatures. Mostly, when the copper content is 4 to 5.5% Cu, alloys respond strongly to thermal treatment and display relatively improved casting properties. However, copper generally reduces resistance to general corrosion and in specific compositions and material conditions increases the stress corrosion susceptibility. It also reduces hot tearing resistance and increases the potential for interdendritic shrinkage. In contrast, it was found that low concentrations of Cu in Al-Zn alloys inhibit stress corrosion.

[8]. When the Cu content is close to or above its solubility limit and the alloy is heat treated so that the copper is distributed in the GP zones, it gives the best combination of strength and ductility, as the precipitation of the second phase θ contributes to the strengthening effect. The presence of a brittle network of eutectics (mostly Al-$CuAl_2$) causes impact resistance, notch toughness and fatigue resistance to decrease. On the other hand, strength at high temperature, and resistance to creep and wear increase with increasing Cu content [54] [55].

Titanium (Ti) is added as a grain refiner and is very effective in refining or reducing the as-cast grain size. Titanium is commonly added in combination with boron (TiB_2), and is often used at concentrations greater than those required for grain refinement to reduce hot tearing. If the addition results in a good dispersion of insoluble constituents, porosity and non-metallic inclusions, an improvement in mechanical properties is obtained. Also, it tends to reduce stress corrosion susceptibility [54].

When Ti is added either individually or in combination with boron to refine the grain structure of the α-Al matrix, it creates many nuclei in the melt, which encourages the formation of small equiaxed grains of α-Al, rather than the coarse, columnar grain structure that is produced in the absence of grain refinement. In Al-Si alloys such as A356 and A357, it is noticed that best results are obtained by adding 10-20 ppm of boron in the form of Al-5Ti-1B or Al-3Ti-1B rod. Whereas for Al-Cu and Al-4.5%Cu-0.5%Mn alloys, it was noticed that best results are achieved with the addition of less than 0.05% Ti and 10-20 ppm of boron added, as before, in the form of Al-5Ti-1B or Al-3Ti-1B rod. For Al-Si-Cu alloys, such as A319 (Al-3%Cu-5.5%Si) alloy, 10-20 ppm of boron provides the best results [56] [57].

Boron (B) forms borides by combining with other metals, such as AlB_2 and TiB_2. Titanium boride works as a grain refiner, as it forms stable nucleation sites that interact with active grain-refining phases such as $TiAl_3$ for grain refinement. Tool life in machining operations can be reduced due to metallic borides and they form coarse or agglomerated inclusions with harmful effects on mechanical properties and ductility. Borides also contribute to sludging, the precipitation of intermetallics from liquid solution in furnaces and troughing. Aluminum containing peritectic elements such as titanium, zirconium, and vanadium is boron treated to improve purity and conductivity in electrical applications. Boron content in rotor alloys may exceed titanium and vanadium contents to ensure either the complexing or precipitation of these elements for improved electrical performance [8] [36].

Zirconium (Zr) is generally contained in aluminum alloys in amounts from 0.1 to 0.3wt%. It is used as a grain refiner, as it reduces the as-cast grain size which improves strength and ductility [15]. Zirconium is added also to form fine coherent precipitates of Al_3Zr called dispersoids. Due to the low solubility and diffusivity of Zr in the Al matrix and also due to the low interface energy of the particles with the matrix, these coherent particles are remarkably stable upon heating and they resist coarsening. Therefore, these dispersoids effectively inhibit recrystallization and recovery during heat treatment due to their obstructive action thereby causing an increase in strength and hardness properties. For instance, a minor addition of Zr, in the amount of 0.15 wt%, can significantly improve the strength and hardness of A319 aluminum alloy in both the as-solutionized and age-hardened conditions. This hardening effect of Zr is attributed to the precipitation of the coherent coarsening-resistant Al_3Zr dispersoids during solution heat treatment [53] [58].

Silver (Ag) is only used in a limited range of Al-Cu premium strength alloys at concentrations of 0.5 to 1.0%. It contributes to precipitation hardening and reduces the risk of stress-corrosion resistance. It accelerates aging response [8]. For example, a small addition improves the strength and stress corrosion resistance of Al-Zn-Mg alloys [36].

It should be kept in mind that changes in the chemical composition and/or heat treatment aiming at improving strength or other properties can render the material too brittle for structural applications. Thus, it is important to check simultaneously what effect any changes to the microstructure would have on the material ductility and strength. Therefore, castings are evaluated using strength-ductility diagrams, known as quality index charts [54] [59] [60]. The concept of quality index Q and construction of quality charts will be discussed in section 1.7.

2.6 HOT TEARING

Aluminum-copper alloys tend to have poor castability due to their high susceptibility to hot tearing. Hot tearing, which is a common defect in such alloys, occurs during the solidification of the liquid metal. This phenomenon is also known variously as hot shortness, hot cracking, super solidus cracking, and shrinkage brittleness. It has been the subject of previous investigations as it is deleterious to mechanical properties of aluminum castings. In a solidifying casting, a macroscopic tear forms as a result of stress built up in the solidified metal. This stress arises mainly due to the volume contraction (usually 5-8%), associated with the change from liquid to solid phase in the solidifying metal, but it can get worse due to thermal contractions in the solid and/or by the constraints of the mold. Experimental measurements of hot tearing, modeling of hot tearing, and generation of fundamental properties related to hot tearing, such as strength of the mushy zone, are three approaches that have been used towards generating information about hot tearing.

Between 1914 and 1936, [61] [62] [63] studies on hot tearing showed that the ductility significantly decreases when an alloy is heated above its solidus temperature, and a liquid phase is formed. In 1946, Singer and Cottrell [64] studied the high temperature tensile properties of Al-Si alloys, their results are shown in Figure 2-11 and Figure 2-12. In Figure 2-11, which displays the strengths of ten different alloy compositions versus temperature, a similar behaviour for each alloy may be noticed. There is a smooth decrease in tensile strength until the solidus temperature is reached. At this point, the strength drops much more rapidly, to a zero value at a temperature some 5-30 degrees above the solidus. A detailed view of the test results in the semi-solid region is shown in Figure 2-12.

Comparing the results shown in Figure 2-11 and Figure 2-12 to the aluminum rich portion of the Al-Si phase diagram shown in Figure 2-13, reveals that the strength and ductility decrease at combinations of temperature and composition which place the material inside the region of two-phase (solid and liquid) equilibrium. The regions of brittle fracture are indicated by the bars drawn in this figure, as measured by Singer and Cottrell. It can be observed that in the semi-solid region, the sharp drop in strength is accompanied by almost a complete loss in ductility.

Other studies such as those of Forest and Bercovici [65], who also carried out hot tensile tests in several semi-solid commercial alloys, and Wisniewski [66], who studied fracture of Al-Cu specimens containing 1-10% liquid, confirmed the earlier results. It has been shown that hot tearing is caused by a loss of strength and ductility. Over the years, this has also been referred to as liquid metal embrittlement, or a ductile/brittle transformation.

The temperature interval for hot tearing has become important and is considered to be significant for hot tearing, based on the theory that the hot tearing temperature is higher than the solidus of an alloy. This interval, regarded as the temperature range between the solidus and a temperature higher than, but close to, the solidus, has been termed as the Critical Solidification Range (CSR), Hot Shortness Temperature Range or Brittleness Stage [67]. Many characteristics of the solidifying metal are different in this temperature range from other stages of solidification. When an alloy solidifies through its freezing range, the α-Al dendrites form a dendritic network, where solid crystals form a semi-continuous network that occurs at a temperature called the coherency temperature. The solid dendrites are surrounded by the remaining liquid as thin films. The feeding of the interdendritic regions and the accommodation of deformation of solid metal are impeded, in the presence of the

interlocking dendrites. This, in turn, gives rise to hot tears in the solidifying structure. At this stage, the relative movement of liquid and solid becomes increasingly difficult with increasing solid fraction. Stress accommodation and healing are two important phenomena that are associated with an alloy cooling through the brittle range. The amount of hot tearing can be reduced by stress accommodation and healing. Hot tearing susceptibility may be impacted by any factor that influences the extent of the brittle range [68] [69].

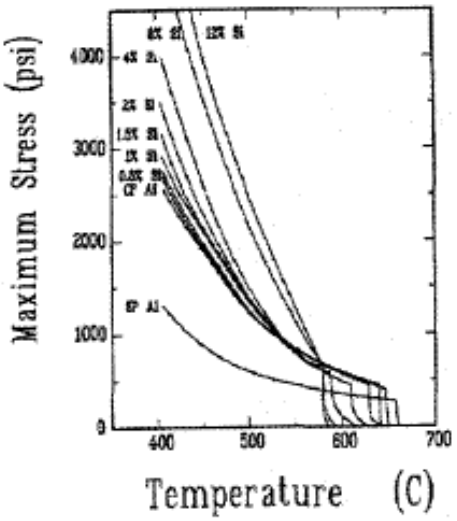

Figure 2-11: Tensile strength of Al-Si alloys at temperatures in the vicinity of the solidus (CP and SP are commercial and special pure aluminum). [64]

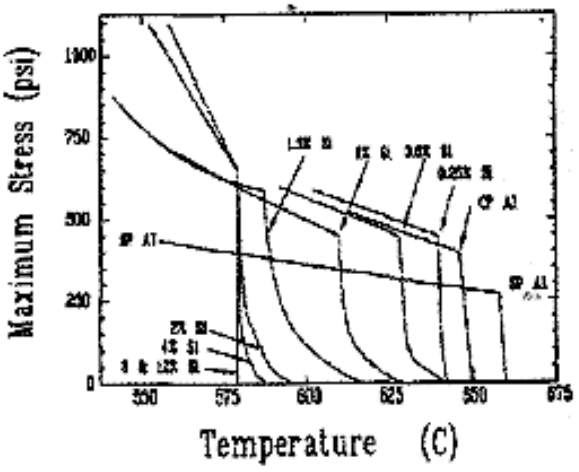

Figure 2-12: Tensile strength of Al-Si alloys. [64]

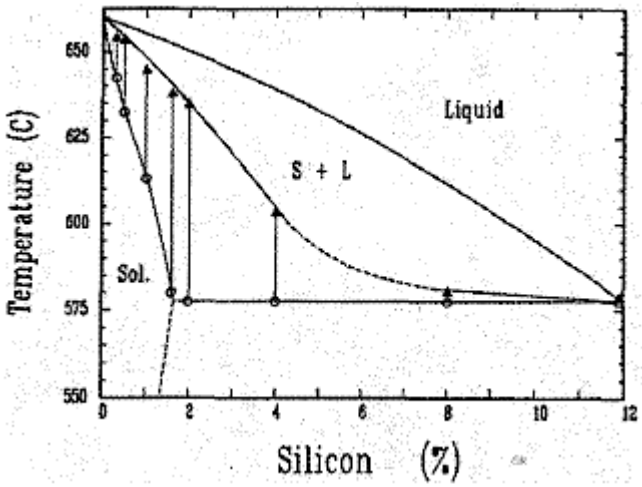

Figure 2-13: Equilibrium phase diagram of the Al-rich portion of the Al-Si system (bars indicate regions of semi-solid coherency). [64]

The reaction of the atmosphere with the metal results in forming a film that covers the surface of most liquid metals. As long as these films remain on the surface, they are harmless. However, when the surface is disturbed, they can be entrained into the bulk of the melt. The surface can be disturbed with additions to the melt, and/or when new surfaces are created, such as during pouring. These entrained films are called bi-films because of their double, film-on-film nature [70]. In aluminum alloys, they remain in the liquid and have a deleterious effect on casting quality, mechanical properties and performance of castings. There are also bi-film opening agents, such as hydrogen dissolved in liquid aluminum and intermetallics such as Fe-containing phases [71]. These bi-film opening agents are harmful as well. In order to produce high quality aluminum castings, it is important to start with a melt that is free from bi-films and bi-film opening agents. Using the best practices in filling and feeding of castings is of no use if the initial melt quality is too low that a good casting cannot be made from it. On the other hand, when surface oxide films are entrained into the

casting during melt transfers and in poorly designed filling systems, high quality melts can be damaged significantly [72].

Castings suffer from defects such as pores, inclusions and hot tears, when the initial melt quality is poor and/or if the liquid metal undergoes significant damage. Generally, pores and hot tears have been traditionally thought to be occurring as a result of metal properties. A recent research [73] has reported that the principal cause of pores and hot tears are bi-films. Moreover, hot tears are initiated by pores or inclusions, as could be observed in situ in experiments with solidifying transparent liquids. In aluminum alloys, bifilms are very deleterious and the cause of many defects. They play an important role in initiating hot tearing during solidification. Their shape, size and distribution are too complex. They act as heterogeneous nucleation sites for liquid to separate, consequently hot tearing increases.

2.7 QUALITY INDEX

The quality of aluminum casting alloys is considered to be a very important factor in selecting an alloy for a particular engineering application. Deciding upon the right alloy quality thus involves reaching a suitable compromise between numerous factors in order to achieve maximum performance with the least possible risk in combination with cost efficiency. The quality of an alloy can be understood as a combination of tensile strength and ductility values, which meet the design prerequisites for using it in a certain application. Alloy composition, solidification rate, heat treatment procedures, casting defects, and such microstructural features as grain size and intermetallic phases, are all parameters which closely affect alloy quality since they also influence the mechanical properties of the casting. [74]. In the design of aeronautical structures, the fracture toughness of materials is also taken into account [75] [76] [77].

The effects of casting conditions, metal composition, and aging time and temperature on the mechanical properties of Al-Si-Mg (356) alloys were studied by the French scientists Drouzy, Jacob and Richard. [59] [60] [78]. In 1980, Drouzy *et al.* proposed the concept of defining the quality of an aluminum alloy by a numerical value, Q, which correlates its mechanical properties. They defined the quality index Q for A356 and A357 casting alloys, based on their tensile test data of Al-7wt%Si-Mg alloys containing different Mg contents and subjected to different heat treatments. The concept was subsequently developed by other researchers in different forms, to evaluate the mechanical properties of other series of cast aluminum alloys used in aerospace and automotive applications.

2.7.1 QUALITY INDEX (Q) PROPOSED BY DROUZY ET AL.

The quality of aluminum alloy castings may be defined using numerical values which correlate their mechanical properties. [78]. The quality of an aluminum alloy may be defined by the equation:

$$Q = UTS + d \log (\%El) \qquad (1)$$

where Q is the quality index in MPa; UTS refers to the ultimate tensile strength in MPa; $\%El$ refers to the percentage elongation to fracture; and d is a material constant. The value of d is equal to 150 MPa for Al-7wt%Si-Mg alloys.

For the same alloy, the probable yield strength (YS) may be defined as follows:

$$YS = a\ UTS - b \log (\%El) + c \qquad (2)$$

where the coefficients a, b, and c are alloy-dependent empirically determined parameters. For the Al-7wt%Si-Mg alloys, the coefficients a, b, and c were determined as 1, 60, and -13, respectively, while the constants b and c are expressed in units of MPa.

The formulas to calculate the quality index Q and the probable yield strength lines YS for aluminum casting alloys were developed empirically by Drouzy *et al*. [54] [59] [60]

Using Equations (1) and (2), it is possible to plot lines of equal quality index or *iso-Q* lines and lines of equal probable yield strength or *iso-YS* lines in the form of a UTS-%El diagram or *quality chart*, as shown in Figure 2-14. The lines of constant "Q" or quality index are said to represent the quality of the alloy. They were found to depend on the soundness of the casting, *i.e.,* on the solidification conditions, and less affected by the heat treatment of the

alloy. Inversely, the "*YS*" lines of equal probable yield strength were found to depend on the degree of hardening, *i.e.* the tempering treatment, and less affected by the solidification conditions [54]. These quality charts are generated for use as a simple means of evaluating, selecting, and also predicting the most appropriate metallurgical conditions which may be applied to the castings so as to obtain the best possible compromise between tensile properties and casting quality. The quality index value (*Q*) is intrinsically related to the level of the quality of the castings, which is susceptible to improvement through adequate control of the impurity elements, casting defects, modification, solution heat treatment and solidification conditions. The probable yield strength (*YS*) depends mainly on the presence of hardening elements such as Mg and Cu, and also on the age-hardening conditions applied to the castings [79].

The right selection of these factors may increase both quality index values and the probable yield strength in the directions shown in Figure 2-14. The quality chart shown in this figure provides sufficient information for each point located on this type of plot so that the appropriate metallurgical conditions may be applied to obtain the specific prerequisite properties demanded of an alloy with respect to a particular application. As may be seen in Figure 2-14, the properties which are known for each point located in the chart are the tensile strength (*UTS*), yield strength (*YS*), percentage elongation to fracture (%*El*), and the quality index value (*Q*) [75] [74, 17] As a straightforward application, the Q-values allow for comparison between different alloys, or between batches of samples of the same alloy. Using this quality chart to plot the experimentally determined tensile strength and tensile ductility for a particular alloy, the material of the best quality will be located near the upper right-hand

corner, an indication that the material has both high UTS and high ductility, *i.e.*, its mechanical quality is high [54].

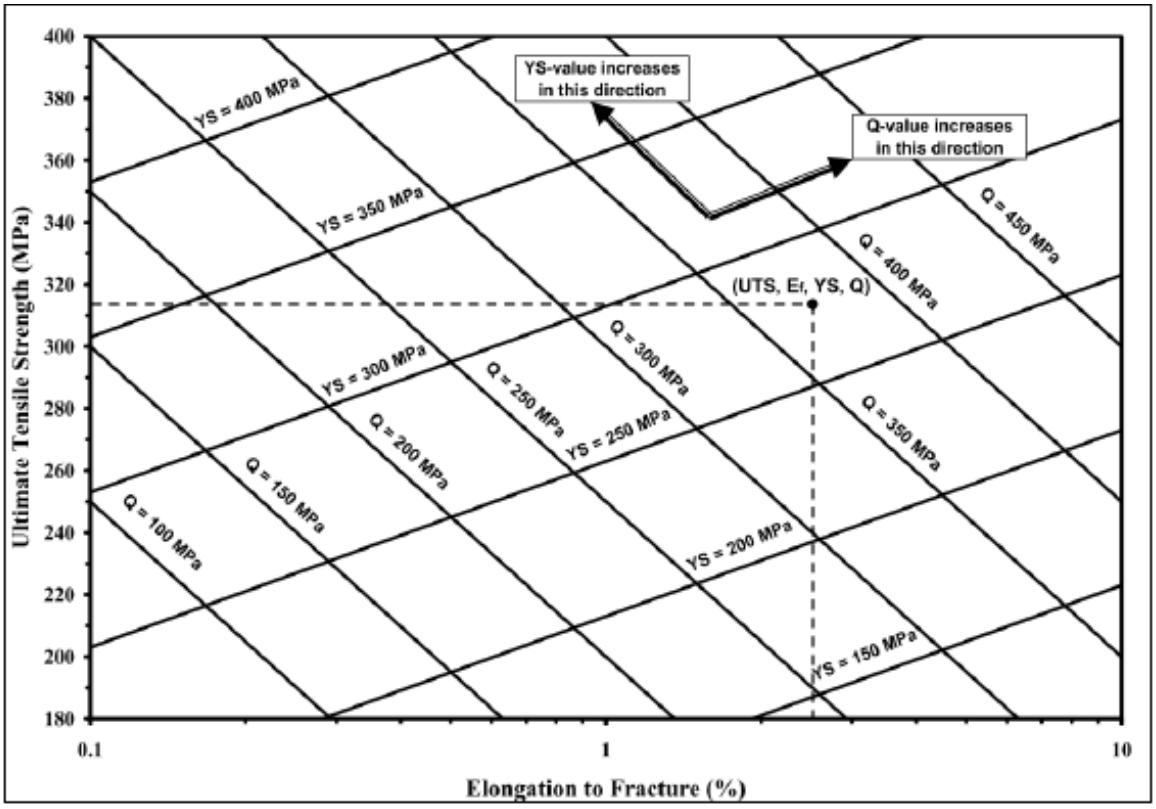

Figure 2-14: Example of the quality chart proposed by Drouzy et al. [78, 78] with iso-Q and iso-YS lines generated using Equations 1 and 2.

To summarize, by evaluating the quality or Q value of a cast aluminum alloy with reference to its mechanical properties, quality charts provide the right direction to follow to improve the quality of the material, and to select the optimum alloy/conditions appropriate for a particular application. In general, quality charts aim at providing the design engineer with a tool for selecting a material with the satisfying properties for any specific application under consideration [80] [81] [82].

CHAPTER 3

EXPERIMENTAL PROCEDURE

CHAPTER 3

3 EXPERIMENTAL PROCEDURE

3.1 INTRODUCTION

This chapter discusses the methodology and experimental procedures followed in this research. A total of five alloys were used, namely the as-received base alloy HT200, two other alloys based on the HT200 alloy containing alloying additions, and 319 and 356 aluminum alloys used as reference alloys, for comparison purposes. In order to fulfill the objectives laid out for this study, the work was divided into four parts: (i) preparation of alloys for melting and casting (which included castings for thermal analysis, for hot tearing investigation and for tensile testing); (ii) heat treatment; (iii) mechanical testing at ambient and elevated temperatures; and (iv) microstructural characterization.

3.2 MATERIALS AND ALLOYS

The chemical composition of the base alloy HT200 is shown in Table 3-1. Two other alloys were prepared from this alloy, using additions of 0.15 wt% Ti + 0.15 wt% Zr, and 0.15 wt% Ti + 0.15 wt% Zr + 0.5 wt% Ag. These additions were made using Al-5% Ti-1% B and Al-15% Zr master alloys, while Ag was added in pure metal form. For the A319 and A356 alloys, 0.15 wt% Ti and 200 ppm Sr were added using Al-5% Ti-1% B and Al-10% Sr master alloys, respectively. The five alloys were coded A, B, C, D and E. Details of the alloy compositions, codes, and master alloys used are provided in Table 3-2 and Table 3-3.

Table 3-1: Chemical composition of the as-received base alloy HT200* and alloys 319 and 356 used in this study

Chemical Analysis (wt%)									
Alloy	**Elements**								
	Cu	Si	Fe	Mn	Mg	Ti	Zr	V	Al
HT200*	6.5	0.054	0.05	0.453	0.006	0.09	0.18	0.01	Balance
319	3.323	7.97	0.418	0.245	0.266	0.03	-	-	Balance
356	0.12	7.19	0.12	-	0.32	0.02	-	-	Balance

* Chemical composition is proprietary to Nemak

Table 3-2: Compositions of the five used alloys for this study

Alloy Code	Composition
Alloy **A**	HT200 (as in in Table 3-2 and Table 3-3. Table 3-1)
Alloy **B**	HT200 +0.15% Ti + 0.15%Zr
Alloy **C**	HT200 +0.15% Ti + 0.15%Zr + 0.5%Ag
Alloy **D**	319 (as in in Table 3-2 and Table 3-3. Table 3-1) + 0.1-0.15%Ti + 200ppm Sr (0.02%)
Alloy **E**	356 (as in in Table 3-2 and Table 3-3. Table 3-1) + 0.1-0.15%Ti + 200ppm Sr (0.02%)

Table 3-3: Master alloys used for alloying additions

Addition	Master Alloy
Ti	Al-5%Ti-1%B
Zr	Al-15%Zr
Ag	Added in pure metal form
Sr	Al-10%Sr

3.3 MELTING AND CASTING PROCEDURES

The HT200 base alloy was received in the form of small ingots, having the composition shown in Table 3-1. The ingots were cut into small pieces and melted in a 40-kg capacity SiC crucible using an electrical resistance furnace, as shown in Figure 3-1 (a). This furnace is equipped with a rotary degassing impeller, shown in Figure 3-1 (b). The melting temperature was maintained at 800°C ± 5°C. For each alloy composition, the specified alloying elements were added using calculated amounts of the corresponding master alloys to obtain the desired level of addition. The additions were made using a perforated graphite bell which was plunged deep into the melt. The molten metal was degassed for about 15 minutes using pure, dry argon gas, injected into the melt at a constant rate of 20 m^3/h, employing the graphite impeller (rotating at ~120 rpm), to minimize the hydrogen absorbed into the melt and to ensure the homogeneous mixing of the additions. To remove oxides and other inclusions before pouring and casting, the melt surface was carefully skimmed. In order to ascertain the exact chemical composition, three samplings for chemical analysis were taken at different times during the casting process for each alloy melt. These samplings were taken at the beginning, at the middle, and at the end of each casting process.

(a) (b)

Figure 3-1: (a) Electrical resistance furnace, (b) Graphite degassing impeller.

The melt was poured into an ASTM B-108 permanent mold preheated to 450°C (to drive out moisture) to prepare test bars for tensile testing (cooling rate 7°C/s). Two standard tensile test bars were obtained for each casting, as shown in Figure 3-2. The standard tensile test bar has a gauge length of 70 mm and a cross-sectional diameter of 12.8 mm, as seen in Figure 3-3. A total of 130 tensile test bars were cast for alloys A, B and C in order to cover all the heat treatments used for this study; while a total of 70 tensile test bars were cast for alloys D and E for the same reason.

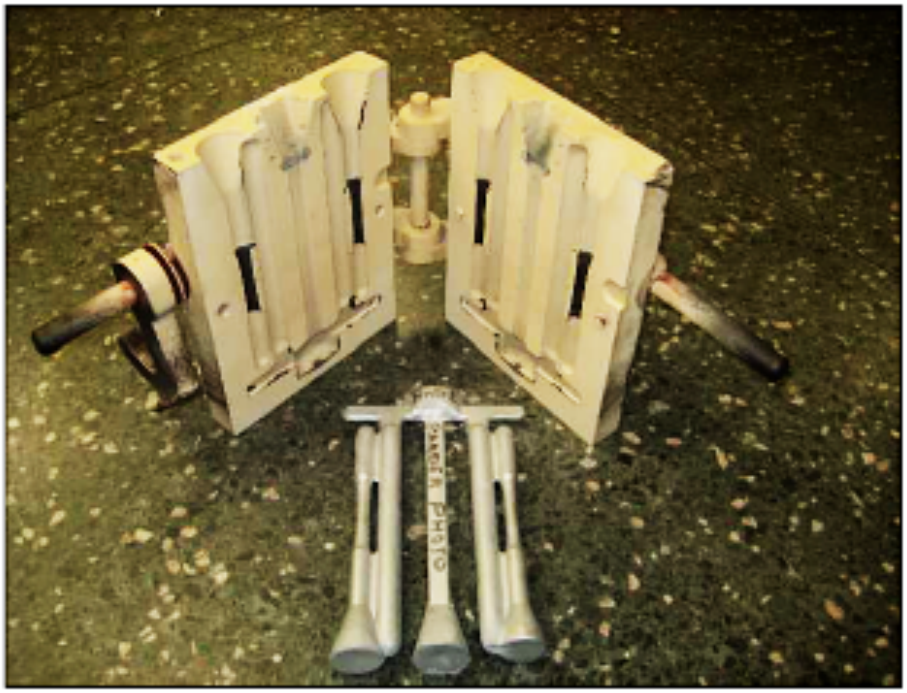

Figure 3-2: ASTM B-108 Permanent Mold and a Casting of two tensile test bars

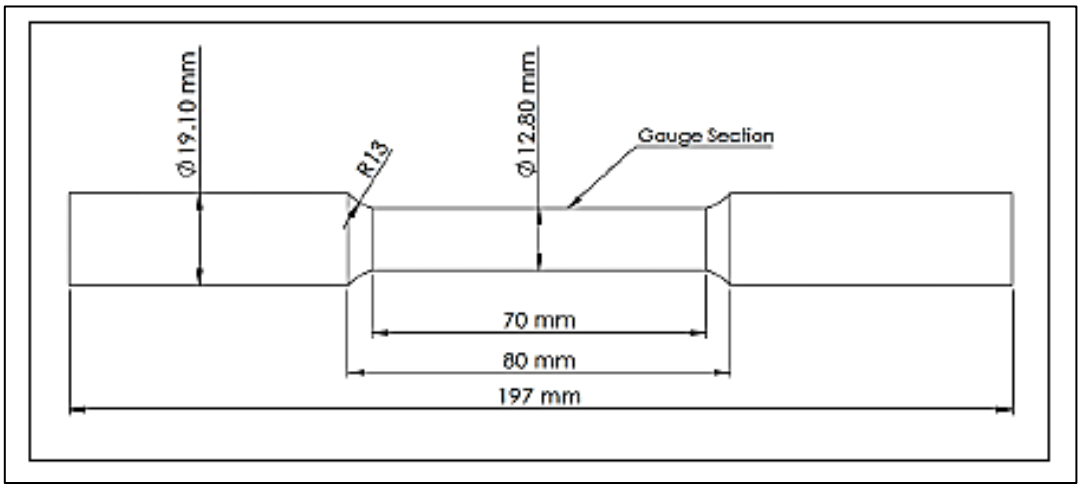

Figure 3-3: Geometry of the standard tensile test bar obtained from ASTM B-108 permanent mold

3.4 HOT TEARING

The effect of chemical composition on the hot-tearing tendency of the Al-6.5wt%Cu base alloy and the four other alloys was investigated, using different mold conditions. These alloys are the base alloy A, and alloys B and C. In addition to alloys D and E which are used as reference alloys to judge the hot-tearing susceptibility (HTS) results of the Al-6.5wt%Cu alloys, as alloys D and E are known commercial alloys. As can be seen in Table 3-1 and Table 3-2, alloy B has the same chemical composition as alloy A in addition to 0.15%Ti and 0.15%Zr. Alloy C has the same chemical composition as alloy A as well, in addition to 0.15%Ti, 0.15%Zr and 0.5%Ag.

A constrained rod casting mold (CRC mold) was used to investigate the hot-tearing susceptibility (HTS) of these alloys, and is shown in Figure 3-4. It is a permanent mould made of cast iron. In order to adjust and select the best hot tearing test specifications, two kinds of coatings (graphite and boron nitride lubricoat-Zv), different dwell times (2, 4, 8 min), and different mold slope angles (0>, 17>) were used. Based on,trial tests the Boron Nitride Lubricoat-ZV coating, a dwell time of 4 min, and a mold slope angle of 0> were selected as the mold parameters for carrying out the hot tearing tests. The dwell time refers to the time period between the pouring of the melt and releasing the casting from the mold. The hot tearing tests were carried out at the following mold temperatures: 400°C, 300°C, and 200°C.

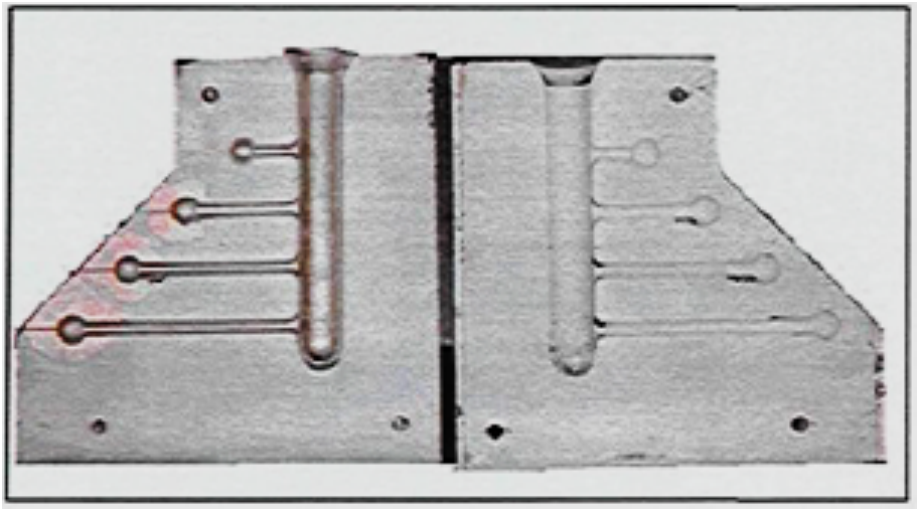

Figure 3-4: The mold used for hot-tearing test, CRC, and a casting

The CRC mold consists of four bars A, B, C, and D of different lengths, namely 2in /5.1cm, 3.5in /8.9cm, 5in /12.7cm and 6.5in /16.51cm, respectively, all measuring 0.5in in diameter, as shown in Figure 3-5. The bars are constrained at one end by a sprue and at the other end by a spherical riser (feeder) of 0.75k (1.9cm) diameter. The distance between each bar is 1.5in (3.81cm) from center to center. The metal is poured through the 7-in (17.8cm) sprue.

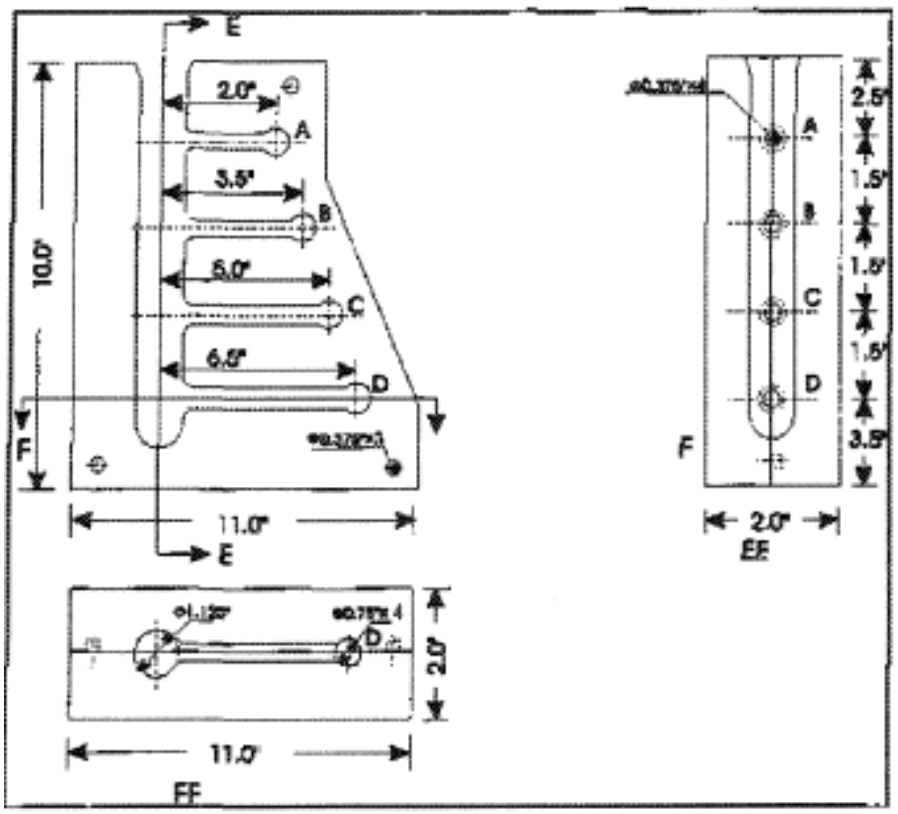

Figure 3-5: The dimensions of the hot-tearing test mold (CRC).

The hot tearing sensitivity (HTS) value for a sample was calculated using the following equation:

$$HTS = \Sigma (C_i * L_i)$$

where C_i is a numerical value used to represent the degree or "level" of crack severity in the bar, as provided in Table 3-4, and L_j is a numerical value assigned to the corresponding bar length, as provided in Table 3-5, where i = A, B, C or D. Four levels were used to classify the crack severity observed in the bars of the CRC mold castings, as illustrated in Figure 3-6. In fact, it was observed that the longer bars were less resistant to hot tearing than the shorter

ones. Each HTS value reported was obtained from an average of five experiments. The best alloy should have an HTS = 0.

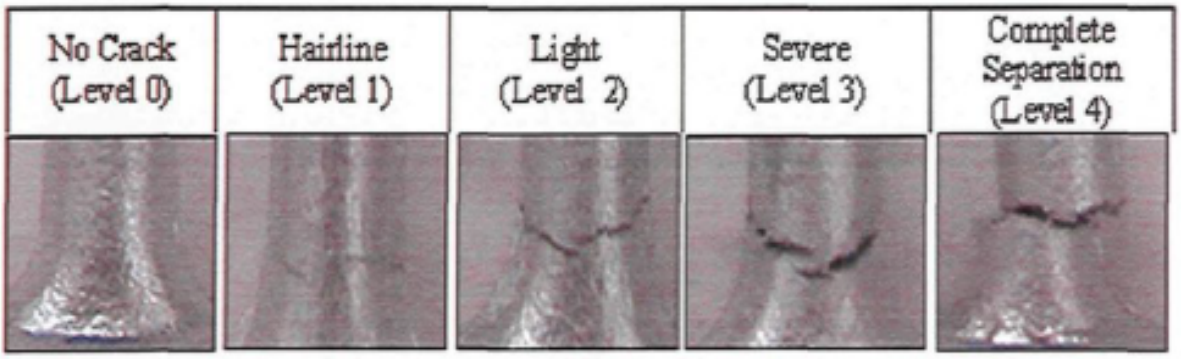

Figure 3-6: Crack severity level categories

Table 3-4: Categories of cracks and hot tearing numerical values (Ci) representing crack severity

Category	Numerical Value of Crack Severity Level (C_i)
Not Cracked	0
Surface Crack	1
Light Crack	2
Severe Crack	3
Complete Crack	4

Table 3-5: Numerical Values of Li representing bars with different lengths

Bar Type (Length inch)	Numerical Value (Li)
A (2.0)	**4**
B (3.5)	**3**
C(5)	**2**
D(6.5)	**1**

3.5 HEAT TREATMENT

Following the casting process, the tensile test bars were divided into bundles of five bars each. The as-cast bars were subjected to different heat treatments to enhance their mechanical properties. The different heat treatment conditions – incorporating solution heat treatment (SHT), quenching, and aging (T6 and T7 tempers) used for this study are as follows:

Table 3-6: Heat treatment conditions for Alloys A, B and C:

1) As Cast
2) SHT* for 4 h followed by air quenching
3) SHT for 4 h followed by water quenching
4) SHT for 4 h followed by water quenching, then artificial aging1 [180°C, 4 h]
5) SHT for 4 h followed by water quenching, then artificial aging 2 [200°C, 4 h]
6) SHT for 4 h followed by water quenching, then artificial aging 3 [250°C, 4 h]
7) SHT for 4 h followed by water quenching, then artificial aging 4 [250°C, 100 h]
8) SHT for 8 h followed by air quenching
9) SHT for 8 h followed by water quenching
10) SHT for 8 h followed by water quenching, then artificial aging 1 [180°C, 4 h]
11) SHT for 8 h followed by water quenching, then artificial aging 2 [200°C, 4 h]
12) SHT for 8 h followed by water quenching, then artificial aging 3 [250°C, 4 h]
13) SHT for 8 h followed by water quenching, then artificial aging 4 [250°C, 100 h]

- *All solution heat treatments (SHT) were carried out at **520°C**.

- Water quenching was done using warm water (~70°C).

- Ten tensile test bars (2 bundles) were subjected to each heat treatment condition, from which five bars were used for tensile testing at ambient temperature (25°C) and five for testing at elevated temperature (250°C).

- Hence, a total of **130 tensile bars** were required per alloy.

Table 3-7: Heat treatment conditions for Alloys D and E:

1) As Cast
2) SHT* followed by air quenching
3) SHT followed by water quenching
4) SHT followed by water quenching, then artificial aging 1 [180°C, 4 h]
5) SHT followed by water quenching, then artificial aging 2 [200°C, 4 h]
6) SHT followed by water quenching, then artificial aging 3 [250°C, 4 h]
7) SHT followed by water quenching, then artificial aging 4 [250°C, 100 h]

- *All solution heat treatments (SHT) for alloy **D** were carried out at **500°C** for **8 h.**

- *All solution heat treatments (SHT) for alloy **E** were carried out at **540°C** for **8 h.**

- Water quenching was done using warm water (~70°C).

- Ten tensile bars (2 bundles) were subjected to each heat treatment condition, rom which five bars were used for tensile testing at ambient temperature (25°C) and five for testing at elevated temperature (250°C).

- Hence, a total of **70 tensile bars** were required per alloy.

A Lindberg Blue M electric furnace was used for carrying out the heat treatment, shown in Figure 3-7. The time elapse between taking out the test-bar bundles from the furnace and quenching was at most ~5 seconds. After heat treatment, the test bars were stored in a freezer at ~ -20°C to preserve their properties until they were used for mechanical testing.

Figure 3-7: Lindberg Blue M electric furnace used for heat treatment

3.6 MECHANICAL TESTING

All as-cast and heat-treated test bars were subjected to tensile testing to obtain the tensile properties of each alloy/heat treatment condition. Testing was carried out at both ambient and elevated temperatures, using one bundle (five test bars) from the two bundles prepared per alloy/condition in each case. Tensile properties, namely, the ultimate tensile strength (UTS), the yield strength (YS) at 0.2% offset strain, and the percentage elongation (%El) were obtained.

3.6.1 TENSILE TESTING AT AMBIENT TEMPERATURE (25°C)

Tensile testing at ambient temperature (25°C) was carried out on half of the total number of test bars (265 bars or 53 bundles) obtained for all the alloys and all conditions (as-cast and heat treated). An MTS Servohydraulic mechanical testing machine was used to carry out the tensile testing at a strain rate of 4×10^{-4} s^{-1}; the MTS machine is shown in Figure 3-8. An attachable extensometer (strain gauge) was used to measure the deformation that took place in each sample during the test. A data acquisition system, attached to the machine, converts the extensometer readings to accurate measurements of the percentage elongation. The system then provides the tensile properties in terms of ultimate tensile strength (UTS), yield strength at 0.2% offset strain (YS), and the percentage elongation to fracture (%El).

Figure 3-8: MTS Mechanical Testing Machine used for ambient temperature tensile testing

The average UTS, YS, and %El values calculated from the values obtained for the five test bars tested per alloy/condition were taken to represent the tensile properties of that alloy composition/condition.

3.6.2 TENSILE TESTING AT ELEVATED TEMPERATURE (250°C)

Tensile testing at elevated-temperature (250°C) was carried out on the other half of the total number of test bars (265 bars or 53 bundles) for all alloys/conditions studied. In this case, the testing was carried out employing an Instron Universal Mechanical Testing machine, as shown in Figure 3-9, using the same strain rate of 4×10^{-4} s^{-1} as in the ambient temperature case. The sample to be tested was mounted in the testing chamber which was maintained at 250°C and left for thirty minutes before starting the test in order to ensure a homogeneous distribution of the temperature throughout the sample. A data acquisition system, attached to the machine, provided the tensile properties in terms of ultimate tensile strength (UTS), yield strength at 0.2% offset strain (YS), and the percentage elongation to fracture (%El). As explained in the previous section, from each set of five test bars (one bundle) used per alloy/condition, the average UTS, YS, and %El, values were calculated, and taken to represent the tensile properties of that alloy composition/condition.

Figure 3-9: Instron Universal mechanical testing machine with a chamber used for elevated temperature tensile testing

3.7 MICROSTRUCTURAL CHARACTERIZATION

The microstructures of the HT200 alloys in the as-cast and heat-treated conditions were examined to correlate the microstructural features observed with the tensile properties and quality indices of the alloys. Several techniques were used in this regard to achieve a qualitative and quantitative analysis of the microstructural constituents and features, which included the intermetallic phases, hardening precipitates and fracture surface characteristics observed in each case.

3.7.1 THERMAL ANALYSIS

Thermal analysis of the alloy melts prepared was carried out in order to obtain the solidification curves (cooling curves) and to identify the main reactions and corresponding temperatures occurring during the solidification of the HT200 alloys. Ingots of the as-received HT200 alloy were cut into smaller pieces, cleaned, and then dried to prepare the required alloys. The melting process was carried out in a cylindrical graphite crucible of 2-kg capacity, using an electrical resistance furnace. The melting temperature was maintained at 780°C. Thermal analysis was carried out for the base alloy (alloy A), as well as for alloys B and C. As mentioned in section 3.2, alloy B is the grain refined form of alloy A, with 0.15%Ti and 0.15%Zr additions, while alloy C has the same composition as alloy B but contains Ag as well.

In order to determine the reactions taking place during solidification, part of the molten metal was poured into an 800g capacity graphite mold preheated to 650°C, which provided close-to-equilibrium solidification conditions at a cooling rate of 0.35 $°Cs^{-1}$. A high sensitivity Type-K (chromel-alumel) thermocouple, insulated using a double-holed ceramic tube, was attached to the centre of the graphite mold. A high-speed data acquisition system linked to a computer system that recorded the data every 0.1 second was used to collect the temperature-time data, as shown schematically in Figure 3-10. From this data, the cooling curves and the corresponding first derivative curves for a number of selected alloys were plotted, to determine the main reactions occurring during solidification and their corresponding temperatures. Figure 3-11 shows a photograph of the actual thermal analysis set-up that was used. Metallographic samples were sectioned from the thermal analysis castings, close to the thermocouple tip as shown in Figure 3-10, mounted and polished for

microstructural examination, to identify the various phases observed in the microstructure with the reactions observed during solidification.

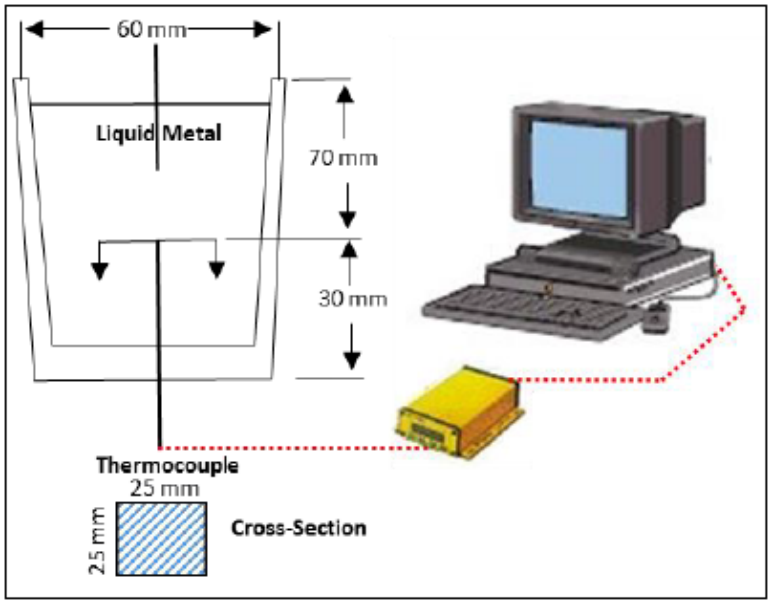

Figure 3-10: A schematic showing the graphite mold and the thermocouple used for thermal analysis.

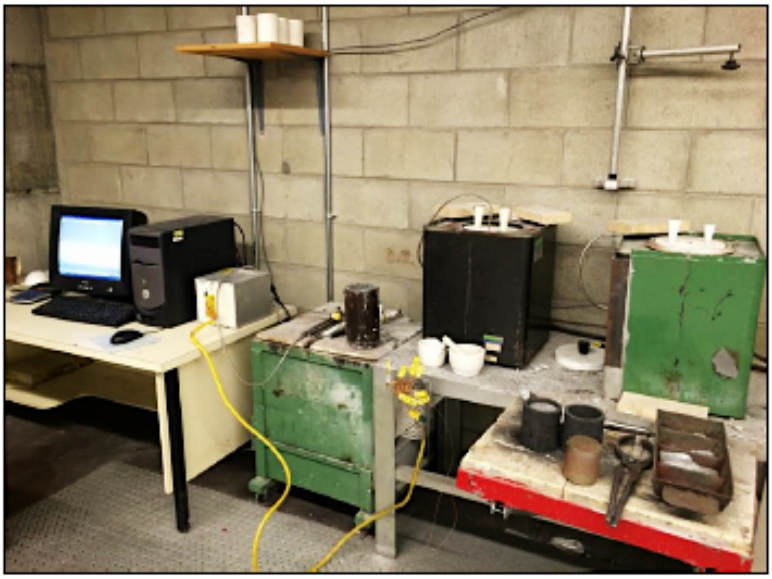

Figure 3-11: The set-up of the thermal analysis.

3.7.2 OPTICAL MICROSCOPY

For metallographic examination, in addition to the samples obtained from the thermal analysis castings, samples were also sectioned from the tensile-tested bars of selected conditions/alloy studied, approximately 10 mm below the fracture surface, as shown in Figure 3-12. The samples were mounted in bakelite using a Struers LaboPress-3 machine, while the grinding and polishing procedures were carried out using a TegraForce-5 machine, as shown in Figure 3-13. Silicon carbide (SiC) abrasive papers were used for grinding, in a sequence of 120 grit, 240 grit, 320 grit, 400 grit, 800 grit and 1200 grit sizes ("grit" representing the measure of fineness for abrasive materials). In this stage of sample preparation, water was used as a lubricant.

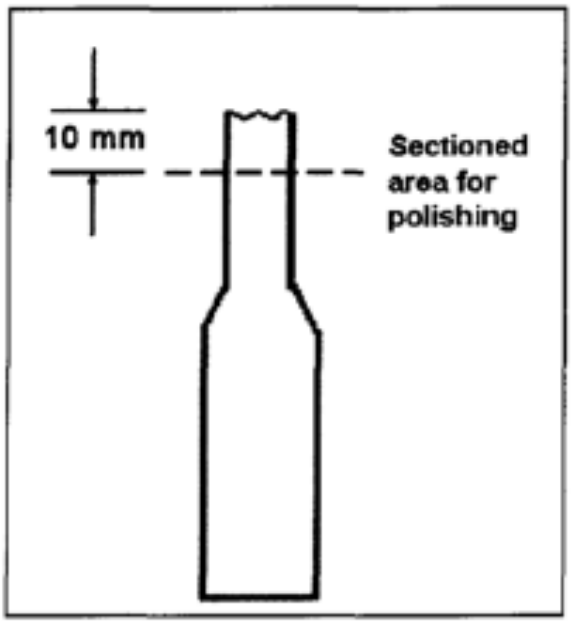

Figure 3-12: Diagram showing the sectioned area used for examining the microstructure of a tensile tested sample using optical microscopy.

In the first step of the polishing process, Struers diamond-suspension, with a diamond particle size of 6µm was used, followed by a finer suspension containing a smaller diamond particle size of 3µm. Struers DP-lubricant was used as the lubricant for this polishing stage. The final stage of polishing was carried out using a Mastermet colloidal silica suspension, SiO_2, having a particle size of 0.6µm, with water used as the lubricant. The samples then displayed a mirror-like surface and were ready for microstructural examination. An Olympus PMG3 optical microscope linked to a Clemex Vision PE image analysis system, shown in Figure 3-14, was used to examine the microstructures of the polished sample surfaces.

Figure 3-13: Struers LaboPress-3 and TegraForce-5 machines used for mounting and polishing the samples for metallography.

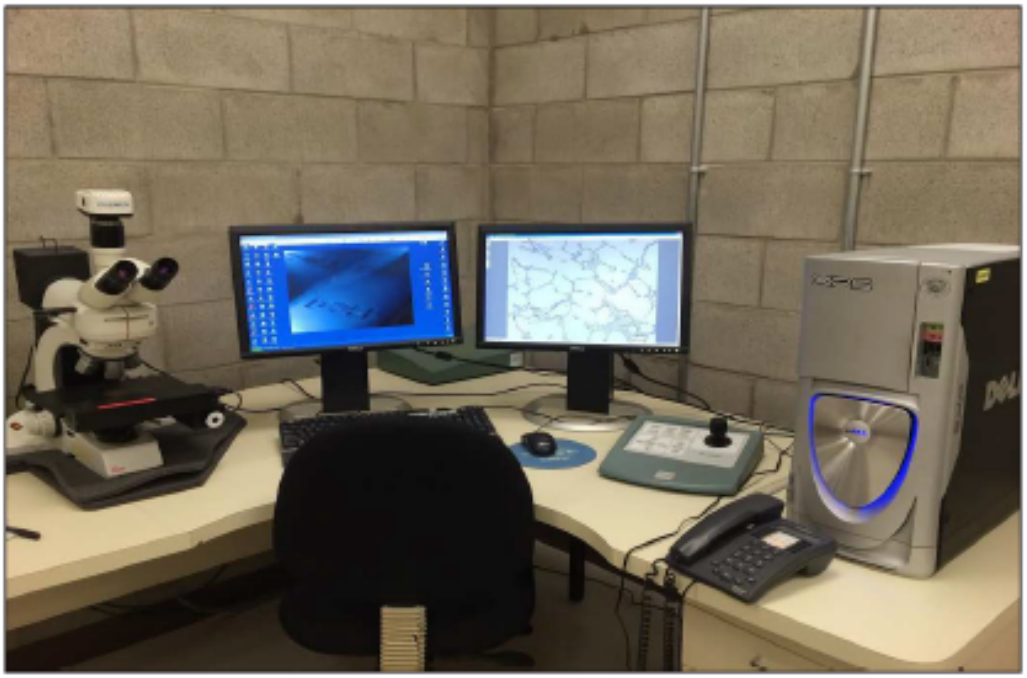

Figure 3-14: Clemex Vision PE 4.0 image analyzer-optical microscope system used in this study.

3.7.3 SCANNING ELECTRON MICROSCOPY

In order to examine the characteristics of the phases and hardening precipitates observed in the HT200 alloys under various heat treatment conditions, scanning electron microscopy (SEM) and field-emission scanning electron microscopy (FESEM) techniques were used. These techniques were used mainly for the purpose of assessing the distribution, size and density of the hardening precipitates in the casting structure under the various aging temperatures and times employed in this study.

Figure 3-16 shows the SEM used for this study, which is a JEOL 840A scanning electron microscope attached to an EDAX Phoenix system designed for image acquisition and energy dispersive X-ray spectroscopy (EDS). The SEM was operated at a voltage of 15 kV, with a maximum filament current of 3 micro amperes. The FESEM provides clear and

less electrostatically distorted high-resolution images even at low voltages, producing images of 2.1 nm resolution at 1 kV and of 1.5 nm resolution at 15 kV. The Hitachi-S-4700 FEGSEM shown in Figure 3-16 was used in this study.

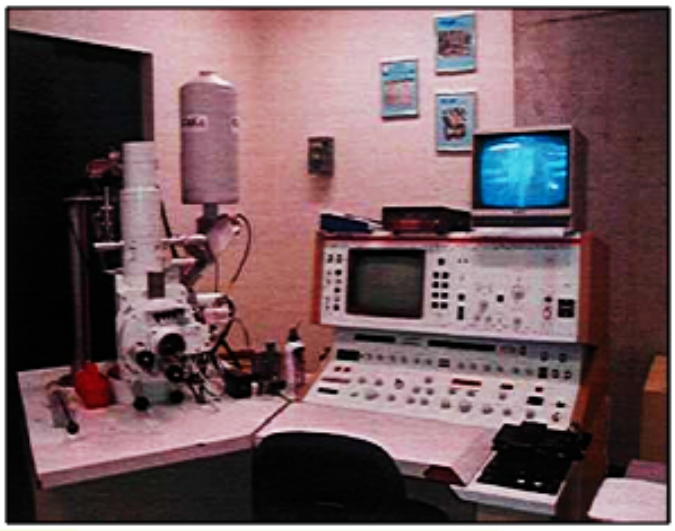

Figure 3-15: Scanning electron microscope (SEM) system used in this study.

Figure 3-16: Field emission scanning electron microscope (FESEM) used in this study.

CHAPTER 4

HOT TEARING AND MICROSTRUCTURAL CHARACTERIZATION

CHAPTER 4

4 HOT TEARING AND MICROSTRUCTURAL CHARACTERIZATION

4.1 INTRODUCTION

Hot tearing is one of the critical casting defects which may occur during solidification, particularly in Al-Cu alloys which exhibit a tendency for hot tearing. Localized stress and strain concentrations caused by solidification shrinkage and linear contraction in weak regions of a casting lead to hot tearing. As the present study covers an investigation of the tensile properties of the HT200 alloys, which are Al-Cu type alloys, this chapter will focus on establishing the parameters leading to:

1- Production of sound castings from these Al-Cu based alloys by minimizing their sensitivity to hot tearing during casting; and

2- Achievement of a fine-grained microstructure in order to obtain optimum mechanical properties at ambient and high temperature.

The relation between yield stress and grain size is described mathematically by the Hall–Petch equation [83] [84]:

$$\sigma_y = \sigma_0 + k_y/d^{1/2}$$

where σ_y is the yield stress, σ_0 is a materials constant for the starting stress for dislocation movement, k_y is the strengthening coefficient, and d is the average grain diameter.

Achieving a smaller grain size is thus the common link in obtaining the above objectives of reducing hot tearing and enhancing the alloy properties. This aspect will be the main focus of the microstructural characterization presented in section 4.3.

4.2 HOT TEARING

Figure 4-1(a) shows the fracture of alloy A when the melt was poured from 750°C. Apparently, the fluidity of the liquid metal was not high enough to fill the mold completely, leading to the formation of some cracks. In order to overcome this problem, the temperature of the molten metal was raised to 830°C which resulted in much lesser sensitivity for cracking, as presented in Figure 4-1(b). An effective way to improve the alloy resistance to hot tearing is the addition of grain refiner [62] [63] as displayed in Figure 4-1(c) for the casting obtained from alloy B (i.e., base alloy A, grained refined with the addition of TiB_2). It is evident that the casting is crack-free without the need for superheating the melt to 830°C. However, reducing the mold temperature to about 200°C led to a defective casting due to poor fluidity of the molten metal. Increasing the alloy Si content is another efficient parameter to consider when controlling the hot tearing severity [69] [73] in cast alloys as may be seen from Figure 4-1(e) and Figure 4-1(f) for alloys 319 and 356, respectively, cast under the same conditions as alloy B in Figure 4-1(c). Both alloys were grain refined using Al-5%Ti-1%B master alloy (0.15%Ti).

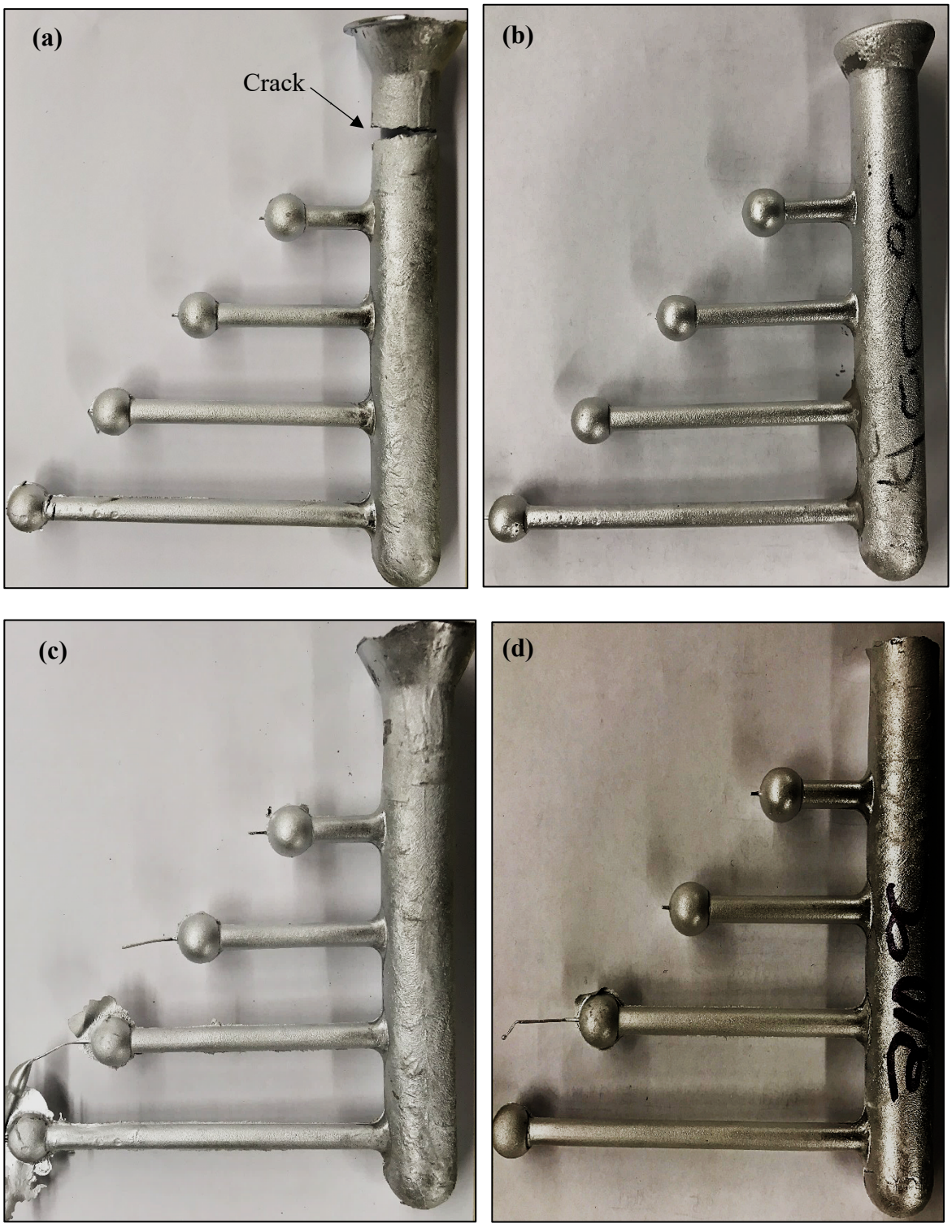
(a)
Crack
(b)
(c)
(d)

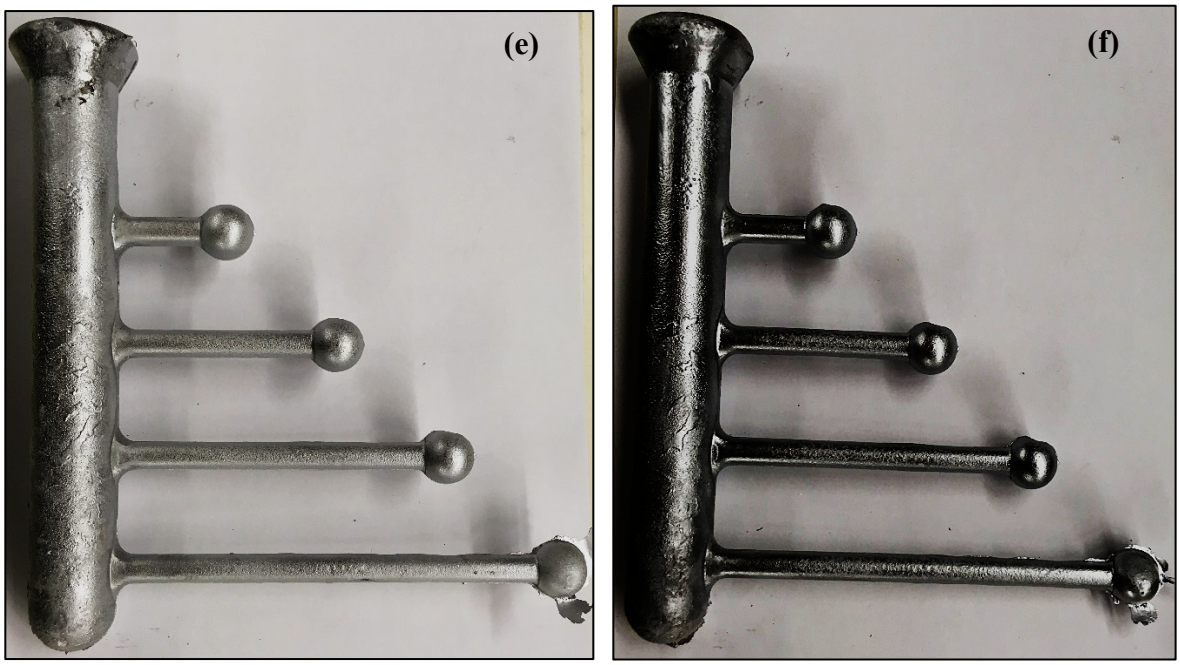

Figure 4-1: Hot tearing in: (a) alloy A poured from 750°C-mold temperature 400°C, (b) alloy A poured from 830°C-mold temperature 400°C, (c) alloy B poured from 750°C-mold temperature 400°C, (d) alloy B poured from 750°C-mold temperature 210°C, (e) alloy D poured from 750°C-mold temperature 400°C, and (f) alloy E poured from 750°C-mold temperature 400°C.

4.3 MICROSTRUCTURAL CHARACTERIZATION

As mentioned previously in Chapter 3, microstructures of the alloys studied were examined using optical microscopy and scanning electron microscopy in conjunction with EDS analysis for identifying the phases observed. Thermal analysis was used to monitor the reactions which occurred during solidification and from the resulting solidification curves obtained, the phases formed corresponding to these reactions were identified.

4.3.1 SOLIDIFICATION CURVES

Figure 4-2 presents the solidification curves (~0.8°C/s) and their first derivatives obtained for alloys B, D and E. The details of the observed reactions are listed in Table 4-1. Due to the absence of Si in alloy B, the solidification temperature range is about 140 °C compared to ~40°C reported for alloys D and E. Campbell and Harding [85] have explained how the fluidity of short freezing range alloys is different from that of long freezing range alloys, based on the mode of solidification and the solidification front (planar *vs* dendritic) in the two cases. The dendritic solidification front in the latter case results in turbulence as the moving liquid which flows through the solidifying dendrites, bringing pockets of hot liquid into the cooler dendritic regions, causing fragmenting and remelting of dendrite arms, resulting in a slurry that eventually thickens and makes the liquid too viscous to flow. This occurs at a certain solid fraction depending on the alloy. The authors also pointed out that the fluidity of Al-Si alloys increases with increasing Si content, due to the high latent heat of solidification of silicon.

The long freezing zone in alloy B explains the difficulty in filling the mold without the alloy being grain refined, which would otherwise enhance its fluidity and therefore the casting soundness. Thus, the absence of Si in alloy B resulted in reducing the temperature of the commencement of solidification i.e., 640 °C (alloy B) *vs* 596 °C for alloy D, which may be attributed in part to the alloy sensitivity to hot tearing.

Figure 4-3 (a, b) shows the main phases observed in alloy B. In addition to the α-Al dendrites, the Al_2Cu phase, the script-like α-Fe and the platelet-like β-Fe intermetallic phases are also present. In this context, it ought to be mentioned here that as the alloys D and E

corresponding to 319 and 356 alloys are very well known, and have been extensively studied, only their solidification curves and corresponding reactions have been provided for purposes of comparison.

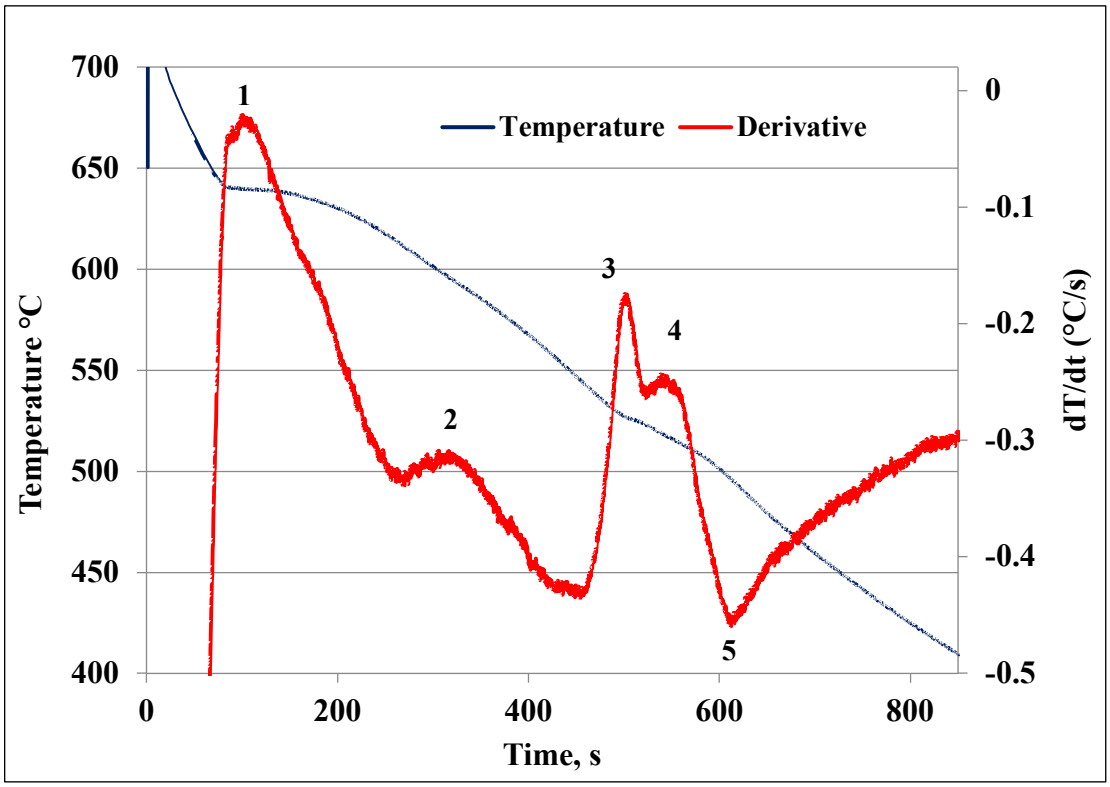

(a)

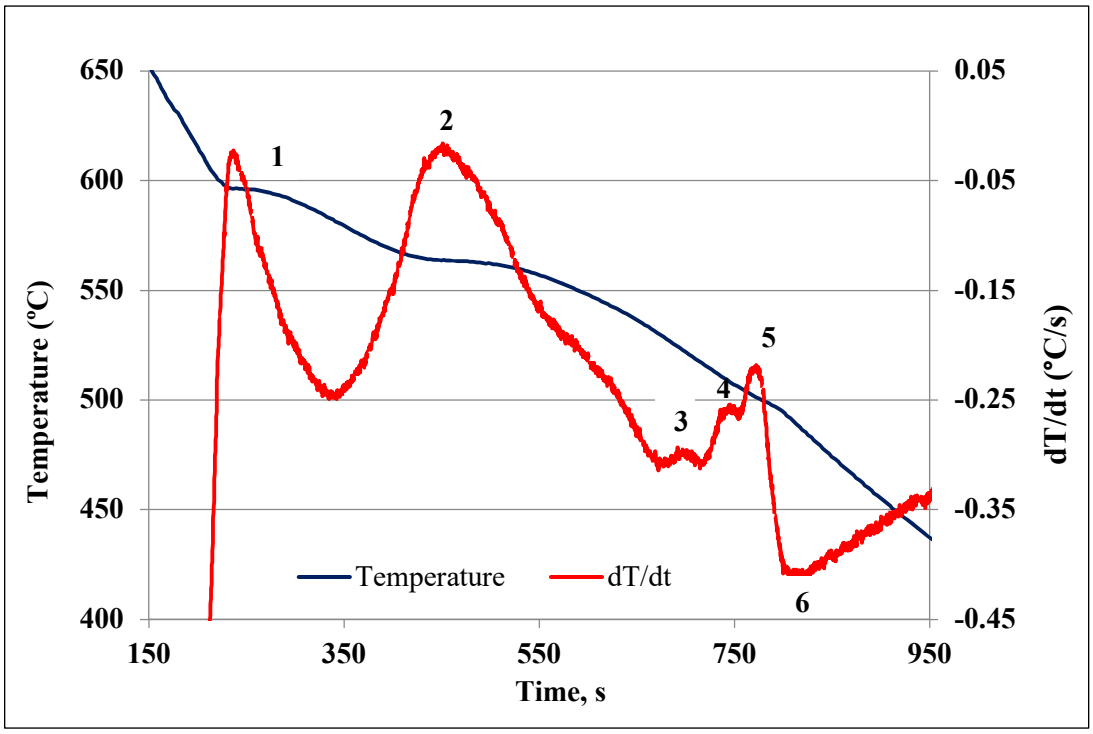

(b)

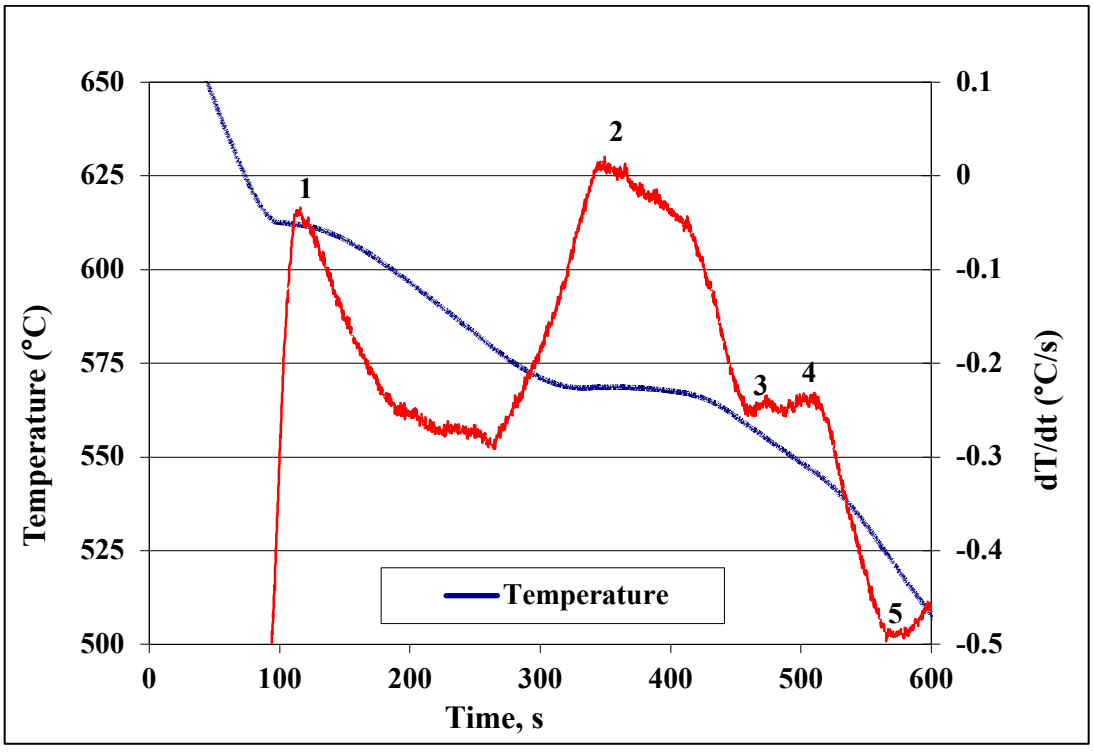

(c)

Figure 4-2: Solidification curves and their first derivatives obtained from (a) alloy B, (b) alloy D, and (c) alloy E. It should be noted here that alloys D and E were grain refined and Sr-modified.

Table 4-1: Reactions obtained from the solidification curves of alloys B, D and E.

Alloy code	Reaction #	Temperature, °C	Details
B	1	640	Precipitation of α-Al
	2	600	Precipitation of α-Fe
	3	523	Precipitation of Al_2Cu phase
	4	516	Precipitation of Q-phase
	5	500	End of solidification
D	1	596	Precipitation of α-Al
	2	562	Precipitation of Al-Si eutectic
	3	524	Partial transformation of β-Fe to π-Fe
	4	509	Precipitation of Mg_2Si phase
	5	500	Precipitation of Al_2Cu phase
	6	490	End of solidification
E	1	612	Precipitation of α-Al
	2	568	Precipitation of Al-Si eutectic
	3	555	Partial transformation of β-Fe to π-Fe
	4	545	Precipitation of Mg_2Si phase
	5	525	End of solidification

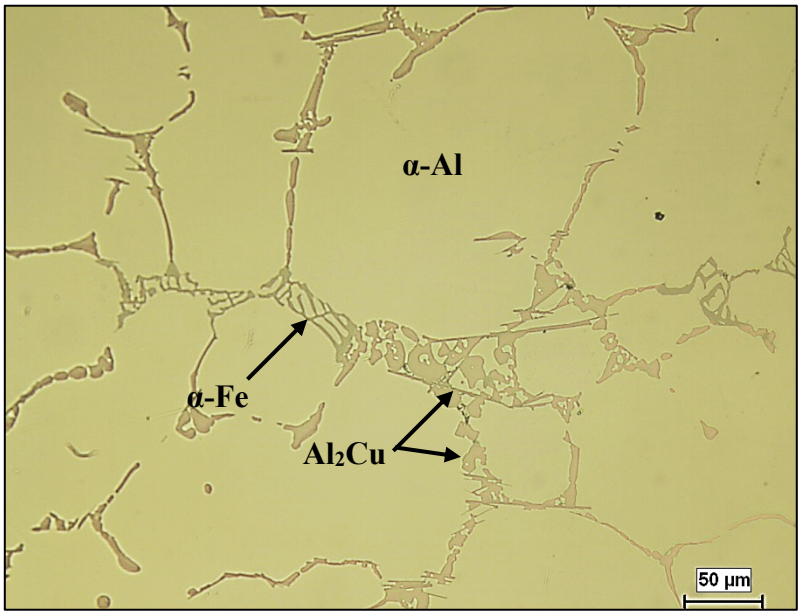

(a)

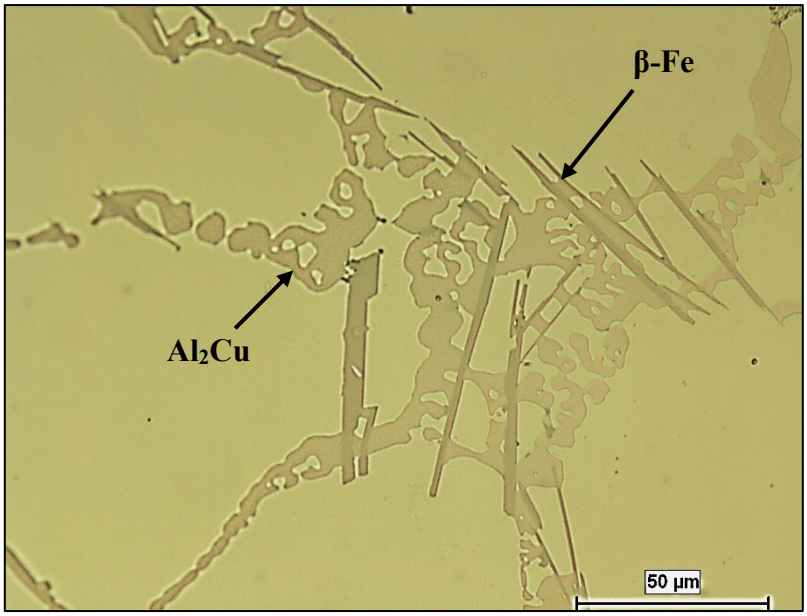

(b)

Figure 4-3: (a) Optical microstructure showing the main phases precipitated in alloy B during solidification, (b) high magnification micrograph of (a) showing the presence of fine β-Fe platelets.

4.3.2 GRAIN SIZE

4.3.2.1 LOW SOLIDIFICATION RATE (~0.8°C/S)

Figure 4-4 shows the macrostructures of deeply etched samples prepared from the thermal analysis castings obtained at low solidification rate (~0.8°C/s). It may be seen that the addition of grain refiner to alloy A resulted in a marked decrease in the alloy grain size, from about 350-400µm to about 100-150µm in alloy B, as seen from Figure 4-4(a) and Figure 4-4(b). The black spots observed in Figure 4-4(a), as marked by the white arrows, are mainly due to the precipitation of Al_2Cu phase particles, which are characterized by their low corrosion resistance [86]. In the case of Al-Si alloys such as alloy D, Figure 4-4(c) shows that the grain refining effect is markedly more significant than in the case of Al-Cu alloys, and results in a grain size in the range of 50-70 µm.

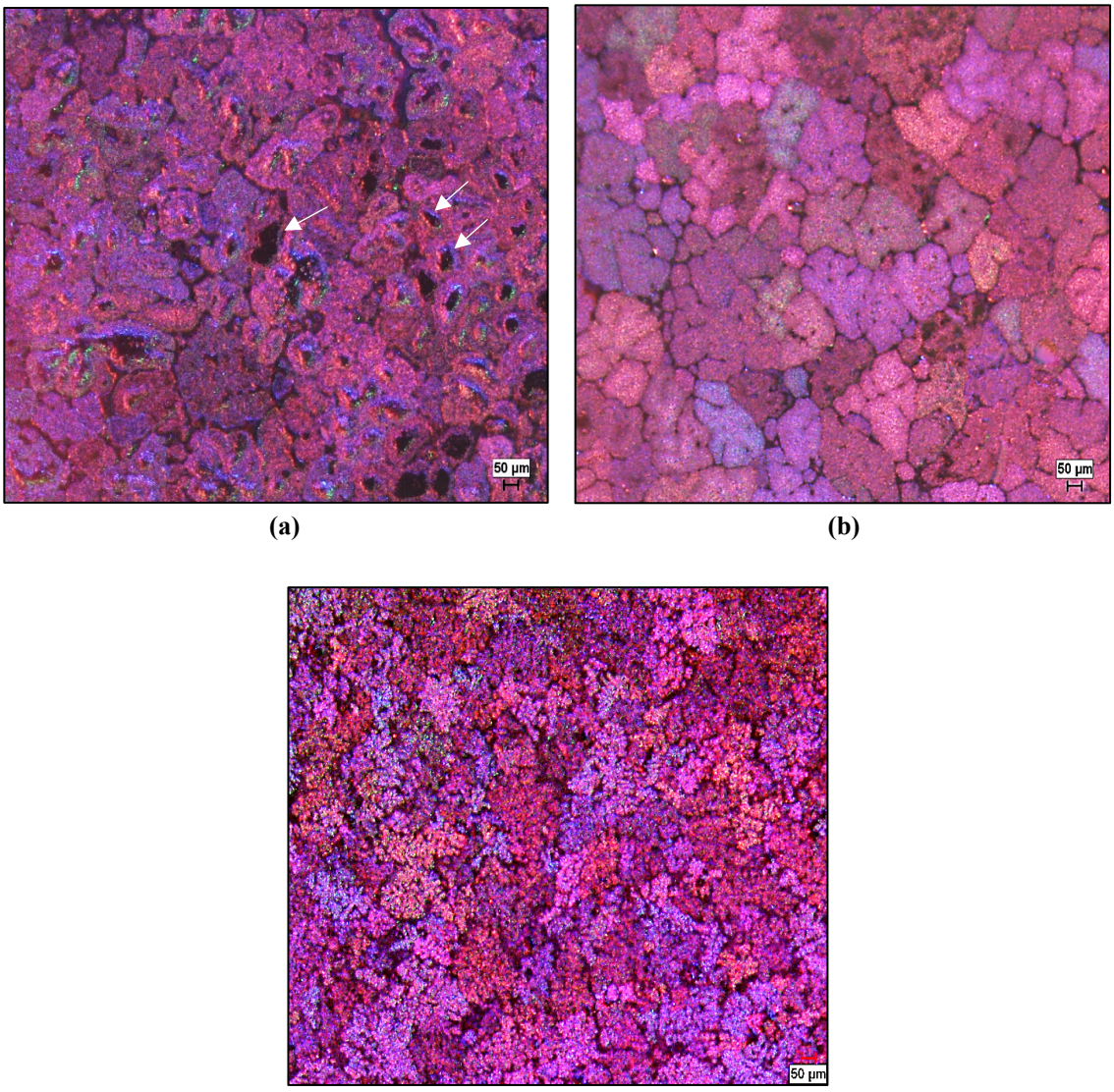

(a) **(b)**

(c)

Figure 4-4: Macrostructures of deeply etched samples of (a) alloy A, (b) alloy B, and (c) alloy D obtained from thermal analysis castings.

4.3.2.2 HIGH SOLIDIFICATION RATE (~8°C/S)

An important parameter to be considered in obtaining castings with high performance is the solidification rate. Figure 4-5 exhibits the microstructures obtained from as-cast tensile

test bar samples of alloys A and B, solidified at approximately 8°C/s. Compared to the micrographs shown in Figure 4-3, the much finer microstructure resulting from the high solidification rate of these samples is clearly noted.

Optical micrographs of these samples in the etched condition are shown in Figure 4-6. The average grain size in alloy A was found to be about 85 μm, as shown in Figure 4-6(a), compared to 350 μm reported for samples solidified at the rate of 0.8°C/s. A combined high solidification rate with proper grain refining resulted in a grain size of approximately 50 μm in alloy B, as seen in Figure 4-6(b).

The microstructural characteristics of the HT200 Al-Cu alloys presented in this chapter have provided qualitative evidence of the importance of such metallurgical parameters as the solidification rate and grain refining in controlling the hot tearing tendency of these alloys and in refining the microstructure in order to improve their mechanical properties. The results on the tensile properties which will be presented in Chapters 5 and 6 will be discussed on the basis of these observations.

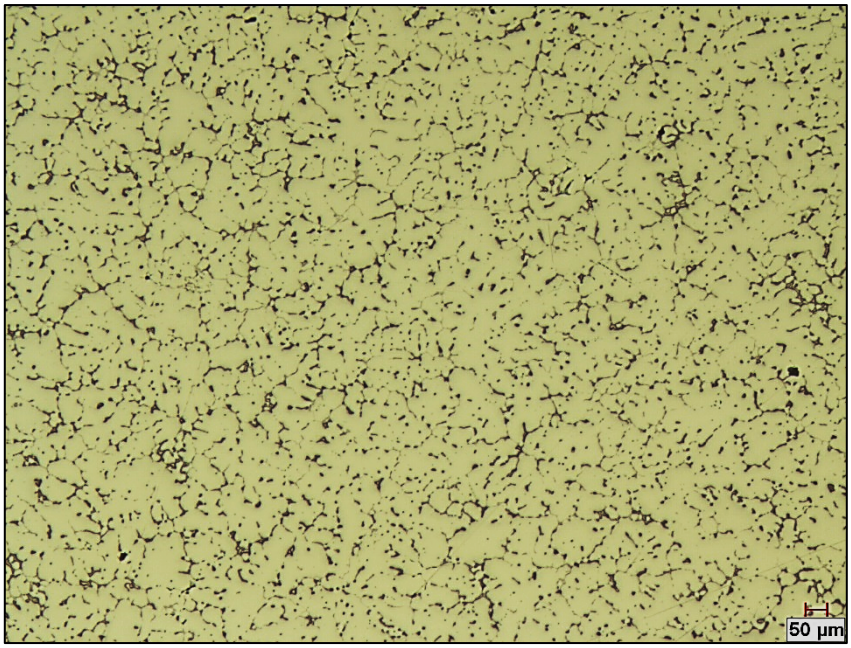

(a)

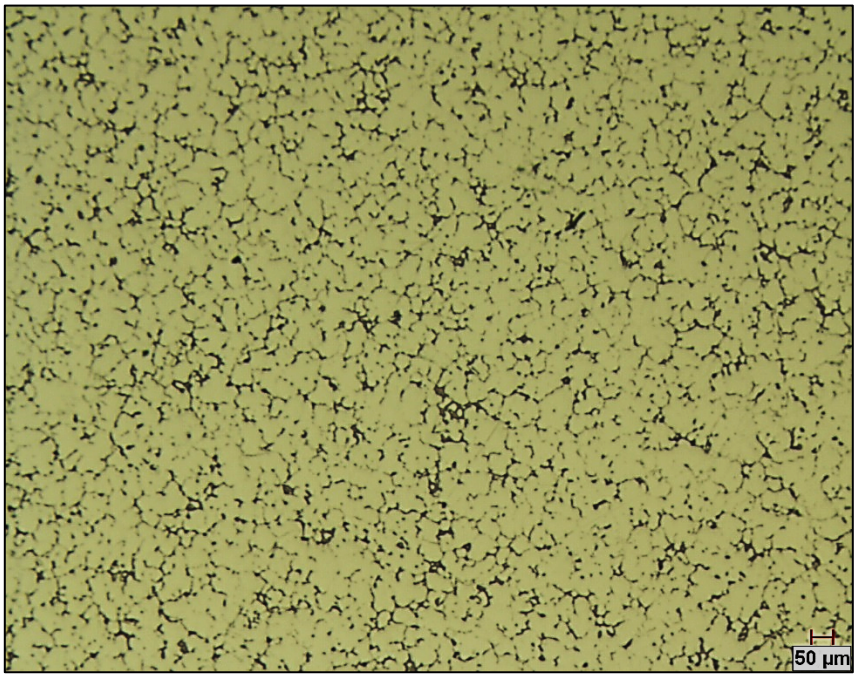

(b)

Figure 4-5: Optical microstructures of (a) alloy A, and (b) alloy B prepared from tensile bars in the as-cast condition.

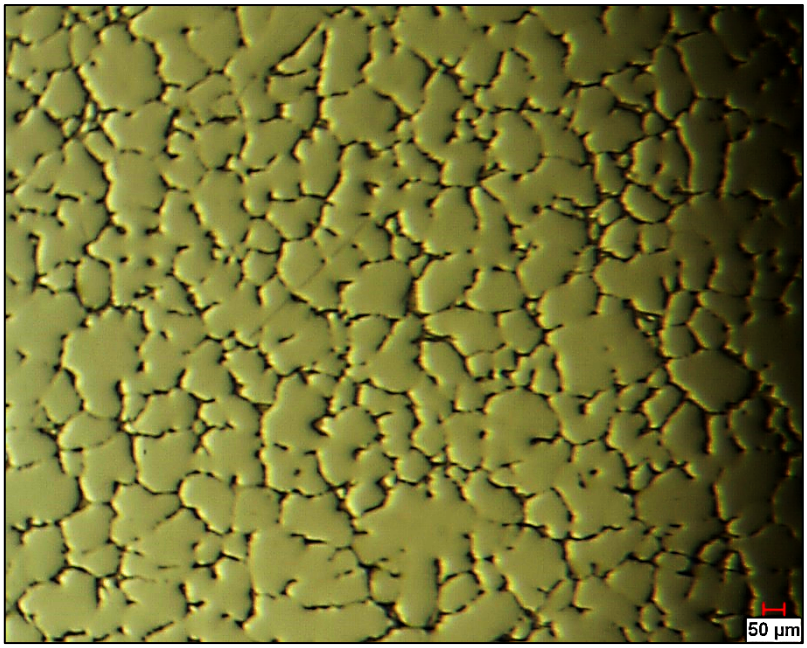

(a)

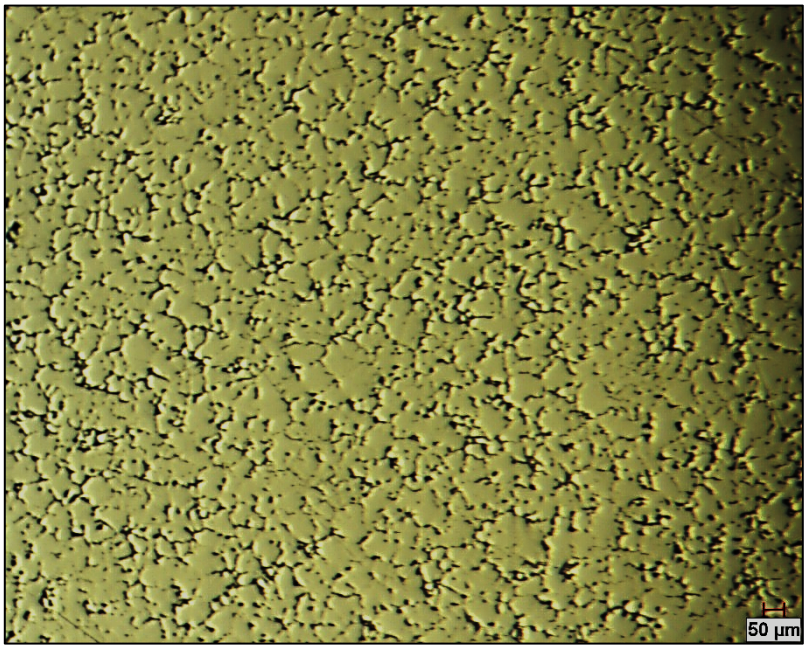

(b)

Figure 4-6: Macrostructures corresponding to the same as-cast tensile bar samples of (a) alloy A, and (b) alloy B in Figure 4.5, revealing the grain size after etching.

CHAPTER 5

AMBIENT TEMPERATURE TENSILE PROPERTIES

CHAPTER 5

5 AMBIENT TEMPERATURE TENSILE PROPERTIES

5.1 INTRODUCTION

This chapter analyzes and discusses the tensile test results of the alloys A, B, C, D and E in the as-cast and heat-treated conditions. The tensile tests were carried out at ambient temperature (25°C). The tensile properties of the HT200 alloys (alloys A, B and C) are compared with those of the reference alloys (alloys D and E). The parameters investigated were the effect of alloying element additions of titanium, zirconium and silver, and the influence of different heat treatment conditions.

The tensile test results at ambient temperature are divided into two groups. The first group covers the results for alloys A, B and C in the as-cast condition and when solution heat treated for four hours. The second group covers the results for alloys A, B, C, D and E in the as-cast condition and when solution heat treated for eight hours.

In order to understand and compare the alloy properties in relation to the various alloying elements as well as determine the effect of the additions made in relation to the heat treatment conditions applied, quality charts were generated. The alloy quality was analyzed using quality index Q values calculated from the tensile test data obtained for the five alloys at ambient temperature, in order to recommend the optimum alloy composition/heat treatment condition for HT200 alloy, and compare the Q values with those of the reference alloys D and E.

In addition to the use of quality charts, plots of property difference, ΔP, are also presented. Such plots represent the difference in a property (P) value obtained for a specific alloy composition/heat treatment condition with respect to that obtained for the base alloy. In the present study and for the ambient temperature testing data, the ΔP values will be plotted taking alloy A (HT200) in the as-cast condition as the base or reference line. The ΔP plots of the ultimate tensile strength, yield strength and percent elongation values obtained are generated for the alloys relative to the values obtained for the base alloy A in the as-cast condition.

5.2 MECHANICAL PROPERTIES

Tensile tests were carried out on all the alloys used for this study, (A, B, C, D and E) to obtain their ultimate tensile strength (UTS), yield strength (YS) and the percentage elongation (%El) values. In addition to the as-cast condition, the alloys were heat treated using different heat treatment conditions, twelve in the case of alloys A, B and C, and six in the case of alloys D and E. The chemical compositions of the five alloys investigated in this study were provided previously in Chapter 3, in Table 3-1 and Table 3-2. Details regarding the heat treatments used for each alloy were provided in Table 3-6 and Table 3-7. For purposes of simplicity, however, the shortened descriptions and codes of these heat treatment conditions shown in Table 5-1 and Table 5-2 will be used to discuss the results. The solution heat treatments used for each alloy are given in Table 5-3. For each alloy/heat treatment condition, five tensile bars were tested and the average values obtained were taken as representing the tensile properties of that alloy/heat treatment condition.

Table 5-1: As cast and heat treatment conditions and codes - shortened descriptions

No.	As Cast and Heat Treatment Conditions	Code
1	As_Cast	AC
2	SHT4_AQ	S4A
3	SHT4_WQ	S4W
4	SHT4_WQ+Aging1	S4WA1
5	SHT4_WQ+Aging2	S4WA2
6	SHT4_WQ+Aging3	S4WA3
7	SHT4_WQ+Aging4	S4WA4
8	SHT8_AQ	S8A
9	SHT8_WQ	S8W
10	SHT8_WQ+Aging1	S8WA1
11	SHT8_WQ+Aging2	S8WA2
12	SHT8_WQ+Aging3	S8WA3
13	SHT8_WQ+Aging4	S8WA4

Table 5-2: Explanation of heat treatment conditions listed in Table 5-1

Heat Treatment Condition	Description
SHT4	Solution Heat Treatment, 4 h
SHT8	Solution Heat Treatment, 8 h
AQ	Air Quenching
WQ	Water Quenching
Aging1	Aging at 180°C for 4 h
Aging2	Aging at 200°C for 4 h
Aging3	Aging at 250°C for 4 h
Aging4	Aging at 250°C for 100 h

Table 5-3: Solution heat treatments used for alloys A, B, C, D and E

Alloy	Solution Heat Treatment
A, B, and C	SHT at 520°C, once for 4 h and once for 8 h
D	SHT at 500°C, for 8 h
E	SHT at 540°C, for 8 h

5.2.1 RESULTS FOR AS-CAST AND 4 HRS-SOLUTION HEAT TREATED CONDITIONS

5.2.1.1 TENSILE TEST RESULTS

This section discusses the tensile properties of the alloys A, B and C in the as-cast condition and when solution heat treated at 520 °C for four hours. Six heat treatment conditions were used in this group, namely S4A, S4W, S4WA1, S4WA2, S4WA3 and S4WA4, as described in Table 5-1 and Table 5-2. The tensile test results for this group are shown in Table 5-4 and were used to obtain the plots displayed in Figure 5-1, Figure 5-2 and Figure 5-3. As may be seen, the tensile properties of the alloys improved significantly after heat treatment.

A micrograph corresponding to the as-cast sample of alloy B (as an example) is shown in Figure 5-4, and reveals the presence of precipitates in the as-cast matrix. The appearance of these precipitates may be explained as follows: during casting, the tensile bars were cast in a preheated mold at 450 °C and then left to cool in the air, resulting in a cooling rate of 7 °C/s, which is relatively a high cooling rate; this in turn caused natural aging. Hence, the as-received alloy (alloy A) in the as-cast condition gave relatively good tensile properties of

283.45 MPa for the UTS, 227.27 MPa for YS and 2.2% for the %El, as compared to the reference alloys D and E, the results for which are shown later on in this chapter, in section 5.2.2.1.

With solution heat treatment (SHT) for four hours, followed by quenching, the tensile properties are improved in the three alloys, especially when water quenching is used, which provides a higher cooling rate. As the solution heat treatment process aims at retaining the maximum amount of hardening solutes of Cu in solid solution in the Al matrix, a homogeneous supersaturated solid solution at elevated temperatures is obtained by dissolving the existing phases like θ-Al_2Cu in the as-cast structure into solution. Other phases, like those containing Fe, are harder to dissolve, due to the limited diffusivity of Fe in Al. This is illustrated in Figure 5-5 which shows a micrograph of alloy B, as an example, when solution heat treated; all phases are dissolved except for those containing Fe. With the quenching that follows SHT, the supersaturated solid solution formed during the solution treatment is preserved, by means of a rapid cooling to some lower temperature, usually near the room temperature. It retains the solute atoms in the solution and blocks them in their positions where they got to at the high temperature during SHT. The higher cooling rate (in water quenching) gives better results (higher strength) than the lower cooling rate (in air quenching), as with lower cooling rate, retaining the precipitates in solution decreases and may fail. The precipitates can form on the grain boundaries as coarse particles, which have a very limited effect on mechanical properties and will not be useful to contribute to the subsequent strengthening.

With the S4W heat treatment, the UTS, YS and %El values of alloy A reached as high as 339 MPa, 232.07 MPa, and 5.8%, respectively, compared to the as-cast values of 283.45

MPa, 227.27 MPa and 2.2%. In the case of Alloy B, the values increased to 327.37 MPa, 206.1 MPa and 4.0%, respectively (cf. 249.76 MPa, 166.94 MPa and 3.72% in the as-cast condition); while for alloy C, the UTS, YS and %EL values improved to 345.58 MPa, 196.97 MPa and 6.14%, respectively (cf. 235.59 MPa, 162.83 MPa and 3.1% the as-cast case).

When the S4W treatment was followed by aging, further significant improvement in the strength of the alloys A, B and C was observed, however, with some decrease in the ductility. This could be seen in the T6 heat treatments, which are represented in this study by the S4WA1 and S4WA2 conditions, and the T7 heat treatments, represented by the S4WA3 and S4WA4 conditions. A description of these four heat treatment processes is given in Table 5-1 and Table 5-2. In the alloys A, B and C, it can be seen that the strength reached its maximum with the T6 heat treatment and then started to decrease with the T7 heat treatment. This is due to the different aging conditions in the two heat treatment processes.

Aging treatment follows the solution treatment and quenching processes, where the castings are subjected to a specified temperature for a certain period of time. It starts by clustering of Cu atoms which are formed from decomposition of the supersaturated solid solution. These clusters appear homogeneously, forming GP zones that are considerably enriched in solute. With further time, the GP zones increase in number, however, their size remains almost constant. Then the GP zones start to dissolve and form particles of θ'' precipitates. The θ'' fine particles nucleate uniformly and are coherent with the matrix lattice structure. Extensive coherency-strain fields are developed due to the high degree of coherency, which leads to a significant increase in the strength of the alloy. The θ'' precipitates are fine and display small inter-particle distances which impede dislocation movement during plastic deformation, leading to high strength and hardness until peak

strength is achieved. As aging continues, the θ'' precipitates dissolve later, forming the θ' phase. As the precipitates of θ' grow, they start to lose coherency with the matrix, leading to reduction in the lattice distortion and consequently a decrease in strength. Any further aging causes the formation of equilibrium θ-Al_2Cu particles. These equilibrium precipitates are totally incoherent with the matrix, relatively large in size, and have a coarse distribution in the matrix as well as large inter-particle spacing. These characteristics lead to softening effects, and thereby a reduction in the strength and increase in ductility. The sequence of formation of these precipitates is as follows:

$$\alpha\text{ssss} \rightarrow \text{GP zones} \rightarrow \theta'' \rightarrow \theta' \rightarrow \theta\ (Al_2Cu)$$

When the alloys undergo T6 heat treatments (i.e. S4WA1 and S4WA2), maximum strength is reached, due to the formation of fine precipitates with high density in the aluminum matrix, with small inter-particle spacing, as illustrated in Figure 5-6(a). These changes make dislocation motion very difficult and result in strengthening effects, thereby increasing the strength. Whereas when the alloys A, B and C undergo T7 heat treatments (i.e. S4WA3 and S4WA4), the castings are over-aged and the strength starts to decrease. This is due to the formation of coarser precipitates with lesser density in the matrix, and displaying large inter-particle spacing, as displayed in Figure 5-6(b). These changes facilitate dislocation motion and result in softening effects, thereby reducing the strength. An EDS spectrum corresponding to the precipitates observed in (b) and showing the Cu content in the alloy is illustrated in Figure 5-6(c).

The three alloys showed the same trend regarding their response to the strengthening process. As these alloys reached their highest strength with the T6 heat treatment, in using

the T7 treatment, viz., increasing the aging temperature and time, they were over-aged, so that the strength decreased and the ductility increased, as explained above in detail. For example, for alloy B, the UTS, YS and %El values in the as-cast condition are 249.76 MPa, 166.94 MPa, 3.72%, respectively. With T6 heat treatment, specifically S4WA2, it achieved its highest strength with 373.67 MPa UTS, 304.22 MPa YS, and a ductility of 2.72%. Whereas after the T7 heat treatments (S4WA3 and S4WA4), the alloy started to soften and exhibit lower strength values and higher ductility. At ambient temperature, and with solution heat treatment for four hours, alloy B gave the highest strength values with the S4WA2 heat treatment.

Table 5-4: Average values of UTS, YS and %El obtained at ambient temperature for alloys A, B and C in the as-cast condition and when subjected to different heat treatment conditions with SHT for 4 h.

Alloy	Condition	UTS [MPa]	YS [MPa]	%EL [%]
Alloy A	AC	283.45	227.27	2.2
	S4A	311.31	194.42	3.94
	S4W	339.0	232.07	5.77
	S4WA1	372.76	297.28	1.25
	S4WA2	333.71	293.32	1.56
	S4WA3	331.2	260.11	2.16
	S4WA4	325.76	246.39	2.83
Alloy B	AC	249.76	166.94	3.72
	S4A	314.13	173.4	6.71
	S4W	327.37	206.1	4.0
	S4WA1	356.24	280.4	2.58
	S4WA2	373.67	304.22	2.72
	S4WA3	334.98	237.25	3.23
	S4WA4	311.61	220.63	3.53
Alloy C	AC	235.59	162.83	3.06
	S4A	267.38	160.89	3.56
	S4W	345.58	196.97	6.14
	S4WA1	353.31	281.67	2.17
	S4WA2	311.54	252.92	2.88
	S4WA3	308.63	221.59	3.03
	S4WA4	294.24	202.7	3.16

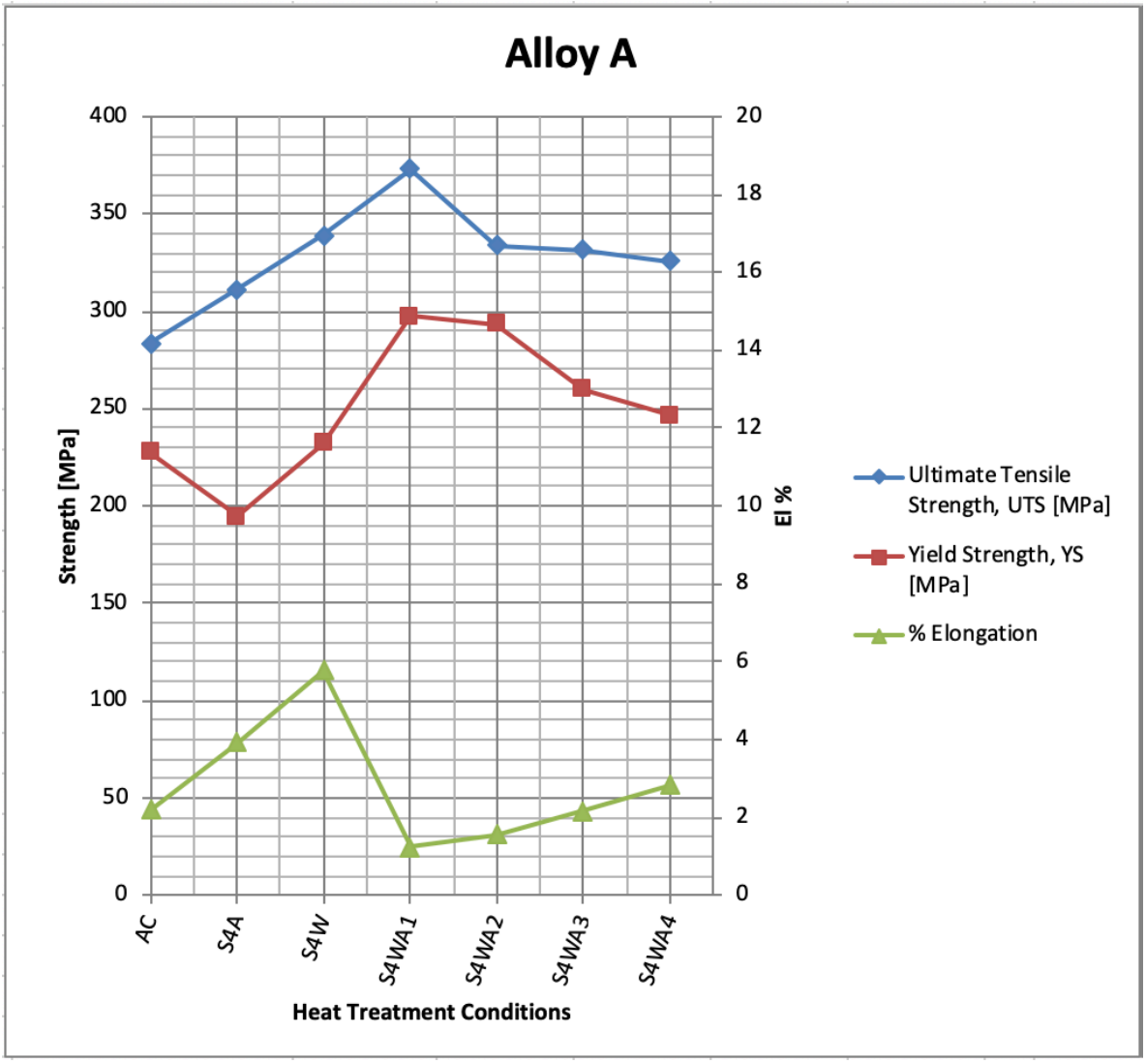

Figure 5-1: Average values of UTS, YS, %El obtained at ambient temperature, for alloy A in the as-cast condition, and after heat treatments comprising SHT for 4 h.

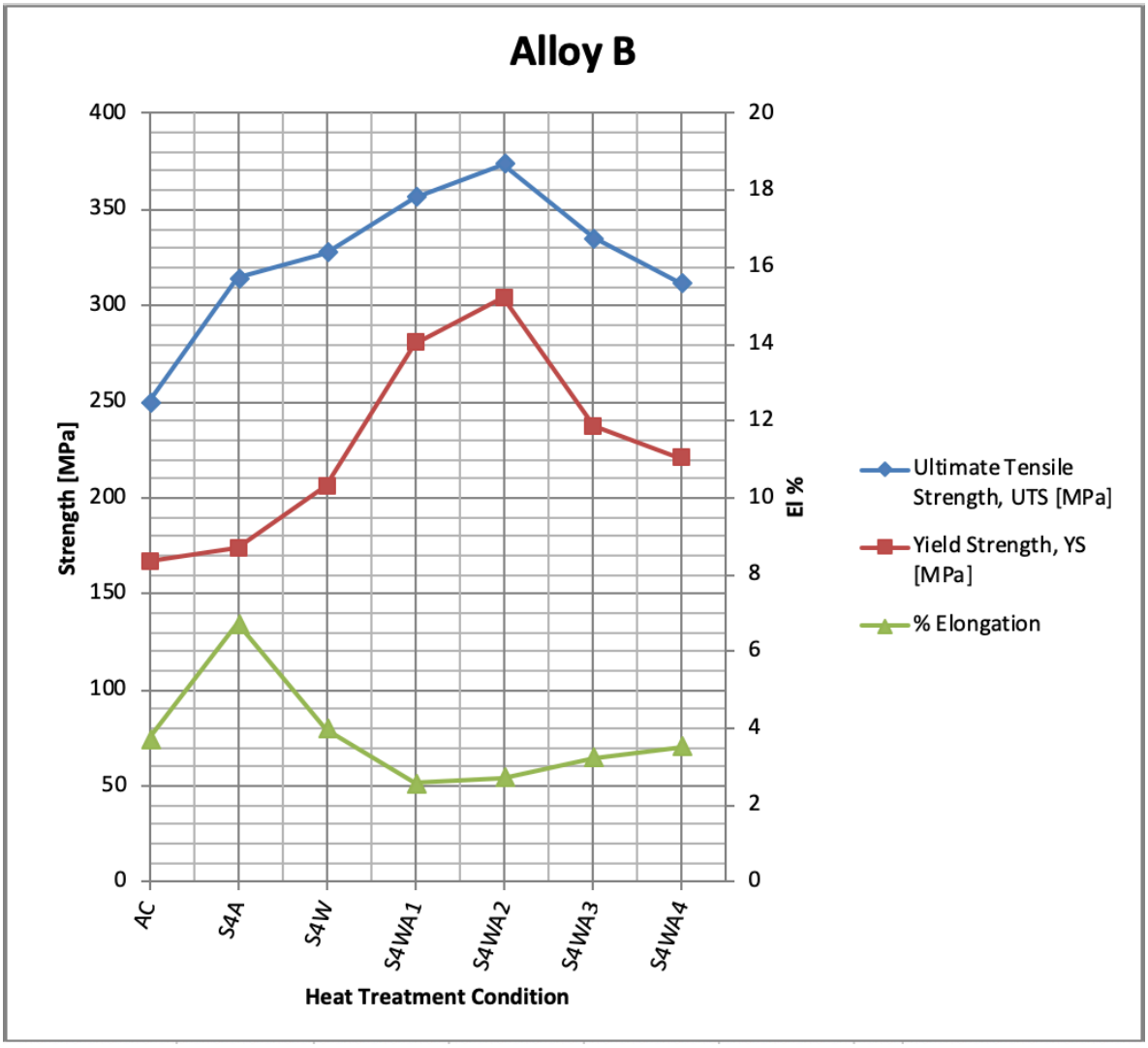

Figure 5-2: Average values of UTS, YS, %El obtained at ambient temperature, for alloy B in the as-cast condition, and after heat treatments comprising SHT for 4 h.

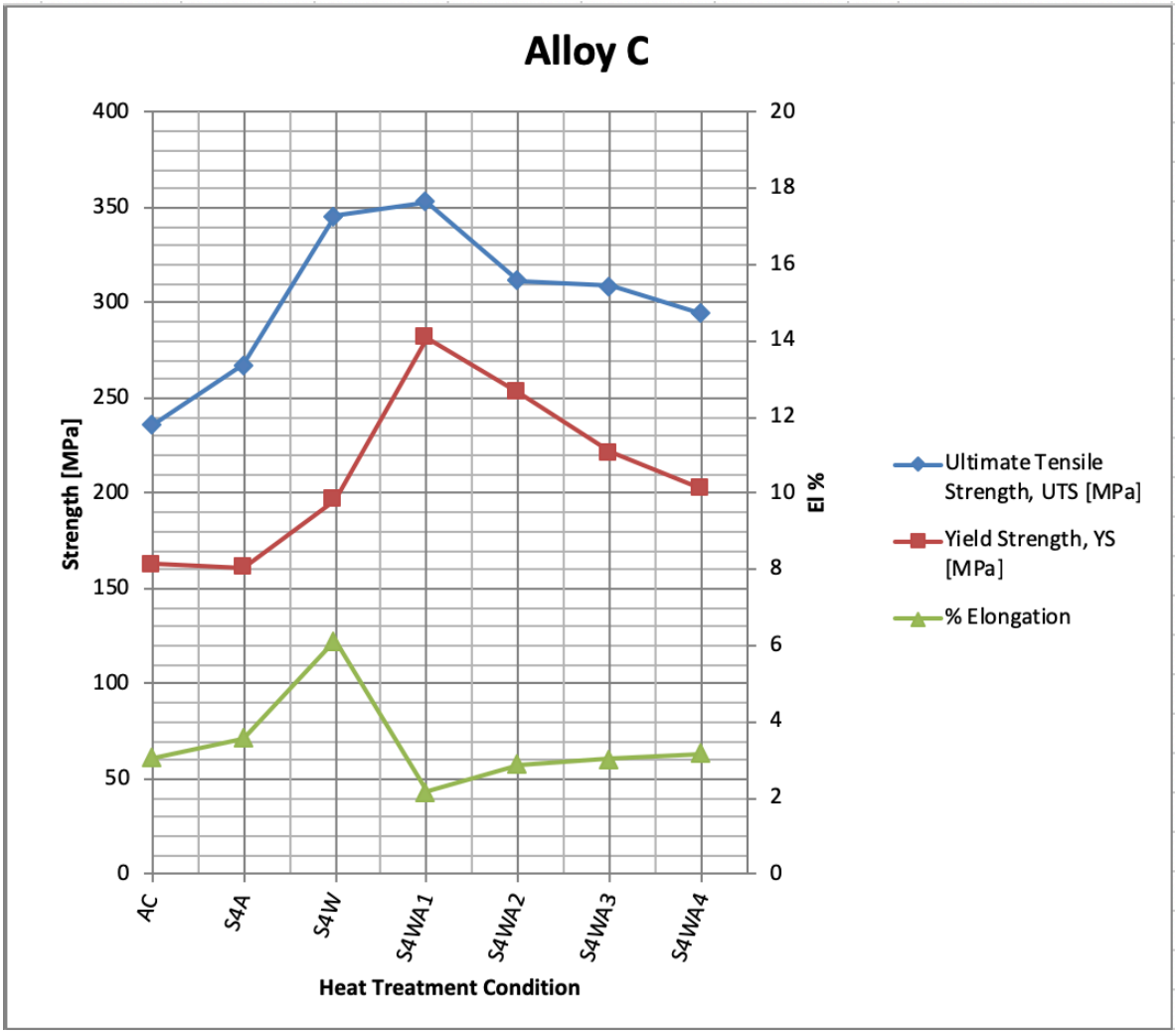

Figure 5-3: Average values of UTS, YS, %El obtained at ambient temperature, for alloy C in the as-cast condition, and after heat treatments comprising SHT for 4 h.

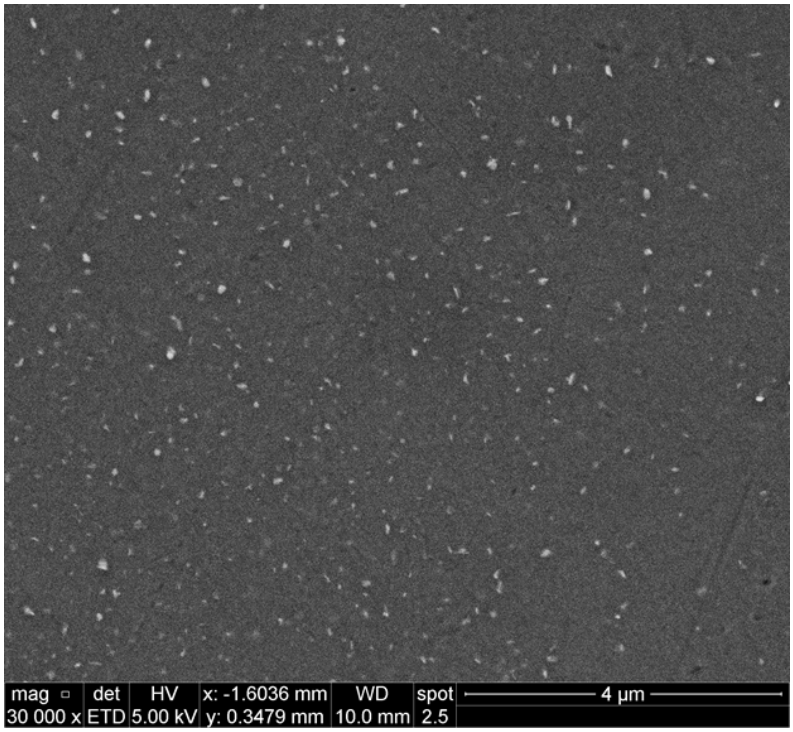

Figure 5-4: Micrograph of alloy B in the as-cast condition showing presence of precipitates in the matrix.

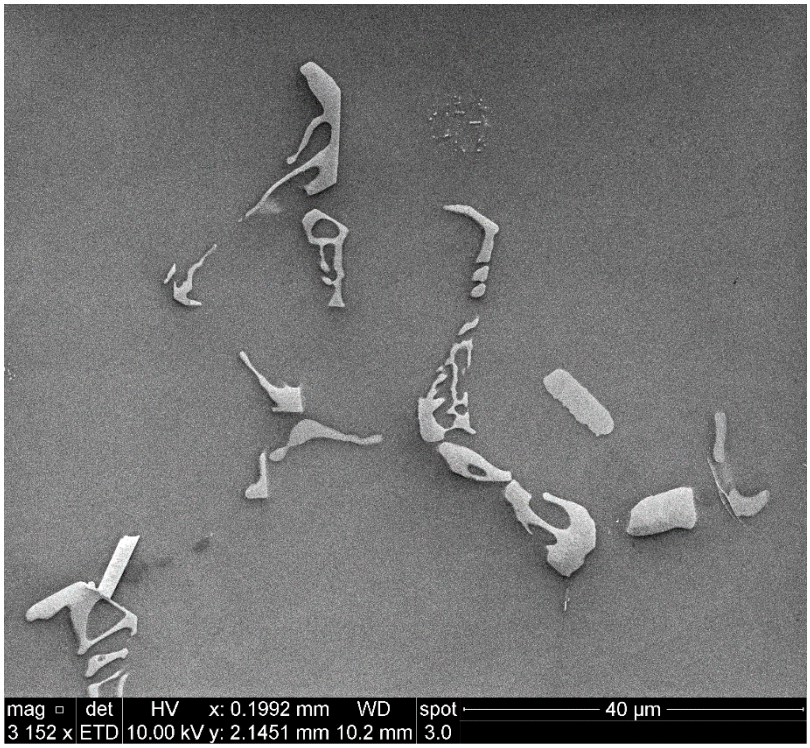

Figure 5-5: Micrograph of alloy B after SHT showing the script-like α-Fe phase.

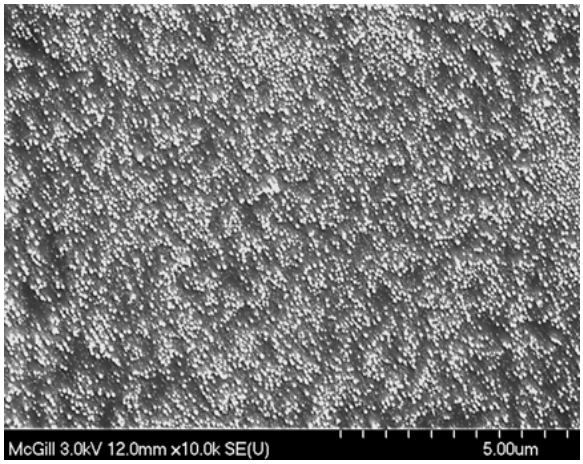

(a)

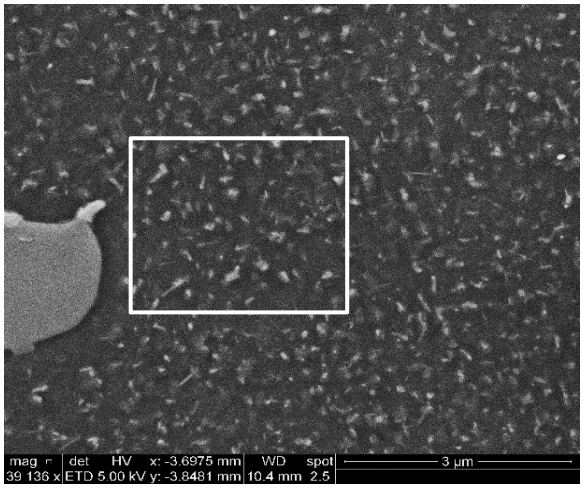

(b)

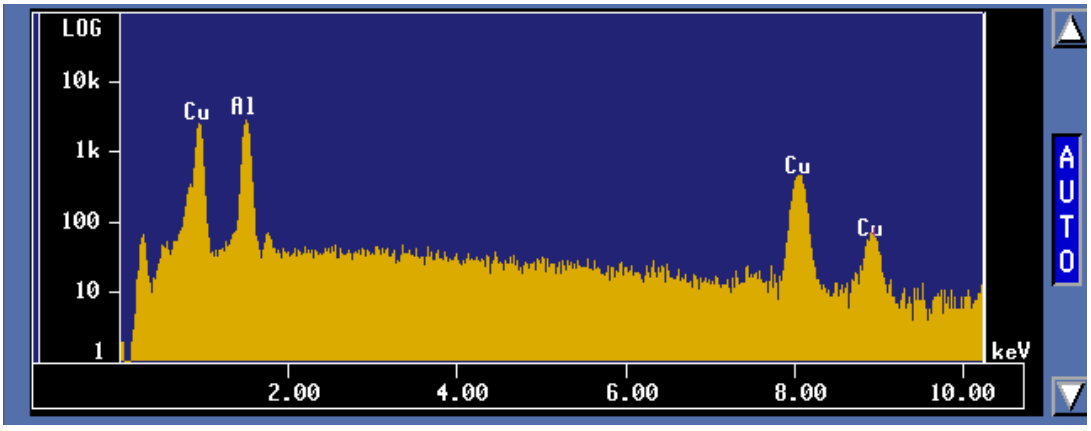

(c)

Figure 5-6: Alloy B corresponding to (a) T6 heat-treated, and (b) T7 heat-treated conditions; (c) EDS spectrum corresponding to the precipitates observed in the white square in (b).

The differences in the characteristics of the precipitates obtained following T6 and T7 heat treatments and their resultant influence on the alloy strength are illustrated schematically in Figure 5-7(a) and Figure 5-7(b), respectively. It can be seen clearly how the dense precipitation of fine particles in (a) with the T6 treatment, and the coarse particles with large inter-particle spacing obtained with the increased aging temperature and time in (b) with the T7 treatment would block the movement of dislocations in the first case, while facilitating it in the latter case, and subsequently strengthen the alloy or cause softening.

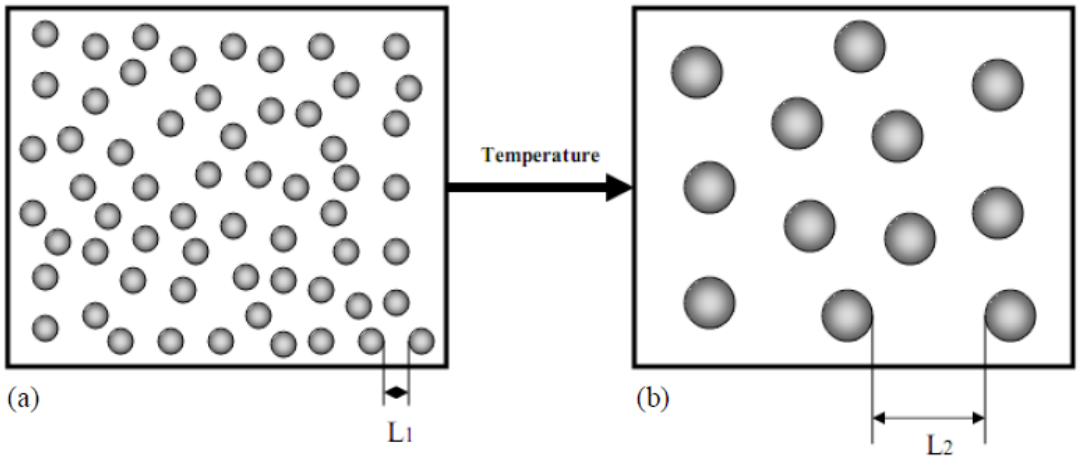

Figure 5-7: Schematic representation showing the influence of increasing aging temperature on the size, density, and inter-particle spacing of the hardening precipitates: (a) at a low aging temperature, and (b) at a high aging temperature (L1 and L2 indicate the inter-particle spacing in each case).

5.2.1.2 ANALYSIS OF TENSILE PROPERTIES USING THE QUALITY INDEX CONCEPT

As mentioned previously in Chapter 2, Drouzy *et al.* [78] [87], in their study of Al-7%Si-Mg or 356-type alloys, proposed the concept of the Quality Index Q as a means of better expressing the tensile properties of Al-Si-Mg alloys, in terms of how variations in Mg content and aging conditions affected the alloy "quality" or performance. This was done by the use of equations that allowed plotting charts of *iso-Q* lines versus *iso-Yield Strength* lines on a quality chart such that it became easy to see how the alloy quality was affected by the heat treatment and alloy composition.

Quality charts were generated in the present study for evaluating the influence of metallurgical parameters on the tensile properties. Equations 1 and 2 from Chapter 2 were used to generate *iso-Q* lines and *iso-Yield Strength* lines, respectively. The *iso-Q* and *iso-YS* lines in these charts facilitate knowing which additions are beneficial for improving the alloy properties. It is possible to improve the strength of the alloys, by increasing the copper content, although this would result in a reduction in ductility [88] [89] [90]. The strengthening effect obtained by adding Cu to an Al-9wt%Si-0.5wt%Mg alloy is based on the formation of Cu- and Cu-Mg-containing precipitates such as θ-Al_2Cu, S-$Al_5Cu_2Mg_8Si_6$, Q-$Al_5Cu_2Mg_8Si_6$, and may be further optimized by applying adequate heat treatment procedures [91] [92] [93]. The quality of these castings will be affected according to the net amount by which the increase in strength is balanced by the reduction in ductility, since the Q-values are derived as a function of the ultimate tensile strength (UTS) and the percentage elongation (%El).

From the tensile test data shown in Table 5-4, quality index or Q values as well as the probable yield strength were calculated and are listed in Table 5-5. Quality charts were then generated for evaluating the influence of the metallurgical parameters involved on the tensile properties and quality of the HT200 aluminum alloys investigated.

Table 5-5: Q and Probable YS (PYS) values obtained from the tensile test results in Table 5-4, and using Equations 1 and 2 from Chapter 2.

Average values of UTS (MPa) and El (%) used to obtain Q and Probable YS values using: Q=UTS+150log(%El) … (1) PYS=UTS-60log(%El)+13 … (2)			
Alloy	**Condition**	**Q [MPa] Eqn (1)**	**PYS [MPa]. Eqn (2)**
Alloy A	AC	334.67	275.96
	S4A	400.61	288.59
	S4W	453.21	306.32
	S4WA1	387.1	380.03
	S4WA2	362.72	335.11
	S4WA3	381.32	324.13
	S4WA4	393.47	311.67
Alloy B	AC	335.29	228.54
	S4A	438.16	277.51
	S4W	417.54	304.3
	S4WA1	417.93	344.57
	S4WA2	438.84	360.6
	S4WA3	411.36	317.43
	S4WA4	393.86	291.71
Alloy C	AC	308.4	219.47
	S4A	350.14	247.27
	S4W	463.82	311.28
	S4WA1	403.75	346.13
	S4WA2	380.41	297.0
	S4WA3	380.91	292.73
	S4WA4	369.26	277.23

The ultimate tensile strength (UTS) is normally used for the specification and quality control of the casting, while the ductility of the casting, expressed as percent elongation to fracture, is usually used as an indicator of casting quality because of its sensitivity to the presence of any impurity or defect in the cast structure. On the other hand, yield strength does not represent the quality of the casting since it is a material property which is not affected by the level of defects or impurities present in the casting, but is influenced, rather, by the movement of dislocations in the casting structure, and depends on the resistance expected by the hardening precipitates to the movement of dislocations [94]. In general, therefore, quality charts provide a simple tool for estimating and recommending the appropriate processing conditions to obtain specified properties and hence to facilitate the selection of castings to meet these specifications.

Figure 5-8 presents the quality chart showing the relationship between UTS and %El for the alloys A, B and C in the as-cast and six heat treatment conditions, for tests carried out at ambient temperature. The optimum results would be located in the upper-right corner of the chart (high Q and high YS). The best combination of Q and PYS values was selected for each of the alloys investigated, for the different heat treatments applied, in order to determine the optimum alloy composition/heat treatment condition. Alloy A reads a Q-value of 453.2 MPa and a PYS-value of 306.3 MPa in the S4W heat treatment condition. Alloy B reads a Q-value of 438.8 MPa and a PYS-value of 360.6 MPa in the S4WA2 heat treatment condition. Alloy C reads a Q-value of 463.8 MPa and a PYS-value of 311.2 MPa in the S4W heat treatment condition. Although the Q-value of alloy B is slightly less than in alloys A and C, the PYS of alloy B is significantly higher. Therefore, alloy B composition, in the S4WA2

heat treatment condition (T6), is considered to be the optimum alloy composition/heat treatment condition for the four hours solution heat treatment group at the room temperature.

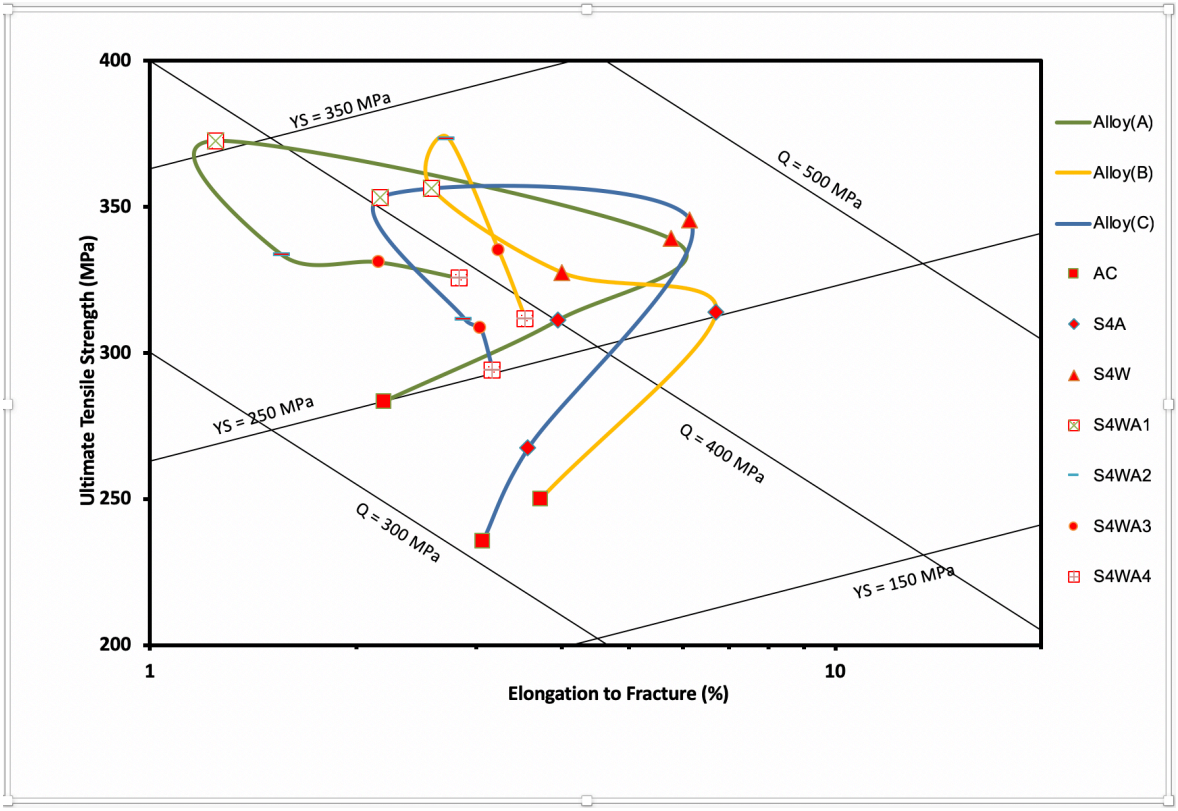

Figure 5-8: Quality chart showing relationship between UTS and %El for the A, B and C alloys investigated in the as-cast and six heat treatment conditions with SHT for 4 h.

5.2.1.3 STATISTICAL ANALYSIS (COMPARISON BETWEEN BASE ALLOY AND OTHER ALLOYS)

This section presents comparison of the tensile properties (UTS, YS and %El) of the different alloys under different heat treatments, following solution heat treatment for four hours, with the base alloy A in the as-cast condition. Figure 5-9 depicts the tensile properties obtained at ambient temperature for Alloys A, B and C for these different heat treatment conditions, *relative* to the values obtained for the base alloy A in the as-cast condition, i.e., after subtracting the values obtained for the base alloy A for each condition, and plotted as ΔP values on the Y-axis (P = Property = UTS, YS or %El), with the X-axis representing the base line for alloy A. The numbers on the X-axis represent the as cast condition and the different heat treatment conditions used. These conditions are indicated by numbers to facilitate reading the data. The condition to which each of these numbers refers to is provided in Table 5-1. The use of this method provides an effective means of knowing how the various additions made and the different heat treatment conditions applied affect the properties of the HT200 casting alloy.

From Figure 5-9, it can be seen that the mechanical properties of the base alloy A are enhanced after the heat treatments. The strength and the ductility are both improved with the S4W and S4WA4 heat treatment conditions; whereas with the S4WA1, S4WA2 and S4WA3 heat treatments, the strength is improved but the ductility is decreased. Regarding alloy B, the mechanical properties were improved with the addition of the grain refiners (Ti and Zr) as well as the heat treatments applied, particularly when artificial aging was included, namely, with the S4WA1, S4WA2 and S4WA3 treatments. Similarly, in the case of alloy C, also, the mechanical properties improved with the addition of Ti, Zr and Ag, and with heat

treatment, particularly with the S4WA2 treatment. With S4WA1 heat treatment, however, the improvement in strength was accompanied by a decrease in the ductility.

As may be seen from Figure 5-9(c), the ductility of the base alloy A (HT200 alloy) is enhanced in alloys B and C regardless the heat treatment condition. The improvement in ductility is therefore due to the addition of the alloying elements to the base alloy, since alloy B and alloy C are derived from the HT200 alloy following 0.15%Ti + 0.15%Zr and 0.15%Ti + 0.15%Zr + 0.5%Ag additions, respectively. Thus, the addition of the grain refiners Ti and Zr plays an important role in enhancing the ductility of HT200 alloys. From an analysis of the ΔP values, it can be concluded that alloy B in the S4WA2 heat treated condition (following SHT for four hours), provides the optimum alloy composition/heat treatment condition for the HT200 alloy.

Comparison of the tensile properties of the five alloys A, B, C, D and E with those of the as-received base alloy A are shown in Figure 5-10. At room temperature, alloy A exhibits good tensile properties (UTS, YS and %El) in the as-cast condition with respect to the as-cast reference alloys D and E. This is due to the high percentage of Cu content (6.5 wt%) which provides high strength. In general, adding grain refiners and alloying elements together with heat treatments (using SHT for four hours) led to good combinations of mechanical properties (UTS, YS and %El) of the HT200 alloys investigated in this study.

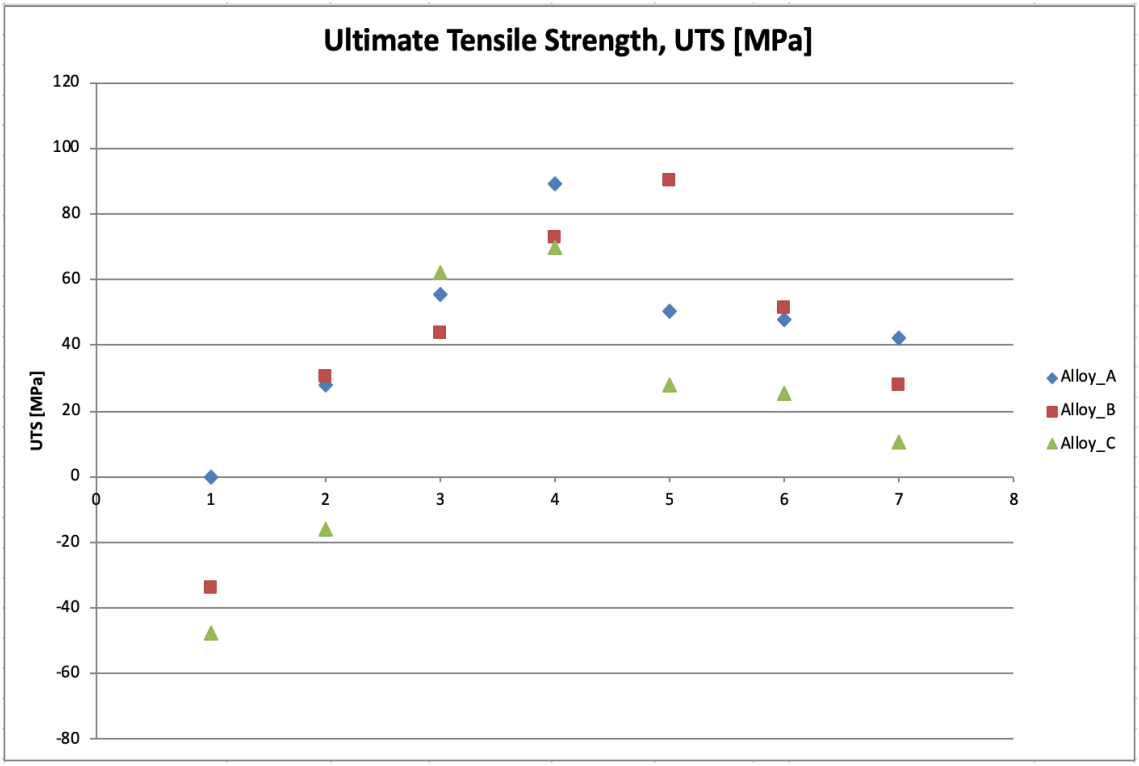
Ultimate Tensile Strength, UTS [MPa]
UTS [MPa]
120
100
80
60
40
20
0
-20
-40
-60
-80
0
1
2
3
4
5
6
7
8
Alloy_A
Alloy_B
Alloy_C

(a)

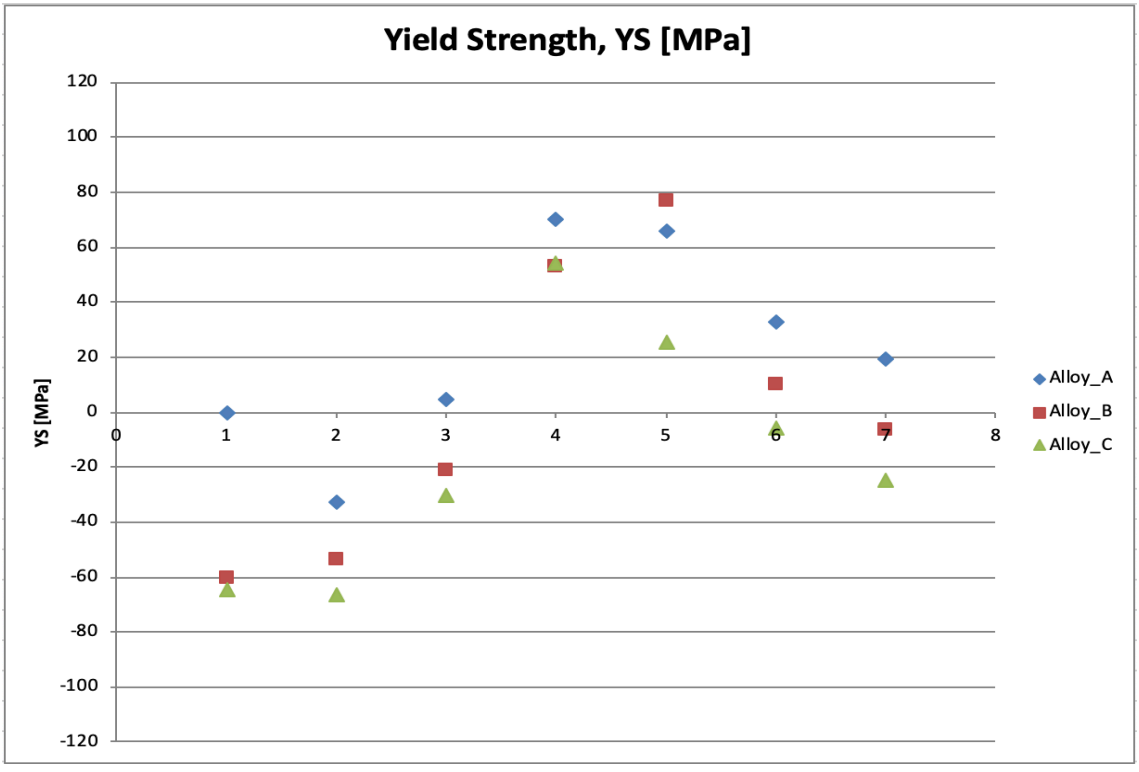
Yield Strength, YS [MPa]
YS [MPa]
120
100
80
60
40
20
0
-20
-40
-60
-80
-100
-120
0
1
2
3
4
5
6
7
8
Alloy_A
Alloy_B
Alloy_C

(b)

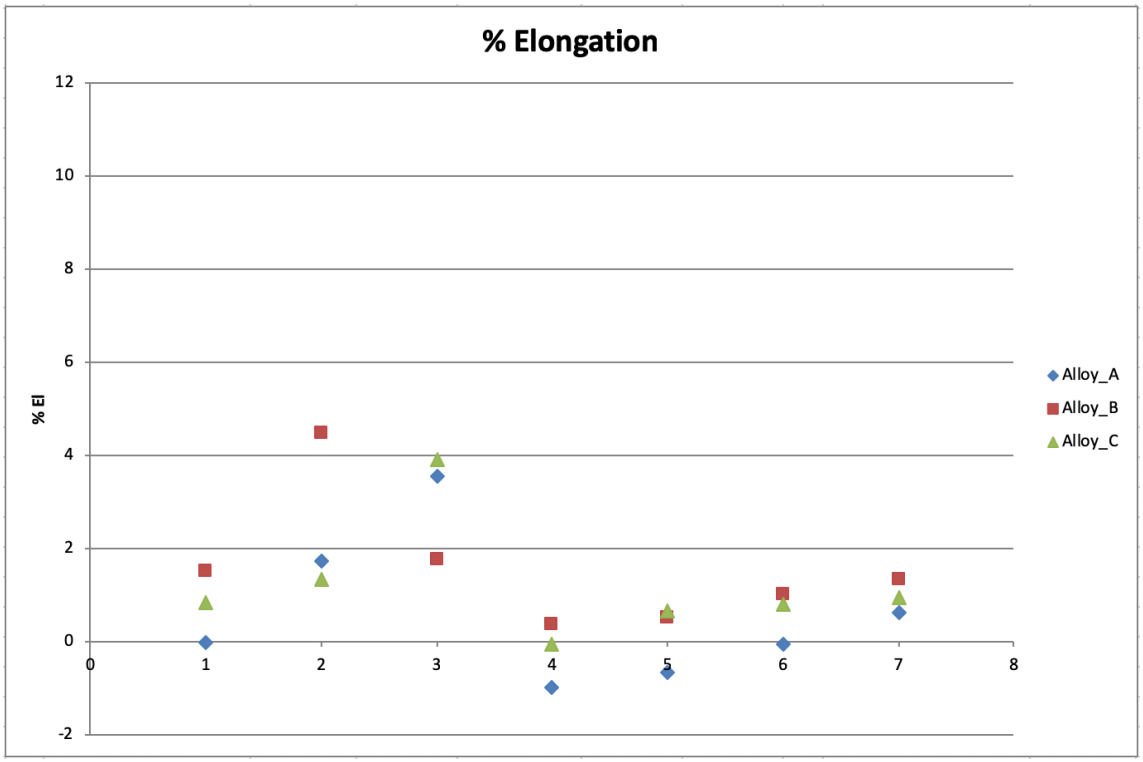

(c)

Figure 5-9: Comparison of tensile properties of A, B and C alloys relative to those of as-cast base alloy A: (a) ΔP-UTS, (b) ΔP-YS, and (c) ΔP-%El as a function of heat treatment condition with SHT for 4 h.

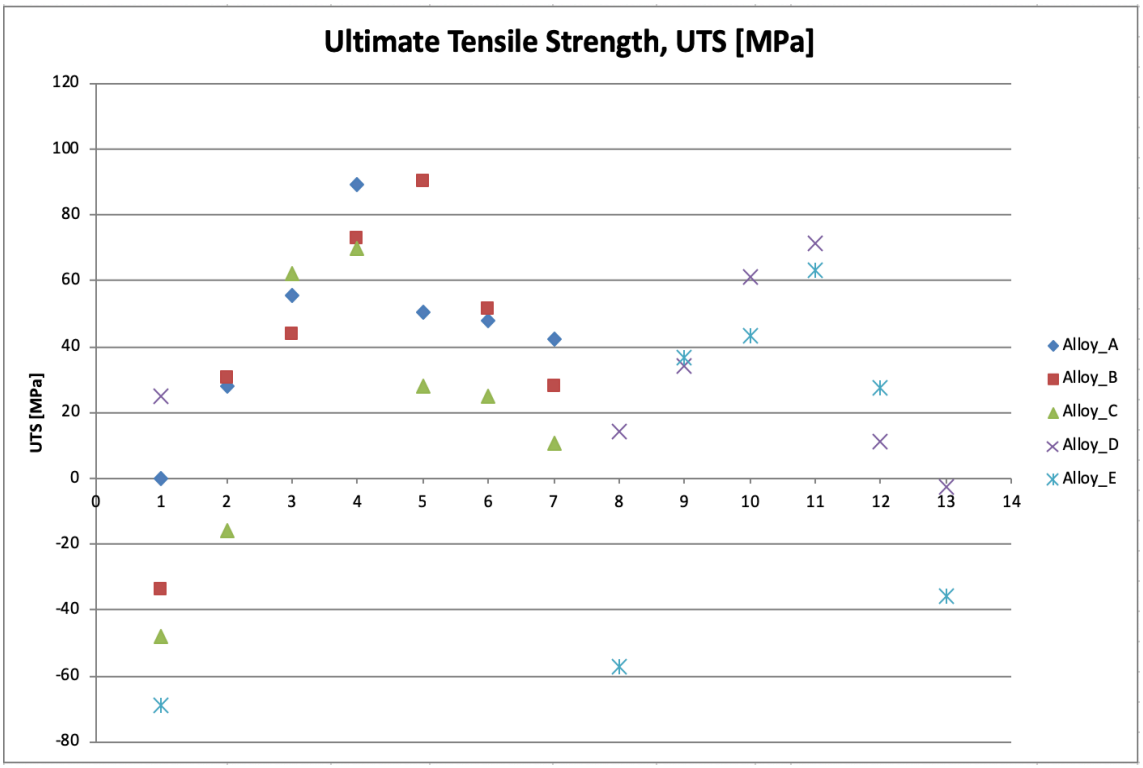

(a)

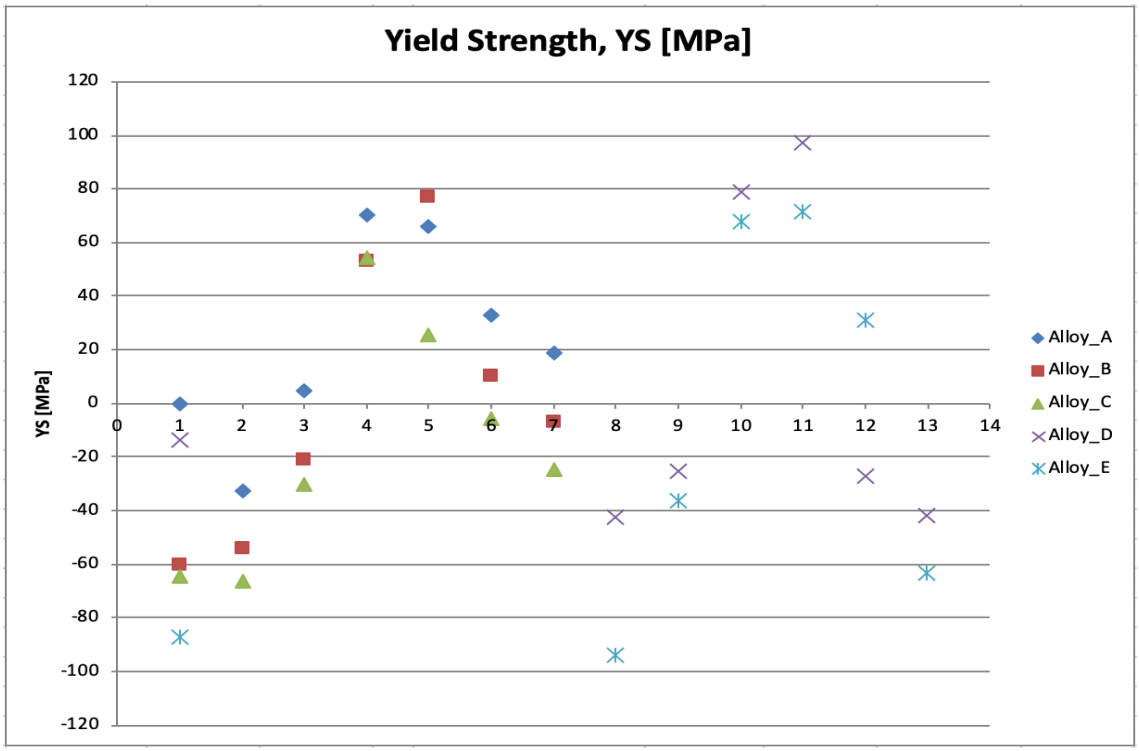

(b)

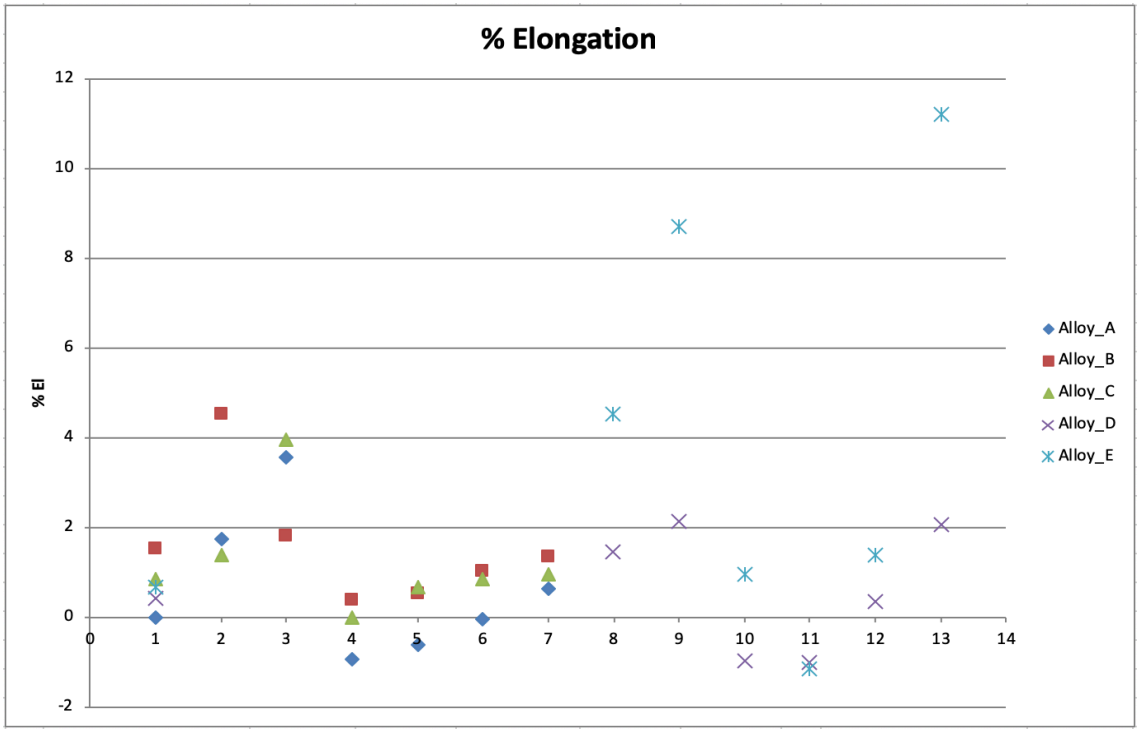

(c)

Figure 5-10: Comparison of tensile properties of A, B, C, D and E alloys relative to those of as-cast base alloy A: (a) ΔP-UTS, (b) ΔP-YS, and (c) ΔP-%El as a function of heat treatment condition with SHT for 4 h.

5.2.2 RESULTS FOR AS-CAST AND 8 HRS-SOLUTION HEAT TREATED CONDITIONS

5.2.2.1 TENSILE TEST RESULTS

This section discusses the tensile properties results of the alloys A, B, C, D and E in the as-cast and heat-treated conditions following solution heat treatment for eight hours. Six heat treatment conditions were used in this group, namely S8A, S8W, S8WA1, S8WA2, S8WA3 and S8WA4. The description of these heat treatment conditions is shown in Table 5-1 and Table 5-2. Alloys A, B and C, were solution treated at 520°C for eight hours, Alloy D was solution treated at 500°C for eight hours, and Alloy E was solution treated at 540°C for eight hours. The tensile properties (UTS, YS and %El) of alloys A, B, C, D and E are provided in Table 5-6 and shown in Figure 5-11 through Figure 5-15. Again, as in the case of the four hours SHT group, the charts in the figure show that the tensile properties are improved for the three alloys A, B and C when heat-treated. The same behavior is exhibited by the reference alloys D and E when heat-treated; they have shown improvements in the tensile properties; as shown in Figure 5-14 and Figure 5-15.

In the first two heat treatment conditions, S8A and S8W, when solution treatment is followed by air or water quenching, the improvement in the tensile properties is attributed to the solution heat treatment (SHT) and the high cooling rate. As with SHT, the maximum amount of hardening solutes of Cu are retained in solid solution in the matrix. That is to obtain and to form a homogeneous supersaturated solid solution at elevated temperatures, which is done by dissolving the existing phases like θ-Al_2Cu in the as cast structure into solution. When the sample is quenched, or cooled rapidly, thereafter, the supersaturated solid

solution formed during the solution treatment is preserved, by means of rapid cooling to some lower temperature, usually near the room temperature. It retains the solute atoms in the solution and blocks them in the positions where they got to at the high temperature during the SHT, and makes the casting ready for subsequent strengthening during the aging stage. As seen from the results for the five alloys, solution treatment followed by water quenching produces better tensile properties. The reason for this is the higher cooling rate achieved with water quenching than air quenching. Some exceptions were noted, that is when the heat-treated samples showed lower values than the as cast condition. The reason for this can be explained based on the casting process, as when the tensile bars were cast they were left to cool in the air, which caused natural aging. This natural aging resulted in some precipitates which provided some strength to the castings, as illustrated in Figure 5-4.

In the solution heat-treated/water quenched condition, alloy A exhibited values of 289.61 MPa, 213.2 MPa and 6.23% for the UTS, YS and %El, respectively, compared to 283.44 MPa, 227.27 MPa and 2.2%, respectively, in the as-cast condition. Alloy B attained values of 363.56 MPa UTS, 190.13 MPa YS, and 12.15% percentage elongation, from 249.76 MPa UTS, 166.94 MPa YS, and 3.72% in the as-cast condition; while the UTS, YS and %El values for alloy C improved to 345.13 MPa, 175.15 MPa and 8.52%, respectively, from 235.59 MPa, 162.83 MPa and 3.05% f in the as-cast condition. The tensile properties of the reference alloy D increased to 317.36 MPa, 201.7 MPa and 4.34% for the UTS, YS and %El, respectively, from 308.21 MPa, 213.5 MPa and 2.62% in the as-cast condition, while alloy E exhibited values of 320 MPa, 191.13 MPa and 10.9% for the UTS, YS and %El, respectively, compared to 214.59 MPa, 140.11 MPa and 2.85% in the as-cast case. The improvement in

tensile properties may be explained based on the same reasons discussed in the preceding paragraphs.

Aging treatment, which follows solution heat treating and quenching, as in the S8WA1, S8WA2, S8WA3 and S8WA4 heat treatment conditions, is used for strengthening, and is controlled by the aging temperature and time. Strengthening is achieved through precipitation hardening (or age hardening), and the main strengthening precipitates in Al-Cu alloys are those of the θ-Al_2Cu phase. After solution treatment and quenching, the solute atoms, which exist in the supersaturated solid solution, SSSS, start to form clusters of atoms known as Guinier-Preston (GP) zones. The solute atoms in these GP zones consist of ordered groups that are coherent with the lattice structure and dispersed within the matrix. Usually these atoms have different sizes than those of the lattice structure of the aluminum matrix; therefore distortion occurs in the lattice structure, producing coherency-strain fields, which leads to a significant improvement in strength. These GP zones are metastable and they dissolve later in the presence of a more stable phase. As the aging treatment progresses, the GP zones dissolve, and metastable coherent or semi-coherent precipitates start forming. These precipitates continue to grow by diffusion of atoms from the SSSS, which results in achieving maximum or peak strength. As aging continues further, the metastable coherent precipitates later become totally incoherent. In this condition, the opposition of the precipitates to dislocation movement is reduced, and in turn leads to a consequent reduction in strength.

When T6 treatment is used, as in S8WA1, S8WA2 heat treatment conditions, peak aging was achieved, as the precipitates were fine, coherent and displayed small inter-particle spacing; therefore the strength increased significantly. As may be seen in Figure 5-11 through

Figure 5-15, alloy A reached its highest strength in the S8WA1 condition, displaying 355.68 MPa, 285.25 MPa and 1.24% as its UTS, YS and %El values, respectively (*cf.* 283.45 MPa, 227.27 MPa and 2.2% in the as-cast case). Alloy B reached its highest strength in the S8WA2 condition, giving 388.57 MPa UTS, 292.24 MPa YS, and 3.15% ductility values, compared to 249.76 MPa, 166.94 MPa and 3.72%, respectively, in the as-cast condition. Alloy C reached its highest strength following S8WA1 treatment (*cf.* 352.0 MPa UTS, 274.86 MPa YS and 2.88% with 235.59 MPa, 162.83 MPa, and 3.06% in the as-cast condition). Alloy D reached its highest strength after S8WA2 treatment, showing 354.8 MPa UTS, 324.36 MPa YS, and 1.2% El, respectively, compared to 308.21 MPa, 213.5 MPa, and 2.62% in the as-cast condition. Alloy E also achieved its highest strength with the S8WA2 treatment, giving 346.46 MPa UTS, 298.46 MPa YS, and 1.05 %El (*cf.* 214.59 MPa, 140.11 MPa and 2.85%, respectively, in the as-cast case).

When the T7 heat treatment was used, i.e., as in the S8WA3 treatment when the aging temperature was increased, or as in the S8WA4 treatment, when both temperature and time were increased, over-aging occurred. That is to, say that the precipitates coarsened and increased in size, so that a lower density of precipitates displaying large inter-particle distances was obtained. This facilitated dislocation movement, producing softening effects that decreased the alloy strength. Thus, when the test bars were over-aged, the strength decreased and the ductility increased. Again, for ambient temperature testing of the HT200 alloys, alloy B showed the highest strength values in the S8WA2 heat treated condition (with SHT for eight hours).

Table 5-6: Average values of UTS, YS and %El obtained at ambient temperature for alloys A, B, C, D and E in the as-cast condition and when subjected to different heat treatment conditions with SHT for 8 h.

Alloy	Condition	UTS [MPa]	YS [MPa]	%EL [%]
Alloy A	AC	283.45	227.27	2.2
	S8A	319.72	182.95	5.12
	S8W	289.61	213.2	6.23
	S8WA1	355.68	285.25	1.24
	S8WA2	322.32	254.22	1.26
	S8WA3	317.33	250.74	2.07
	S8WA4	311.43	219.51	2.57
Alloy B	AC	249.76	166.94	3.72
	S8A	311.88	166.49	6.87
	S8W	363.56	190.13	12.15
	S8WA1	367.47	281.39	3.2
	S8WA2	388.57	292.24	3.15
	S8WA3	346.25	247.59	3.27
	S8WA4	331.0	219.58	3.73
Alloy C	AC	235.59	162.83	3.06
	S8A	268.75	155.67	4.45
	S8W	345.13	175.15	8.52
	S8WA1	352.0	274.86	2.88
	S8WA2	344.8	272.65	3.2
	S8WA3	335.77	236.14	3.32
	S8WA4	304.11	209.63	3.39
Alloy D	AC	308.21	213.5	2.62
	S8A	297.84	184.62	3.65
	S8W	317.37	201.7	4.34
	S8WA1	344.54	306.26	1.21
	S8WA2	354.8	324.36	1.2
	S8WA3	294.77	199.97	2.55
	S8WA4	280.93	185.56	4.24
Alloy E	AC	214.59	140.11	2.85
	S8A	226.0	133.65	6.71
	S8W	320.01	191.13	10.91
	S8WA1	326.62	294.91	3.16
	S8WA2	346.46	298.46	1.05
	S8WA3	310.83	258.47	3.57
	S8WA4	247.81	164.11	13.41

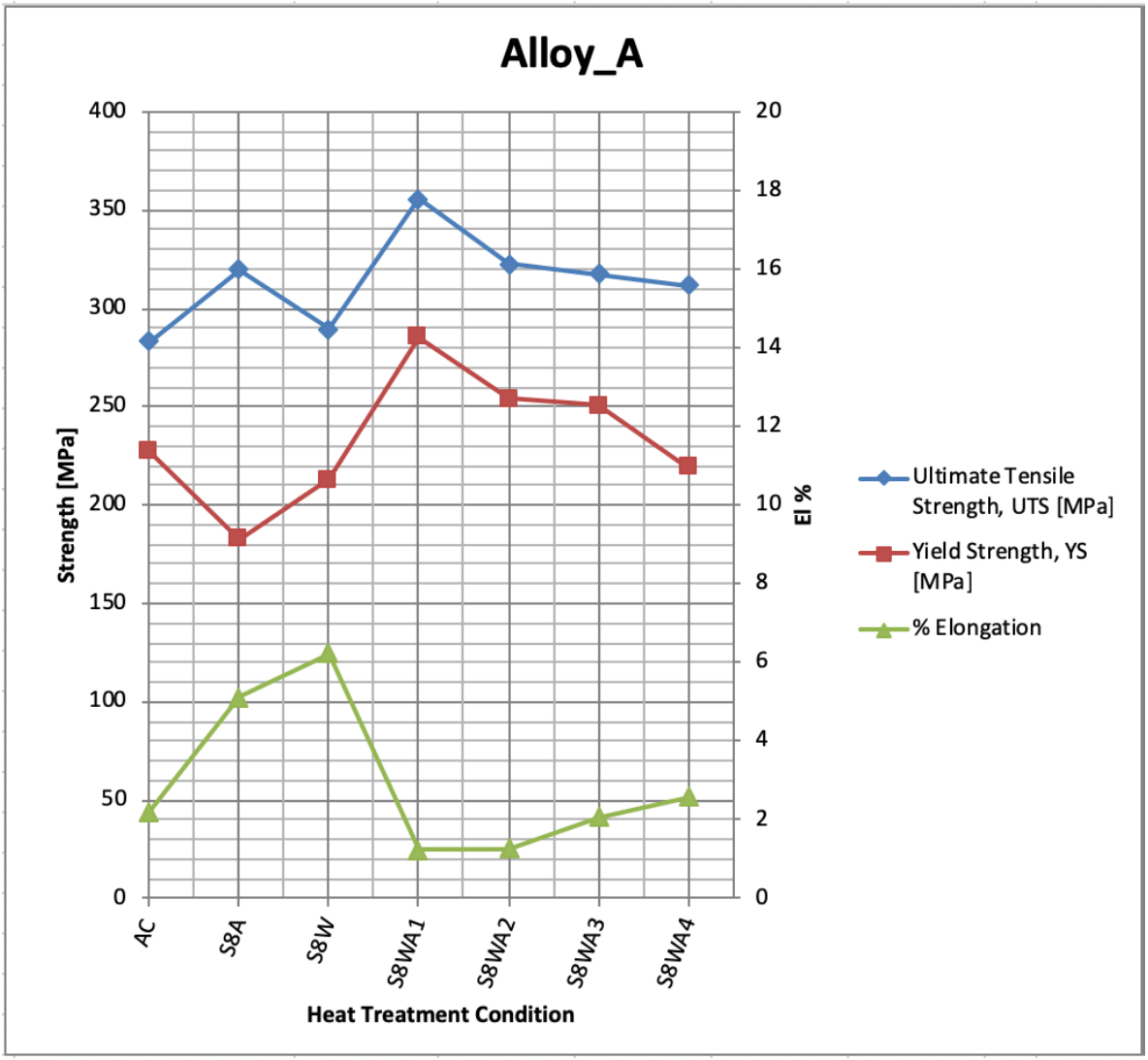

Figure 5-11: Average values of UTS, YS, %El obtained at ambient temperature, for alloy A in the as-cast condition, and after heat treatments comprising SHT for 8 h.

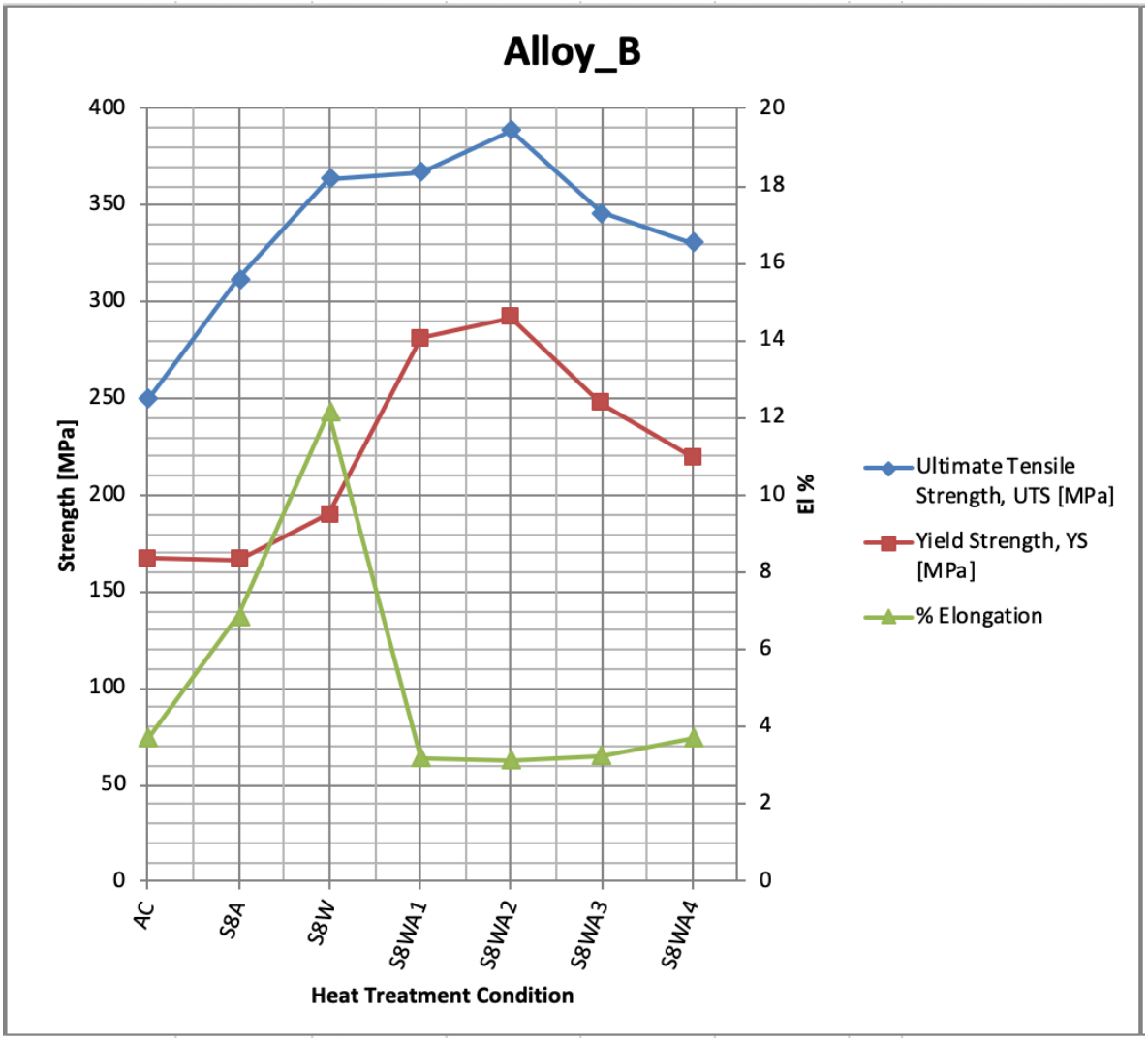

Figure 5-12: Average values of UTS, YS, %El obtained at ambient temperature, for alloy B in the as-cast condition, and after heat treatments comprising SHT for 8 h.

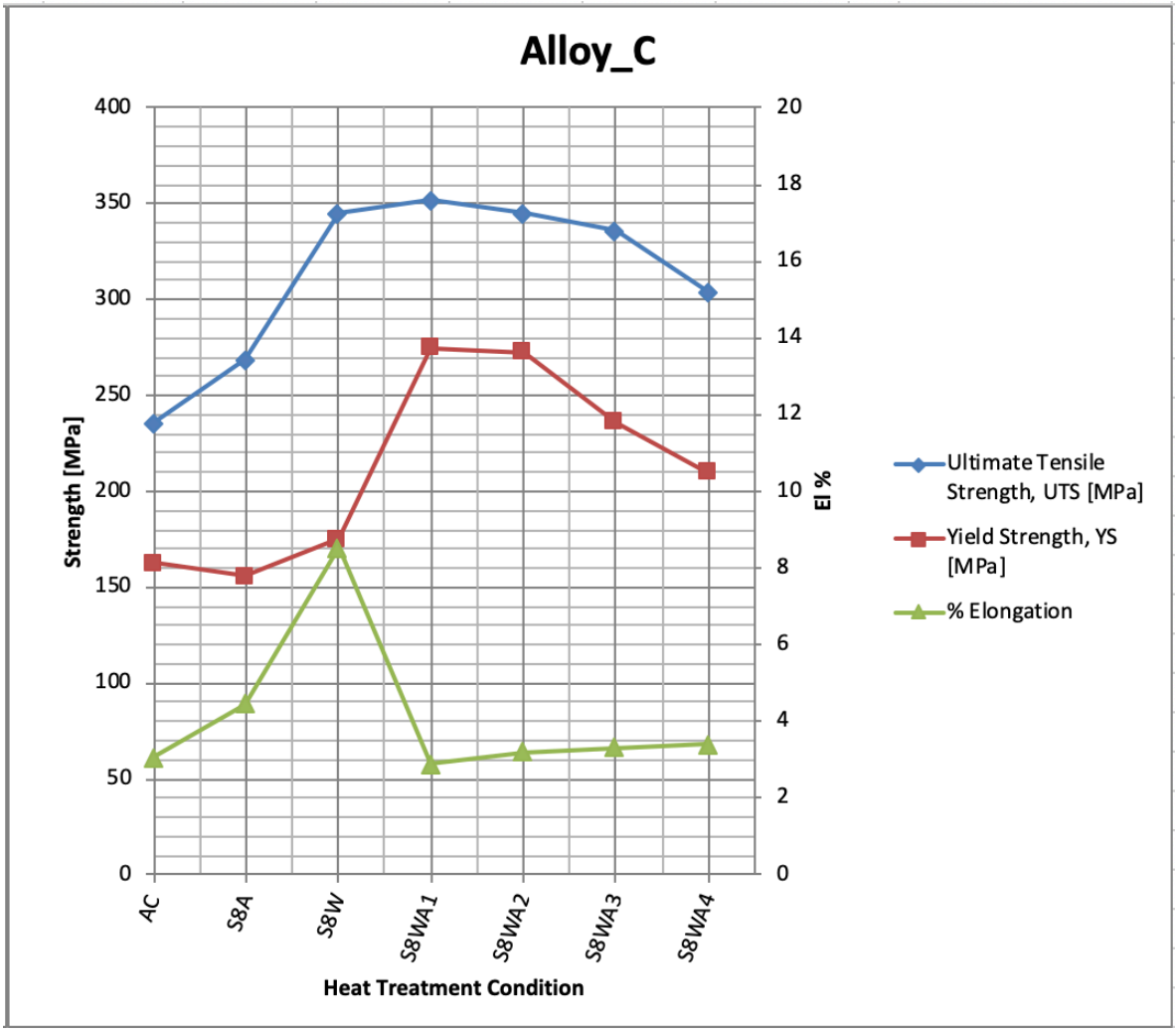

Figure 5-13: Average values of UTS, YS, %El obtained at ambient temperature, for alloy C in the as-cast condition, and after heat treatments comprising SHT for 8 h.

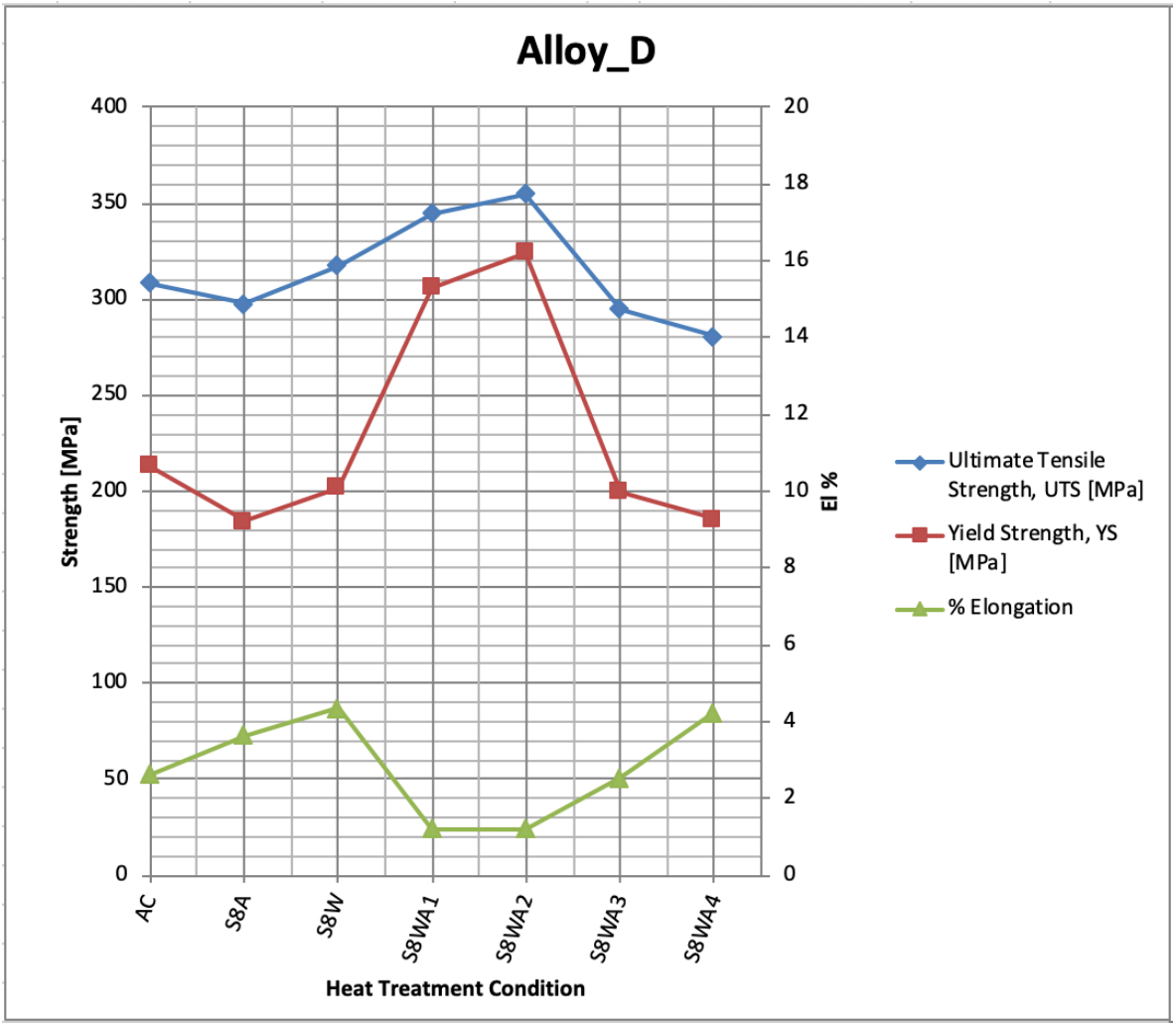

Figure 5-14: Average values of UTS, YS, %El obtained at ambient temperature, for alloy D in the as-cast condition, and after heat treatments comprising SHT for 8 h.

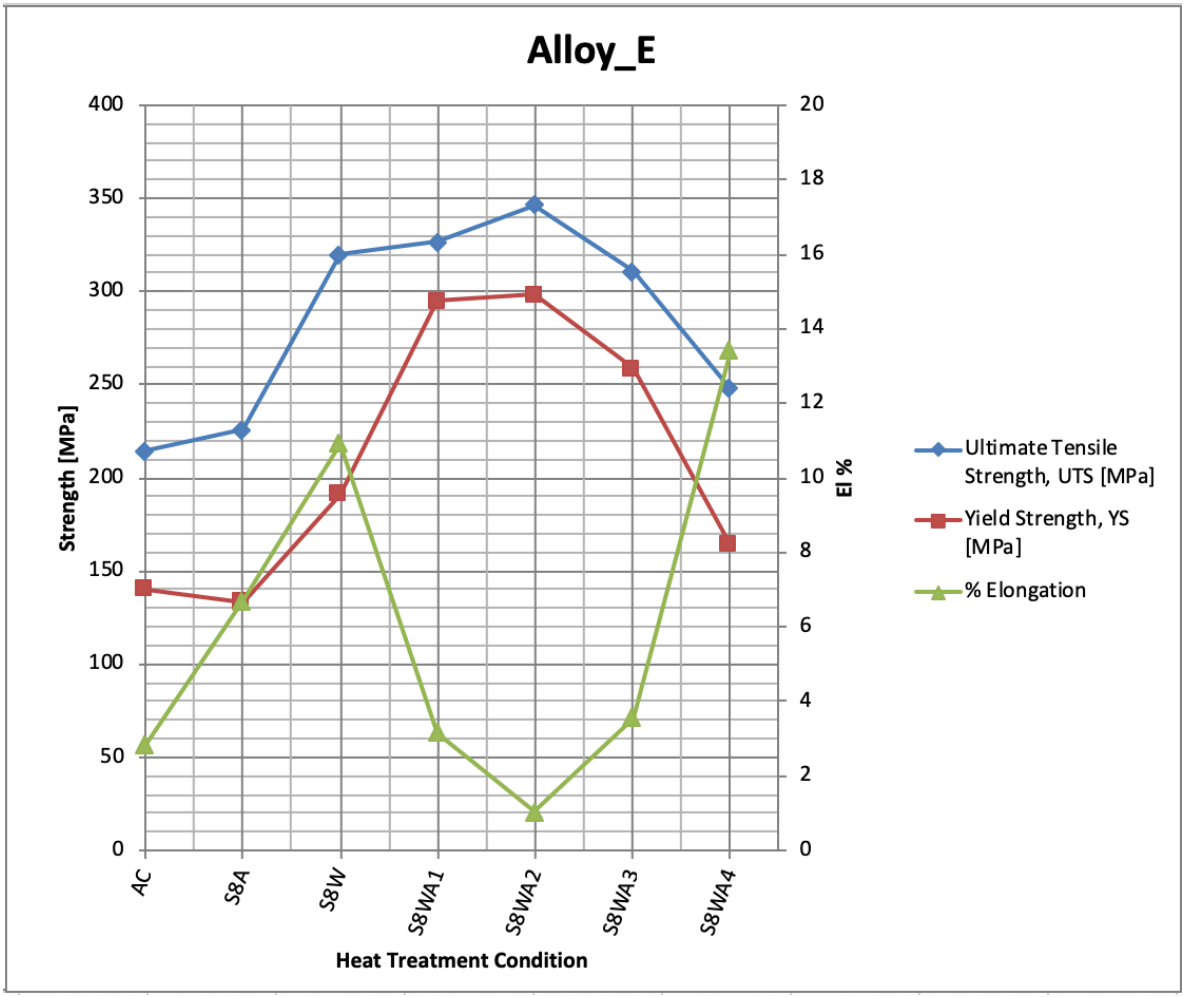

Figure 5-15: Average values of UTS, YS, %El obtained at ambient temperature, for alloy E in the as-cast condition, and after heat treatments comprising SHT for 8 h.

5.2.2.2 ANALYSIS OF TENSILE PROPERTIES USING THE QUALITY INDEX CONCEPT

As mentioned earlier in this chapter, quality charts provide a very good tool in giving an indication for the effect of different heat treatments and/or chemical composition changes on the strength and ductility of casting alloys.

Using the tensile test data shown in Table 5-6, quality index or Q values as well as the probable yield strength were calculated and are listed in Table 5-7. Quality charts were then generated for evaluating the influence of the metallurgical parameters involved on the tensile properties and quality of the HT200 aluminum alloys investigated.

Table 5-7: Q and Probable YS (PYS) values obtained from the tensile test results in Table 5-6, and using Equations 1 and 2 from Chapter 2.

Average values of UTS (MPa) and El (%) used to obtain Q and Probable YS values using: Q=UTS+150log(%El) … (1) PYS=UTS-60log(%El)+13 … (2)			
Alloy	**Condition**	**Q [MPa] Eqn (1)**	**PYS [MPa]. Eqn (2)**
Alloy A	AC	334.67	275.96
	S8A	426.06	290.18
	S8W	408.78	254.95
	S8WA1	369.77	363.04
	S8WA2	337.62	329.21
	S8WA3	364.86	311.32
	S8WA4	372.93	299.83

Alloy B	AC	335.29	228.54
	S8A	437.38	274.68
	S8W	526.25	311.48
	S8WA1	443.26	350.16
	S8WA2	463.24	371.7
	S8WA3	423.47	328.36
	S8WA4	416.74	309.71
Alloy C	AC	308.4	219.47
	S8A	365.98	242.85
	S8W	484.73	302.29
	S8WA1	420.86	337.45
	S8WA2	420.4	327.55
	S8WA3	413.98	317.49
	S8WA4	383.65	285.29
Alloy D	AC	371.05	296.07
	S8A	382.26	277.07
	S8W	412.98	292.12
	S8WA1	356.92	352.58
	S8WA2	366.54	363.11
	S8WA3	355.63	283.43
	S8WA4	375.03	256.29
Alloy E	AC	282.77	200.32
	S8A	350.03	189.38
	S8W	475.71	270.73
	S8WA1	401.65	309.61
	S8WA2	349.56	358.22
	S8WA3	393.79	290.65
	S8WA4	416.95	193.16

Quality charts showing the relationship between UTS and %El are shown in Figure 5-16 for the alloys A, B and C, and in Figure 5-17 for alloys D and E. The as-cast and six heat treatment conditions, comprising solution heat treatment for eight hours, are plotted in these charts. The optimum results can be found in the upper-right corner (high Q and high YS). The best combination of Q-value and PYS-value was chosen for each of the alloys investigated under different heat treatment conditions, in order to determine the optimum alloy composition/heat treatment condition. Alloy A had a Q-value of 426 MPa and a PYS-value of 254.9 MPa following S8A heat treatment, and a Q-value of 369.7 MPa and PYS-value of 363 MPa after S8WA1 heat treatment. Alloy B exhibited a Q-value of 526.2 MPa and a PYS-value of 311.4 MPa in the S8W heat-treated condition, and a Q-value of 463.2 MPa and a PYS-value of 371.7 MPa after S8WA2 heat treatment. Alloy C showed a Q-value of 484.7 MPa and a PYS-value of 302.2 MPa after S8W heat treatment, and a Q-value of 420.8 MPa and a PYS-value of 337.4 MPa after S8WA1 treatment. Regarding the reference alloys, alloy D had a Q-value of 412.9 MPa and a PYS-value of 292.1 MPa in the S8W heat-treated condition, and a Q-value of 366.5 MPa and a PYS-value of 363.1 MPa after S8WA2 heat treatment. Lastly, alloy E reached a Q-value of 475.7 MPa and a PYS-value of 270.7 MPa with S8W heat treatment, and a Q-value of 349.5 MPa and a PYS-value of 358.2 MPa following S8WA2 heat treatment.

In the Quality (Q) and probable yield strength (PYS) values listed above, two heat treatment conditions were selected per alloy, one without aging and the other included aging. The Q-values for the heat treatments comprising solution heat treatment for eight hours, with no aging were higher due to the higher ductility values. Whereas with aging, in the T6 heat treatments, the Q-values decreased and the PYS-values were higher due to the higher strength

caused by aging. From the results mentioned above, alloy B showed higher values, for both heat treatment conditions - without and with aging, than alloys A and C. Alloy B also showed higher values for both heat treatment conditions without and with aging than the reference alloys D and E.

By comparing the results for alloy B in the T6 heat-treated condition S4WA2 with solution heat treatment for four hours (438.8 MPa Q-value; 360 MPa PYS), with those obtained in the T6 heat-treated condition S8WA2 but with solution heat treatment for eight hours (463 MPa Q-value; 371 MPa PYS), it can be concluded that alloy B in the T6 heat treatment condition S8WA2 provides the optimum alloy composition/heat treatment condition among both solution heat treatment groups (4 hrs and 8 hrs) for achieving the best tensile properties and alloy quality for HT200 alloy at room temperature.

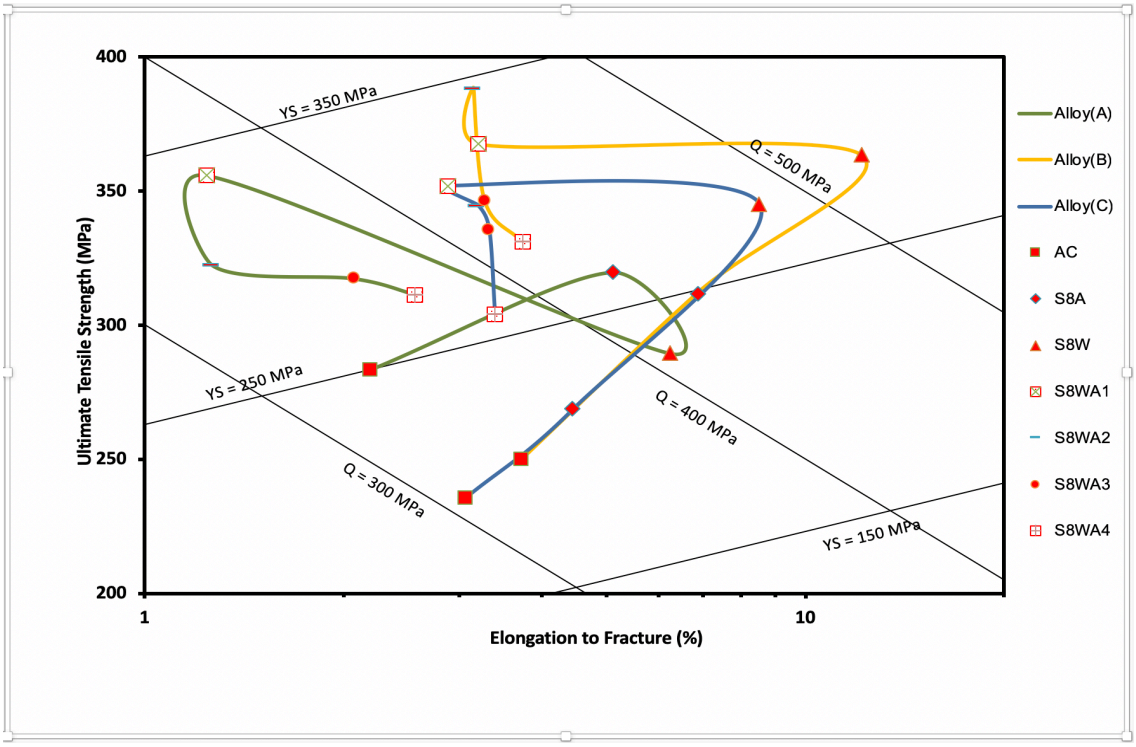

Figure 5-16: Quality chart showing relationship between UTS and %El for the A, B and C alloys investigated in the as-cast and six heat treatment conditions with SHT for 8 h.

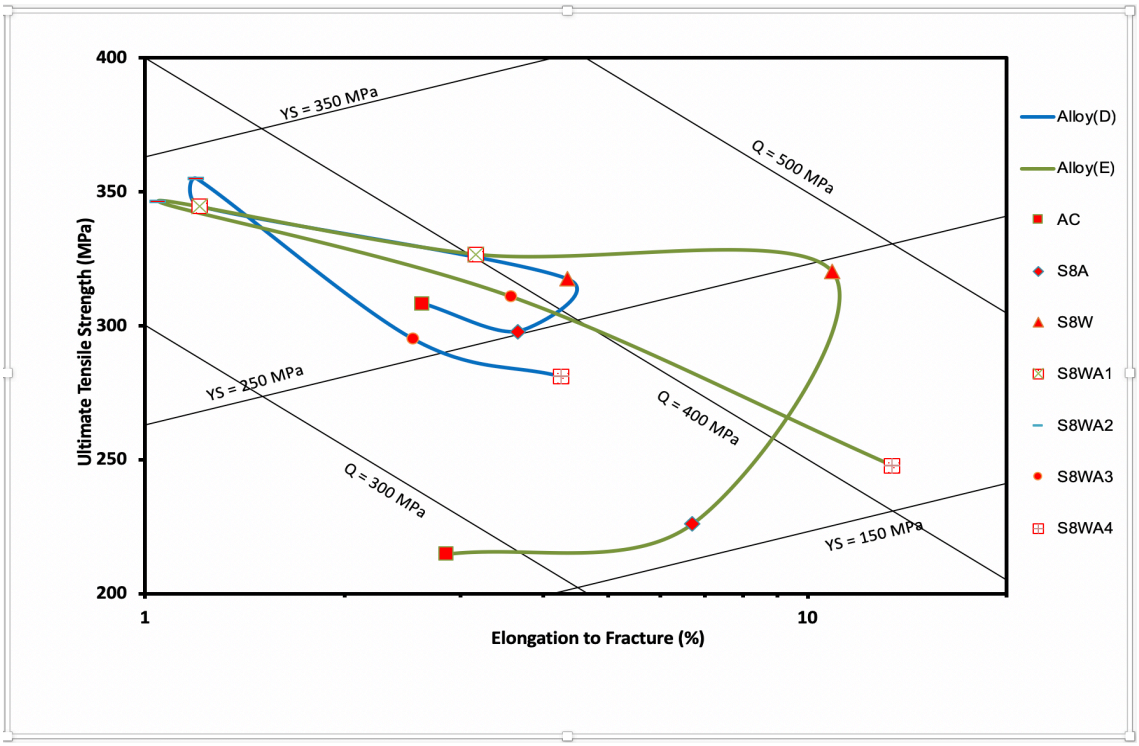

Figure 5-17: Quality chart showing relationship between UTS and %El for the D and E alloys investigated in the as-cast and six heat treatment conditions with SHT for 8 h.

Figure 5-18 presents a panel chart showing the Q-values corresponding to alloys A, B, C, D and E, in the as-cast condition and for the two groups of heat treatment conditions, comprising six heat treatment conditions with solution heat treatment for four hours and another six with solution heat treatment for eight hours. The chart in Figure 5-19 compares the Q-values of the five alloys, in the as-cast, and all the heat treatment conditions studied. As may be seen, alloy B gives the best overall performance across the range of heat treatments employed. With respect to the reference alloys, the HT200 alloy with a composition corresponding to alloy B appears to be a better choice. An interesting observation is that a comparable alloy quality is obtained for HT200 alloy with shorter solution/heat treatments.

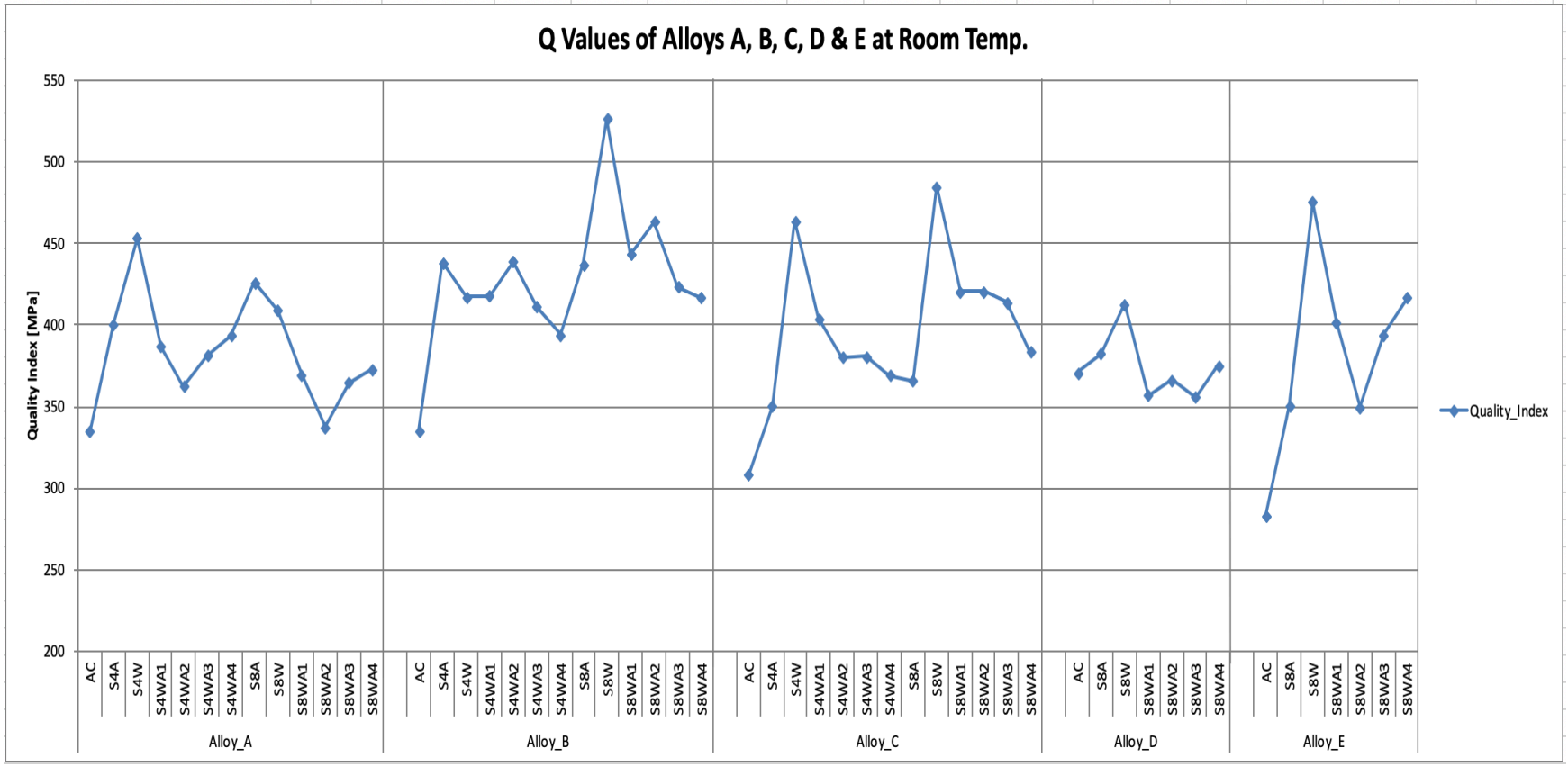

Figure 5-18: A panel chart for the quality values of alloys A, B, C, D and E in the as-cast condition and the 12 heat treatment conditions used in this study.

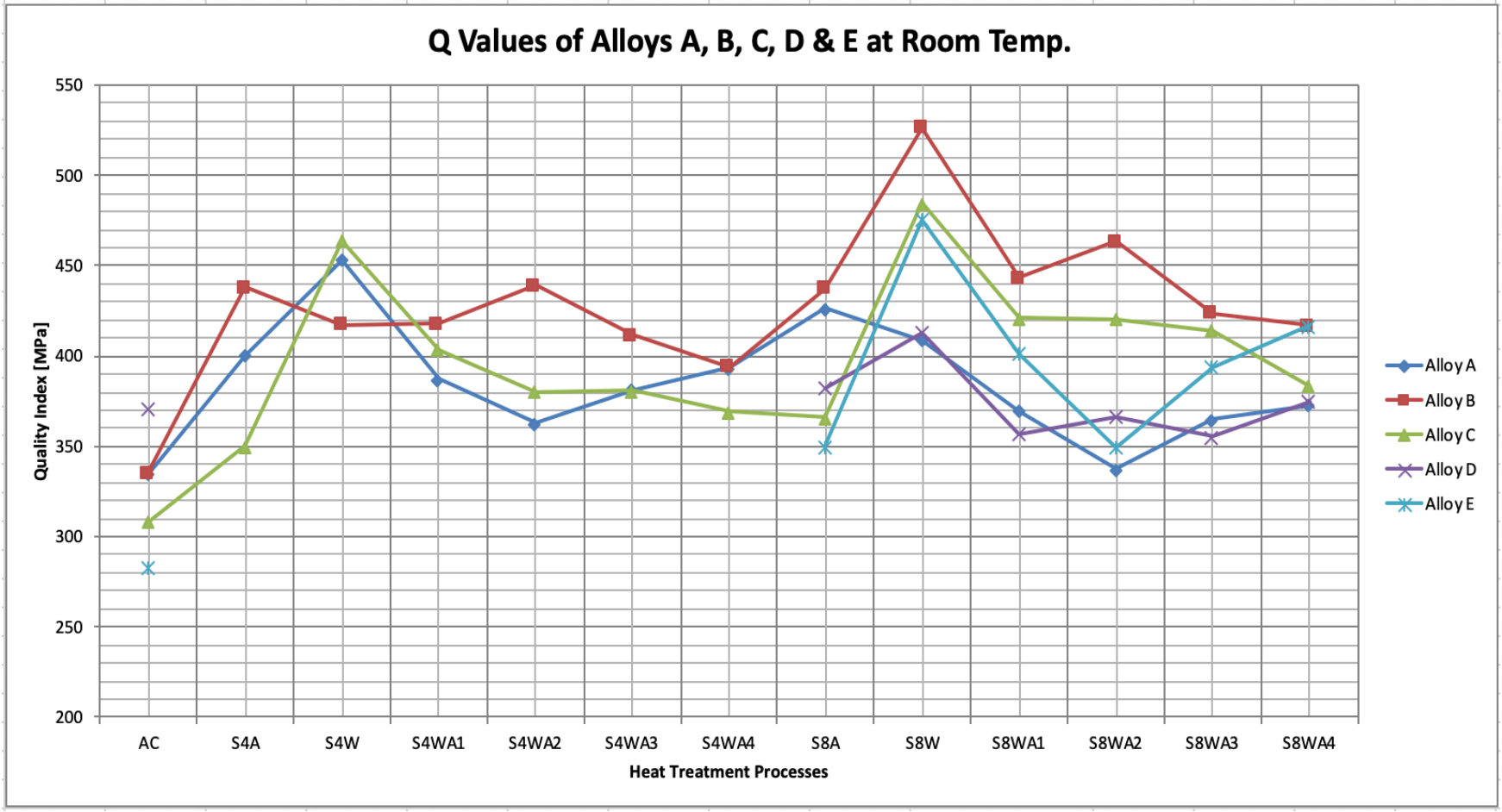

Figure 5-19: Quality values of alloys A, B, C, D and E in the as-cast condition and the 12 heat treatment conditions used in this study.

5.2.2.3 STATISTICAL ANALYSIS (COMPARISON BETWEEN BASE ALLOY AND OTHER ALLOYS)

This section presents a comparison of the tensile properties (UTS, YS and %El) of the different alloys under different heat treatment conditions, following solution heat treatment for eight hours, with those of the as-cast base alloy A. Figure 5-20 depicts the tensile properties obtained at room temperature for Alloys A, B and C for these different heat treatment conditions, with SHT for eight hours, relative to the values obtained for the base alloy A at the as-cast condition, i.e., after subtracting the values obtained for the base alloy A for each condition, and plotted as ΔP values on the Y-axis (P = Property = UTS, YS or %El), with the X-axis representing the base line for alloy A. The numbers on the X-axis represent the as-cast condition and the different heat treatment conditions used. These conditions are indicated by numbers to facilitate reading the data. As before, each of the numbers and the condition they refer to is provided in Table 5-1. Property differences in values, ΔP, with respect to the different heat treatments, with SHT for eight hours, are also presented for the reference alloys D and E, which are shown in Figure 5-21. The use of this method provides an effective means of knowing how the various additions made and the different heat treatment conditions applied affect the properties of the HT200 casting alloy.

Regarding alloys A, B and C, it may be seen from Figure 5-20, that their mechanical properties were generally enhanced. The strength of the base alloy A was improved with some of the applied heat treatment conditions, namely; S8WA1, S8WA2 and S8WA3, whereas the ductility decreased. Regarding alloy B, both the strength and the ductility were improved due to the addition of the grain refiners (Ti and Zr) as well as the heat treatments

applied, particularly when artificial aging was included, as was noted with the heat treatment conditions S8WA1, S8WA2 and S8WA3. Similar observations were made for alloy C; the mechanical properties improved with the addition of the Ti, Zr and Ag, as well as the heat treatments S8WA1, S8WA2 and S8WA3, as in the case of alloy A and alloy B.

As may be seen from Figure 5-20 (c), the ductility of the base alloy A is enhanced in alloys B and C regardless the heat treatment condition. Thus, the presence of the grain refiners Ti and Zr in alloy B as well as in alloy C plays an important role in enhancing the ductility of HT200 alloys.

Regarding the reference alloys D and E, it may be seen from Figure 5-21 that their mechanical properties were generally enhanced. The strength of alloy D improved with S8WA1 and S8WA2 heat treatments, whereas the ductility decreased. In the case of alloy E, both the strength and the ductility were improved with the heat treatments S8WA1 and S8WA3.

Figure 5-22 compares the room temperature tensile properties of the five alloys A, B, C, D and E with those of the as received base alloy A. As may be seen, alloy A showed comparable tensile properties (UTS, YS and %El) in the as cast condition with respect to the reference alloys D and E in the as cast condition as well as in the heat treatment conditions with SHT for eight hours. This is due to the high percentage of Cu content (6.5 wt% Cu) which provides high strength.

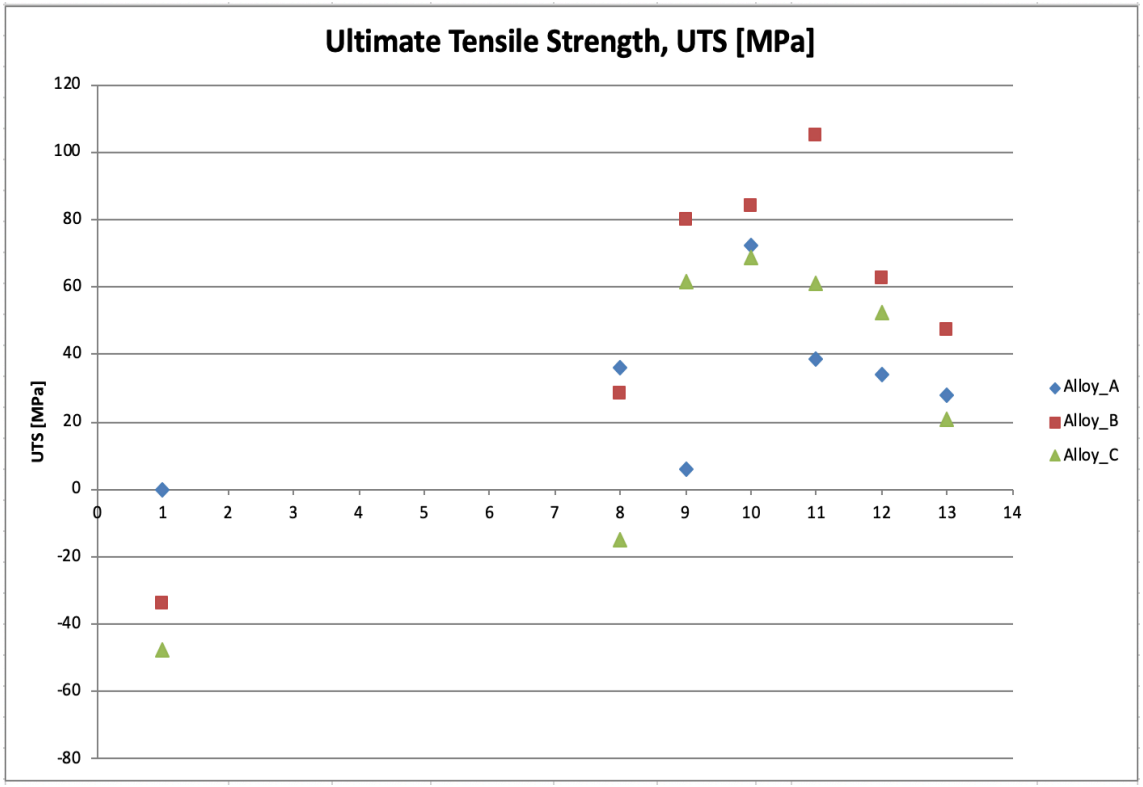
Ultimate Tensile Strength, UTS [MPa]
UTS [MPa]
120
100
80
60
40
20
0
-20
-40
-60
-80
0 1 2 3 4 5 6 7 8 9 10 11 12 13 14
Alloy_A
Alloy_B
Alloy_C

(a)

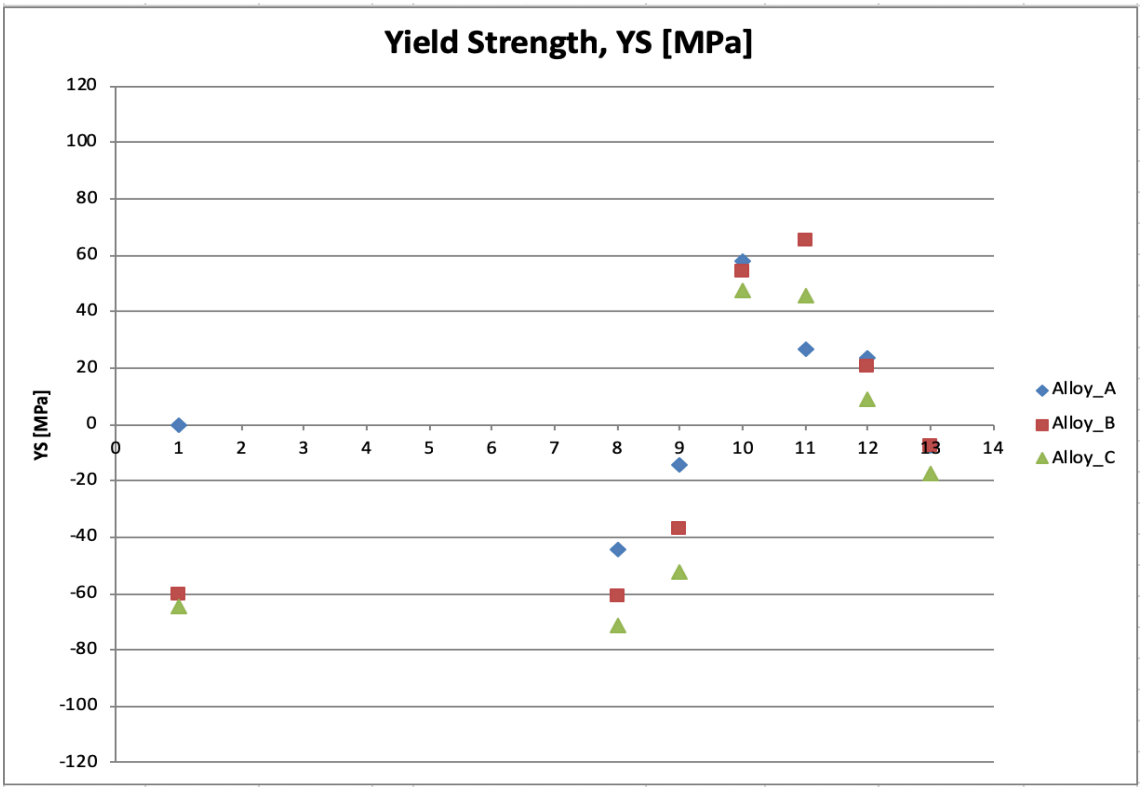
Yield Strength, YS [MPa]
YS [MPa]
120
100
80
60
40
20
0
-20
-40
-60
-80
-100
-120
0 1 2 3 4 5 6 7 8 9 10 11 12 13 14
Alloy_A
Alloy_B
Alloy_C

(b)

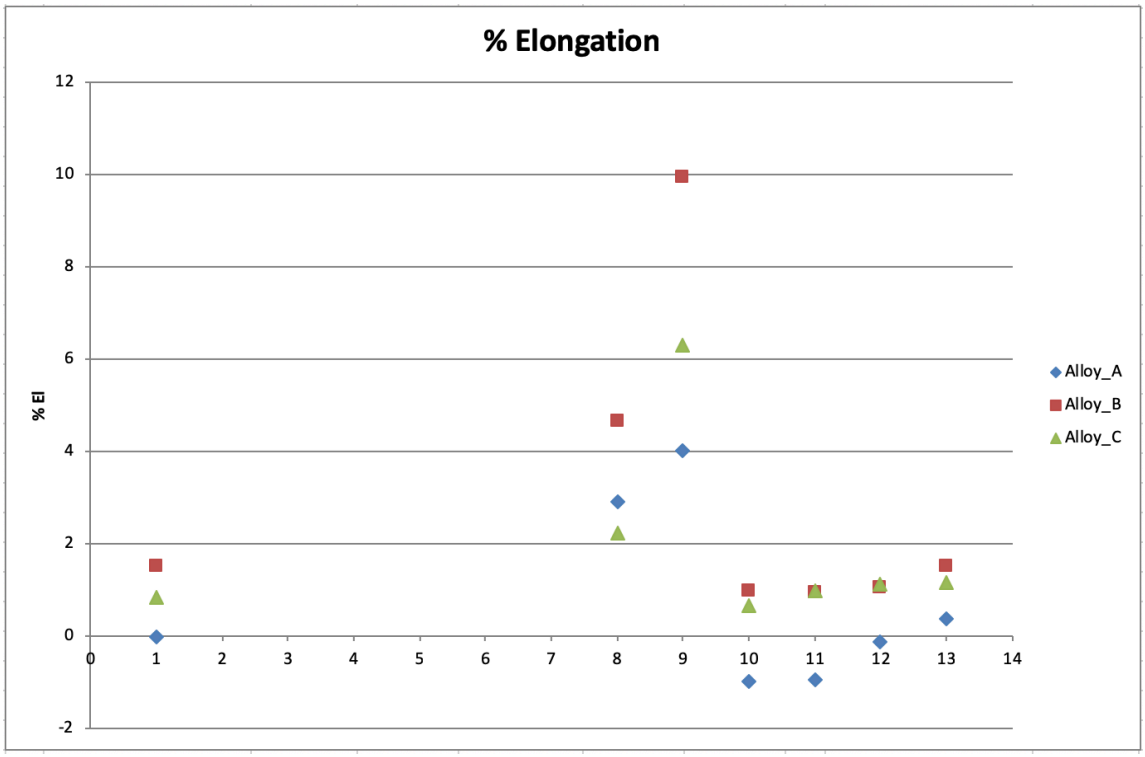

(c)

Figure 5-20: Comparison of tensile properties of A, B and C alloys relative to those of as-cast base alloy A: (a) ΔP-UTS, (b) ΔP-YS, and (c) ΔP-%El as a function of heat treatment conditions with SHT for 8 h.

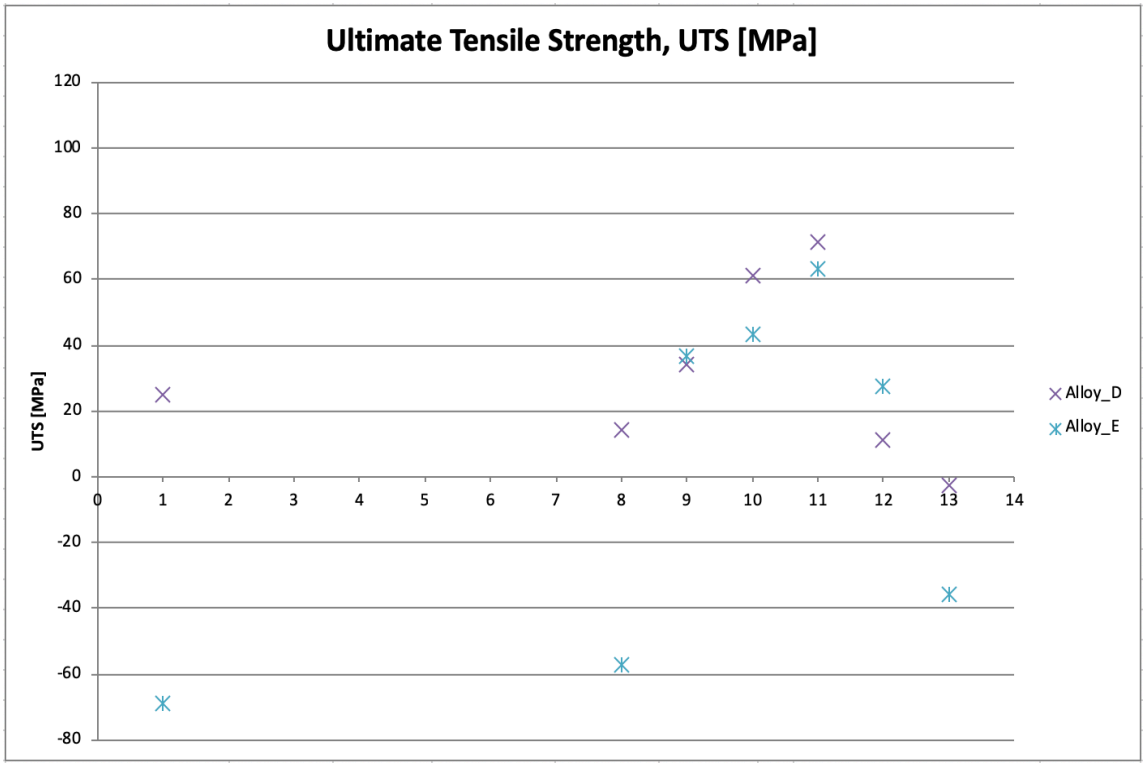

(a)

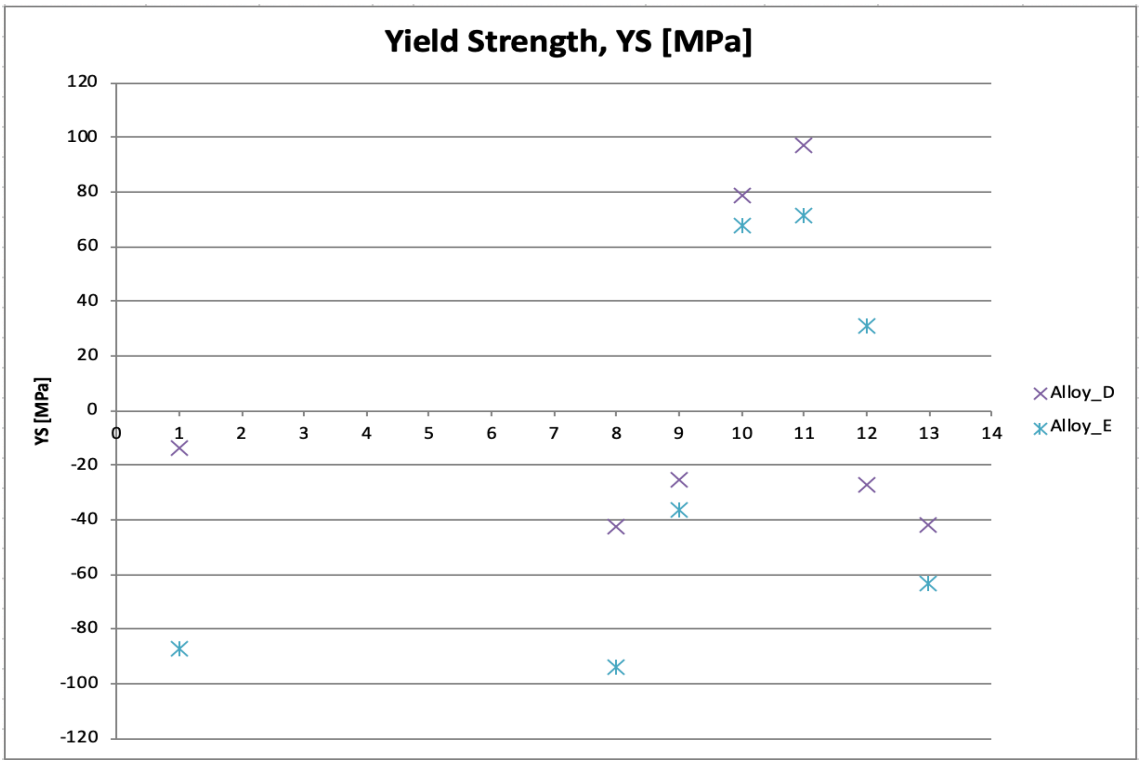

(b)

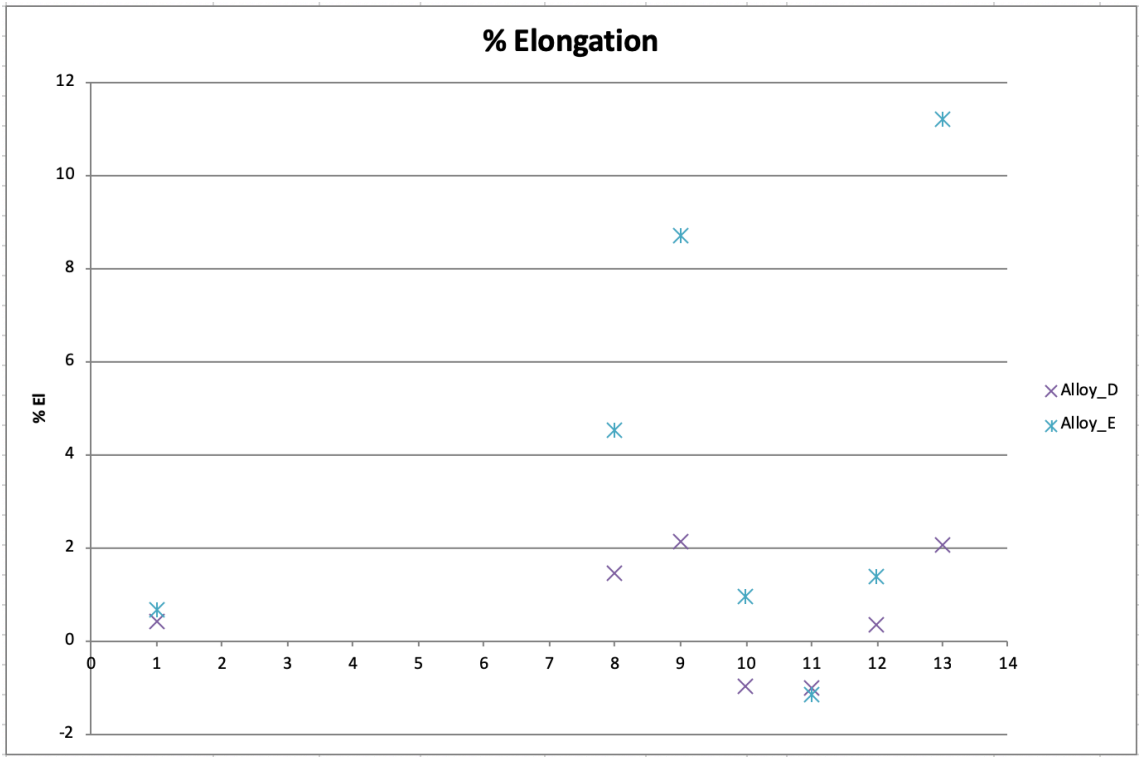

(c)

Figure 5-21: Comparison of tensile properties of D and E alloys relative to those of as-cast base alloy A: (a) ΔP-UTS, (b) ΔP-YS, and (c) ΔP-%El as a function of heat treatment conditions with SHT for 8 h.

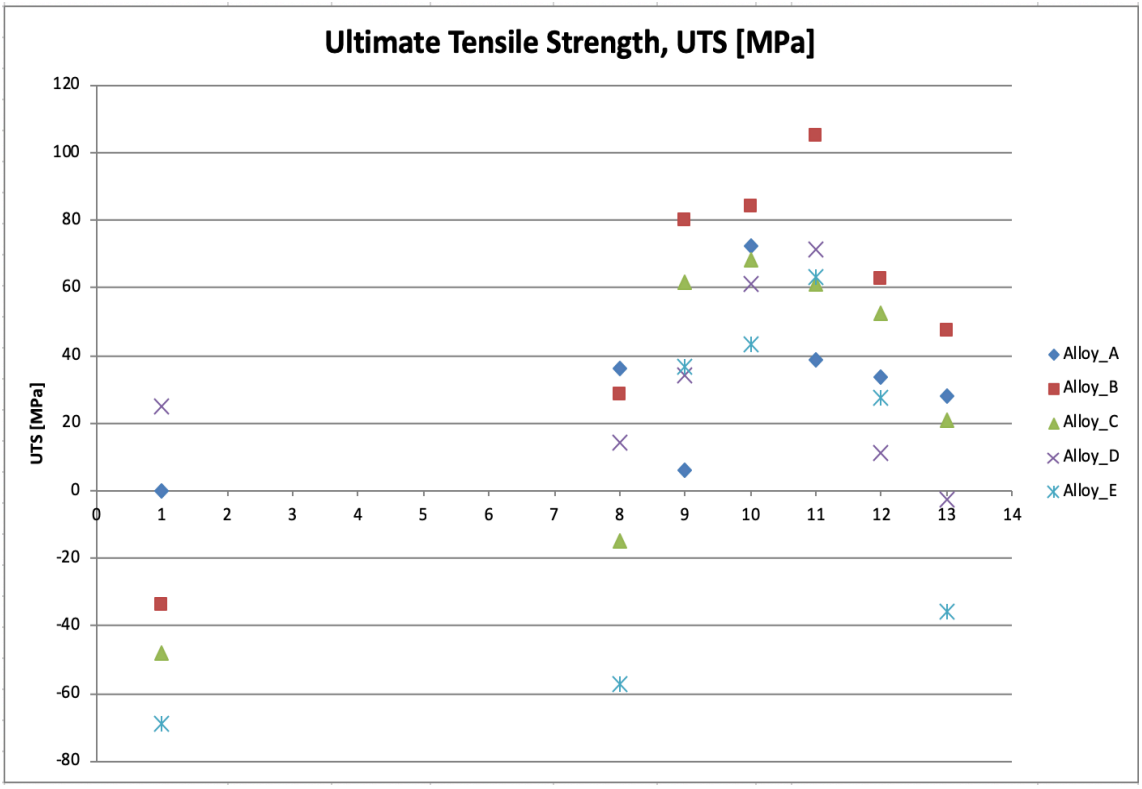
Ultimate Tensile Strength, UTS [MPa]
UTS [MPa]
120
100
80
60
40
20
0
-20
-40
-60
-80
0 1 2 3 4 5 6 7 8 9 10 11 12 13 14
Alloy_A
Alloy_B
Alloy_C
Alloy_D
Alloy_E

(a)

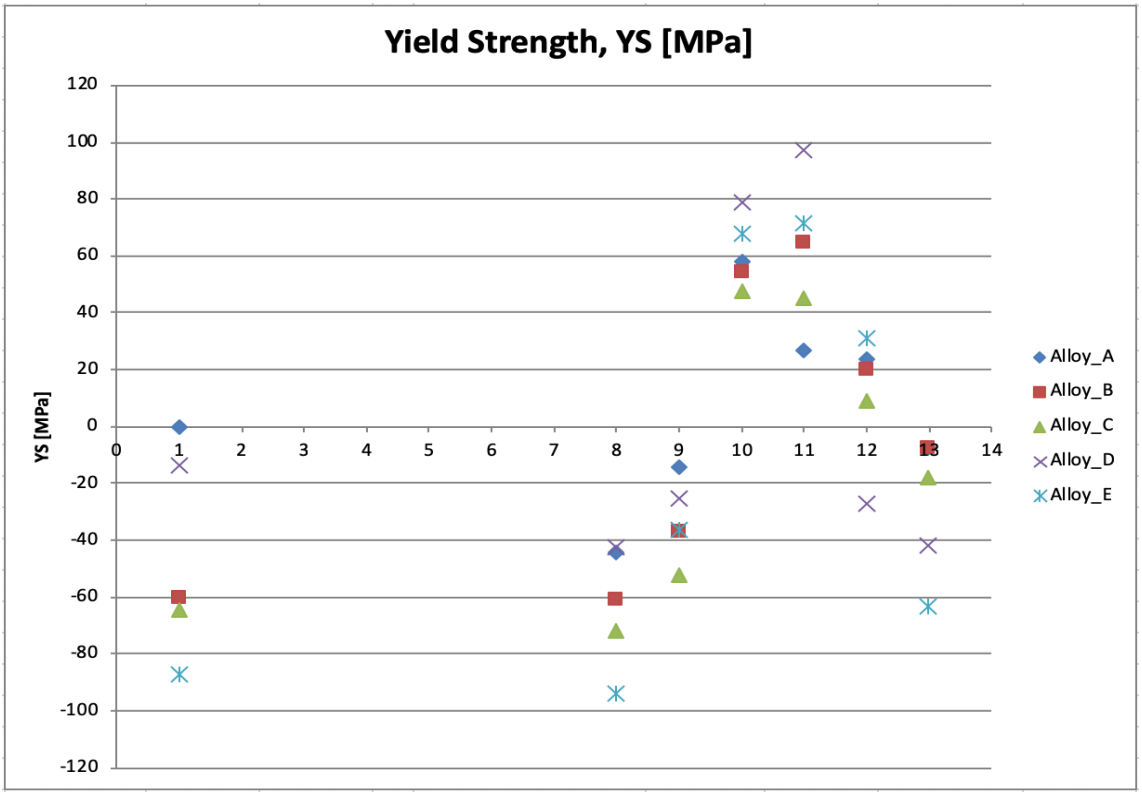
Yield Strength, YS [MPa]
YS [MPa]
120
100
80
60
40
20
0
-20
-40
-60
-80
-100
-120
0 1 2 3 4 5 6 7 8 9 10 11 12 13 14
Alloy_A
Alloy_B
Alloy_C
Alloy_D
Alloy_E

(b)

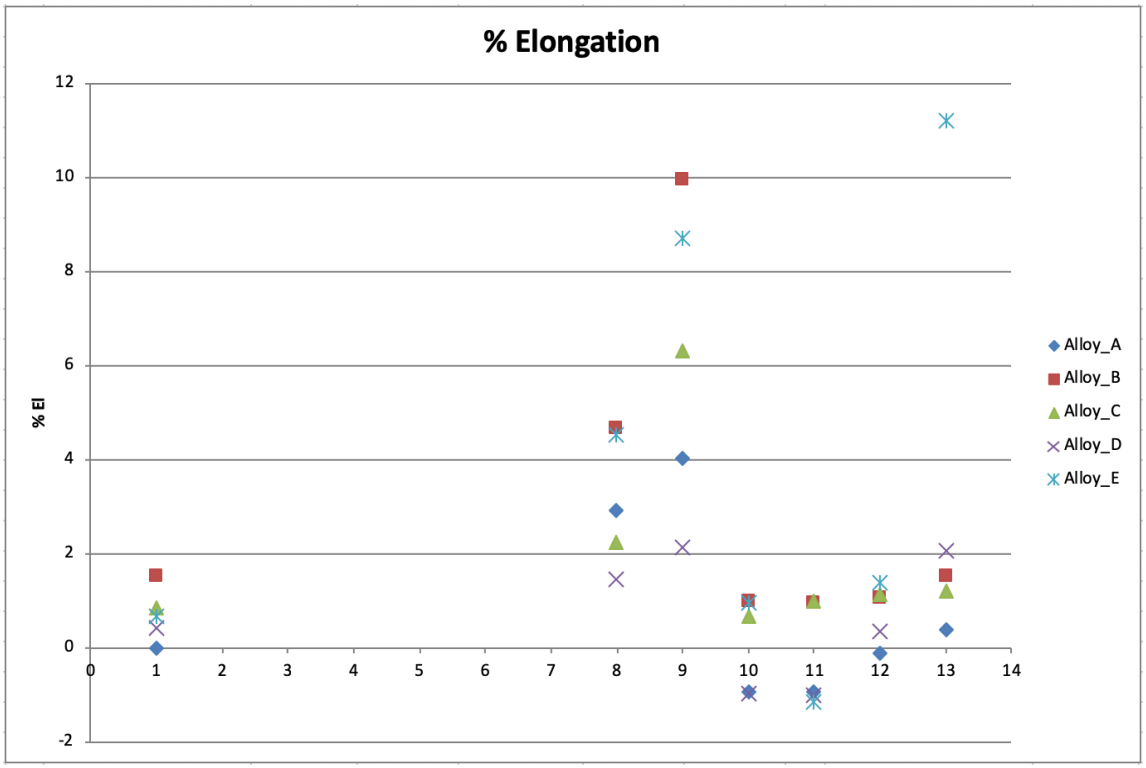

(c)

Figure 5-22: Comparison of tensile properties of A, B, C, D and E alloys relative to those of as-cast base alloy A: (a) ΔP-UTS, (b) ΔP-YS, and (c) ΔP-%El as a function of heat treatment conditions with SHT for 8 h.

Figure 5-23 shows a comparison of the tensile properties (UTS, YS and %El), in all the thirteen conditions used in this research for alloys A, B and C, relative to those of as-cast base alloy A, while Figure 5-24 shows the tensile properties for all the alloys A, B, C, D and E, relative to those of the as-cast base alloy A for the same thirteen conditions. The results obtained may be explained based on the same factors as discussed earlier on in this section and in section 5.2.1.3. In general, the additions and heat treatments used lead to good combinations of tensile properties, comparable to those of the reference alloys. From an analysis of the ΔP values in these two figures, it can be concluded that alloy B in the S8WA2 heat-treated condition, with SHT for eight hours, is the best composition/heat treatment condition to achieve optimum properties for HT200 alloy.

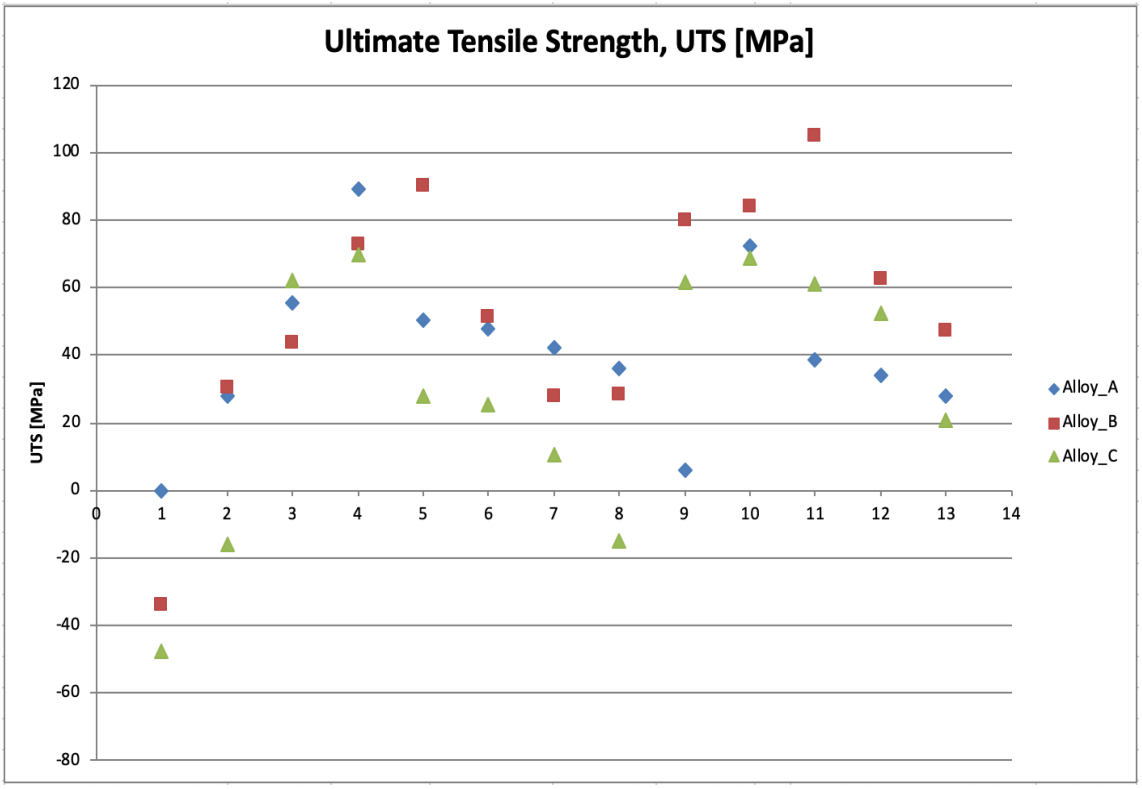
Ultimate Tensile Strength, UTS [MPa]
UTS [MPa]
120
100
80
60
40
20
0
-20
-40
-60
-80
0 1 2 3 4 5 6 7 8 9 10 11 12 13 14
Alloy_A
Alloy_B
Alloy_C

(a)

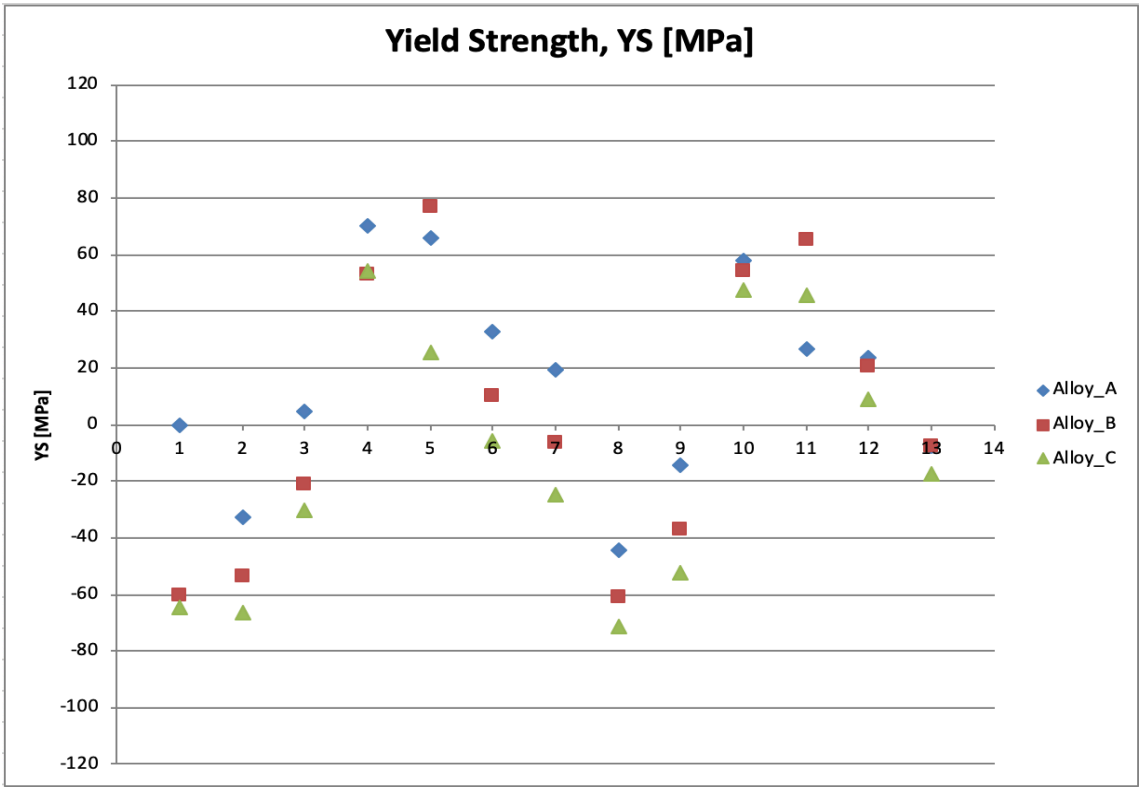
Yield Strength, YS [MPa]
YS [MPa]
120
100
80
60
40
20
0
-20
-40
-60
-80
-100
-120
0 1 2 3 4 5 6 7 8 9 10 11 12 13 14
Alloy_A
Alloy_B
Alloy_C

(b)

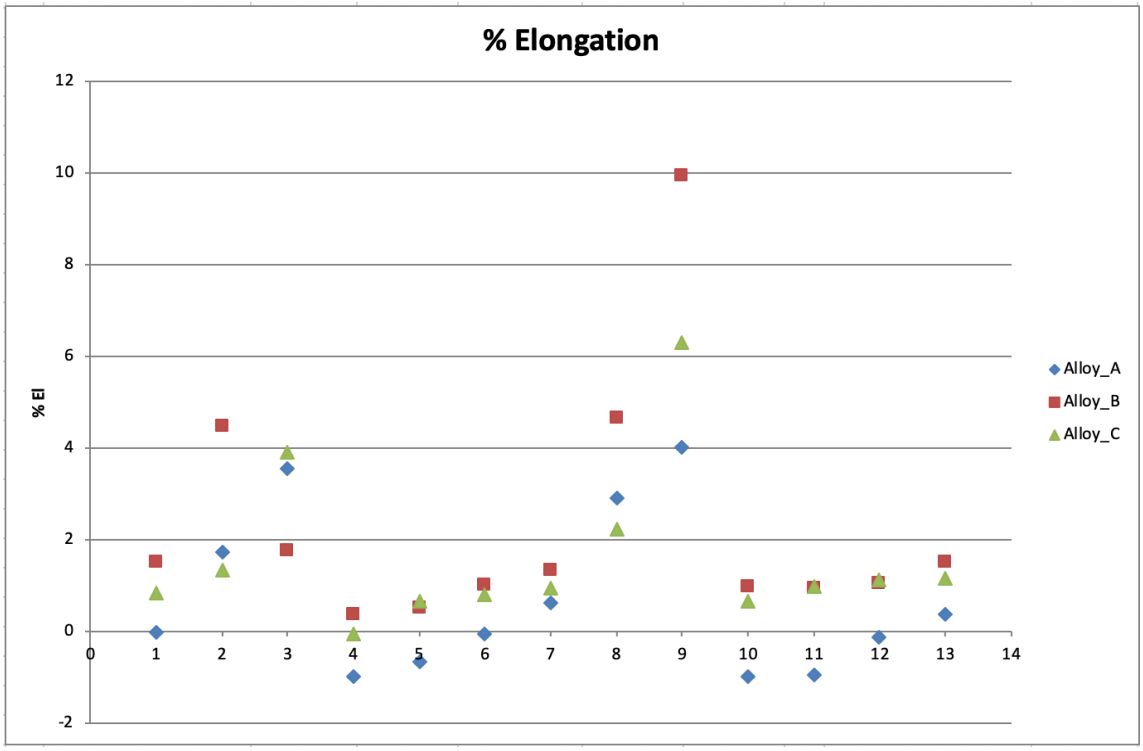

(c)

Figure 5-23: Comparison of tensile properties of A, B and C alloys relative to those of as-cast base alloy A: (a) ΔP-UTS, (b) ΔP-YS, and (c) ΔP-%El as a function of heat treatment conditions with SHT for 4 h and 8 h.

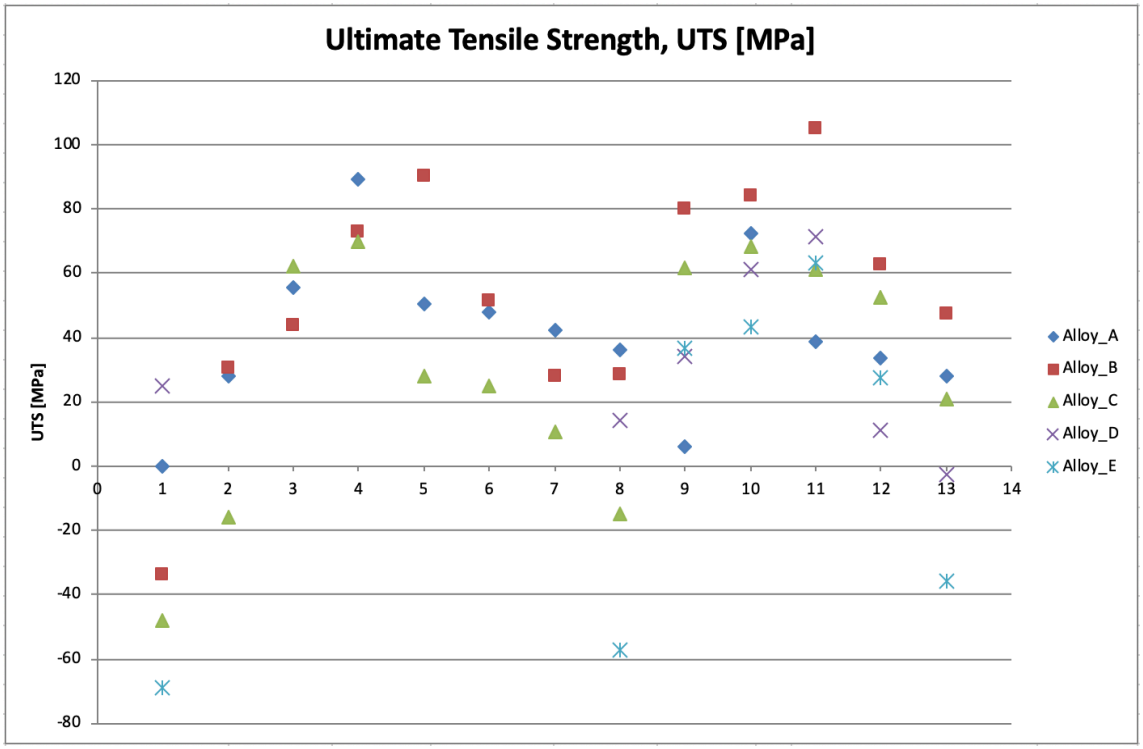

(a)

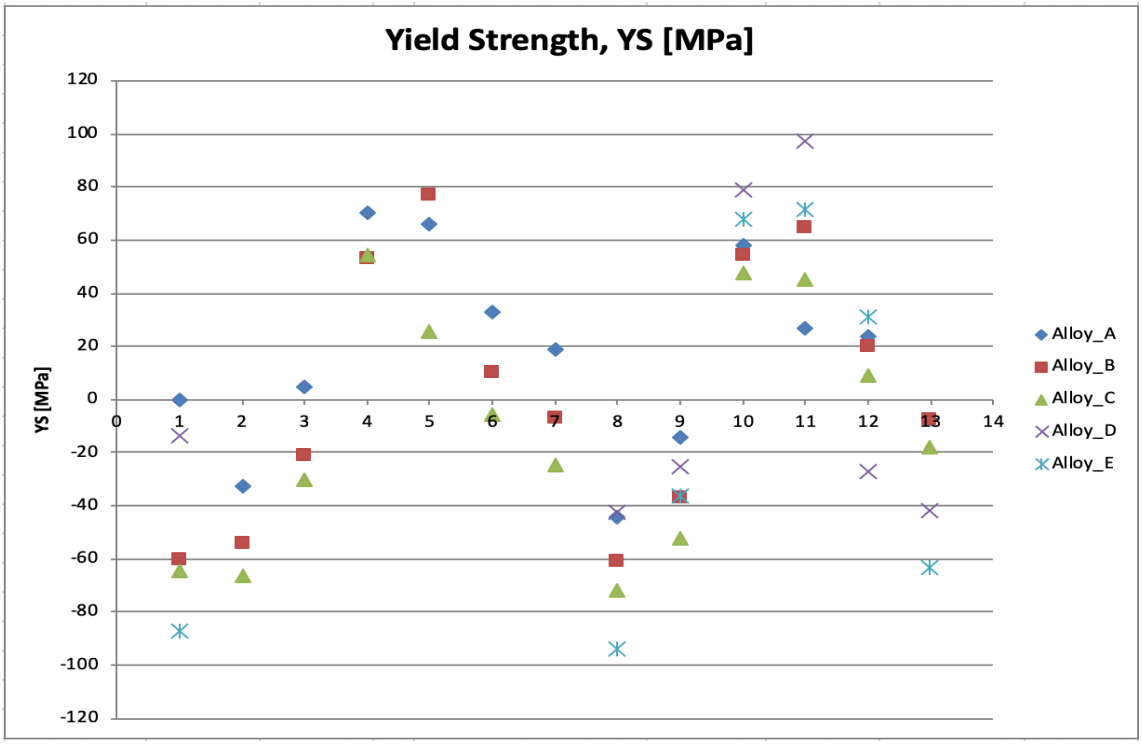

(b)

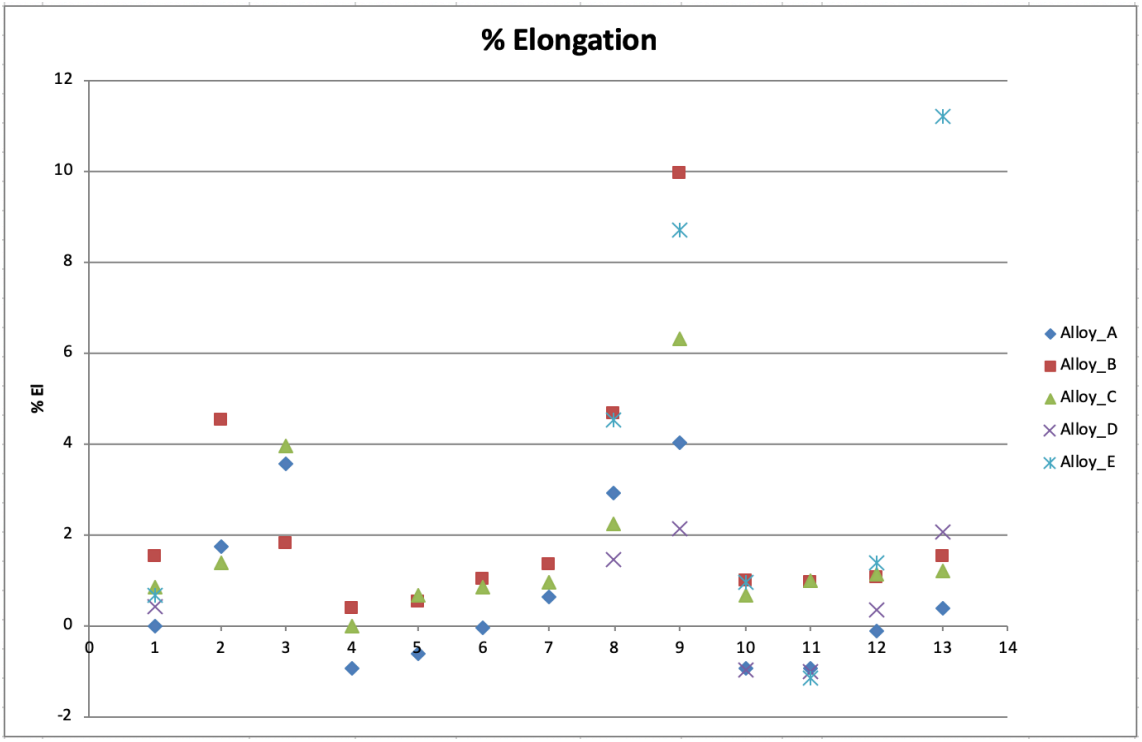

(c)

Figure 5-24: Comparison of tensile properties of A, B, C, D and E alloys relative to those of as-cast base alloy A: (a) ΔP-UTS, (b) ΔP-YS, and (c) ΔP-%El as a function of heat treatment conditions with SHT for 4 h and 8 h.

CHAPTER 6

ELEVATED-TEMPERATURE TENSILE PROPERTIES

CHAPTER 6

6 ELEVATED-TEMPERATURE TENSILE PROPERTIES

6.1 INTRODUCTION

This chapter presents and discusses the tensile properties of the alloys A, B, C, D and E in the as-cast and heat-treated conditions, for the tensile tests carried out at the elevated temperature of 250°C. The test bars were maintained at the high temperature for a specified stabilization time before carrying out the tensile tests. The tensile properties of the HT200 alloys A, B and C are compared with those of the reference alloys D and E. The parameters investigated were the effect of alloying element additions of titanium, zirconium and silver, and the influence of different heat treatment conditions.

The tensile test results at elevated-temperature are divided into two groups. The first group covers the results for alloys A, B and C in the as-cast condition and when solution heat treated for four hours. The second group covers the results for alloys A, B, C, D and E in the as-cast condition and when solution heat treated for eight hours.

The alloy quality was analyzed using the quality index concept. Q values for the five alloys were calculated from the high temperature tensile test data obtained. Quality charts were generated in order to understand the alloy properties in relation to the various alloying elements as well as determine the effect of the additions made in relation to the heat treatment conditions applied. This would help in recommending the optimum alloy composition/heat

treatment condition for HT200 alloy. The Q-values of the HT200 alloys were compared with those of the reference alloys D and E.

Plots of property difference, ΔP, are also presented. Such plots represent the difference in a property (P) value obtained for a specific alloy composition/heat treatment condition with respect to that obtained for the base alloy. In the present study and for the elevated temperature testing data, the ΔP values will be plotted taking the HT200 alloy A in the as-cast condition as the base or reference line. The ΔP plots of the ultimate tensile strength, yield strength and percent elongation values obtained are generated for the alloys relative to the values obtained for the base alloy A in the as-cast condition.

6.2 MECHANICAL PROPERTIES

Tensile tests were carried out on all the alloys used for this study to obtain their ultimate tensile strength (UTS), yield strength (YS) and the percentage elongation (%El) values. In addition to the as-cast condition, the alloys were heat treated using different heat treatment conditions, twelve in the case of alloys A, B and C, and six in the case of alloys D and E. Before the tests were carried out, each tensile bar mounted for testing was kept in the test chamber for thirty minutes at the elevated-temperature of 250°C to stabilize the sample, after which the test was carried out. The chemical compositions of the five alloys investigated in this study are provided in Table 3-1 and Table 3-2. Details regarding the heat treatments used for each alloy are provided in Table 3-6 and Table 3-7. For purposes of simplicity, however, the shortened descriptions and codes of these heat treatment conditions shown in Table 5-1 and Table 5-2 will be used to discuss the results. The solution heat treatments used

for each alloy are given in Table 5-3. For each alloy/heat treatment condition, five tensile bars were tested, and the average values obtained were taken as representing the properties of that alloy/heat treatment condition.

6.2.1 RESULTS FOR AS-CAST AND 4 HRS-SOLUTION HEAT TREATED CONDITIONS

6.2.1.1 TENSILE TEST RESULTS

This section discusses the tensile properties of the alloys A, B and C when tested at 250 °C. The test bars of each alloy were divided into bundles of five, one representing the as-cast condition, and the rest used for heat treatment. Six heat treatment conditions were used for this group, namely S4A, S4W, S4WA1, S4WA2, S4WA3 and S4WA4, as described in Table 5-1 and Table 5-2. The alloys were solution heat treated at 520°C for four hours. For each test, the test bar was kept in the testing chamber at 250°C for thirty minutes before running the test, to guarantee a homogeneous temperature distribution throughout the bar; then the test was carried out. The tensile test results for this group are shown in Table 6-1 and plotted as curves in Figure 6-1, Figure 6-2 and Figure 6-3. The results reveal that, as in the case of the ambient temperature testing, the high temperature tensile properties of the alloys also improved significantly after heat treatment.

Further heating the samples in the testing chamber and then running the tests at 250°C coarsened the precipitates, decreased their density, increased their size and increased the inter-particle spacing, so that the strength decreased and the ductility increased, when compared with the ambient temperature tensile test results. This is demonstrated visually in

the micrographs shown in Figure 6-4 and in Figure 6-5, which compare the microstructures of T7-heat treated alloy B tested at ambient temperature and at 250°C. It can be seen that the precipitates in Figure 6-5 are coarser, bigger, lower in density, and with greater inter-particle spacing than the precipitates in Figure 6-4. Hence, the lower strength values obtained for this group at the elevated temperature.

In the first two heat treatment conditions, i.e., S4A and S4W (solution treatment followed by air or water quenching), the improvement in the tensile properties is attributed to the SHT and the high cooling rate achieved with water quenching, as explained previously in Chapter 5. The supersaturated solid solution obtained by the dissolution of existing phases like θ-Al_2Cu in the as-cast structure is preserved, by means of rapid cooling to room temperature during the water quenching. As seen from the results for the three alloys, solution treatment with water quenching provided better tensile properties than when the bars were air quenched, due to the higher cooling rate obtained with water quenching.

Thus, following solution heat treatment and water quenching, alloy A exhibited 201.94 MPa, 134.2 MPa and 6.24% for the UTS, YS and %El, respectively (cf. 152.8 MPa, 87.69 MPa and 6.11% in the as-cast condition); alloy B had UTS, YS and %El values of 218.25 MPa, 171.97 MPa and 5.96% (cf. 157.13 MPa, 88.32 MPa and 8.54% in the as-cast case), while alloy C showed 223 MPa, 158.4 MPa and 7.41% as its UTS, YS and %El values (cf. 156.8 MPa, 102.69 MPa and 5.92% in the as-cast condition). These results may be explained based on the same reasons mentioned in the preceding paragraphs.

Aging treatment, as in the S4WA1, S4WA2, S4WA3 and S4WA4 heat treatment conditions, follows solution heat treating and quenching, and is controlled by the *temperature*

and *time* used. Precipitation or age hardening increases the strength in Al-Cu alloys, the main strengthening precipitates being those of the θ-Al_2Cu phase. After solution treatment and quenching, the solute atoms, which exist in the supersaturated solid solution, SSSS, start to form clusters of atoms known as Guinier-Preston or GP zones. The solute atoms in these GP zones consist of ordered groups, which are coherent with the lattice structure and dispersed within the matrix. Usually these atoms have different sizes than those of the lattice structure of the aluminum matrix; therefore, distortion occurs in the lattice, producing coherency-strain fields which lead to a significant improvement in strength. These GP zones are metastable, and they dissolve later in the presence of a more stable phase. As the aging treatment progresses, the GP zones dissolve, and metastable coherent or semi-coherent precipitates start forming. These precipitates continue to grow by diffusion of atoms from the SSSS, which results in achieving maximum or peak strength. As aging continues further, the metastable coherent precipitates later become totally incoherent. In this condition, the opposition of the precipitates to dislocation movement is reduced, and this in turn leads to a consequent reduction in strength.

Peak aging is obtained when T6 heat treatment is used (as in S4WA1, S4WA2), as the resulting precipitates are fine, coherent and display small inter-particle spacing, which increases the opposition to dislocation motion, so that the strength is significantly increased. As can be seen in Figure 6-1, Figure 6-2 and Figure 6-3, alloy A alloy A reached its highest strength with the S4WA2 treatment, with values of 258.25 MPa, 255.93 MPa and 2.1% for the UTS, YS and %El, respectively, compared to 152.8 MPa, 87.69 MPa and 6.1% in the as-cast condition. Alloy B also reached its highest strength in the S4WA2 heat-treated condition, with UTS, YS and %El values of 286.49 MPa, 276.23 MPa and 3.12% respectively (cf.

157.13 MPa, 88.32 MPa and 8.54% in the as-cast condition). Alloy C, however, reached its highest strength after S4WA1 treatment (cf. 259.19 MPa, 254.86 MPa and 3.22% with 156.8 MPa, 102.69 MPa and 5.92% in the as-cast case).

The application of T7 treatment, when the aging temperature was increased as in S4WA3, or when both aging temperature and time were increased as in S4WA4, caused over-aging. That is to say that the precipitates became coarse, bigger in size, lower in density, and displayed large inter-particle distances. As was seen from Figure 6.5, the precipitates in the T7 heat-treated alloy B coarsened even further, when the alloy sample was maintained at the 250°C temperature prior to testing.

As discussed before in the preceding chapter, such characteristics facilitate dislocation motion, which in turn causes softening effects that decreases the strength. Thus, when the castings were over-aged, the strength decreased and the ductility increased. For the elevated temperature tests and with four hours SHT, among the HT200 alloys, alloy B showed the highest strength values in the S4WA2 heat treatment condition.

Table 6-1: Average values of UTS, YS and %El obtained at 250°C for alloys A, B and C in the as cast condition and when subjected to different heat treatment conditions with SHT for 4 h.

Alloy	Condition	UTS [MPa]	YS [MPa]	%EL [%]
Alloy A	AC	152.8	87.69	6.11
	S4A	154.06	107.97	6.21
	S4W	201.94	134.21	6.24
	S4WA1	255.09	253.41	2.0
	S4WA2	258.25	255.93	2.1
	S4WA3	208.21	169.81	2.81
	S4WA4	198.77	166.27	3.68
Alloy B	AC	157.13	88.32	8.54
	S4A	159.0	111.48	11.15
	S4W	218.25	171.97	5.96
	S4WA1	255.26	253.51	2.76
	S4WA2	286.49	276.23	3.12
	S4WA3	235.78	195.78	3.99
	S4WA4	223.05	193.82	4.38
Alloy C	AC	156.81	102.69	5.92
	S4A	170.92	128.75	3.89
	S4W	223.01	158.4	7.41
	S4WA1	259.19	254.86	3.22
	S4WA2	245.59	243.26	3.26
	S4WA3	204.59	177.61	3.92
	S4WA4	195.89	171.28	4.06

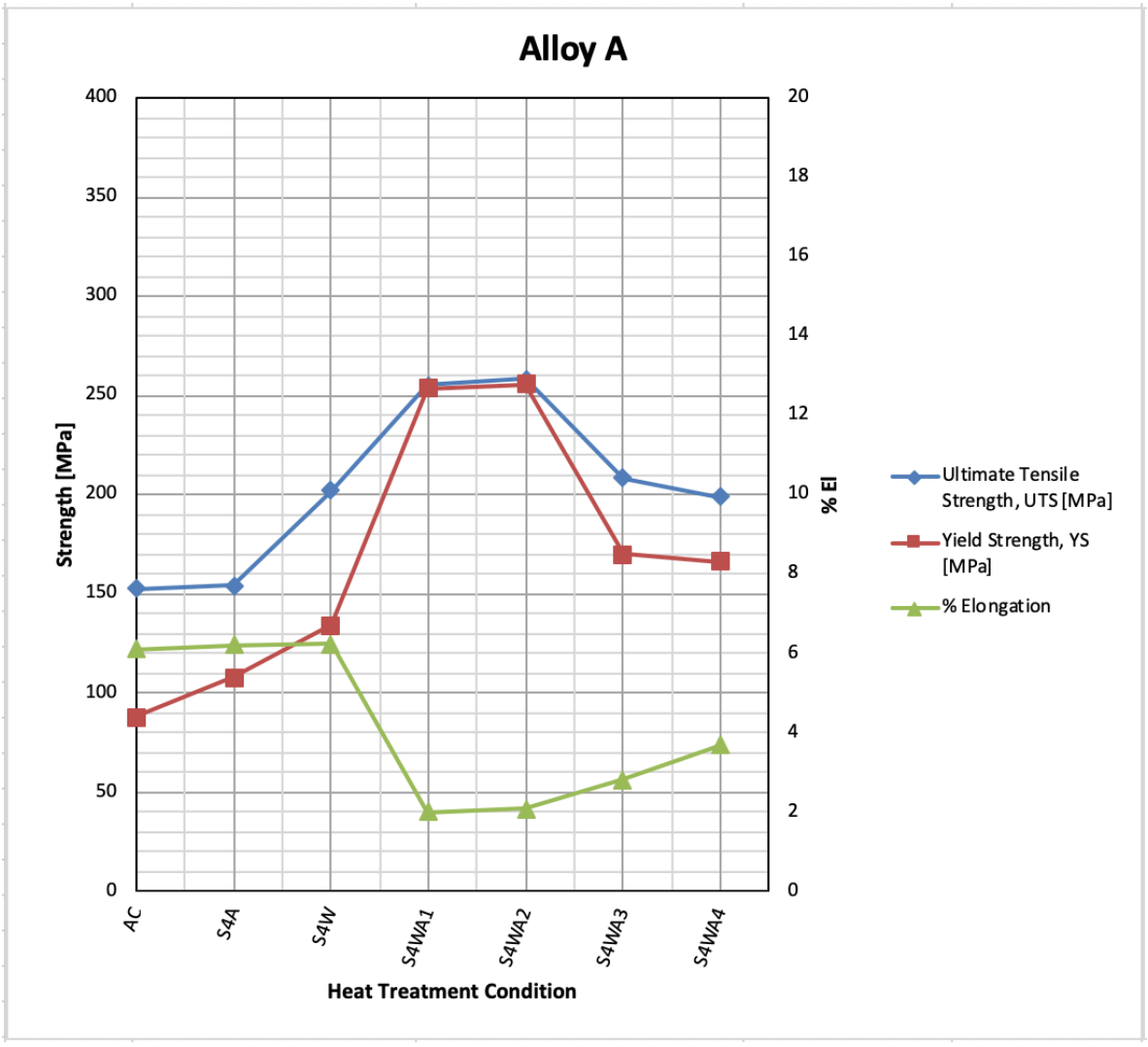

Figure 6-1: Average values of UTS, YS, %El for alloy A in the as-cast condition and after heat treatments comprising SHT for 4 h (tested at 250°C).

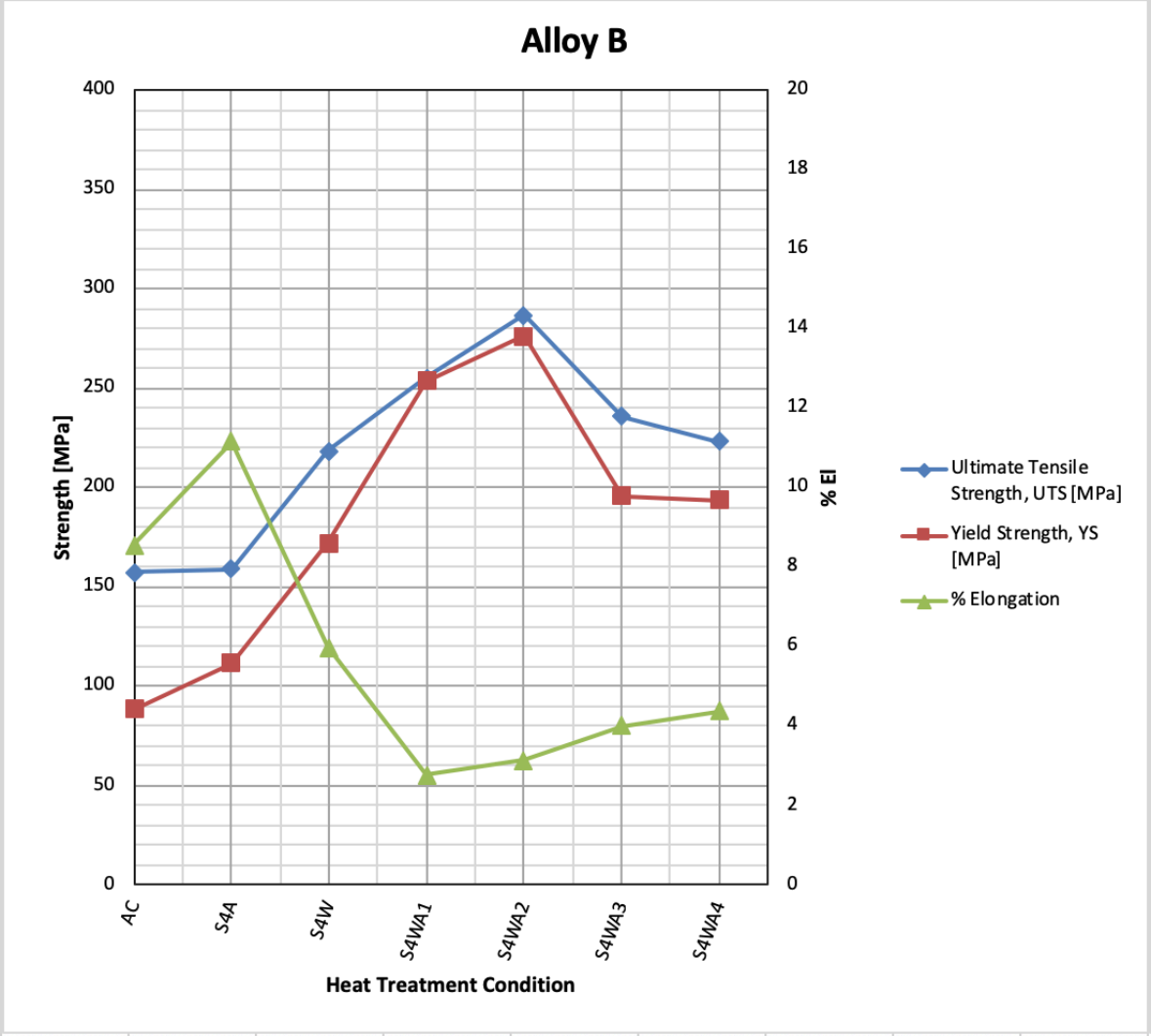

Figure 6-2: Average values of UTS, YS, %El for alloy B in the as-cast condition and after heat treatments comprising SHT for 4 h (tested at 250°C).

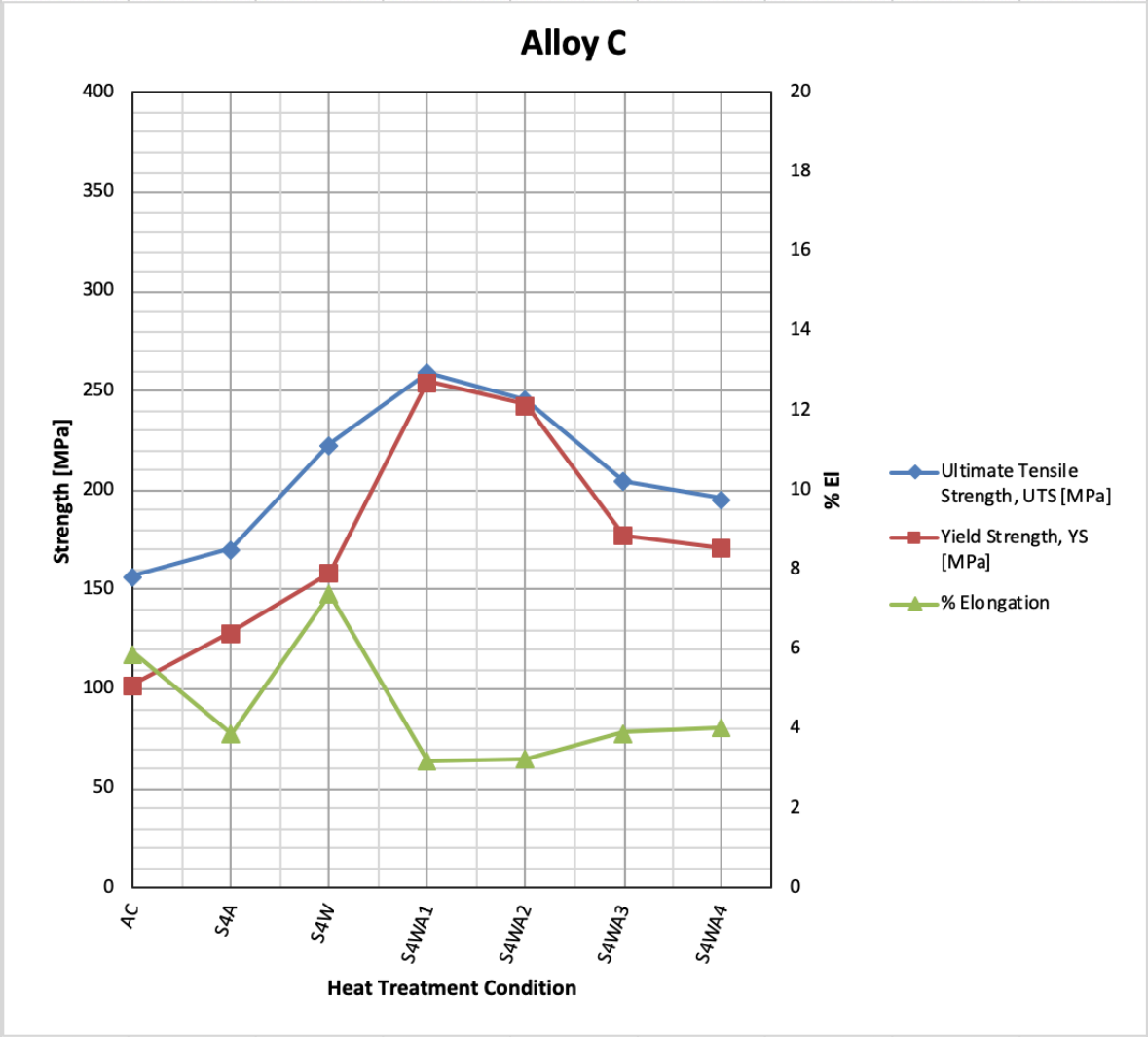

Figure 6-3: Average values of UTS, YS, %El for alloy C in the as-cast condition, and after heat treatments comprising SHT for 4 h (tested at 250°C).

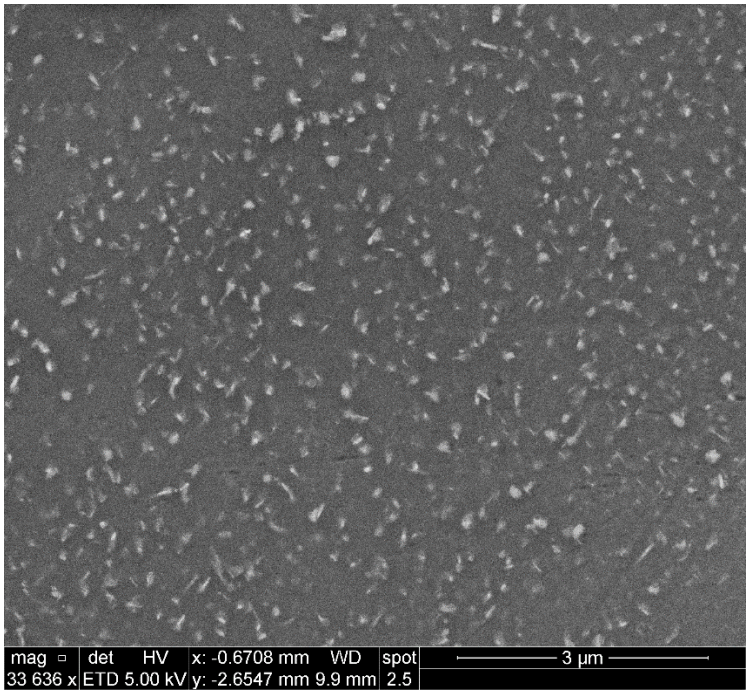

Figure 6-4: Micrograph of T7 heat-treated alloy B tested at ambient temperature.

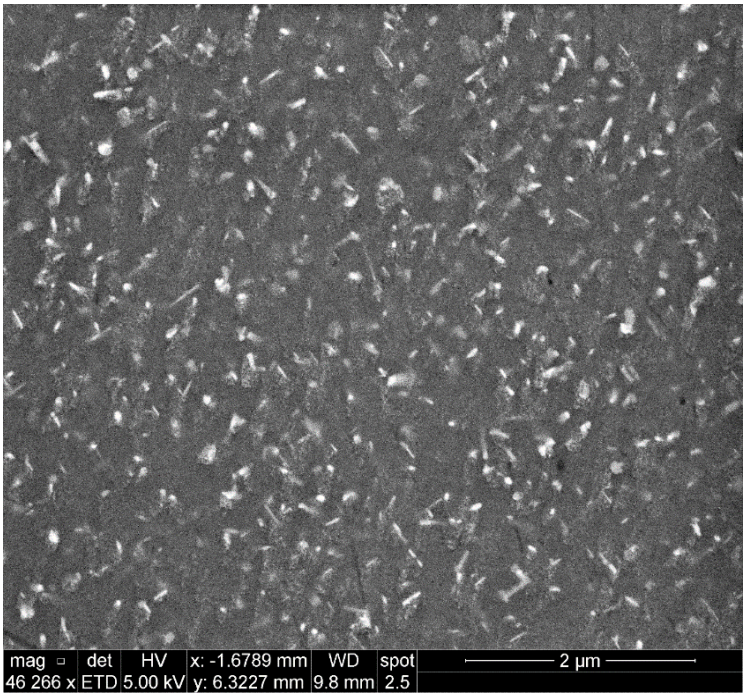

Figure 6-5: Micrograph of T7 heat-treated alloy B tested at 250°C.

6.2.1.2 ANALYSIS OF TENSILE PROPERTIES USING THE QUALITY INDEX CONCEPT

It should be kept in mind that changes in the chemical composition and/or heat treatment aiming at improving strength or other properties can render the material too brittle for structural applications. Thus, it is important to check simultaneously what effect on material ductility and strength any changes to the microstructure would have. Therefore, castings are evaluated using strength-ductility diagrams, referred to as quality index charts.

As mentioned earlier in Chapter 2, the concept of the Quality Index Q was proposed by Drouzy *et al.* [78] [87] as a means of better expressing the tensile properties of Al-Si-Mg alloys, in terms of how variations in Mg content and aging conditions affected the alloy "quality" or performance,. They used equations that allowed plotting iso-Q lines versus iso-Probable Yield Strength lines on a quality index chart, such that it became easy to see how the alloy quality was affected by the heat treatment and alloy composition. These are the Equations 1 and 2 described in Chapter 2, and are shown in Table 6-2 below. The *iso- Q* and *iso-PYS* lines in these charts facilitate knowing which additions are beneficial for improving the alloy properties.

By increasing the copper content in aluminum alloys, the strength of the alloys can be improved significantly, although this would result in a reduction in ductility. The quality of these castings will be affected according to the net amount by which the increase in strength is balanced by the reduction in ductility. As the Q-values are function of the ultimate tensile strength (UTS) and the percentage elongation (%El), thus they can be used as a very good indication of that balance between the strength and ductility of the alloy.

From the tensile test data shown in Table 6-1, quality index or Q values as well as the probable yield strength were calculated and are listed in Table 6-2. Quality charts were then generated for evaluating the influence of the metallurgical parameters involved on the tensile properties and quality of the HT200 aluminum alloys tested at the elevated temperature, following different heat treatment conditions using SHT for four hours.

Table 6-2: Q and Probable (PYS) values calculated from the tensile test results in Table 6-1, and using Equations 1 and 2 from Chapter 2.

Average values of UTS (MPa) and El (%) used to obtain Q and Probable YS values using: Q=UTS+150log(%El) … (1) PYS=UTS-60log(%El)+13 … (2)			
Alloy	**Condition**	**Q [MPa] Eqn (1)**	**PYS [MPa]. Eqn (2)**
Alloy A	AC	270.74	118.63
	S4A	273.0	119.49
	S4W	321.17	167.25
	S4WA1	300.14	250.07
	S4WA2	306.28	252.04
	S4WA3	275.41	194.34
	S4WA4	283.66	177.82
Alloy B	AC	296.83	114.25
	S4A	316.17	109.15
	S4W	334.58	184.72
	S4WA1	321.42	241.80
	S4WA2	360.65	269.83
	S4WA3	325.85	212.75
	S4WA4	319.23	197.58
Alloy C	AC	272.67	123.46
	S4A	259.40	148.52
	S4W	353.52	183.80
	S4WA1	335.26	241.75
	S4WA2	322.56	227.80
	S4WA3	293.64	181.96
	S4WA4	287.14	172.39

Quality charts provide a simple tool for estimating and recommending the appropriate processing conditions to obtain specified properties and facilitate the selection of castings to meet these specifications. Calculation of quality values (Q-values) depends principally on the ultimate tensile strength and the percentage elongation. The ultimate tensile strength (UTS) is normally used for the specification and quality control of the casting, while the ductility of the casting, expressed as percentage elongation to fracture, is usually used as an indicator of casting quality because of its sensitivity to the presence of any impurity or defect in the cast structure. Whereas, yield strength does not represent the quality of the casting since it is a material property which is not affected by the level of defects or impurities present in the casting, but is influenced, rather, by the movement of dislocations in the casting structure, and depends on the resistance expected by the hardening precipitates to the movement of dislocations.

Figure 6-6 shows a quality chart illustrating the relationship between UTS and %El for the alloys A, B and C in the as-cast and six heat treatment conditions, tested at 250°C. The optimum results can be found toward the upper-right corner (high Q and high PYS region) of the chart. The best combination of Q and PYS values was chosen for each of the alloys following the different heat treatments, in order to determine the optimum alloy composition/heat treatment condition. Alloy A gave a Q-value of 321.17 MPa and a PYS value of 167.25 MPa in the S4W heat treated condition and Q/PYS values of 306.28 MPa/252 MPa after S4WA2 heat treatment. Alloy B gave a Q-value of 360.65 MPa and a PYS value of 269.8 MPa in the S4WA2 heat treatment condition. Alloy C gave Q/PYS values of 353.5 MPa/183.8 MPa in the S4W heat treated condition, and 335.26 MPa/ 241.75 MPa after S4WA1 heat treatment. As alloy B showed much higher quality and probable yield strength

values in the S4WA2 heat treated condition than alloys A and C, the alloy B composition and the S4WA2 heat treatment condition (T6) may be considered as the optimum alloy composition/heat treatment condition at the elevated-temperature for the HT200 alloy, for the four hours solution heat treatment group.

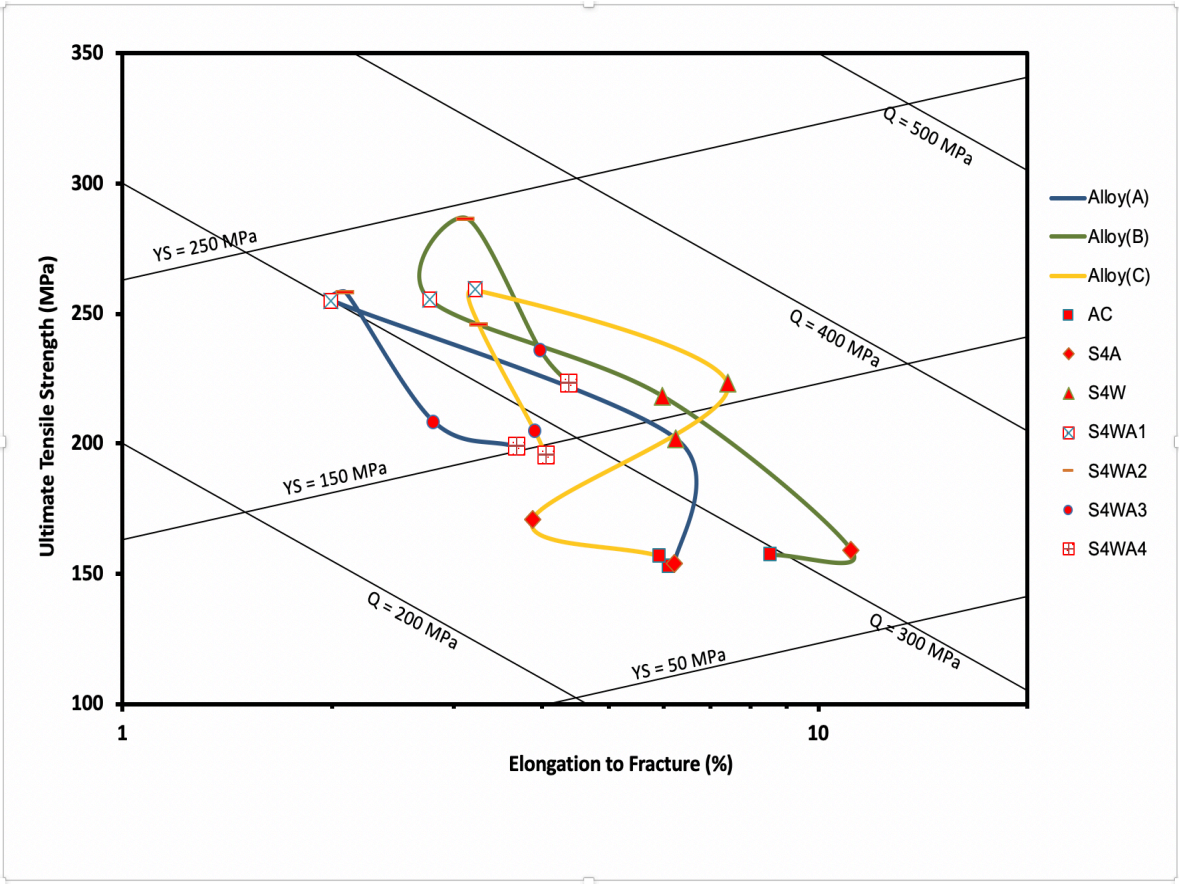

Figure 6-6: Quality chart showing relationship between UTS and %El for the A, B and C alloys investigated in the as-cast and six heat treatment conditions with SHT for 4 h.

6.2.1.3 STATISTICAL ANALYSIS (COMPARISON BETWEEN BASE ALLOY AND OTHER ALLOYS)

This section presents a comparison of the elevated temperature tensile properties (UTS, YS and %El) of the different alloys under different heat treatments, following solution heat treatment for four hours, with the base alloy A in the as-cast condition. Figure 6-7 depicts the tensile properties obtained for alloys A, B and C following different heat treatment conditions, relative to the values obtained for the base alloy A in the as-cast condition, i.e., after subtracting the values obtained for the base alloy A from each condition, and plotted as ΔP values on the Y-axis (P = Property = UTS, YS or %El), with the X-axis representing the base line for alloy A. The numbers on the X-axis represent the as cast condition and the different heat treatment conditions used. These conditions are indicated by numbers to facilitate reading the data. Each of these numbers with the condition it refers to is provided in Table 5-1. The use of this method provides an effective means of knowing how the various additions made and the different heat treatment conditions applied affect the properties of the HT200 casting alloy.

From Figure 6-7, it can be seen that the strength of the base alloy A is improved in general after heat treatment, except for the S4A treatment where only the YS shows some improvement, but not the UTS. In comparison, the S4W heat treatment provides much better strength, although the ductility does not change from its as-cast value with either of these two heat treatments. As expected, when artificial aging is also carried out, as with S4WA1, S4WA2 (T6), and S4WA3, S4WA4 (T7) treatments, the strength is improved considerably, while the ductility is decreased in proportion to the increase in strength. Regarding alloy B, the mechanical properties were improved with the addition of the grain refiners (Ti and Zr)

as well as the heat treatments applied, particularly when artificial aging was included, namely with S4WA1, S4WA2 and S4WA3 treatments. Similarly, improvements in the strength occurred for alloy C, with the addition of Ti, Zr and Ag, as well as heat treatment, particularly when artificial aging was implemented, using S4WA2 heat treatment, accompanied by the corresponding decrease in ductility.

Thus, the Ti and Zr grain refiner additions to alloys B and C play an important role in enhancing the strength of the HT200 alloy. From an examination of the ΔP values, it can be concluded that the alloy B composition combined with the S4WA2 heat treatment condition, with SHT for four hours, provides the optimum alloy composition/heat treatment condition for maximizing the strength of the HT200 alloy at elevated temperature.

Figure 6-8 compares the tensile properties of alloys A, B, C, D and E and the as-received HT200 base alloy. At the elevated temperature, and for the as-cast condition, the as-received alloy (alloy A) showed somewhat lower strength with respect to the reference alloys D and E. Generally, adding grain refiners and alloying elements in addition to applying heat treatments using SHT for four hours led to tensile properties (UTS, YS and %El) of the HT200 alloys that followed a similar trend as those of the reference alloys using the same heat treatments, but after a solution treatment of 8 hours. The higher strengths obtained for the HT200 alloys with the T7 heat treatments clearly indicates their resistance to softening at the higher temperatures and aging times.

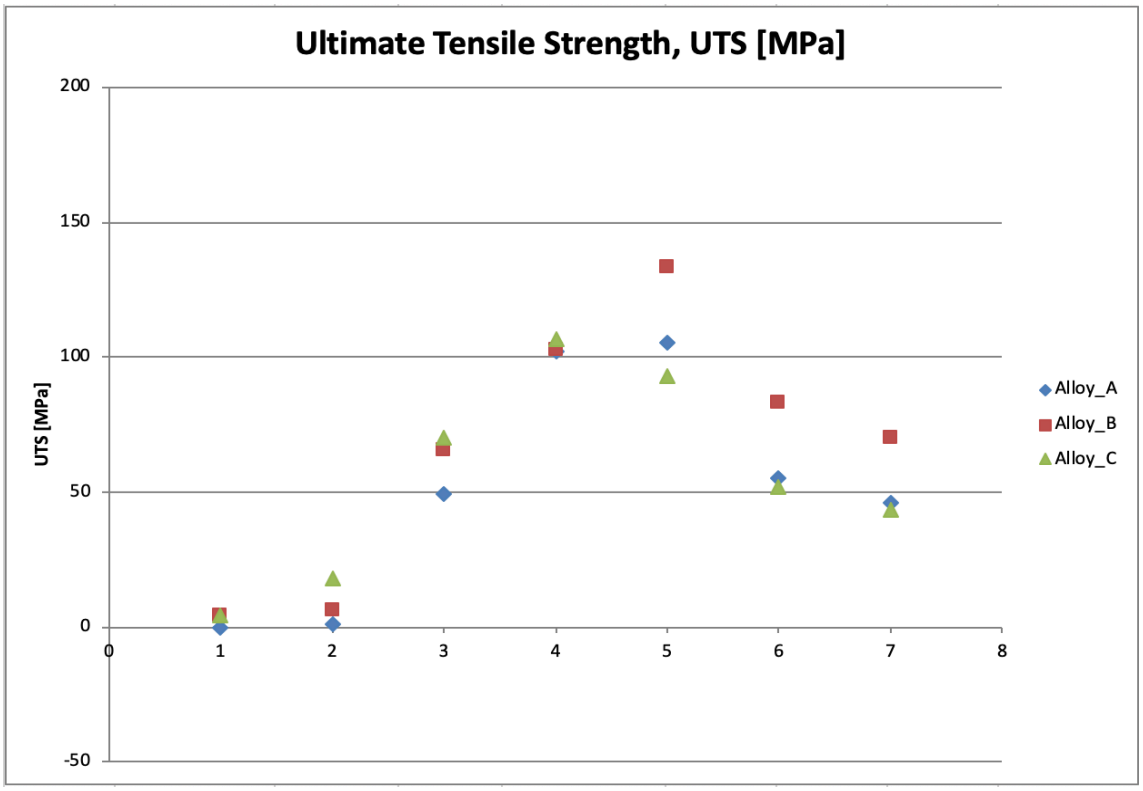
Ultimate Tensile Strength, UTS [MPa]
UTS [MPa]
200
150
100
50
0
-50
0
1
2
3
4
5
6
7
8
Alloy_A
Alloy_B
Alloy_C

(a)

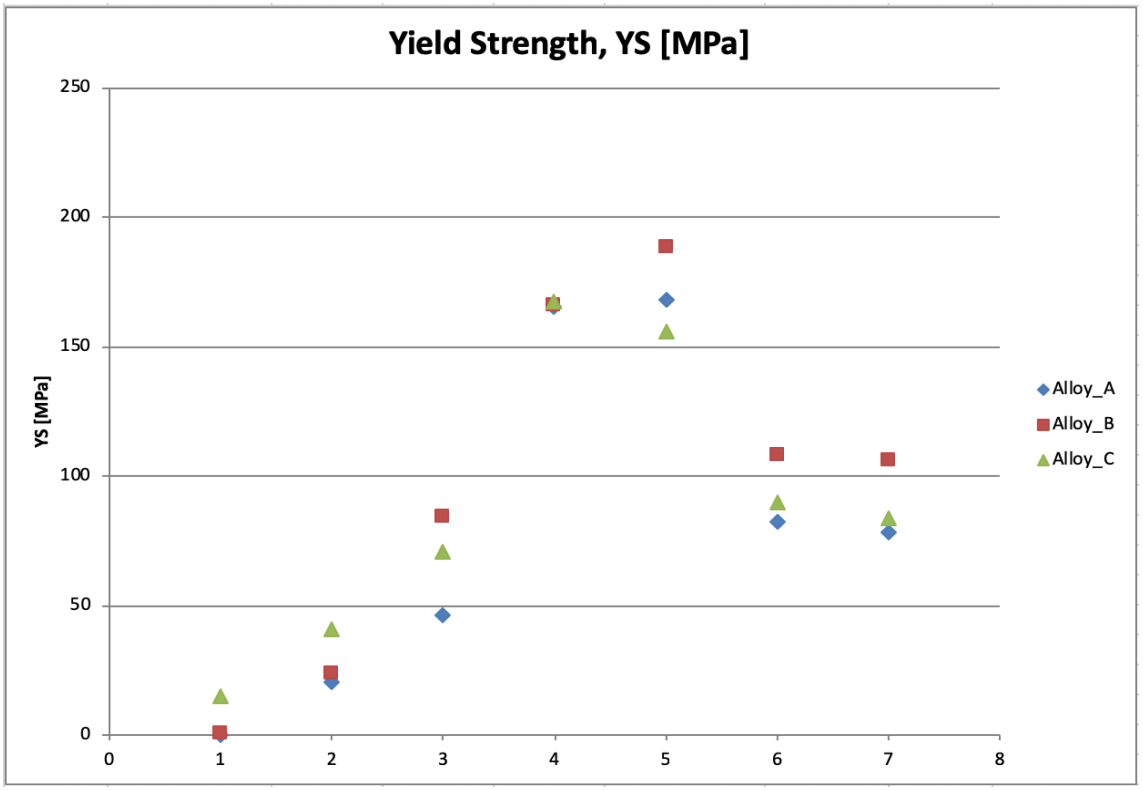
Yield Strength, YS [MPa]
YS [MPa]
250
200
150
100
50
0
0
1
2
3
4
5
6
7
8
Alloy_A
Alloy_B
Alloy_C

(b)

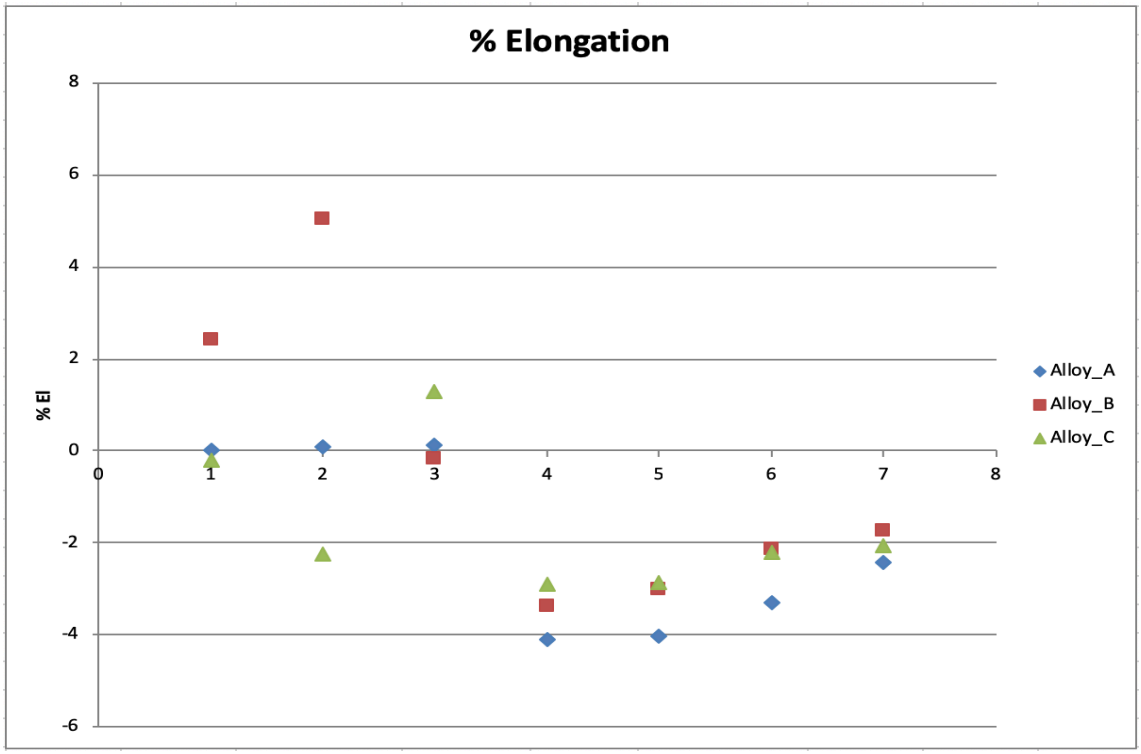

(c)

Figure 6-7: Comparison of tensile properties of A, B and C alloys relative to those of as-cast base alloy A: (a) ΔP-UTS, (b) ΔP-YS, and (c) ΔP-%El as a function of heat treatment condition with SHT for 4 h.

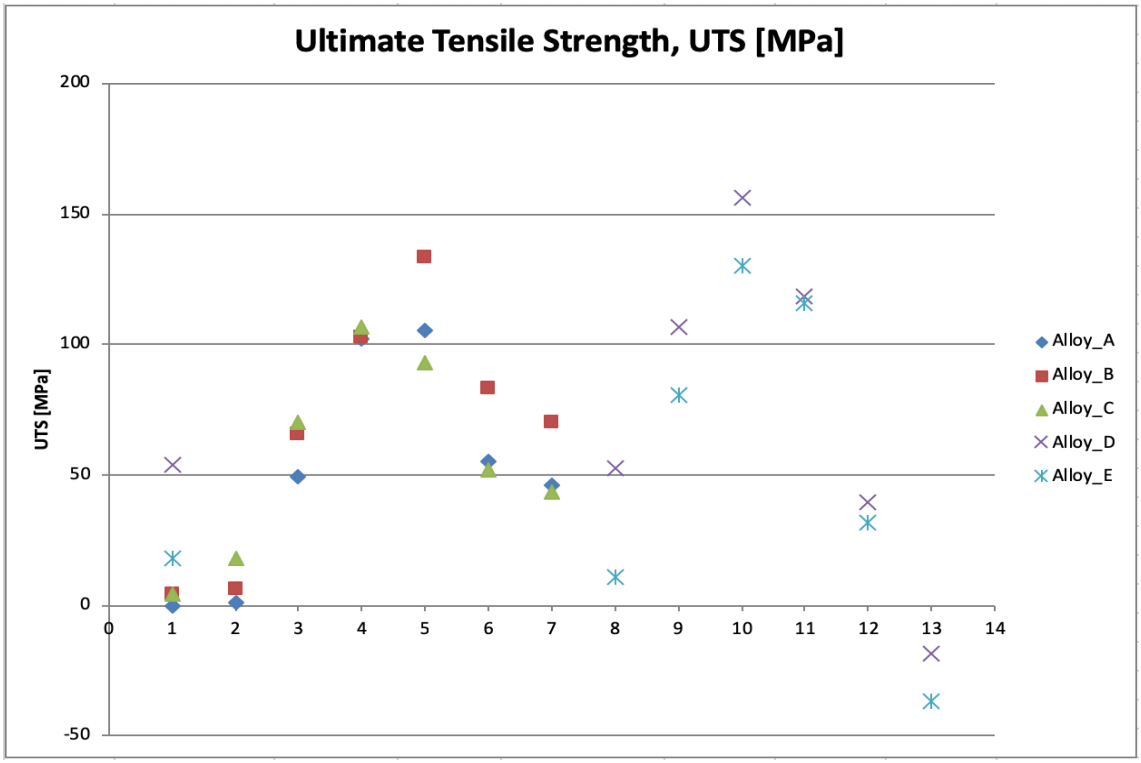

(a)

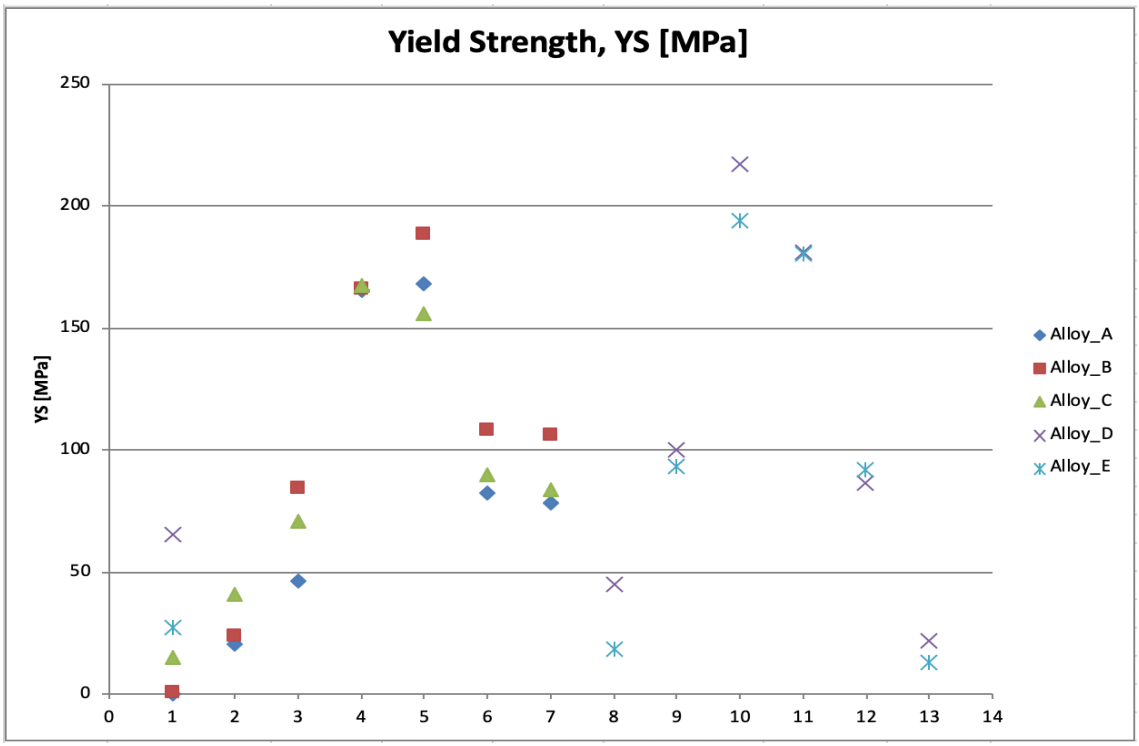

(b)

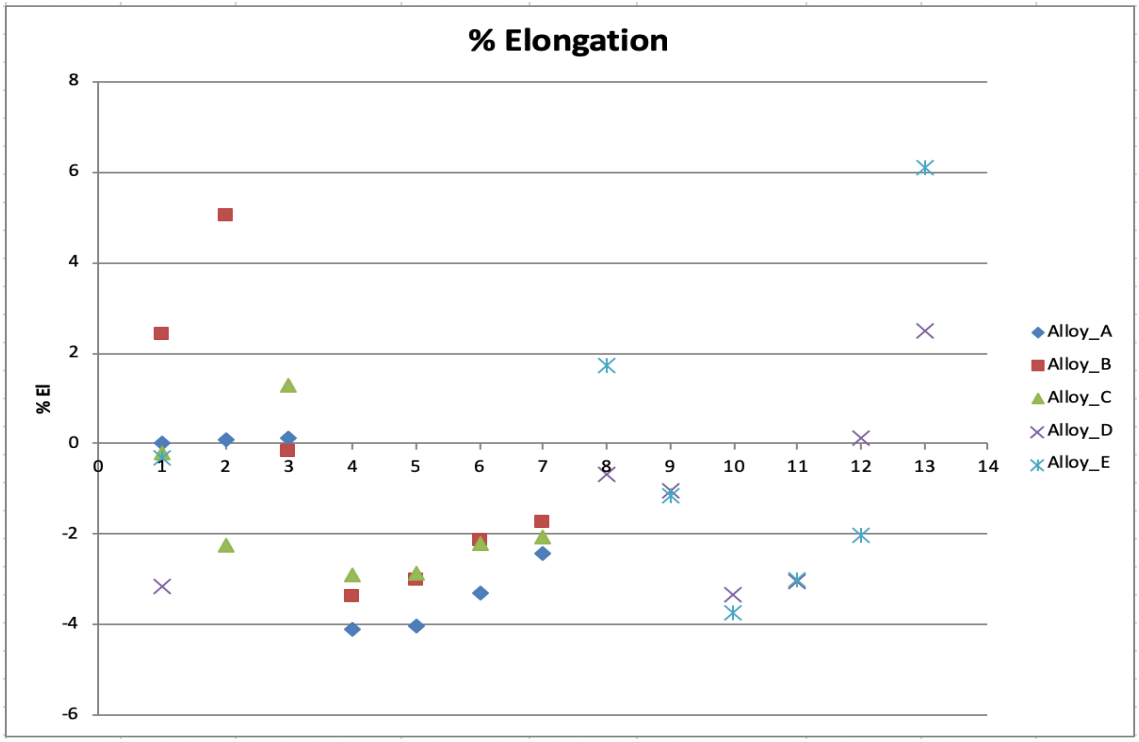

(c)

Figure 6-8: Comparison of tensile properties of A, B, C, D and E alloys relative to those of as-cast base alloy A: (a) ΔP-UTS, (b) ΔP-YS, and (c) ΔP-%El as a function of heat treatment condition with SHT for 4 h and 8 h.

6.2.2 RESULTS FOR AS-CAST AND 8 HRS-SOLUTION HEAT TREATED CONDITIONS

6.2.2.1 TENSILE TEST RESULTS

The tensile properties of the alloys A, B, C, D and E, when tested at 250°C, using test bars in the as-cast and heat-treated conditions following solution heat treatment for eight hours, are presented in this section. Six heat treatment conditions were used in this group, namely S8A, S8W, S8WA1, S8WA2, S8WA3 and S8WA4. Their descriptions are provided in Table 5-1 and Table 5-2. Alloys A, B and C were solution treated at 520°C for eight hours, alloy D was solution treated at 500°C for eight hours, and alloy E was solution treated at 540°C for eight hours. Prior to testing, the test bars were kept in the testing chamber at 250°C for thirty minutes, to ensure a homogeneous temperature distribution throughout the bar before the test was carried out. The high temperature tensile properties (UTS, YS and %El) of alloys A, B, C, D and E are listed in Table 6-3 and shown in Figure 6-9 through Figure 6-13.

Again, as in the case of the four hours SHT group, the charts in the figure show that the tensile properties of alloys A, B and C are improved upon heat treatment. The same behavior was exhibited by the reference alloys D and E when heat-treated, with improvements in the tensile properties; as shown in Figure 6-12 and Figure 6-13. Further heating of the samples in the testing chamber and then running the tests at 250°C coarsened the precipitates, decreased their density, increased their size and increased the inter-particle spacing, so that the strength decreased and the ductility increased, when compared with the ambient temperature tensile test results.

When tested at 250°C, the HT200 alloys showed lower values of strength and higher values of ductility in the as-cast condition compared to the as-cast reference alloys D and E. In the as-cast condition, alloy A exhibited UTS, YS and %El values of 152.8 MPa, 87.7 MPa, 6.1%, respectively, alloy B gave 157.1 MPa, 88.3 MPa, 8.5%, while alloy C showed 156.8 MPa, 102.68 MPa, 5.9% for the UTS, YS and %El, respectively. Compared to these values, alloy D showed 206.3 MPa, 152.96 MPa, 2.95% for the UTS, YS and %El, respectively, in the as-cast condition, and alloy E gave 170.9 MPa, 114.8 MPa, 5.79% for the UTS, YS and %El, respectively, in the as-cast condition.

Using heat treatment enhanced the mechanical properties of the HT200 alloys. Considering the first two heat treatment conditions, S8A and S8W, which comprise solution heat treatment followed by air or water quenching, it can be seen that the strength of the alloys improved. The improvement in the alloy strength is attributed to the solution heat treatment (SHT) as well as the high cooling rate that followed. As with SHT, the maximum amount of hardening solutes of Cu are retained in the solid solution in the matrix, forming a homogeneous supersaturated solid solution, SSSS, at elevated temperatures. When quenched, the SSSS formed during the solution treatment stage is preserved, by means of the rapid cooling to a lower temperature, usually near the room temperature. The quenching retains the solute atoms in solution and blocks them in the positions where they got to at the high temperature during the SHT, so that the casting is ready for subsequent strengthening mechanisms, as discussed earlier in section 6.2.1.1 of this chapter.

As seen from the results for the five alloys, better tensile properties were obtained, when solution treatment was followed by water quenching than when air quenching was used, due to the higher cooling rate achieved with water quenching. Alloys D and E showed

somewhat lower strength values in the S8A heat-treated condition than in the as-cast condition. This may be explained by the casting process as, when the tensile bars were cast they were left to cool in the air, which caused natural aging. This natural aging resulted in the formation of some precipitates as was shown in Chapter 5 which gave the extra strength to the castings.

In the S8W heat-treated condition, alloy A showed UTS, YS and %El values of 234.5 MPa, 197.9 MPa and 4.24%, respectively; alloy B displayed 216.7 MPa, 151.78 MPa and 4.5%, respectively, and alloy C gave 217.97 MPa, 198.3 MPa and 4.1%, respectively. The reference alloy D showed 259.7 MPa, 187.7 MPa and 5.1% as its UTS, YS and %El values, respectively, while alloy E gave 233.3 MPa, 180.87 MPa and 4.97%. The improvement in properties can be checked by comparing these results with those for the as-cast condition noted earlier in this section.

The remainder of the heat treatments used, namely S8WA1, S8WA2, S8WA3 and S8WA4, included artificial aging, with S8WA1 and S8WA2 representing T6 heat treatments and S8WA3 and S8WA4 representing T7 heat treatments. The precipitation hardening or age hardening follows solution heat treating and quenching and is used for strengthening. Aging treatment is controlled by temperature and time. Aging increases the strength and the main strengthening precipitates in Al-Cu alloys are those of the θ-Al_2Cu phase. During this aging process the alloy reaches its peak strength and then starts to soften when the aging temperature or aging time is increased further, known as over-aging; further increase in temperature may lead to annealing.

The five alloys achieved peak strength when T6 heat treatments were used (i.e. S8WA1 and S8WA2), as the precipitates were fine, coherent and displayed small inter-particle spacing; therefore the strength increased significantly. From Figure 6-9 to Figure 6-11, it can be seen that alloys A, B and C reached their peak strength in the S8WA2 heat treatment condition. The UTS, YS and %El values for the three alloys were 281.2 MPa, 280.17 MPa, 1.97%; 307.94 MPa, 303.9 MPa, 2.26%; and 276 MPa, 274.96 MPa, 3.2%, respectively. From Figure 6-12 and Figure 6-13, it can be seen that alloys D and E achieved their peak strength in the S8WA1 heat-treated condition, displaying 309 MPa, 304.85 MPa, 2.77%, and 282.6 MPa, 281.47 MPa and 2.36% as their UTS, YS and %El values, respectively. Compared to the as-cast values of each alloy, significant improvement in strength can be remarked.

When T7 treatment is used (i.e. S8WA3 and S8WA4), the strength begins to decrease, and the ductility to increase, with the increase in aging temperature, which leads to overaging. In the S8WA4 heat treatment condition, the increase in both aging temperature and aging time cause further overaging, such that the precipitates become coarser, bigger in size and lower in density, displaying large inter-particle distances as a result. This facilitates dislocation motion which in turn produces softening effects that decrease the alloy strength. Thus, in the over-aged condition, the ductility of the alloy increases as its strength is decreased.

At the elevated temperature of 250°C, among the HT200 alloys, alloy B showed the highest strength values in the S8WA2 heat treated condition with SHT for eight hours. Alloy B achieved very comparable and competitive mechanical properties with respect to the reference alloys D and E, exhibiting UTS, YS and %El values of 307.9 MPa, 303.9 MPa,

2.26% (albeit at a somewhat higher aging temperature of 200 °C), compared to 309 MPa, 304.85 MPa, 2.77%, and 282.6 MPa, 281.46 MPa, 2.36% for alloys D and E in the S8WA1 heat-treated condition, at an aging temperature of 180 °C, for the same aging time of 4 hours.

Table 6-3: Average values of UTS, YS and %El obtained at 250°C for alloys A, B, C, D and E in the as-cast condition and when subjected to different heat treatment conditions with SHT for 8 h.

Alloy	Condition	UTS [MPa]	YS [MPa]	%EL [%]
Alloy A	AC	152.80	87.69	6.11
	S8A	163.71	107.58	6.75
	S8W	234.51	197.94	4.24
	S8WA1	260.53	253.67	1.34
	S8WA2	281.21	280.17	1.97
	S8WA3	226.92	200.69	2.11
	S8WA4	172.78	112.98	2.91
Alloy B	AC	157.13	88.32	8.54
	S8A	175.67	117.59	8.07
	S8W	216.72	151.79	4.51
	S8WA1	273.02	270.58	1.87
	S8WA2	307.94	303.92	2.26
	S8WA3	241.69	184.78	3.17
	S8WA4	203.23	178.81	4.62
Alloy C	AC	156.81	102.69	5.92
	S8A	170.12	115.66	6.36
	S8W	217.97	198.36	4.07
	S8WA1	234.15	233.72	3.44
	S8WA2	276.06	274.96	3.20
	S8WA3	211.76	180.80	3.90
	S8WA4	201.54	170.96	4.33
Alloy D	AC	206.33	152.96	2.96
	S8A	205.08	132.89	5.44
	S8W	259.73	187.71	5.09
	S8WA1	309.11	304.86	2.77
	S8WA2	271.15	268.51	3.07
	S8WA3	192.11	173.81	6.24
	S8WA4	134.39	109.60	8.61
Alloy E	AC	170.90	114.85	5.79
	S8A	163.68	105.85	7.85
	S8W	233.30	180.87	4.97
	S8WA1	282.63	281.47	2.37
	S8WA2	268.71	268.0	3.11
	S8WA3	184.50	179.28	4.10
	S8WA4	115.72	100.87	12.21

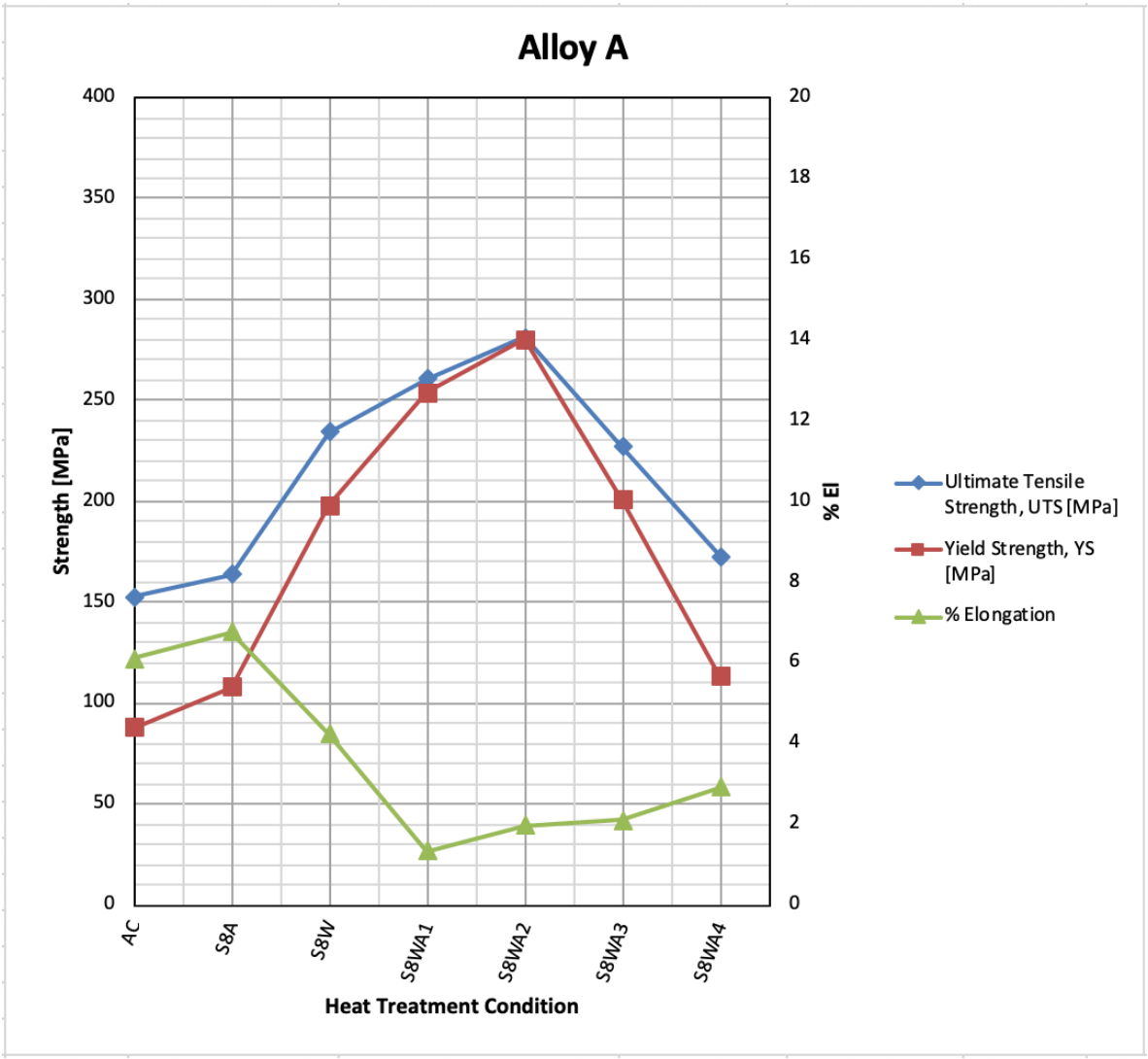

Figure 6-9: Average values of UTS, YS, %El obtained at 250°C, for alloy A in the as-cast condition, and after heat treatments comprising SHT for 8 h.

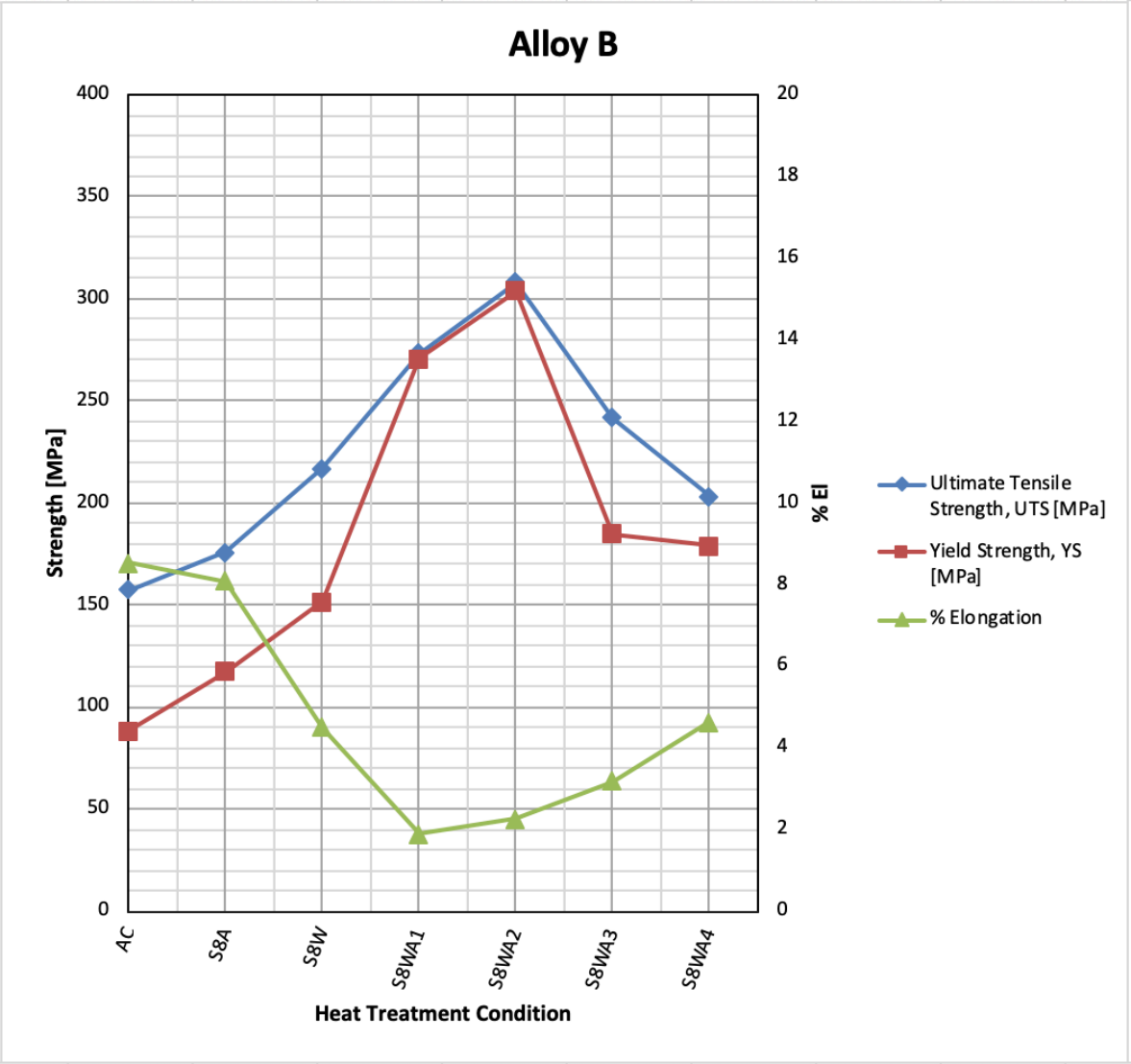

Figure 6-10: Average values of UTS, YS, %El obtained at 250°C, for alloy B in the as-cast condition, and after heat treatments comprising SHT for 8 h.

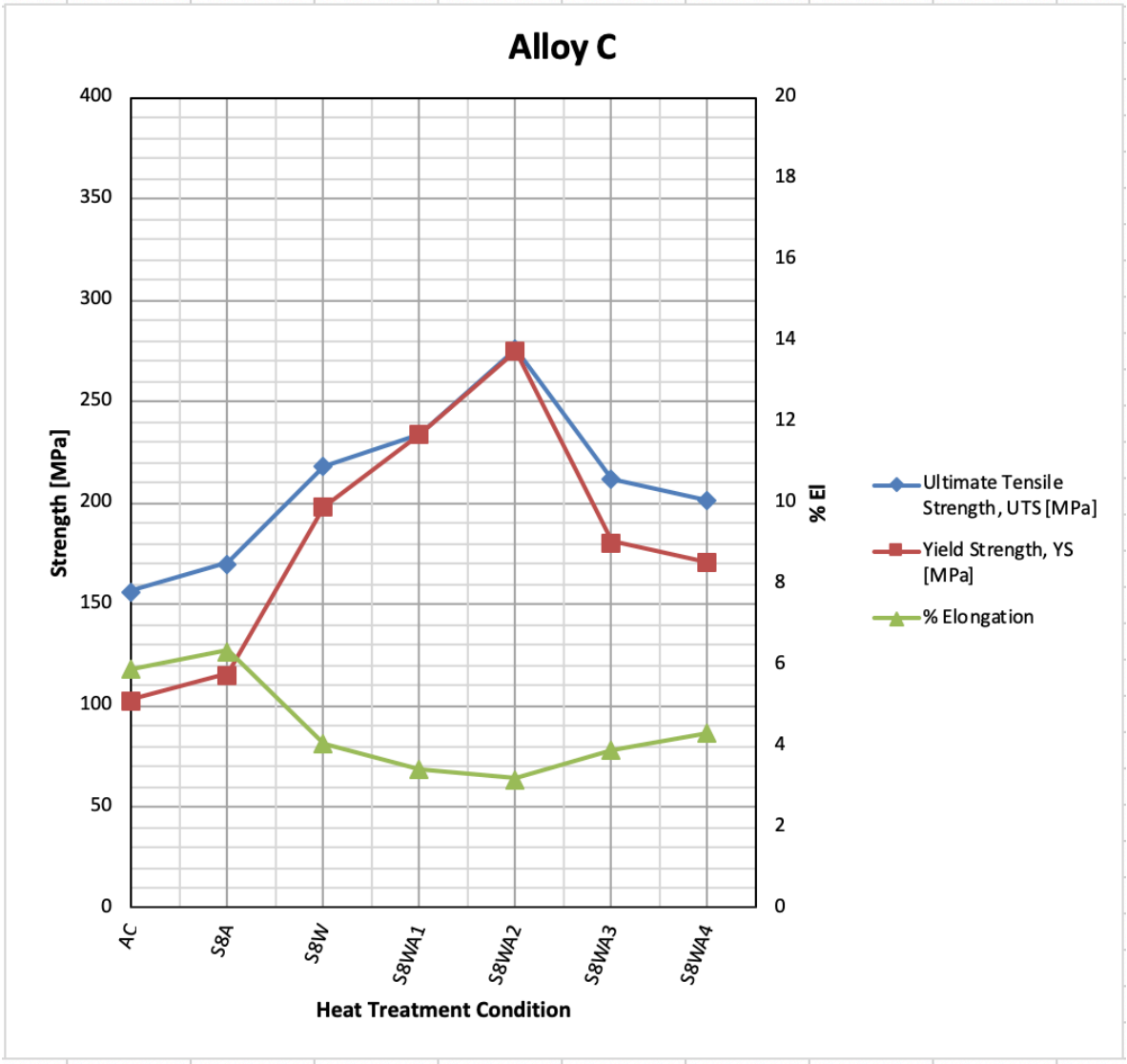

Figure 6-11: Average values of UTS, YS, %El obtained at 250°C, for alloy C in the as-cast condition, and after heat treatments comprising SHT for 8 h.

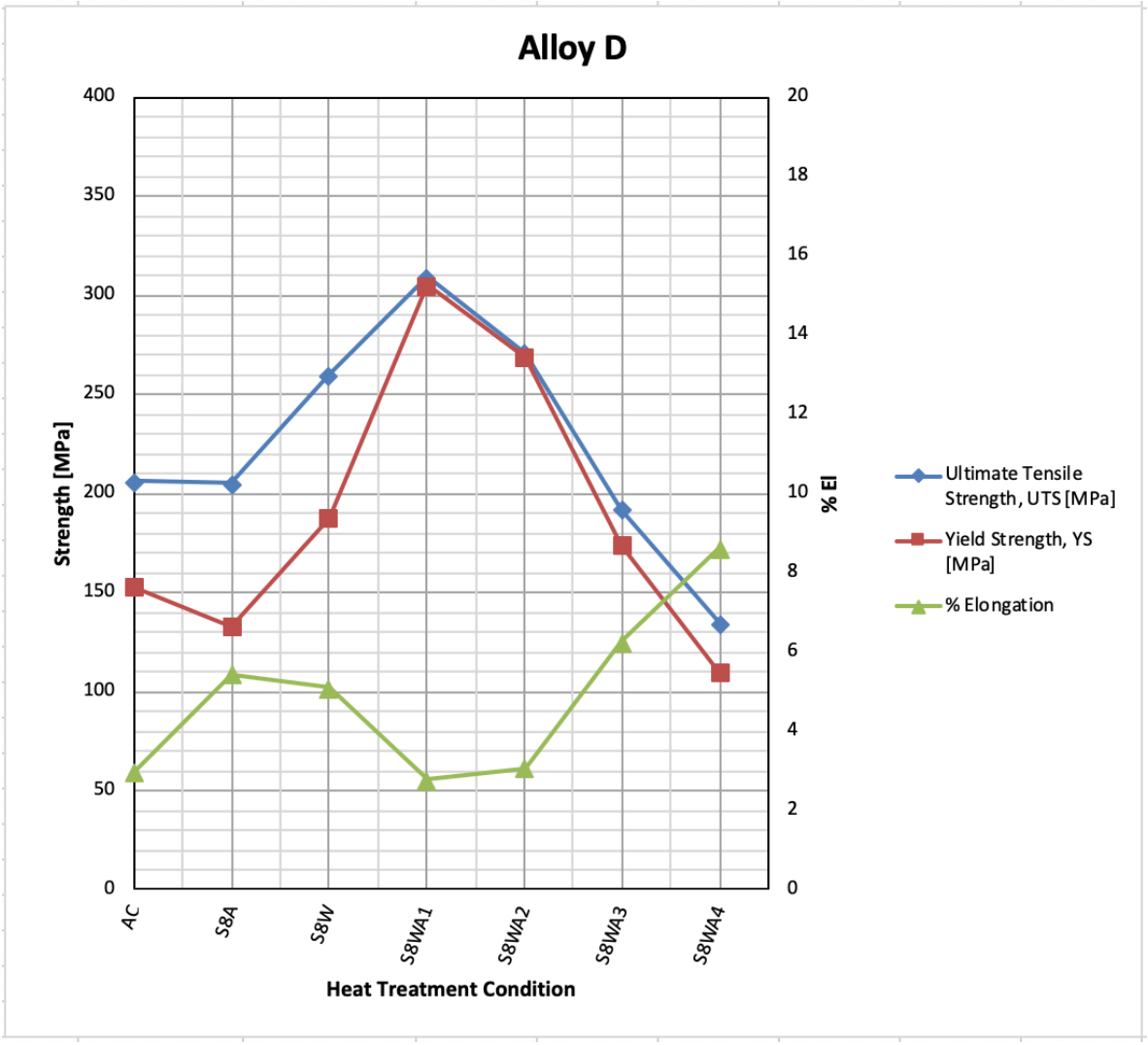

Figure 6-12: Average values of UTS, YS, %El obtained at 250°C, for alloy D in the as-cast condition, and after heat treatments comprising SHT for 8 h.

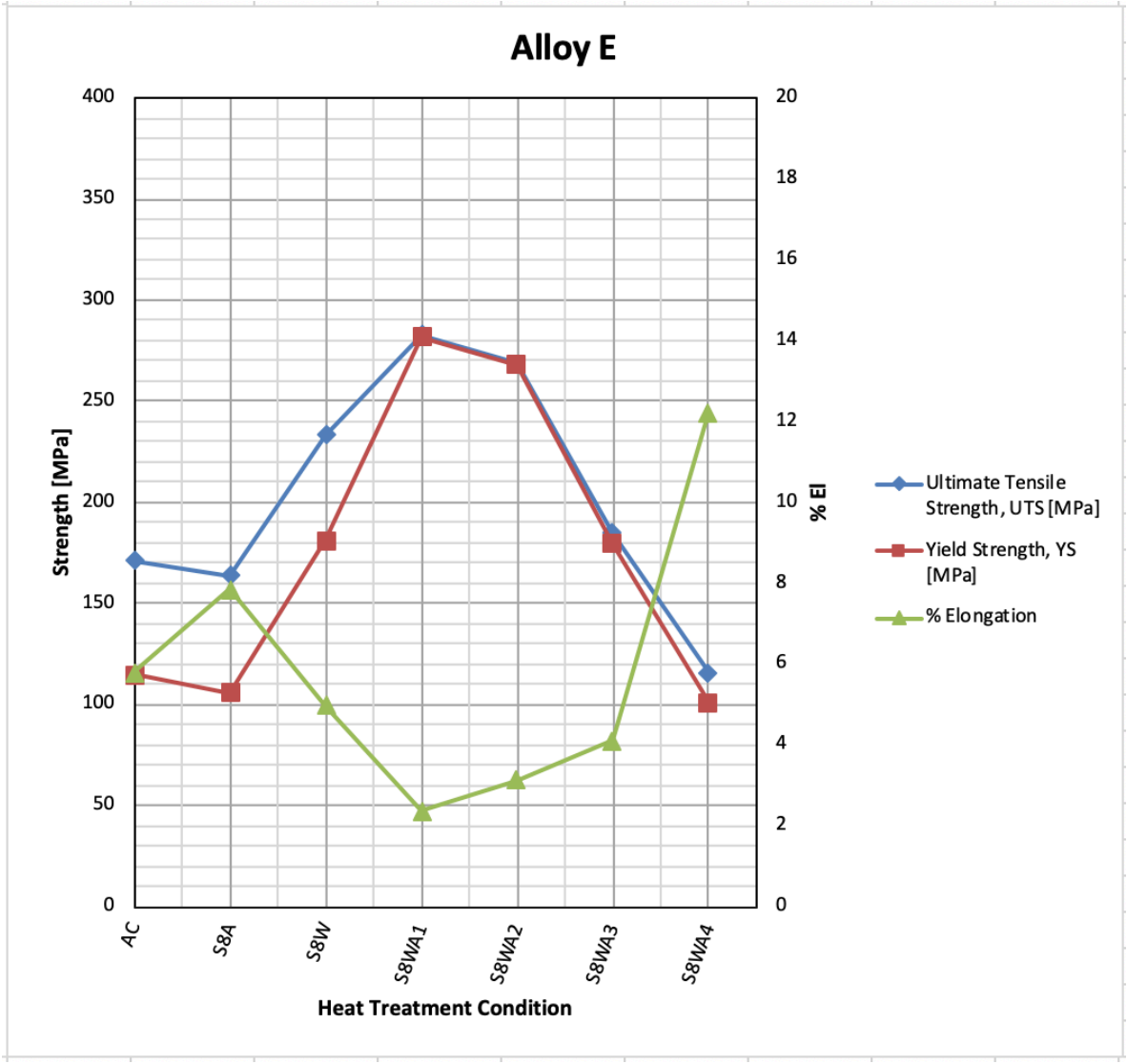

Figure 6-13: Average values of UTS, YS, %El obtained at 250°C, for alloy E in the as-cast condition, and after heat treatments comprising SHT for 8 h.

6.2.2.2 ANALYSIS OF TENSILE PROPERTIES USING THE QUALITY INDEX CONCEPT

As mentioned earlier in this chapter, quality charts provide a very good means of indicating the effect of different heat treatments and/or chemical composition changes on the strength and ductility of cast alloys.

From the tensile test data shown in Table 6-3, quality index or Q values as well as the probable yield strength or PYS values were calculated and are listed in Table 6-4. Quality charts were then generated for evaluating the influence of the metallurgical parameters involved on the tensile properties and quality of the HT200 aluminum alloys at the elevated temperature, under the as-cast and different heat treatment conditions with SHT for eight hours.

Table 6-4: Q and Probable YS (PYS) values obtained from the tensile test results in Table 6-3, and using Equations 1 and 2 from Chapter 2.

Average values of UTS (MPa) and El (%) used to obtain Q and Probable YS values using: **Q=UTS+150log(%El) … (1)** **PYS=UTS-60log(%El)+13 … (2)**			
Alloy	**Condition**	**Q [MPa] Eqn (1)**	**PYS [MPa]. Eqn (2)**
Alloy A	AC	270.74	118.63
	S8A	288.09	126.95
	S8W	328.61	209.86
	S8WA1	279.40	265.99
	S8WA2	325.31	276.57
	S8WA3	275.46	220.50
	S8WA4	242.29	157.97

Alloy B	AC	296.83	114.25
	S8A	311.67	134.27
	S8W	314.83	190.48
	S8WA1	313.94	269.65
	S8WA2	360.99	299.72
	S8WA3	316.93	224.59
	S8WA4	302.90	176.36
Alloy C	AC	272.67	123.46
	S8A	290.60	134.93
	S8W	309.43	194.39
	S8WA1	314.64	214.95
	S8WA2	351.93	258.71
	S8WA3	300.36	189.33
	S8WA4	296.98	176.36
Alloy D	AC	276.93	191.09
	S8A	315.44	173.94
	S8W	365.72	230.33
	S8WA1	375.58	295.53
	S8WA2	344.27	254.89
	S8WA3	311.43	157.38
	S8WA4	274.64	91.28
Alloy E	AC	285.34	138.13
	S8A	297.91	122.99
	S8W	337.74	204.53
	S8WA1	338.73	273.19
	S8WA2	342.70	252.11
	S8WA3	276.41	160.73
	S8WA4	278.73	63.52

Quality charts showing the relationship between UTS and %El are shown in Figure 6-14 for the alloys A, B and C, and in Figure 6-15 for alloys D and E. Points corresponding to the as-cast and six heat treatment conditions, with solution heat treatment for eight hours, are labeled in each case. The optimum results are expected to be located towards the upper-right corner (high Q and high YS region). The best combination of Q-value and PYS-value was determined for each of the alloys investigated among the different heat treatments applied, to find out the optimum alloy composition/heat treatment condition. The respective Q/YS combinations were found to be 328.6 MPa/209.86 MPa for alloy A in the S8W heat treated condition, and 325.3MPa/276.56 MPa after S8WA2 heat treatment; alloy B showed 361 MPa/299.7 MPa, and alloy C 351.9MPa/258.7MPa, also after S8WA2 treatment in both cases. Regarding the reference alloys, alloys D and E displayed Q/PYS values of 375.57 MPa/295.5 MPa and 338.7 MPa/273.2 MPa, respectively, both after S8WA1 heat treatment, while alloy E exhibited Q/PYS values of 342.7MPa/252 MPa following S8WA2 treatment.

Quality (Q) and probable yield strength (PYS) values of two heat treatment conditions were taken for alloy A, one without aging and the other including aging to differentiate between the two heat treatment types. The Q-value for the heat treatment comprising solution heat treatment for eight hours and no aging was slightly higher due to the higher ductility. Whereas with aging, in the T6 heat treatments, the Q-value was slightly lower and the PYS-value was significantly higher due to the higher strength resulting from aging. From the results noted above, alloy B in the S8WA2 heat treatment condition showed higher values for Q and PYS than alloys A and C. With respect to the reference alloys, alloy B showed very comparable quality values. The highest Q-value of alloy B is very close to the highest Q-value of alloy D, while the highest PYS-value of alloy B is higher than the highest PYS-

value of the same alloy. In comparing the Q- and PYS- values of alloy B with alloy E, alloy B gave higher results.

By comparing the Q/PYS results of alloy B in the T6 heat-treated condition S4WA2 with solution heat treatment for four hours (360.65 MPa/269.8 MPa), with those of alloy B in the T6 heat treatment condition S8WA2 but with solution heat treatment for eight hours (361 MPa/299.7 MPa), it can be concluded that alloy B in the S8WA2 condition corresponds to the optimum alloy composition/heat treatment condition for the HT200 alloy at the elevated temperature.

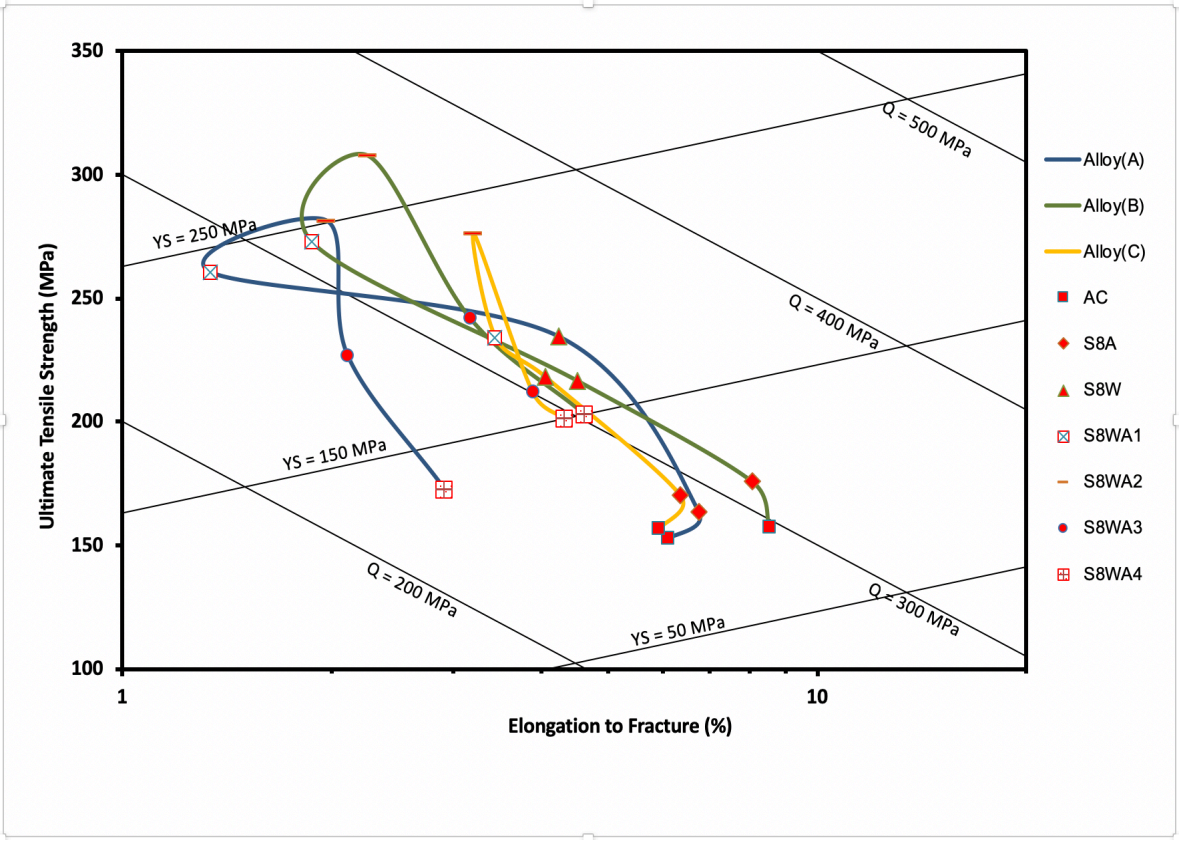

Figure 6-14: Quality chart showing relationship between UTS and %El for the A, B and C alloys investigated in the as-cast and six heat treatment conditions with SHT for 8 h.

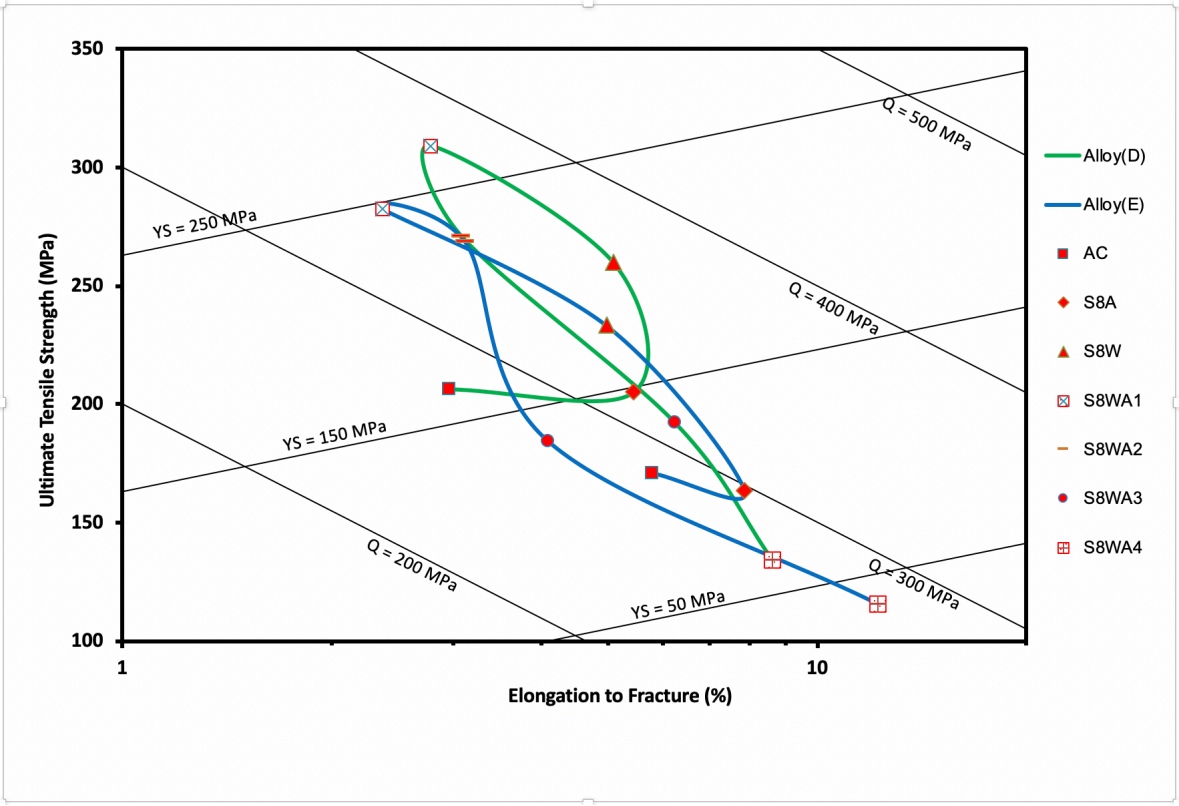

Figure 6-15: Quality chart showing relationship between UTS and %El for the D and E alloys investigated in the as-cast and six heat treatment conditions with SHT for 8 h.

Figure 6-16 presents a panel chart showing the Q-values for each of the five alloys A, B, C, D and E in the as-cast condition, and following the 12 heat treatment conditions (six with solution heat treatment for four hours and six with solution heat treatment for eight hours), obtained from the tests carried out at 250 °C. On an individual basis, alloy B gives the most consistent quality across the range of heat treatments used, within a variation of 50 MPa. The maintenance in strength may be attributed to the Zr which would form precipitates that retain their strength at high temperature.

While Figure 6-17 shows how the Q-values of the five alloys vary on going from the as-cast condition through all the heat treatment conditions used in this study. The reference

alloy D or 319 alloy exhibits higher quality than the other alloys after 8 hours of solution treatment followed by water quenching, up until an aging temperature of 180 C (S8WA1 treatment). At higher aging temperatures, the alloy quality decreases rapidly as the alloy softens; with alloy B showing a better quality than the other alloys at these temperatures, again attributed to retention of its strength due to the presence of Zr.

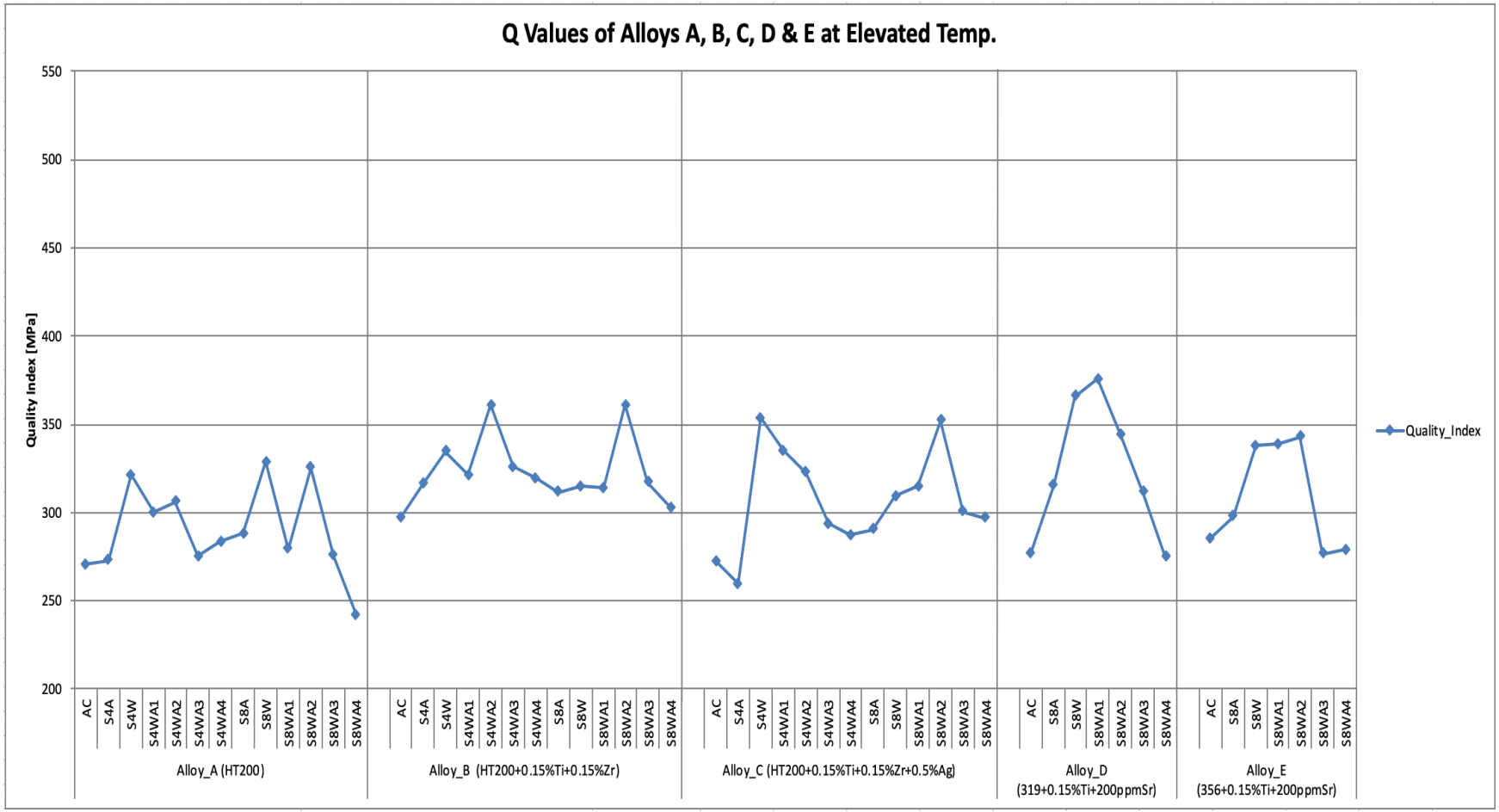

Figure 6-16: A panel chart for the quality values of alloys A, B, C, D and E in the as-cast condition and the 12 heat treatment conditions used in this study.

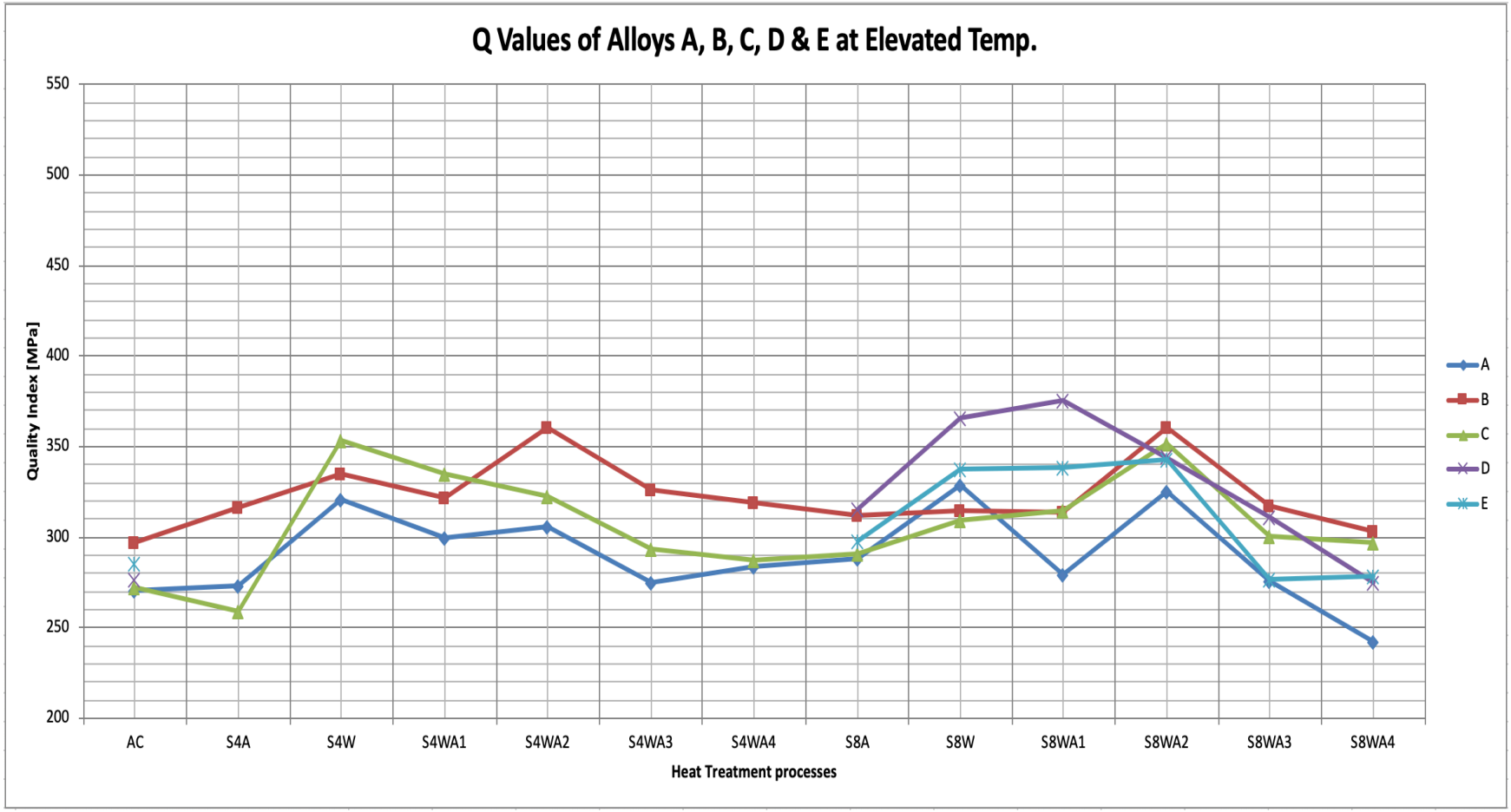

Figure 6-17: Quality values of alloys A, B, C, D and E in the as-cast condition and the 12 heat treatment conditions used in this study.

6.2.2.3 STATISTICAL ANALYSIS (COMPARISON BETWEEN BASE ALLOY AND OTHER ALLOYS)

This section presents a comparison of the tensile properties (UTS, YS and %El) of the different alloys under different heat treatment conditions, following solution heat treatment for eight hours, with those of the base alloy A in the as-cast condition, for tests carried out at 250 °C. Figure 6-18 depicts the tensile properties obtained for Alloys A, B and C for these different heat treatment conditions, relative to the values obtained for the base alloy A at the as-cast condition, i.e., after subtracting the values obtained for the base alloy A for each condition, and plotted as ΔP values on the Y-axis (P = Property = UTS, YS or %El), with the X-axis representing the base line for alloy A. The numbers on the X-axis represent the as-cast condition and the different heat treatment conditions used. These conditions are indicated by numbers to facilitate reading the data. Each of the numbers with the conditions they refer to is provided in Table 5-1. The ΔP values with respect to the different heat treatments, with SHT for eight hours, are also presented for the reference alloys D and E, which are shown in Figure 6-19. The use of this method provides an effective means of knowing how the various additions used and the different heat treatment conditions applied affect the properties of the HT200 casting alloy.

Regarding alloys A, B and C, it may be seen from Figure 6-18, that their mechanical properties were generally enhanced. The strength of the base alloy A improved by as much as 70-130 MPa with some of the aging treatments applied, namely S8WA1, S8WA2 and S8WA3, while the ductility showed a corresponding decrease. Highest strengths were displayed by alloy B, due to the addition of the grain refiners (Ti and Zr), as well as the heat

treatments applied, particularly in the case of the S8WA1 and S8WA2 treatments. With respect to alloys B and A, the improvements observed for alloy C for these treatments were slightly lower.

As Figure 6-18 (c) shows how the much higher strengths achieved with heat treatment are reflected in the corresponding low ductility values exhibited in each case, except for the S8A condition (solution treatment + air quenching) which exhibited the lowest gain in strength.

Compared to the as-cast HT200 base alloy A, the reference alloys D and E display better as-cast strength, as seen in Figure 6-19 (a, b). The strength of the alloys improved with heat treatment, particularly with S8WA1 and S8WA2 T6 treatments, alloy D showing higher improvements, in general, and correspondingly, lower ductility values compared to alloy E. Considerable softening of the alloy was observed when the aging temperature and time were highest i.e., 250 °C and 100 hours when the S8WA4 treatment was applied, the UTS reaching values lower than the as-cast HT200 base alloy. It must be borne in mind that the effects of temperature were further emphasized by the high temperature testing conditions.

Figure 6-20 compares the tensile properties of the five alloys A, B, C, D and E with those of the as received base alloy A. At the elevated testing temperature, the as received HT200 alloy (alloy A) showed lower tensile properties (UTS, YS and %El) with respect to the reference alloys D and E in the as-cast and solution heat-treated conditions (with SHT for eight hours). This is attributed to the 7% Si content of the 319 and 356 alloys which would provide a significant contribution to the strength, particularly after solution treatment, compared to the HT200 alloy. On the other hand, the higher strength values exhibited by the

HT200 alloys compare to the 319 and 356 alloys after peak aging has been achieved shows the advantage of the Zr addition in maintaining the alloy resistance to softening at high temperatures.

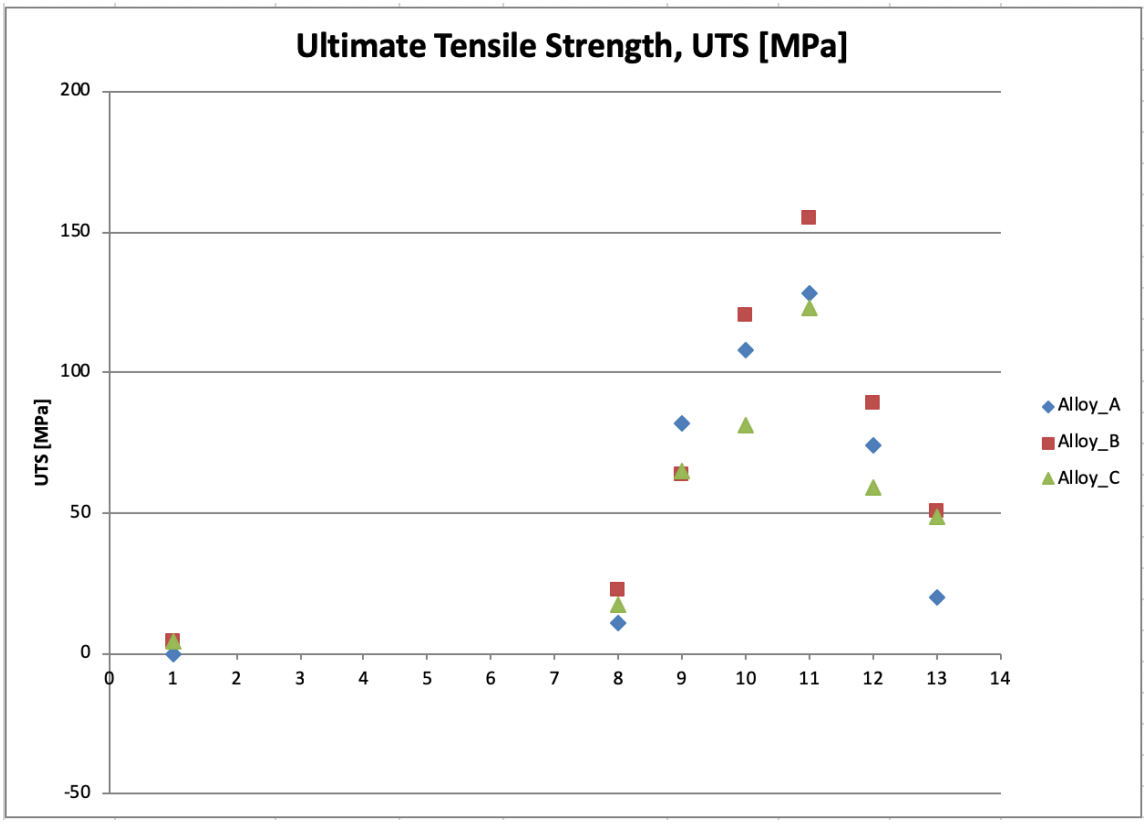

(a)

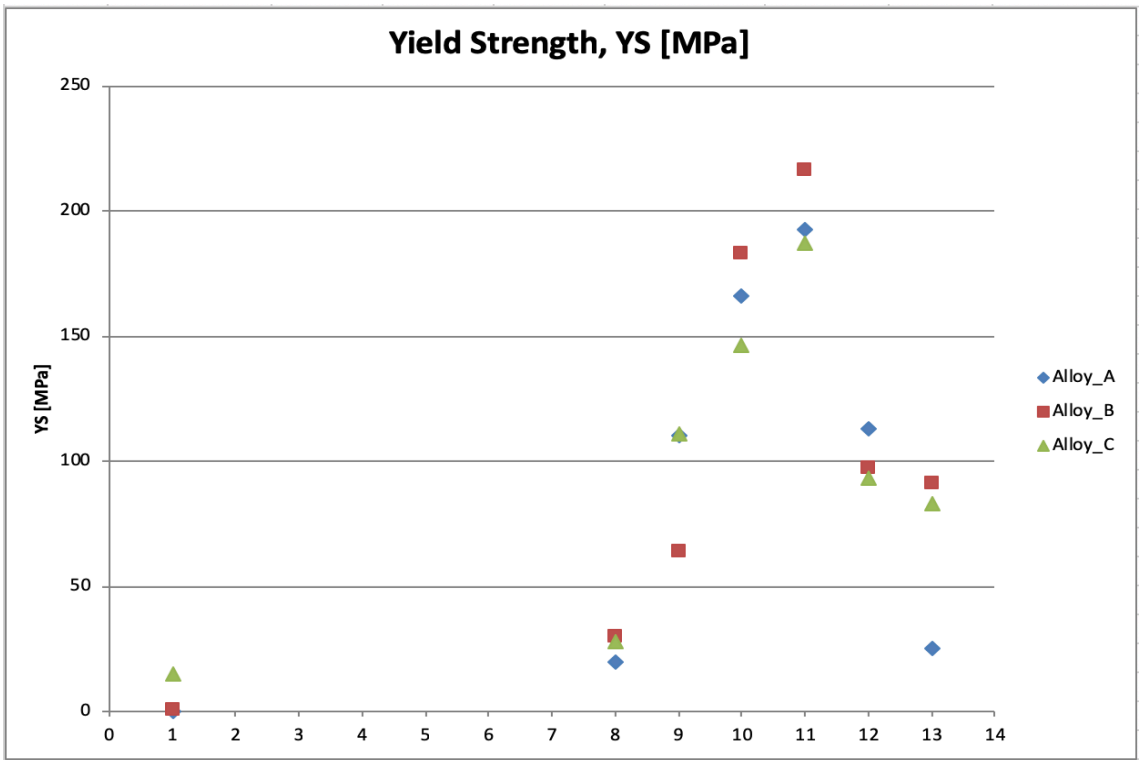

(b)

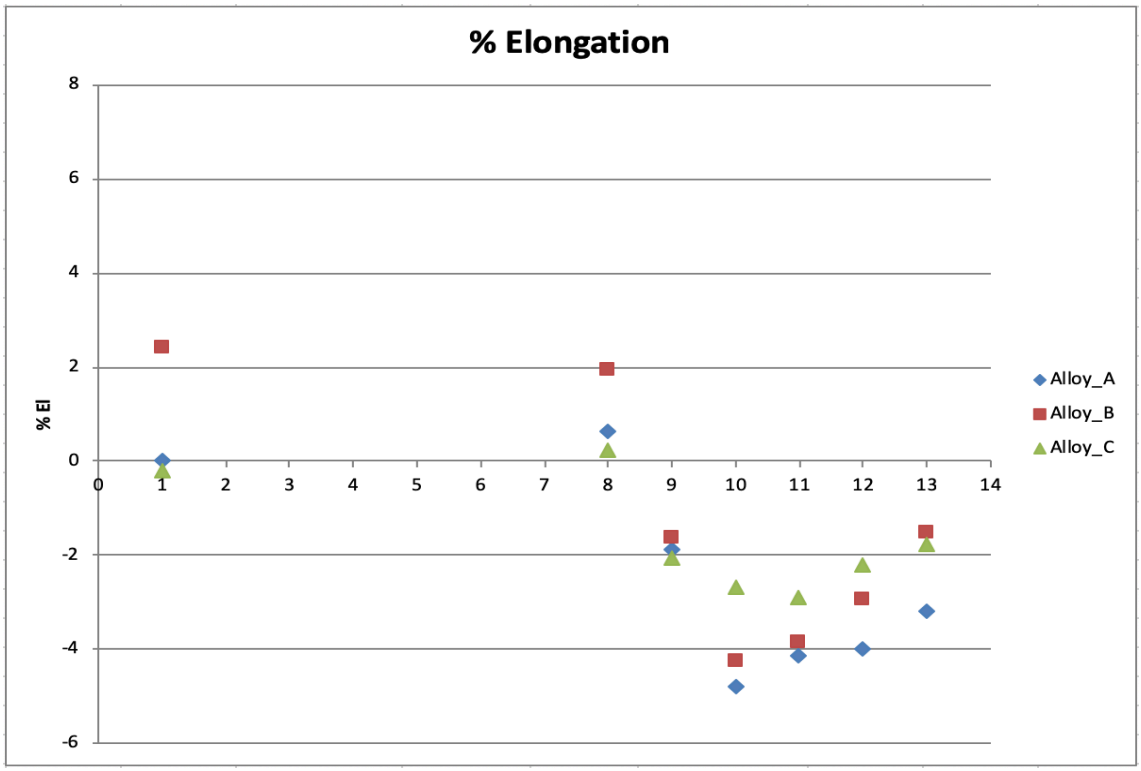

(c)

Figure 6-18: Comparison of tensile properties of A, B and C alloys relative to those of as-cast base alloy A: (a) ΔP-UTS, (b) ΔP-YS, and (c) ΔP-%El as a function of heat treatment conditions with SHT for 8 h.

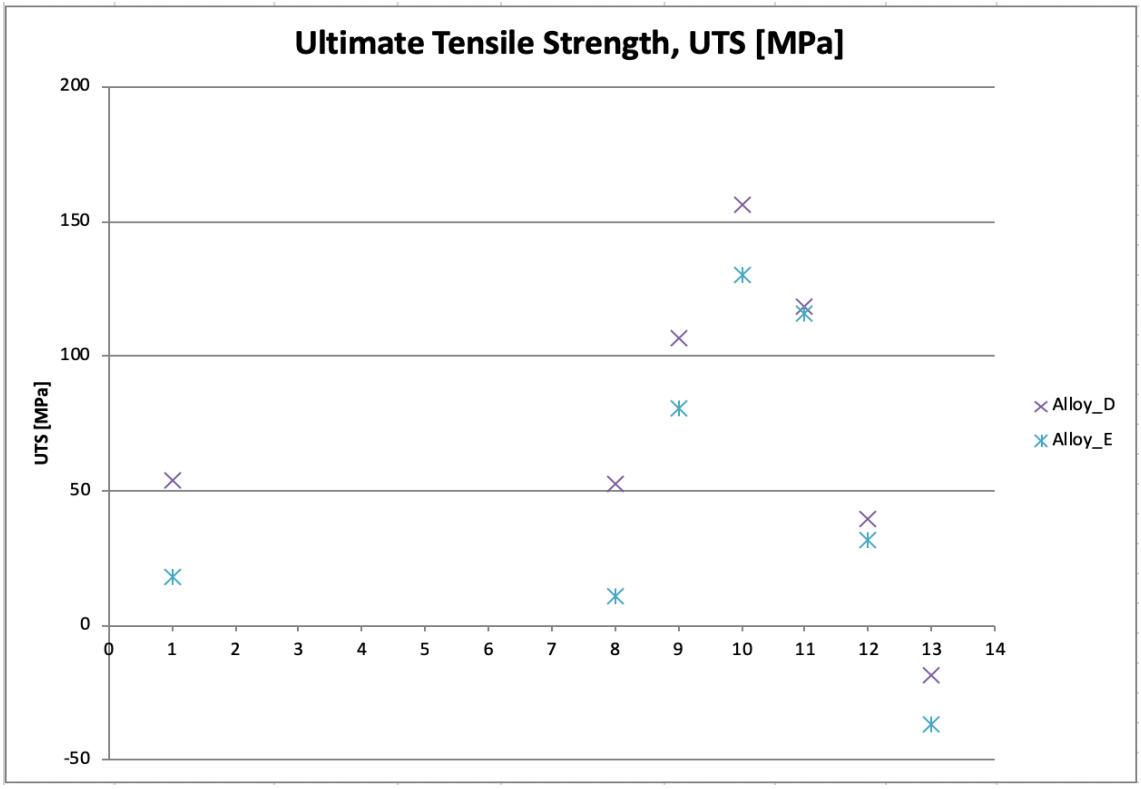
Ultimate Tensile Strength, UTS [MPa]
UTS [MPa]
200
150
100
50
0
-50
0 1 2 3 4 5 6 7 8 9 10 11 12 13 14
Alloy_D
Alloy_E

(a)

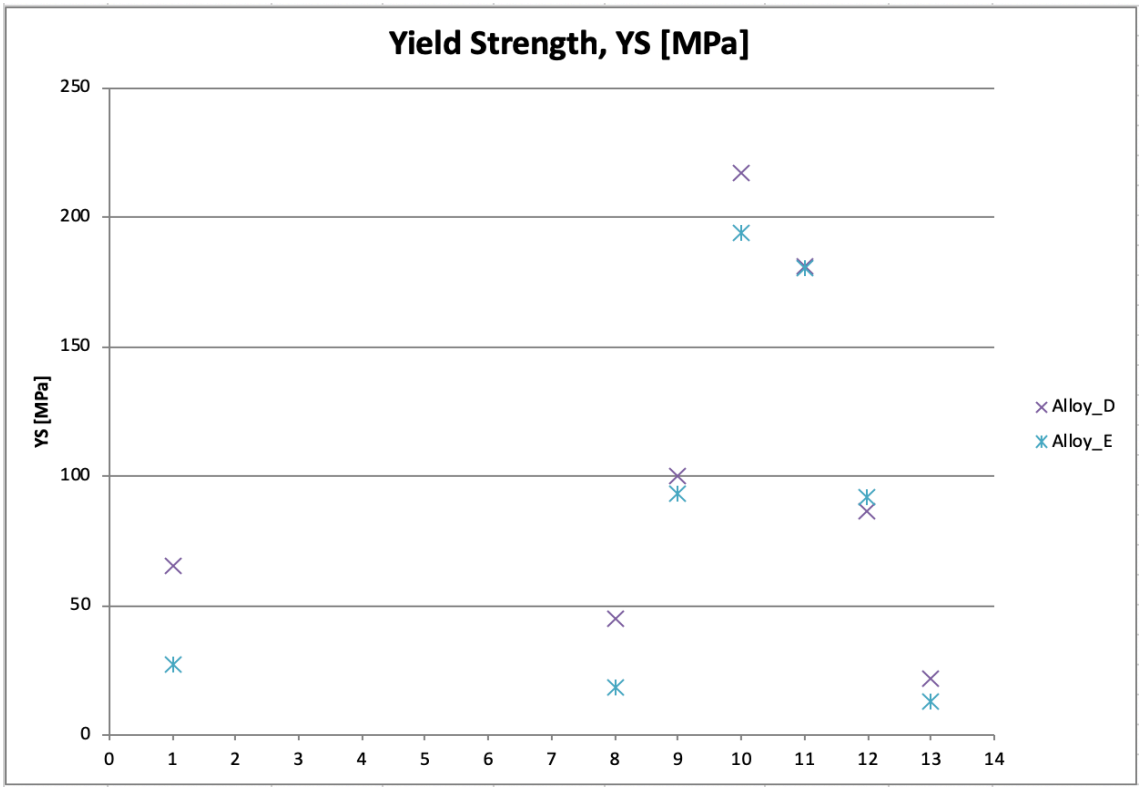
Yield Strength, YS [MPa]
YS [MPa]
250
200
150
100
50
0
0 1 2 3 4 5 6 7 8 9 10 11 12 13 14
Alloy_D
Alloy_E

(b)

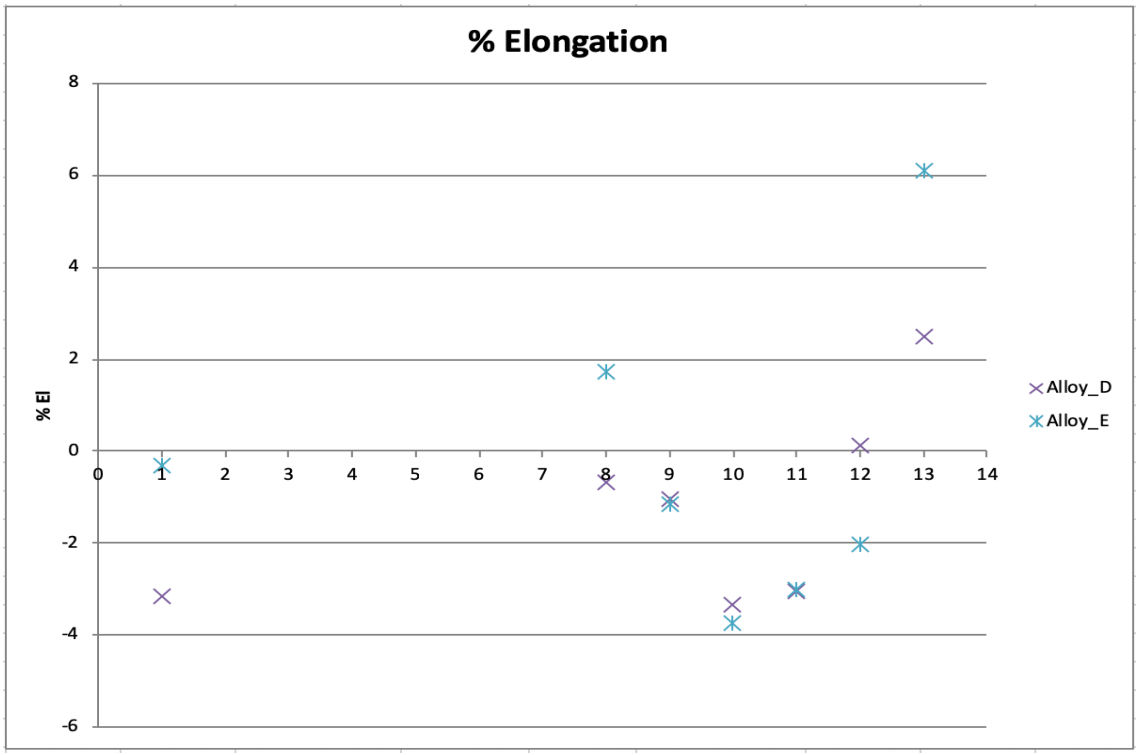

(c)

Figure 6-19: Comparison of tensile properties of D and E alloys relative to those of as-cast base alloy A: (a) ΔP-UTS, (b) ΔP-YS, and (c) ΔP-%El as a function of heat treatment conditions with SHT for 8 h.

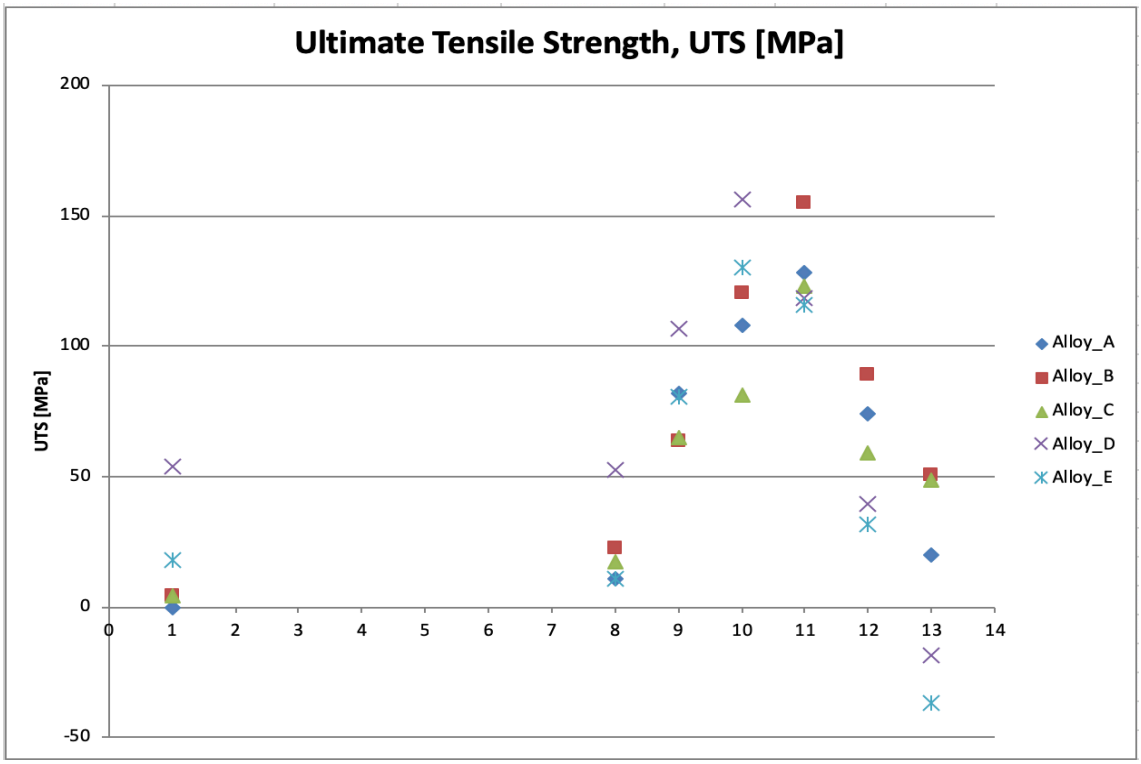

(a)

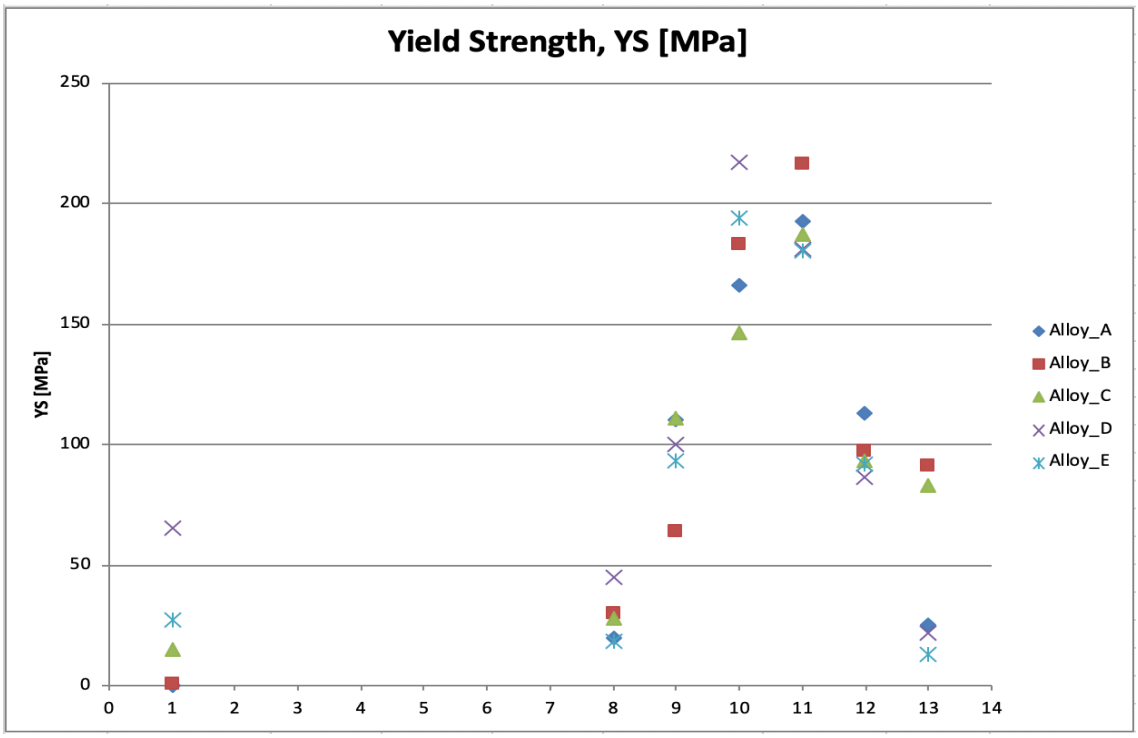

(b)

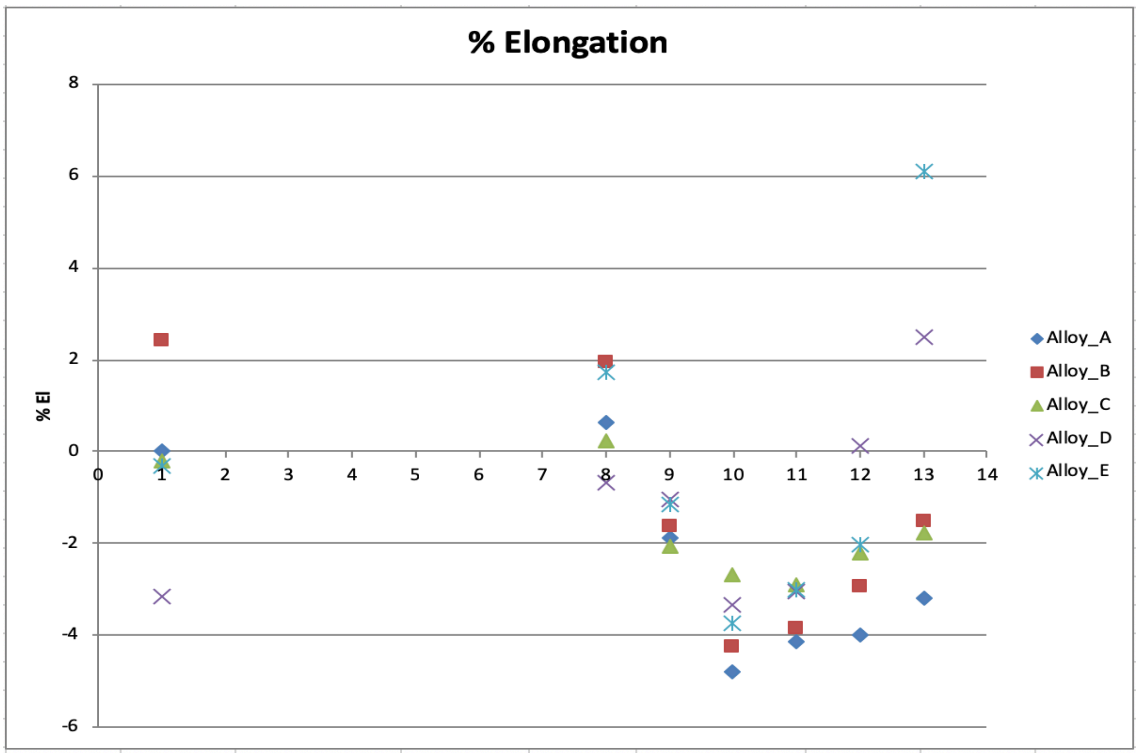

(c)

Figure 6-20: Comparison of tensile properties of A, B, C, D and E alloys relative to those of as-cast base alloy A: (a) ΔP-UTS, (b) ΔP-YS, and (c) ΔP-%El as a function of heat treatment conditions with SHT for 8 h.

Figure 6-21 shows comparison of the tensile properties (UTS, YS and %El) in the as-cast and twelve heat treatment conditions used in this study for the HT200 alloys A, B and C, relative to those of as-cast base alloy A, while Figure 6-22 compares the tensile properties of the five alloys A, B, C, D and E, for the same thirteen conditions. From Figure 6-21, it can be seen that the strength begins to improve with solution heat treatment, but increases more when followed by water quenching. Artificial aging further enhances the strength with the T6 heat treatments, and thereafter the strength starts to decrease as softening commences with the use of the T7 heat treatments. The same trend is observed more or less for solution times of 8 hours as in the case of the 4 hour solution treatments. Overall, alloy B in the S8WA2 heat-treated condition provides the highest strength.

Figure 6-22 shows that compared to the HT200 alloys, the reference alloys 319 and 356 show higher strength values in the as-cast condition and following 8 hours solution heat treatment, as well as in the T6 condition. The higher strength in their case is attributed to the silicon content of the alloys which provides an added contribution to the strength besides that of the precipitates. Coarsening of these constituents in the T7 condition and the additional exposure to temperature at the elevated temperature testing conditions results in the increase in ductility values observed for the 319 and 356 alloys condition #13 in Figure 6-22 (c).

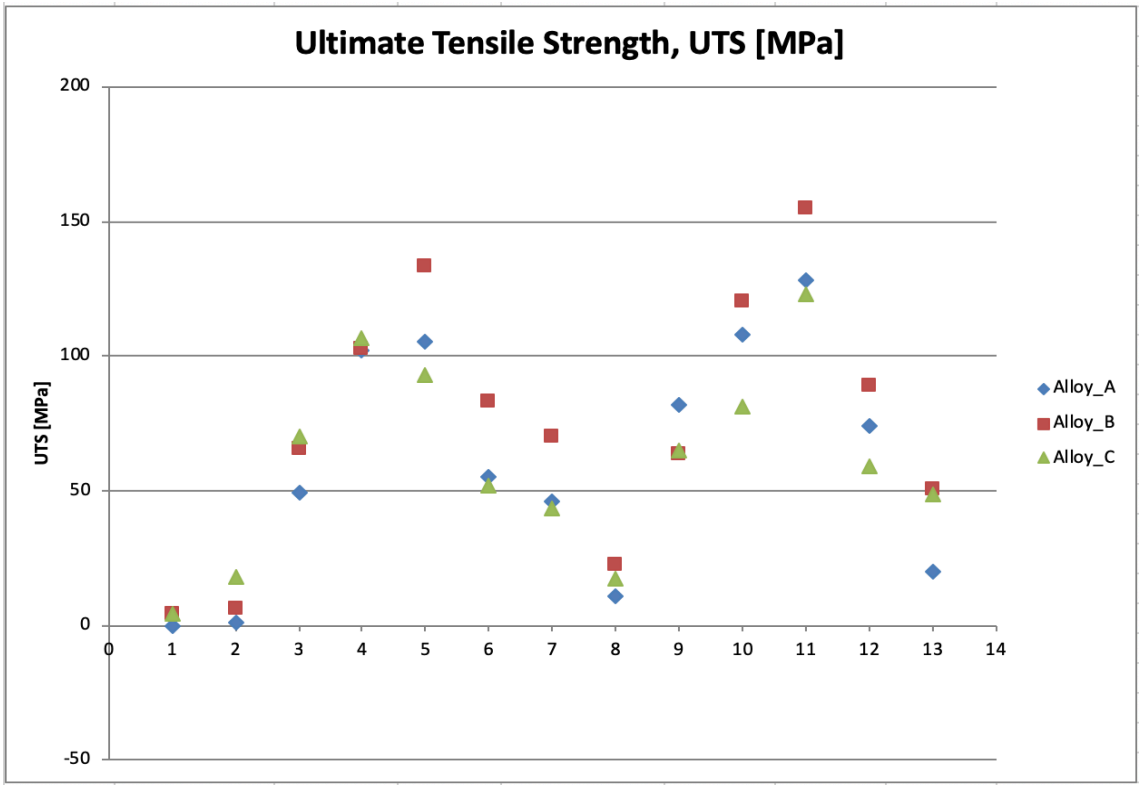
Ultimate Tensile Strength, UTS [MPa]
UTS [MPa]
200
150
100
50
0
-50
0 1 2 3 4 5 6 7 8 9 10 11 12 13 14
Alloy_A
Alloy_B
Alloy_C

(a)

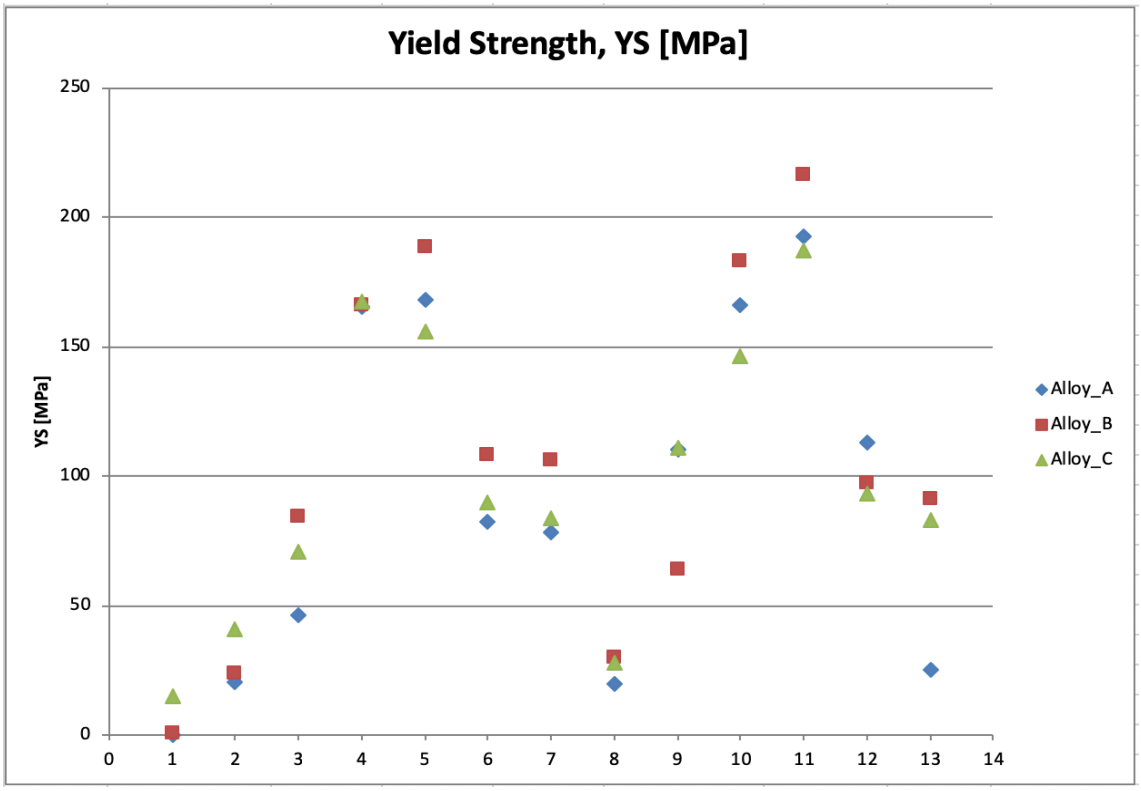
Yield Strength, YS [MPa]
YS [MPa]
250
200
150
100
50
0
0 1 2 3 4 5 6 7 8 9 10 11 12 13 14
Alloy_A
Alloy_B
Alloy_C

(b)

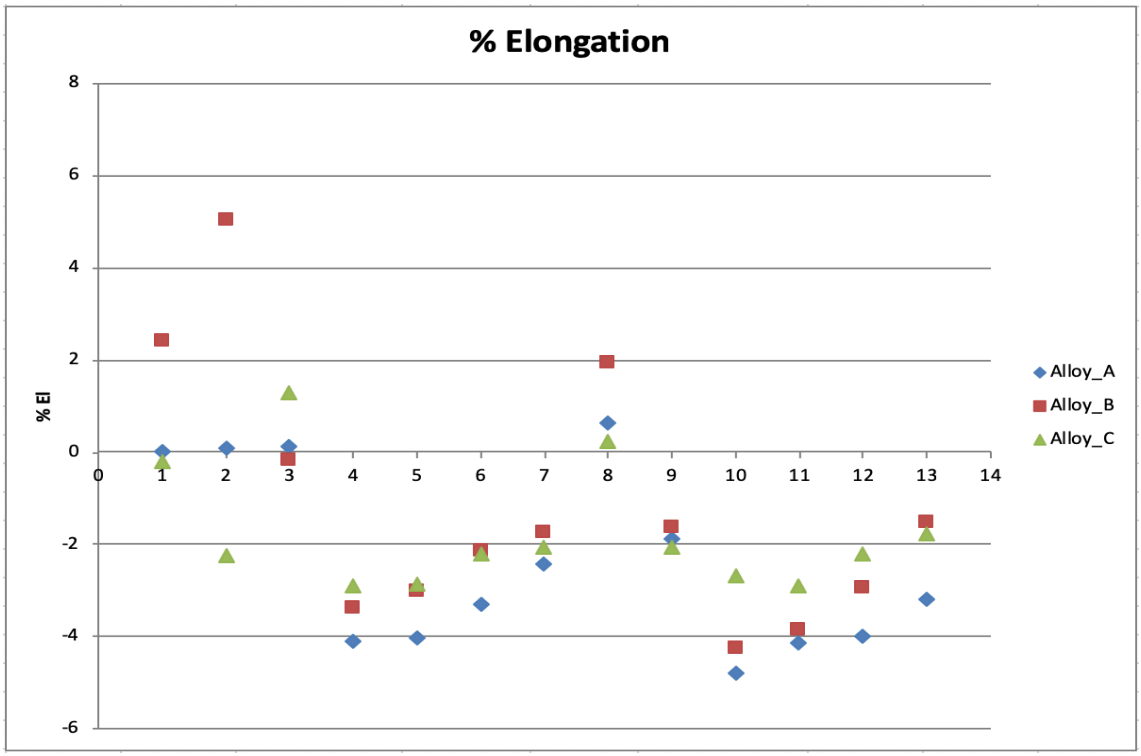

(c)

Figure 6-21: Comparison of tensile properties of A, B and C alloys relative to those of as-cast base alloy A: (a) ΔP-UTS, (b) ΔP-YS, and (c) ΔP-%El as a function of heat treatment conditions with SHT for 4 h and 8 h.

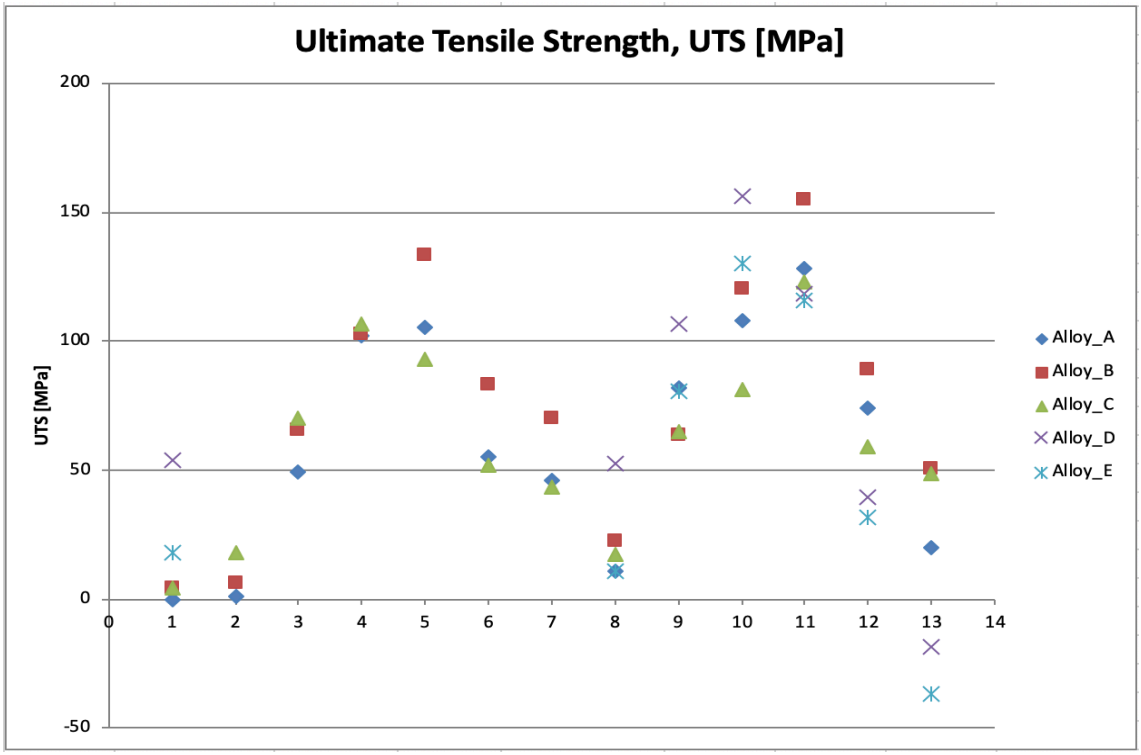

(a)

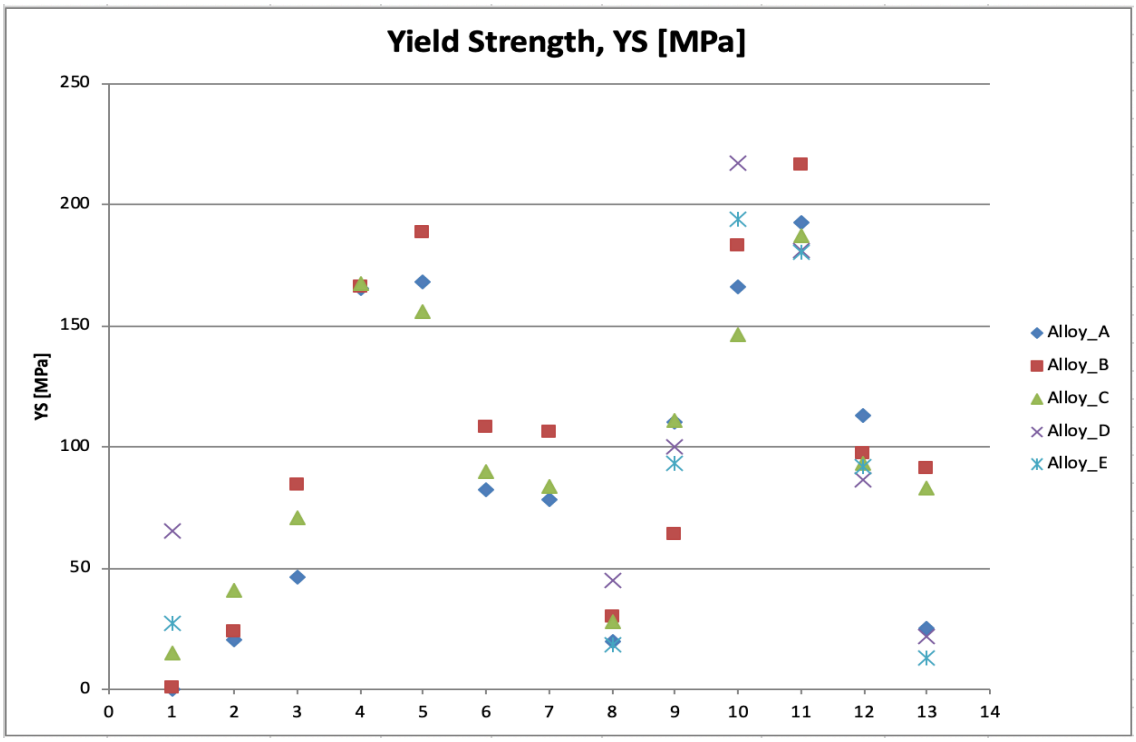

(b)

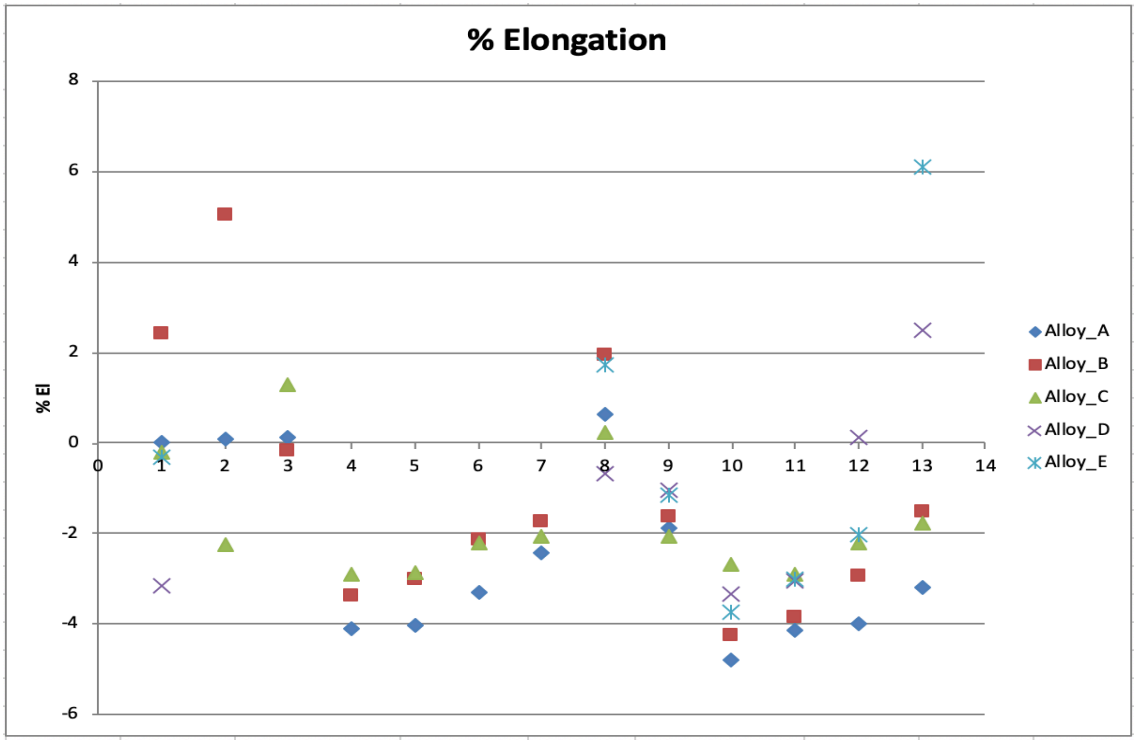

(c)

Figure 6-22: Comparison of tensile properties of A, B, C, D and E alloys relative to those of as-cast base alloy A: (a) ΔP-UTS, (b) ΔP-YS, and (c) ΔP-%El as a function of heat treatment conditions with SHT for 4 h and 8 h.

CHAPTER 7

CONCLUSION

CHAPTER 7

7 CONCLUSIONS

This research study was carried out to investigate the effects of different heat treatments and alloying additions on the ambient and high temperature tensile properties of a new Al-6.5%Cu based alloy, designated HT200 alloy. Three alloys were used: the base HT200 alloy (coded A), and two others, containing 0.15% Ti + 0.15%Zr, and 0.15% Ti + 0.15%Zr + 0.5%Ag additions (coded B and C, respectively). The properties of the three HT200-types alloys were compared with those of 319 (coded D) and 356 (coded E) alloys, subjected to the same heat treatment conditions. Based on their extensive use in the automotive industry, the 319 and 356 alloys were selected as reference alloys, for comparing the performance of the new alloy, with respect to these popular alloys.

From an analysis and discussion of the results presented in Chapters 4, 5 and 6 of this thesis, a number of conclusions were drawn and are presented in this chapter in the sections that follow.

7.1 HOT TEARING AND MICROSTRUCTURE

1. The temperature of the molten HT200 alloy A was raised to 830°C to decrease the alloy sensitivity to cracking as, when the melt was poured from 750°C, the fluidity of the liquid metal was not high enough to fill the mold completely, leading to the formation of some cracks. Thus, melt superheating was used to overcome this problem.

2. Addition of grain refiners, as in alloys B and C, in addition to controlling the mold temperature, is an effective means of improving the alloy resistance to hot tearing without the need for superheating the melt. Alloy B showed good evidence of this, as it produced a crack-free casting.

3. From thermal analysis, five main reactions were detected during the solidification of alloy B: (i) precipitation of α-Al at 640°C, followed by (ii) precipitation of α-Fe at 600°C; (iii) precipitation of Al_2Cu phase at 523°C; (iv) precipitation of Q-phase at 516°C; and lastly, (v) end of solidification at 500°C.

4. At low cooling rate of 0.8°C/s obtained with the thermal analysis castings, the addition of grain refiner to HT200 alloy resulted in a marked decrease in the alloy grain size, from about 350-400μm in alloy A to about 100-150μm in alloy B.

5. At the high cooling rate of 8°C/s obtained with the tensile test bar castings, the average grain size in alloy A was found to be about 85 μm, compared to 350 μm reported for samples solidified at 0.8°C/s. A combined high solidification rate with proper grain refining resulted in a grain size of approximately 50 μm in alloy B.

6. The metallurgical parameters of solidification rate and grain refining have a remarkable effect in controlling the hot tearing susceptibility and in refining the microstructure of the HT200 Al-Cu alloys, to improve their mechanical properties.

7.2 TENSILE TESTS CARRIED OUT AT AMBIENT TEMPERATURE

7. Addition of the grain refiners TiB2 and Zr enhanced the overall ductility of the HT200 alloy, giving %El values of 3.7% and 3% in alloys B and C compared with 2.2% for alloy A.

8. In the as-cast condition, the HT200, 319 and 356 alloys exhibited UTS, YS and %El values of 283.45 MPa, 227.3 MPa and 2.2% (alloy A), 308.2 MPa, 213.5 MPa and 2.6% (alloy D) and 214.6 MPa, 140 MPa and 2.85% (alloy E).

9. The strength of the HT200 alloys improved significantly with heat treatment. The best strength results were obtained when aging was implemented using T6 and T7 heat treatments. T6 heat treatments gave higher strength than T7 heat treatments where overaging resulted in alloy softening.

10. Optimum room temperature tensile properties and Q-values for the five alloys investigated and the corresponding heat treatment conditions which provided these properties are summarized in the table below.

Alloy	Optimum tensile properties			Q-value (MPa)	Heat treatment condition
	UTS (MPa)	YS (MPa)	%El		
A	372.76	297.3	1.24%	387.0	S4WA1
B	388.6	292.24	3.1%	463.2	S8WA2
C	352.0	274.86	2.9%	420.86	S8WA1
D	354.8	324.36	1.2%	366.54	S8WA2
E	346.5	298.5	1.0%	349.6	S8WA2

11. Among the three HT200 alloys, alloy B in the S8WA2 heat-treated T6 condition is considered the optimum composition/heat treatment condition for the HT200 alloy. The

UTS improved by ~37%, the YS improved by ~29% and the %El improved by ~41%, compared to those of the as-received alloy A at the as-cast condition. The observed enhancement in the tensile properties may be interpreted in terms of the precipitation of ultra-fine particles of the θ-Al_2Cu phase, as well as the grain refining.

12. Comparing alloy B with the reference alloys D and E, all three alloys display optimum properties in the S8WA2 heat-treated condition. However, alloy B exhibits the highest UTS, %El, PYS and Q values in comparison, with an alloy quality exceeding that of alloys D and E by ~26.4% and ~32.5%, respectively.

13. Alloy B also gives the best overall performance across the range of heat treatments employed with respect to the HT200 alloys. Hence, the alloy B version of HT200 alloy could be considered as a very suitable alternative to the 319 and 356 alloys for use in the automotive industry.

14. The addition of Ag, contrary to expectations, did not produce noticeable improvement in the strength properties (UTS and YS).

7.3 TENSILE TESTS CARRIED OUT AT THE ELEVATED-TEMPERATURE

15. Addition of TiB_2 and Zr enhanced the overall ductility of the as received HT200 alloy, from 6.11% in alloy A to 8.54% in alloy B.

16. The strength of the HT200 alloys improved significantly with heat treatment. However, the strength values of the alloys at elevated temperature (250°C) were lower than those observed at room temperature (25°C).

17. The HT200 alloy A showed lower tensile properties with respect to the 319 and 356 reference alloys in as-cast and solution heat-treated conditions. The higher strengths observed in these alloys is attributed to the strengthening effects resulting from their higher Si content.

18. Optimum high temperature tensile properties and Q-values for the five alloys investigated and the corresponding heat treatment conditions which provided these properties are summarized in the table below.

Alloy	Optimum tensile properties			Q-value (MPa)	Heat treatment condition
	UTS (MPa)	YS (MPa)	%El		
A	281.2	280.2	1.97%	325.3	S8WA2
B	307.9	303.9	2.3%	361.0	S8WA2
C	276.0	274.9	3.2%	351.9	S8WA2
D	309.1	304.9	2.8%	375.6	S8WA1
E	282.6	281.5	2.4%	338.7	S8WA1

19. The best strength results were obtained when aging was carried out. T6 heat treatments gave higher strength than T7 heat treatments, where over aging and alloy softening commenced.

20. Alloy B in the S8WA2 (T6) heat-treated condition is considered the optimum alloy composition/heat treatment condition for the HT200 alloy, as it gave the highest UTS, YS, %El and Q-values compared with alloys A and C (cf. 307.9 MPa UTS, 303.9 MPa YS with 152.8 MPa UTS, 87.7 MPa YS for alloy A). The observed enhancement in

tensile properties is related to the precipitation of ultra-fine particles of the θ-Al_2Cu phase, as well as the grain refining.

21. Alloy B gives the best overall performance across the range of heat treatments employed with respect to the HT200 alloys, with properties comparable to the widely used 319 and 356 reference alloys, making a very suitable alternate for use in the automotive industry.

22. The presence of Ag in alloy C enhanced the YS of alloy A by ~17% in the as-cast condition, and also showed a slight improvement in UTS, going from 152.8 MPa to 156.8 MPa.

RECOMMENDATIONS FOR FUTURE WORK

Based on the results obtained in this study, the following aspects may be further explored to provide a deeper and more comprehensive understanding of the HT200 alloys investigated in this study.

- Study the precipitates obtained and precipitation behavior using transmission electron microscopy to identify their exact composition and characteristics.

- Conduct creep tests at high temperature to determine the effect of heat treatment on the alloy life time.

- Investigate the effects of the different heat treatments used on other mechanical properties of these alloys, such as the impact and fatigue properties.

REFERENCES

REFERENCES

[1] ASM International Handbook Committee, ASM Handbook Volume 2: Properties and Selection: Nonferrous Alloys and Special-Purpose Materials, ASM International, 1990.

[2] M. Kutz, Mechanical Engineers' Handbook: Materials and Mechanical Design, Book 1, Third Edition, New Jersey: John Wiley & Sons, Inc., 2006.

[3] ASM International, "Aluminum and Aluminum Alloys," *ASM International,* 2015.

[4] F. Paray and J. Gruzleski, "Factors to Consider in Modification," *AFS Transactions,* vol. 102, pp. 833-842, 1994.

[5] U. Vatsayan, K. Pandey and A. Biswas, "Effects of Heat Treatment on Materials Used In Automobiles: A Case Study," *IOSR Journal of Mechanical and Civil Engineering (IOSR-JMCE),* pp. 90-95, 2014.

[6] G. H. Garza-Elizondo, S. A. Alkahtani, A. M. Samuel and F. H. Samuel, "Role of Ni and Zr in Preserving the Strength of 354 Aluminum Alloy at High Temperature," *Springer International Publishing, In Light Metals 2014,* pp. 305-314, 2014.

[7] G. Mathers, The welding of aluminium and its alloys, Woodhead Publishing Ltd and CRC Press LLC, 2002.

[8] J. G. Kaufman and E. L. Rooy, Aluminum Alloy Castings: Properties, Processes, and Applications, ASM International, 2004.

[9] A. Mohamed and F. Samuel, "Microstructure, tensile properties and fracture behavior of high temperature Al–Si–Mg–Cu cast alloys," *Materials Science and Engineering,* Vols. A, 577, pp. 64-72, 2013.

[10] C. Kammer, Castingin Aluminium Handbook, Vol. 2, Dusseldorf: Aluminium-Verlag, 1999.

[11] M. Flemings, Solidification Processing, New York: McGraw-Hill, 1974.

[12] J. Campbell, Castings, London, UK: Butterworth-Heinemann Ltd., 1991.

[13] T. H. Muster, A. E. Hughes and G. E. Thompson, Copper Distributions in Aluminium Alloys, New York: Nova Science Publishers, Inc., 2009.

[14] A. Hossain, A. S. W. Kurny and M. A. Gafur, "Effect of 2wt% Cu Addition on the Tensile Properties and Fracture Behavior of Peak Aged Al-6Si-0.5Mg-2Ni Alloy at Various Strain Rates," *International Journal of Chemical, Nuclear, Metallurgical and Materials Engineering,* vol. 8 No: 5, pp. 356-364, 2014.

[15] G. E. Totten and D. S. MacKenzie, Handbook of Aluminum Volume 1 - Physical Metallurgy and Processes, New York: Marcel Dekker, Inc., 2003.

[16] G. H. G. Elizondo, "Machinability of Al-(7-11%)Si Casting Alloys: Role of Free-Cutting Elements," MSc Thesis, Université du Québec à Chicoutimi, Chicoutimi, Quebec, 2010.

[17] M. H. A. Abdelaziz, "Microstructural and Mechanical Characterization of Transition Elements-Containing Al-Si-Cu-Mg Alloys for Elevated-Temperature Applications," PhD Thesis, Université du Québec à Chicoutimi, Chicoutimi, Quebec, 2018.

[18] L. Bâckerud, Guocai and J. Tamminen, "Solidification Characteristics of Aluminum Alloys," *AFS/SKANALUMINUM, USA,* vol. 2, p. 255, 1990.

[19] G. G. Garcia, J. E. Cuadra and H. M. Molinar, "Copper Content and Cooling Rate Effects over Effects Second Phase Particles Behavior in Industrial Aluminum-Silicon Alloy 319," *Materials and Design,* vol. 28, pp. 428-433, 2007.

[20] E. Rincon, H. F. Lopez, M. M. Cisneros, H. Mancha and M. A. Cisneros, "Effect of Temperature on the Tensile Properties of an As-Cast Aluminum Alloy A319," *Materials Science and Engineering A,* Vols. 452-453, pp. 682-687, 2007.

[21] P. N. Crepeau, "Effect of Iron in Al-Si Casting Alloys: A Critical Review," *AFS Transactions,* vol. 110, pp. 361-366, 1995.

[22] Z. Ma, A. M. Samuel, F. H. Samuel, H. W. Doty and S. Valtierra, "A Study of Tensile Properties in Al-Si-Cu and Al-Si-Mg Alloys: Effect of β-Iron Intermetallics and Porosity," *Materials Science and Engineering A,* vol. 490, pp. 36-51, 2008.

[23] L. Lu and A. K. Dahle, "Iron-Rich Intermetallic Phases and Their Role m Casting Defect Formation in Hypoeutectic Al-Si Alloys," *Metallurgical and Materials Transactions A,* vol. 36A, pp. 819-835, 2005.

[24] J. Y. Hwang, H. W. Doty and M. J. Kaufman, "The Effects of Mn Additions on the Microstracture and Mechanical Properties of Al-Si-Cu Casting Alloys," *Materials Science and Engineering A,* vol. 488A, pp. 496-504, 2008.

[25] N. Han, X. F. Bian, Z. K. Li, T. Muo and C. D. Wung, "Effect of Si on the Microstructure and Mechanical Properties of the Al-4.5%Cu Alloys," *Acta Metallurgica Sinica,* vol. 19, pp. 405-410, 2006.

[26] L. Ceschini , I. Boromei, A. Morri, S. Seifeddine and I. L. Svensson, "Microstructure, Tensile and Fatigue Properties of Al-10%Si-2%Cu Alloy with Different Fe and Mn Content Cast under Controlled Conditions," *Journal of Materials Processing Technology,* vol. 209, pp. 5669-5679, 2009.

[27] S. G. Shabestari and H. Momeni, "Effect of Copper and Solidification Conditions on the Microstructure and Mechanical Properties of Al-Si-Mg Alloys," *Journal of Materials Processing Technology,* Vols. 153-154, pp. 193-198, 2004.

[28] D. Eskin, Q. Du, D. Ruvalcaba and L. Katgerman, "Experimental Study of Structure Formation in Binary Al-Cu Alloys at Different Cooling Rates," *Materials Science and Engineering A,* vol. 405 A, pp. 1-10, 2005.

[29] L. Y. Zhang, Y. H. Jiang and W. K. Wang, "Effect of Cooling Rate on Solidified Microstructure and Mechanical Properties of Alurninum-A356 Alloy," *Journal of Materials Processing Technology,* vol. 207, pp. 107-111, 2008.

[30] D. Argo and J. E. Gruzleski, "Porosity in Modified Aluminum Alloy Castings," *AFS Transactions,* vol. 16, pp. 65-74, 1988.

[31] D. Emadi and J. E. Gruzleski, "Effects of Casting and Melt Variables on Porosity in Directionally-Solidified Al-Si Alloys," *AFS Transactions,* vol. 95, pp. 307-312, 1994.

[32] ASM Handbook Committee, ASM Handbook Volume 4 - Heat Treating, ASM International, 1991.

[33] W. Callister, Fundamentals of Materials Science and Engineering: An Interactive E. Text. ed., ed. Vol. 5, Wiley New York, 2001.

[34] F. Fracasso, "Influence of Quench Rate on the Hardness Obtained after Artificial Ageing of an Al-Si-Mg Alloy," University of Padova, 2010.

[35] A. M. A. Mohamed and F. H. Samuel., *A review on the heat treatment of Al-Si-Cu/Mg casting alloys,* Dr. Frank Czerwinski (Ed.), ISBN: 978-953-51-0768-2, InTech, DOI: 10.5772/50282, 2012.

[36] J. E. Hatch, Aluminum Properties and Physical Metallurgy, ASM International, 1984.

[37] ASM International Alloy Phase Diagram and the Handbook Committees, ASM Handbook Volume 3: Alloy Phase Diagrams, ASM International, 1992.

[38] W. Callister and D. Rethwisch, *Fundamentals of Materials Science and Engineering: An Integrated Approach. ed.,* John Wiley & Sons, 2012.

[39] V. I. Elagin, *Ways of Developing high-Strength and high-Temperature Structural Aluminum alloys in the 21st Century,* 2007.

[40] C. Caceres, I. Svensson and J. Taylor, *Strength-Ductility Behaviour of Al-Si-Cu-Mg Casting Alloys in T6 Temper,* 2003.

[41] A. Mohamed and F. Samuel, "Influence of Mg and Solution Heat Treatment on the Occurrence of Incipient Melting in Al–Si–Cu–Mg Cast Alloys," *Materials Science and Engineering: A,* vol. 543, pp. 22-34, 2012.

[42] M. Moustafa, F. Samuel and H. Doty, "Effect of Solution Heat Treatment and Additives on the Hardness, Tensile Properties and Fracture Behaviour of Al-Si (A413. 1) Automotive Alloys," *Journal of materials science,* vol. 38 (22), pp. 4523-4534, 2003.

[43] G. Sigworth, J. Howell, O. Rios and M. Kaufman, "Heat Treatment of Natural Aging Aluminum Casting Alloys," *International Journal of Cast Metals Research,* vol. 19 (2), pp. 123-129, 2006.

[44] K. A. Ragab, "The use of fluidized sand bed as an innovative technique for heat treating aluminum based castings," PhD Thesis, Université du Québec à Chicoutimi, Chicoutimi, Quebec, 2012.

[45] A. Samuel, H. Doty, S. Valtierra and F. Samuel, "Defects Related to Incipient Melting in Al–Si–Cu–Mg Alloys," *Materials & Design,* vol. 52, pp. 947-956, 2013.

[46] A. Mohamed, A. Samuel, F. Samuel and H. Doty, "Influence of Additives on the Microstructure and Tensile Properties of near-Eutectic Al–10.8% Si Cast Alloy," *Materials & Design,* vol. 30 (10), pp. 3943-3957, 2009.

[47] E. Sjölander and S. Seifeddine, "The Heat Treatment of Al–Si–Cu–Mg Casting Alloys," *Journal of Materials Processing Technology,* vol. 210 (10), pp. 1249-1259, 2010.

[48] E. Sjölander and S. Seifeddine, "Artificial Ageing of Al–Si–Cu–Mg Casting Alloys," *Materials Science and Engineering: A,* vol. 528 (24), pp. 7402-7409, 2011.

[49] D. Zhang and L. Zheng, "The Quench Sensitivity of Cast Al-7 Wt Pct Si-0.4 Wt Pct Mg Alloy," *Metallurgical and Materials Transactions A,* vol. 27 (12), pp. 3983-3991, 1996.

[50] I. Polmear, *Light alloys: from traditional alloys to nanocrystals,* 2005.

[51] D. Porter, K. Easterling and M. Sherif, Phase Transformations in Metals and Alloys, (Revised Reprint). ed., ed. Vol, CRC press, 2011.

[52] L. Bäckerud, E. Krol and J. Tamminen, Solidification Characteristics of Aluminum Alloys Volume I: Wrought Alloys, Sweden: Tangen Trykk A/S, 1986.

[53] E.-E. M. Elgalad, "Effect of Additives on the Mechanical Properties and Machinability of a New Aluminum-Copper Base Alloy," PhD Thesis, Université du Québec à Chicoutimi, Chicoutimi, Quebec, 2010.

[54] H. K. Kamga, "Influence of Alloying Elements Iron and Silicon on Mechanical Properties of Aluminum-Copper Type B206 Alloys," PhD Thesis, Université du Québec à Chicoutimi, Chicoutimi, Quebec, 2010.

[55] D. Xiao, J. Wang, D. Ding and S. Chen, "Effect of Cu content on the mechanical properties of an Al–Cu–Mg–Ag alloy," *Journal of Alloys and Compounds,* vol. 343, pp. 77-81, 2002.

[56] G. Sigworth and T. Kuhn, *Grain Refinement of Aluminum Casting Alloys,* 2007.

[57] S. Zor, M. Zeren, H. Özkazanc and E. Karakulak, "Effect of Titanium Addition on Corrosion Properties of Al–Si Eutectic Alloys," *Protection of Metals and Physical Chemistry of Surfaces,* Vols. 48, no. 5, pp. 568-571, 2012.

[58] R. Mahmudi, P. Sepehrband and H. Ghasemi, "Improved Properties of A319 Aluminum Casting Alloy Modified with Zr," *Materials Letters,* vol. 60, pp. 2606-2610, 2006.

[59] M. Drouzy, S. Jacob and M. Richard, "L'Indice de Qualité et la Limite D'élasticité des Alliages A-S7 G," *Fonderie 360,* pp. 345-349, 1975.

[60] M. Drouzy, S. Jacob and M. Richard, "Le Diagramme Charge de Rupture Allongement des Alliages D'Aluminium : L'Indice de Qualité - Application aux A-S7 G," *Fonderie 355,* pp. 139-147, 1976.

[61] G. a. J. Archbutt, "Properties and Production of Aluminum Alloy Die Castings," *Journal of Institute of Metals,* vol. 40, p. 219, 1928.

[62] J. Vero, "The Hot Shortness of Aluminum Alloys," *The Metal Industry,* vol. 48, pp. 431-442, 1936.

[63] A. Norton, "Hot Shortness Testing Machine for Aluminum Alloys," *ASME Transactions,* vol. 8, p. 124, 1914.

[64] A. Singer and S. Cottrell, "Properties of the AL-Si Alloys at Temperatures in the Region of the Solidus," *Journal of Institute of Metals,* vol. 73, pp. 33-54, 1946.

[65] B. Forest and S. Bercovici, "Experimental Study of Mechanical Properties of Aluminum Alloys During Controlled Solidification: Application to Hot Tearing," *Solidification Technology in the Foundry and Cast House, Proceed, Conf, Univ. of Warwick, Coventry, U.K, Paper 93, 12 pages,* 1980.

[66] P. Wisniewski, "Tensile Properties of Binary Al-Cu Alloys in Solid plus Liquid State," PhD Thesis, Univ. of Pittburgh, Pittburgh, PA, 1990.

[67] J. Borland, "Generalized Theory of Super-Solidus Cracking in Welds and Casting," *British Welding Journal,* Vols. 7, No.8, pp. 508-512, 1960.

[68] W. Pumphrey and P. Jennings, "A Consideration of the Nature of Brittleness at Temperature above the Solidus in Castings and Welds in Aluminum Alloys," *Journal of Institute of Metals,* vol. 75, p. 235, 1948.

[69] W. Pellini, "Strain Theory of Hot Tearing," *Foundry,* vol. 80, pp. 124-199, 1952.

[70] J. Campbell, "Entrainment defects," *Materials Science and Technology,* vol. 22 (2), pp. 127-145, 2006.

[71] J. Campbell, Complete Casting Handbook: Metal Casting Processes, Metallurgy, Techniques and Design, Elsevier Science, 2015.

[72] R. Ç. D. D. M. T. Muhammet Uludağ, "The effects of degassing, grain refinement & Sr-addition on melt quality-hot tear sensitivity relationships in cast A380 aluminum alloy," *Engineering Failure Analysis,* pp. 90-102, 2018.

[73] L. Katgerman and D. Eskin, "In search of prediction of hot cracking in aluminium alloys," *in: H.H. Thomas Bollinghaus, Carl E. Cross, John C. Lippold (Eds.), Hot Cracking Phenomena in Welds II, Springer, Berlin,* p. 3–18, 2008.

[74] H. Ammar, "Influence of Metallurgical Parameters on the Mechanical Properties and Quality Indices of Al-Si-Cu-Mg and Ai-Si-Mg Casting Alloys," PhD Thesis, Université du Québec à Chicoutimi, Chicoutimi, Quebec, 2010.

[75] G. H. G. Elizondo, "Effect of Ni, Mn, Zr and Sc Additions on The Performance of Al-Si-Cu-Mg Alloys," PhD Thesis, Université du Québec à Chicoutimi, Chicoutimi, Quebec, 2016.

[76] N. Alexopoulos, "Generation of Quality Maps to Support Material Selection by Exploiting the Quality Indices Concept of Cast Aluminum Alloys," *Materials and Design,* vol. 28, pp. 534-543, 2007.

[77] N. Alexopoulos, "Definition of Quality in Cast Aluminum Alloys and Its Characterization with Appropriate Indices," *Journal of Materials Engineering and Performance,* vol. 15(1), pp. 59-66, 2006.

[78] M. Drouzy, S. Jacob and M. Richard, "Interpretation of Tensile Results by Means of Quality Index and Probable Yield Strength," *AFS International Cast Metals Journal,* vol. 5, pp. 43-50, 1980.

[79] H. Ammar, A. Samuel, F. Samuel, E. Simielli, G. Sigworth and J. Lin, "Influence of Aging parameters on the Tensile Properties and Quality Index of Al-9 Pct Si-1.8 Pct Cu-0.5 Pct Mg 354-Type Casting Alloys," *Metallurgical and Materials Transactions A,* vol. 43A, pp. 61-73, 2012.

[80] M. Verbrugge, "Mass Decompounding and Vehicle Lightweighting," *Materials Science Forum,* vol. 5, pp. 618-619, 2009.

[81] J. Hernandez-Sandoval, G. Garza-Elizondo, A. Samuel, S. Valtierra and F. Samuel, "The ambient and high temperature deformation behavior of Al-Si-Cu-Mg alloy with minor, Ti, Zr, Ni additions," *Material and Design,* vol. 58, pp. 89-101, 2014.

[82] H. Ammar, C. Moreau, A. Samuel, F. Samuel and H. Doty, "Effects of Aging Parameters on the Quality of 413-Type Commercial Alloys," *Materials and Design,* vol. 30, pp. 1014-1025, 2009.

[83] R. W. Armstrong, "Hall-Petch Relationship: Use in Characterizing Properties of Aluminum and Aluminum Alloys," Taylor & Francis Group, U.K., 2016.

[84] Y.-J. Kwon, I. Shigematsu and N. Saito, "Mechanical Property Improvements in Aluminum Alloy through Grain Refinement using Friction Stir Process," *Materials Transactions,* Vols. 45, No. 7, p. 2304 to 2311, 2004.

[85] J. Campbell and R. Harding, "The fluidity of Molten Metals," *EEA - European Aluminum Association, TALAT Lecture 3205, 19 pages, 17 figures,* 1994.

[86] I. Odnevall Wallinder, X. Zhang, S. Goidanich, N. Le Bozec, G. Herting and C. Leygraf, "Corrosion and runoff rates of Cu and three Cu-alloys in marine environments with increasing chloride deposition rate," *Science of the Total Environment,* vol. 472, p. 681–694, 2013.

[87] S. Jacob, "Quality Index in Predicting of Properties of Aluminum Castings-A Review," *AFS Transactions,* vol. 108, pp. 811-818, 2000.

[88] A. Dons, G. Heiberg, J. Voje, J. Maeland, J. Loland and A. Prestmo, "On the Effect of Additions of Cu and Mg on the Ductility of Al-Si Foundry Alloys Cast with a Cooling Rate of Approximately 3 K/s," *Materials Science and Engineering A,* Vols. 413-414, pp. 561-566, 2005.

[89] S. Abis, M. Massazza, P. Mengucci and G. Tiontino, "Early Ageing Mechanisms in a High-Copper AlCuMg Alloy," *Scripta Materialia,* vol. 45, pp. 685-691, 2001.

[90] H. R. Ammar, C. Moreau, A. M. Samuel, F. H. Samuel and H. W. Doty, "Influences of alloying elements, solution treatment time and quenching media on quality indices of 413-type Al–Si casting alloys," *Materials Science and Engineering A,* Vols. 489, no. 1, pp. 426-438, 2008.

[91] P. Ratchev, B. Verlinden, P. De Smet and P. Van Houtte, "Precipitation Hardening of an Al-4.2wt%Mg-0.6wt%Cu Alloy," *Acta Materialia,* vol. 46(10), pp. 3523-3533, 1998.

[92] S. Wang, M. Starink and N. Gao, "Precipitation Hardening in Al-Cu-Mg Alloys Revisited," *Scripta Materialia,* vol. 54, pp. 287-291, 2006.

[93] P. Ratchev, B. Verlinden, P. De Smet and P. Van Houtte, "Effect of Cooling Rate and Predeformation on the Precipitation Hardening of an Al-4.2wt%Mg-0.6wt%Cu Alloy," *Scripta Materialia,* vol. 38(8), pp. 1195-1201, 1998.

[94] F. Samuel, A. Samuel and H. Doty, "Factors controlling the type and morphology of Cu-containing phases in 319 Al alloys," *AFS Transactions,* vol. 104, pp. 893-901, 1996.